INTERROGATING MEMORY B-CELL RESPONSES TO RNA VIRUSES OF CLINICAL IMPORTANCE

By

Zoe Leah Lyski

A DISSERTATION

Presented to the Department of Molecular Microbiology and Immunology
and the Oregon Health & Science University
School of Medicine
in partial fulfillment of
the requirements for the degree of
Doctor of Philosophy

March 2022

Table of Contents

List of abbreviations

Abbreviation	Full word
AA	Amino acid
AB	Antibody
ACE-2	Angiotensin converting enzyme -2
ADCC	Antibody-dependent cellular cytotoxicity
ADCP	Antibody-dependent cellular phagocytosis
ADE	Antibody-dependent enhancement
ADP	Antibody-dependent phagocytosis
AF	Alexa Fluor
AID	Activation-induced cytidine deaminase
ALC	Absolute lymphocyte count
ANOVA	Analysis of variance
ARDS	Acute respiratory distress syndrome
ASC	Antibody secreting cells
BCL-2	B-cell lymphoma
BCR	B-cell receptor
BTK	Bruton tyrosine kinase
CDR	Complementary determining region
CHIKV	Chikungunya virus
CLL	Chronic lymphocytic leukemia
CNS	Central nervous system
COVID	Coronavirus disease
DENV	Dengue virus
DHF	Dengue hemorrhagic fever
DSS	Dengue shock syndrome
DZ	Dark zone
EBV	Epstein Barr virus
EDE	E-dimer E epitope
EDI	Envelope protein domain I
EDII	Envelope protein domain II
EDIII	Envelope protein domain III
EDTA	Ethylenediaminetetraacetic acid
EEE	Eastern Equine Encephalitis
ELISA	enzyme-linked immunosorbent assay
ELISPOT	Enzyme linked immuno spot
EM	Electron microscopy

ER	Endoplasmic reticulum
EUA	Emergency use authorization
FACS	Fluorescence activated cell sorting
FBS	Fetal bovine serum
FDA	Federal department of agriculture
FFU	Foci forming unit
FRNT	Foci reduction neutralization titer
GC	Germinal center
GMF	Geometric mean frequency
GMT	Geometric mean titer
HC	Heavy chain
HIV	Human immunodeficiency virus
HRP	Horseradish peroxidase
ICU	Intensive care unit
IFN	Interferon
IGHV	immunoglobulin heavy chain variable region
IL	Interleukin
IP	Intraperitoneal injection
IRB	Internal review board
IRES	Internal ribosomal entry site
ISG	Interferon stimulated gene
IV	Intravenous
JEV	Japanese encephalitis virus
JNJ	Johnson and Johnson
LDA	Limiting dilution assay
LLPC	Long lived plasma cell
LOD	Limit of detection
LPS	Lipopolysaccharide
LZ	light zone
MAYV	Mayaro virus
MBC	Memory B-cell
MBL	Monoclonal B-cell lymphocytosis
MERS	Middle Eastern Respiratory syndrome
MHC	Major histocompatibility complex
ONNV	O`nyong-nyong virus
ORF	Open reading frame
PBMC	Peripheral blood mononuclear cells
PFU	Plaque forming units

PRNT	Plaque reduction neutralization titer
RBD	Receptor binding domain
RRV	Ross River virus
RSV	Respiratory syncytial virus
SARS	Severe acute respiratory syndrome
SFV	Semliki Forest virus
SHM	Somatic hypermutation
SINV	Sindbis virus
TBEV	Tick-borne encephalitis virus
TCR	T-cell receptor
TFH	T-follicular helper cell
TLR	Toll-like receptor
Treg	Regulatory T-cell
UL	microliter
UNAV	Una virus
VDJ	Variable/diversity/joining
VEEV	Venezuelan equine encephalitis virus
VLP	Virus like particle
VOC	Variant of concern
WEEV	Western equine encephalitis virus
WNV	West Nile virus
WT	Wild-type
YFV	Yellow Fever Virus
ZIKV	Zika virus

List of tables

Table of figures

Acknowledgments

This dissertation is the product of years of collaborative work that wouldn't be possible without supportive lab members, mentors, family, and friends. First of all, I have to thank my mentor, Dr. William Messer MD, PhD. for his support, trust, and unwavering enthusiasm, for setting a good example, and for showing me that it's possible to have a happy home life and a successful scientific career. Secondly, I would like to thank the Messer lab members (past and present) for all of their support over the years: Drs Jana Mooster MD, PhD. and Zhengchun Lu, MD, PhD., Bettie Kareko, Jules Weinstein, Felicity Coulter MSc., Courtney Micheletti, and David Xthona Lee, for their words of encouragement, lab treats, and friendship. I would also like to thank those along the way who have given me the opportunity to practice being a mentor, Diana Demchenko, Michelle Garcia, and Peregrine Painter. I would also like to thank my advisory committee members, Dr.'s Dan Streblow PhD., Mark Slifka PhD., and Ann Hessel PhD. for their continued support, guidance, and expert advice. They were always there to share a kind word of encouragement or help me troubleshoot if I was having a problem. I'd also like to thank Ian Amanna PhD. and Archana Thomas PhD., from the Slifka lab, Bill Sutton MS and David Spencer PhD. from the Hessell lab, and Anuja Mathew, PhD for sharing protocols, reagents and helping me troubleshoot, especially early on in my graduate career. Our Ponce collaborators Rachel Rodriguez, Luisa Alvarado MD, and Vanessa Rivera-Amill PhD for being instrumental in getting our endemic cohort up and running, for their critical editing of manuscripts and intellectual contributions to our arbovirus work. I couldn't have done this human subject research without support from our clinical study coordinator team, Brian Booty, Sarah Seigel PhD., Amanda Brunton MPH, Peter Sullivan, and Matt Strnad who worked hard to recruit and enroll all of our human subjects and manage all of the associated data. Dr. Stephen Spurgeon MD and his team who allowed me to run point on the CLL experiments giving me the

opportunity to work on different projects and gain more experience writing. I'd also like to acknowledge Dr. Lydie Trautmann for joining my committee as an external reader, providing helpful feedback and support. Finally, this work would not be possible without support, encouragement, and understanding from my family and friends. My lab sister Bettie Kareko who has been my biggest supporter throughout my graduate career always there with words of encouragement, cookies, or coffee when I needed it the most. My parents, Steve and Diane Sapiro, who always encouraged me to push myself to accomplish great things, no matter what obstacles stood in my way. My husband, AJ, who has been my biggest fan and who has always given 115% to make sure our world keeps turning, especially during all the ups and downs of grad school. Finally, I would like to thank my boys, Gavin, Corbin, and Bear, who have supported me, encouraged me, loved me unconditionally, and made me a better scientist.

Abstract

This dissertation characterizes B-cell mediated immune responses to RNA viruses of clinical importance. Specifically, I examine the responses to dengue virus (DENV), chikungunya virus (CHIKV), and the newly emerged severe acute respiratory syndrome coronavirus 2 (SARS-CoV-2). Following first infection, naïve host B-cells expand and produce antigen-specific antibodies that recognize viral antigens. After viral clearance, some antigen-specific B-cells become long-lived plasma cells (LLPCs) while others become memory B-cells (MBCs) that remain in peripheral blood and lymphoid tissues, poised to respond in the event of repeat infection with the same, or similar pathogen. Populations of antibody secreting LLPCs and resting MBCs are independent and contribute in different ways towards protection against newly infecting/emerging viral pathogens. This work is important because much of much of the durability, breadth, and longevity of antigen-specific MBCs remain incompletely characterized, but the critical role they play in establishing broad immunity should not be underestimated. This is important for DENV which circulates as four distinct serotypes that often overlap geographically, for alphaviruses that have a high emergence potential, as well as SARS-CoV-2 which continues to undergo evolution that results in new SARS-CoV-2 variants of concern.

In Chapter 1, a comprehensive overview of the virology, pathogenesis, adaptive immunity, and vaccinology for each virus family included, as well as an introduction to B-cell biology and immunity.

In chapter 2, I interrogate the B-cell mediated response to dengue virus (DENV), one of the most important vector-borne viral pathogens affecting humans worldwide. Specifically, LLPC-derived antibodies and MBCs recognize epitopes of the envelope glycoprotein (E) that are present on the surface of DENV as well as secreted non-structural protein 1 (NS1). I quantified

DENV-specific MBCs in humans following DENV-1 infection in a cross-sectional manner, using peripheral blood mononuclear cells (PBMCs) from n=39 DENV-1 immune donors with times post-infection ranging from <1-43 years. We used two complementary approaches to quantify the MBC population: flow cytometry and limiting dilution assay; using these approaches, we identified DENV-whole virion envelope and NS1-specific MBCs that remain in circulation decades after infection with varying frequencies in subjects from both boosting (endemic) and non-boosting (non-endemic) transmission settings.

In chapter 3, I, in collaboration with Dr Dan Streblow's lab, interrogated the B-cell mediated response to Chikungunya virus (CHIKV), a mosquito-borne alphavirus. Neutralizing antibodies are the primary immune correlate of protection elicited by CHIKV infection. Using convalescent blood samples collected from 12 subjects with suspected or confirmed CHIKV infection, we identified antibodies with broad neutralizing properties against both CHIKV and other alphaviruses. I also performed memory B-cell analysis, using methods developed in chapter 2. I functionally assessed the ability of memory B-cell-derived antibodies to bind to CHIKV, closely related Mayaro virus, as well as the highly conserved B domain on the viral surface E2 protein, thought to contribute to cross-reactivity between related Old-World alphaviruses.

In chapter 4, I, in collaboration with our clinical team, characterized the magnitude, breadth, and durability of SARS-CoV-2 specific antibody responses (LLPC and MBC) in 35 subjects following natural infection with SARS-CoV-2. Using a cohort of subjects with diverse disease history, I found that the magnitude of antibody responses varied significantly between individuals but is the highest overall in hospitalized subjects. Variant of concern-RBD-reactive MBCs were present in the peripheral blood of 97% of all subjects, including those that experienced asymptomatic or mild disease, providing a reason for optimism regarding the

capacity of vaccination, prior infection, and/or both, to elicit immunity that may have the capacity to limit disease severity and transmission of SARS-CoV-2 variants as they continue to arise and circulate.

In chapter 5, in collaboration with hematologist-oncologist Dr. Stephen Spurgeon, I review the background of the B-cell responses in patients with chronic lymphocytic leukemia (CLL), a hematological malignancy that targets B-cells and is characterized by a dysfunctional, but incompletely characterized, adaptive immune response. In chapters 6 and appendix 2, I then characterize the B-cell responses in CLL patients at different stages of treatment (observation, active treatment, post treatment) in order to better understand how this immunocompromised population responds to vaccination with mRNA COVID-19 vaccines. I applied the same methods of interrogating antigen-specific MBCs used for DENV, CHIKV and COVID-19 patients to thoroughly examine the B-cell immune response to vaccination and booster vaccination in human subjects with CLL. My main finding was that the overall B-cell mediated immune response is reduced compared to healthy controls in a treatment phase dependent manner. Boosting was shown to elicit a response (1of 2 subjects), albeit a lowered responses compared to health control subjects.

Chapter 1: RNA Viruses of Clinical Importance

There are many more RNA viruses of clinical importance than are presented in this dissertation. The RNA viruses of clinical importance that I have chosen to study come from the Messer lab's long-standing interest in mosquito-borne flaviviruses, as well as two unique opportunities to branch out into new pathogens of interest. First, a collaboration with a recent OHSU graduate, John Powers, PhD, from Dr. Dan Streblow's lab examining immunity to mosquito transmitted Chikungunya virus, and secondly, the COVID-19 pandemic, which offered a unique opportunity to study SARS-CoV-2 specific B-cell immunity. All of these viruses cause disease in their human hosts, often resulting in morbidity and mortality. This chapter provides an introduction to the virology, pathogenesis, immunity and vaccinology (available vaccines and those in development) for the three main virus families studied in this dissertation.

1.1.1 **Flavivirus Virology**

Flaviviruses belong to the family flaviviridae and are small (40-60nm), positive-sense single-stranded RNA viruses, enveloped in a host-cell derived lipid membrane.[13,14] The viral genome is ~11kb in length and is translated as a single polyprotein. The genome encodes 3 structural proteins on the 5' end and 7 non-structural proteins (Figure 1). *Flaviviruses* are widely distributed globally and include over 90 viruses, many of them pathogenic which include dengue (DENV), yellow fever (YFV), West Nile (WNV), Japanese encephalitis (JEV), tick-borne encephalitis (TBEV), and Zika (ZIKV) the most recent flavivirus to cause a widespread pandemic across the Americas.[14,15] Dengue alone causes an estimated 400 million infections globally every year, a quarter of which result in symptomatic disease (section 1.1.2).[4,5,16]

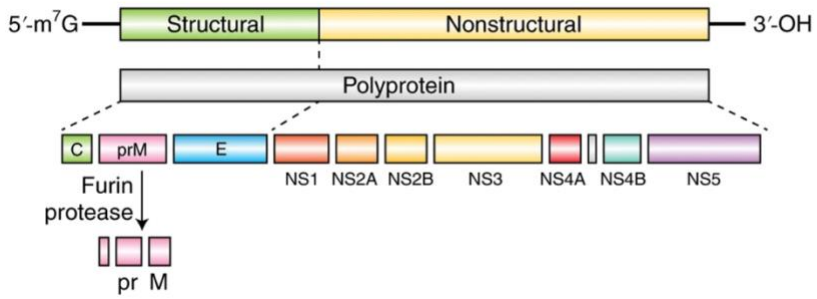

Figure 1 Flavivirus genome

Figure taken from [8] with permission.

Vector hosts

There are two main groups of flaviviruses: insect-specific and mosquito/tick-borne. [17] Those that are transmitted by mosquitoes and ticks - arthropods - are called arboviruses, short for "arthropod-borne" viruses, with the ability to infect and replicate in a wide range of vertebrate and arthropod hosts. [13] Both tick and mosquito-borne flaviviruses alternate between arthropod and vertebrate hosts. Insect-only flaviviruses are restricted to replicating exclusively in insects. In addition, there are some flaviviruses with no known arthropod vector which are found in vertebrate hosts. [17] Vertical transmission, *e.g* from adult female arthropods to progeny, is

responsible for insect-only transmission. Some flaviviruses have a broad host range, for example, WNV and JEV can replicate in a wide variety of hosts from avian species to horses and humans, while others have a very narrow host range, for instance, YFV and DENV have been found to replicate only in non-human primates (NHPs) and humans. [18,19] The transmission cycles that exist for arthropod-borne flaviviruses are summarized below:

- Sylvatic transmission cycles occur in Africa and South America, where the virus is transmitted between forest mosquitos and wild primates. Sporadic spillover events occasionally involve forestry workers and hunters. [20] YFV, ZIKV, and DENV are examples of flaviviruses that can be maintained in a sylvatic cycle between NHPs and tree-dwelling mosquitoes such as *Ae. Africanus*.[2]
- Intermediate transmission cycles occur in zones of emergence, usually in small towns or villages on the edges of forests or jungles where sylvatic cycles are occurring. Outbreaks, occur sporadically as small-scale epidemics and involve semi-domestic mosquitoes, those that live and breed in both the forest and around people. For example, in Africa YFV participates in the intermediate transmission cycle between NHPs and *Aedes simpsoni* mosquitoes. [21,22]
- Enzootic cycles occur between mosquitos and birds or small mammals, which serve as the amplifying hosts. Humans serve as incidental hosts and typically do not contribute to the virus life cycle. Humans are considered dead-end or accidental hosts because they do not typically lead to further virus transmission, although infection may result in clinical disease. [19] JEV, WNV, and TBEV are maintained in the enzootic transmission cycle, between *Culex* mosquito spp. and birds or pigs in the case of JEV and ticks such as *Ixodes persulcatus* or *Haemaphysalis concinna* and small rodents or mammals. [21, 23]

- Urban transmission cycles occur in larger cities, requiring a minimum of 10,000 to 1 million occupants. [2] In this cycle, humans serve as the host and the virus is transmitted human-to-human by peri-domestic mosquitoes such as *Ae. Aegypti* and Ae. *Albopictus,* which live in close proximity to humans and are able to lay eggs in small amounts of water, such as that in water storage containers, and often take multiple blood meals increasing the rate of viral transmission. [2]. ZIKV, DENV, and YFV can all be transmitted in the urban cycle. [2]

Viral replication

Flaviviruses enter host cells via receptor-mediated endocytosis through interactions with a wide range of cell-surface receptors, although no single receptor has been identified. [24] There are several receptors postulated to play a role in flavivirus entry, including C-type lectin receptors, such as dendritic cell-specific intercellular adhesion molecule 3 grabbing non-integrin (DC-SIGN) and T-cell immunoglobulin and mucin domain (TIM). [24] Following clathrin-mediated uptake into endocytic vesicles the endosomal pH lowers triggering conformational changes to the E protein, which leads to fusion between the viral and endosomal membranes releasing the nucleocapsid into the cytoplasm. [25] In the cytoplasm viral RNA undergoes cap-dependent translation by ribosomes on the rough endoplasmic reticulum (ER). [1] Viral translation yields a

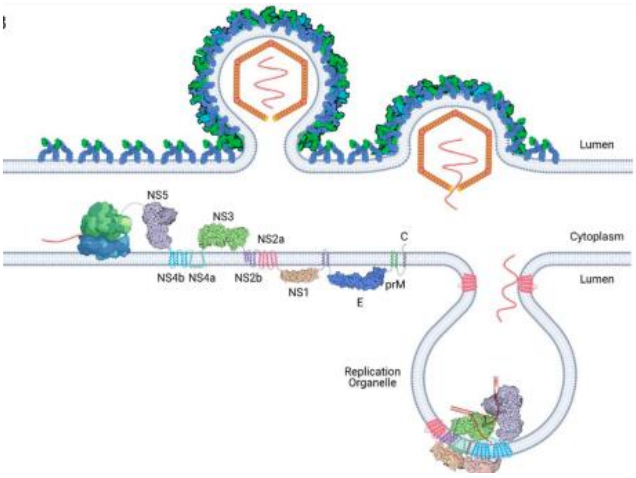

Figure 2 Flavivirus replication in viral replication factories.
Figure from [1] published under Creative Commons licenses.

polyprotein that encodes non-structural and structural proteins that are anchored to the ER membrane. [1] The viral polyprotein is then cleaved into its respective proteins by host proteases and viral protease NS3. Flavivirus replication occurs in membrane invaginations of the endoplasmic reticulum, called replication factories (Figure 2). [26] These serve to protect the replicating virus from innate immune sensors in the cytoplasm and localize viral protein translation close to the ER. Viral replication requires changes in host cell metabolism including increased cholesterol, fatty acid, and sphingomyelin synthesis. [27,28] In the replication factories, negative-strand RNA is synthesized takes place, which acts as a template for positive-sense RNA synthesis. Newly generated positive strand RNA is then destined for packaging into immature virions to be used as a message template to synthesize additional viral proteins.

Non-structural (NS) proteins are highly conserved across flaviviruses. Their functions are summarized below.

- NS1 is a multifunctional protein. When present as a monomer it serves as a cofactor for viral replication. Within infected cells, NS1 is mainly present as a dimer that is associated with cellular membranes. [29] Within the trans-Golgi network complex sugars are removed from the intracellular NS1 dimer, which then forms a soluble hexamer that is secreted extracellularly.[29] Secreted NS1 is present at high concentrations, up to 15 µg/mL during acute infection and has been implicated in pathogenesis and immune evasion (see section 1.1.2).[30] NS1 specific antibodies have been associated with protective immunity (see section 1.1.3).[20,31]
- NS3 is an enzyme that aids in polyprotein processing. Specifically, the N-terminal domain functions with co-factor NS2B to aid in processing the viral polyprotein, while

the C-terminal domain functions as a helicase, separating RNA strands during replication. [20,32]

- NS5 serves two distinct functions: the N-terminal methyl transferase domain is responsible for viral capping while the C-terminal domain serves as an RNA-dependent RNA polymerase. [20,33]
- NS2A, NS2B, NS4A, and NS4B are all highly hydrophobic, membrane-associated proteins that assist in viral replication by localizing NS3 and NS5 to the membrane through protein-protein interactions. [20] These small NS proteins also interfere with host innate immune responses for example, NS2A inhibits the host interferon response through interactions with STAT1 and STAT2 and NS4A/NS4B modulate interferon signaling. [34,35]

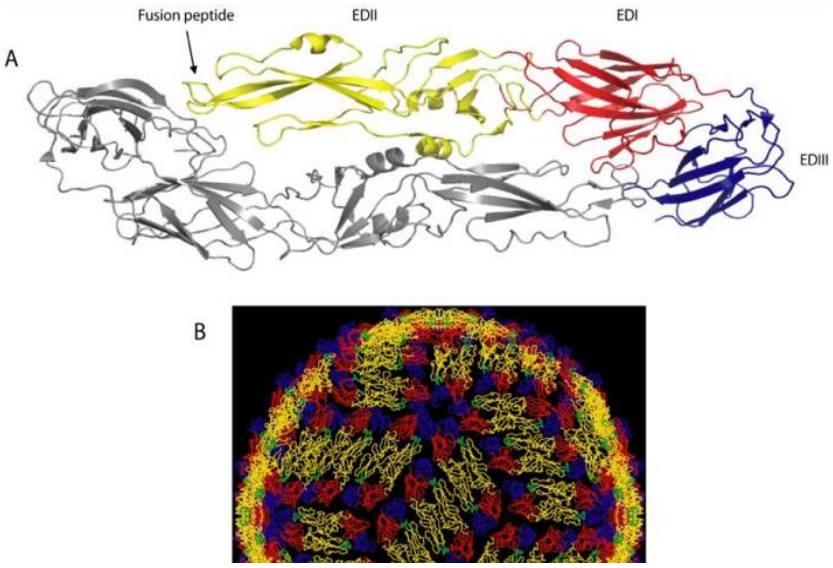

Figure 3 Flavivirus virion structure

A) Head to tail arrangement of two E monomers. EDI in red, EDII in yellow, and EDIII in blue. B) Arrangement of three homodimers making up a E protein raft on the surface of a flavivirus virion. [9] Figure published under Creative Commons licenses.

Structural Proteins

The viral genome encodes for three structural proteins: capsid (C) 11kD, envelope (E) 50kD, and premembrane (prM) 26 kD which is cleaved into secreted Pr (18 kD) and M (8kD) during viral maturation.[14] E covers the surface of the virion and mediates receptor binding and endosomal membrane fusion during infection. E protein consists of 3

domains: EDI, EDII, and EDIII. E monomers form head to tail homodimers and three E homodimers form a trimer raft that covers the surface of the virion. [36] In total, 180 monomers are organized into 90 tightly packed dimers and 30 trimer rafts that lie flat on the surface of the virion (Figure 3).

Virus maturation

Following viral replication, structural protein C interacts with viral RNA to become the nucleocapsid core. [37,38] PrM and E form a stable heterodimer anchored to the ER membrane. [38] These prM and E heterodimers along the ER membrane surround the nucleocapsid core to form immature virions (Figure 4). [38] Once assembled, these virions bud into the ER lumen as immature /non-infectious virions, that are bumpy/rough in appearance due to trimeric prM-E spikes in which E trimers are erect on the surface of the virion. [39] The presence of prM inhibits conformational changes to E that thereby prevent the fusion loop

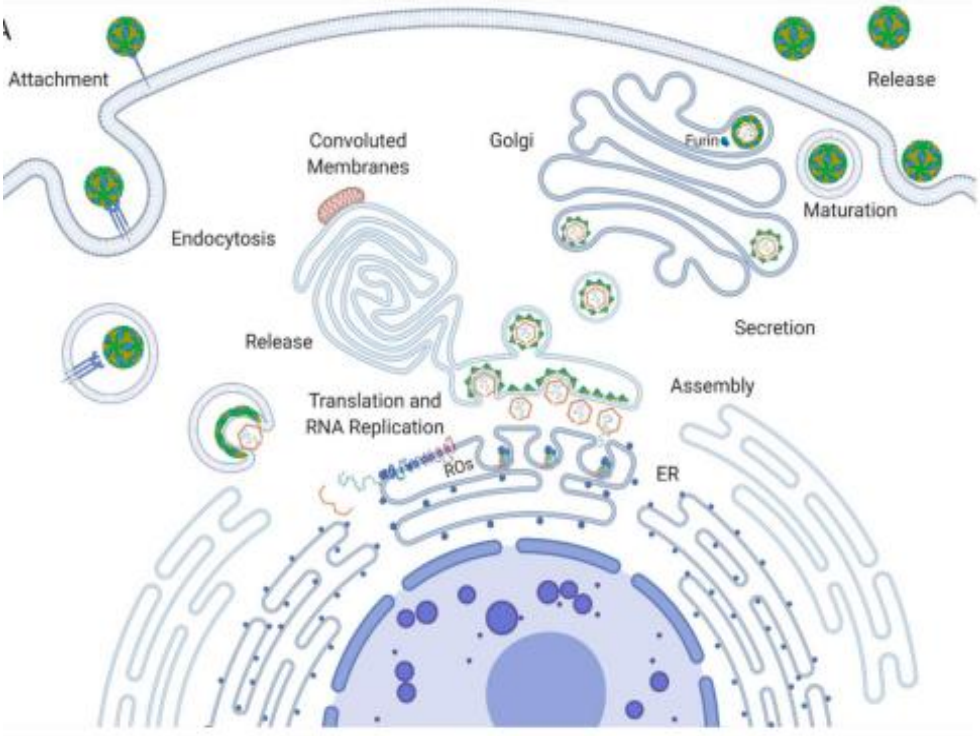

Figure 4 Flavivirus lifecycle

Figure from [1] published under Creative Commons licenses.

on the distal end of E from binding to host membranes during viral egress. As virions traffic through the secretory pathway encountering an increasingly acidic environment, E trimers undergo conformational changes. At low pH, E lays flat against the surface of the virion as homodimers, exposing a prM cleavage site for host protease furin. [39] This results in cleavage of pr, which disassociates from E upon entering a neutral pH environment. The resulting mature/infectious virions are then released by the host cell. [9,14] Cleavage of prM occurs with varying efficiency depending on virus type and host cell, with the greatest ratio of immature to mature virus particles occurring in DENV grown in vertebrate or mosquito cell culture. [9,14,40] Virus isolated from humans, grown in primary human cells, or in furin over-expressing cells contains fully mature virions. [40] The maturation state of virions produced in arthropod vectors remains to be determined. Viral maturation state can have a profound effect on the ability of immune sera, derived from natural infection or vaccination, to neutralize DENV. [30] The fusion loop as well as other conserved regions on E are exposed in immature virions but hidden on the surface of mature virions. Raut *et al*. hypothesize that the smooth surface of mature virions, without exposed fusion loop, results in reduced virus neutralization by cross-reactive antibodies or immune sera, which preferentially bind to epitopes present on the fusion loop. [8,41] This has important consequences for vaccine design. [39,40] The implications of this will be explored in section 1.1.3.

1.1.2 Flavivirus Pathogenesis

Flaviviruses cause a broad range of disease severity ranging from asymptomatic to severe, sometimes resulting in death. This wide spectrum of symptoms includes hepatitis, encephalitis, congenital abnormalities, and vascular shock as the result of tissue-specific tropisms. [15] These

viruses are pathogenic in humans and animals, affecting up to 400 million individuals globally each year, posing a serious public health risk to people who live in or travel to regions where flaviviruses circulate. [16] The majority of flavivirus infections (50-80%) are asymptomatic, with most symptomatic infections resulting in self-limiting febrile illness without long-term effects. A minority of individuals progress to more serious disease. Pathogenesis is an interplay between specific pathogenic effects caused by the virus itself and effects caused by the host response to infection, either as a result of an excessive innate or misdirected adaptive immune response.

Hemorrhagic flaviviruses

Dengue is the most common of all arboviral diseases, resulting in an estimated 400 million infections globally each year.[16] Dengue is caused by one of the four antigenically distinct serotypes (DENV 1- 4) which differ by 30 -35% in amino acid identity across the envelope protein. [42] DENV infection has a low fatality rate of <1% with early recognition and treatment. This rate can increase up to 20% if untreated. [43,44] Following the bite from an infected mosquito, DENV replicates first in Langerhans cells in the skin. The virus then spreads to the draining lymph node, rapidly replicates, and disseminates throughout the host circulatory system and target organs. DENV can replicate in a wide variety of cell types including keratinocytes, monocytes, macrophages, dendritic cells, endothelial cells, hepatocytes, and adipocytes. [44,45] Acute illness, if symptomatic, is characterized by mild undifferentiated febrile illness. DENV infection can progress to serious dengue, with or without warning signs. [44] Severe disease is characterized by plasma leakage, hemorrhage, and severe organ involvement including cardiac, liver, and central nervous system. [46] Warning signs include liver enlargement, decrease in platelet count, abdominal pain, and fluid accumulation which can occur in the lungs (pleural effusion) or the abdominal cavity (ascites). [47] Risk factors have been identified for the

development of severe dengue. These risk factors include prior dengue T-cell and B-cell mediated immunity, differences in viral and host genetics, and impairment or exacerbation of anti-viral immune response. [44] Peak symptom onset coincides with high levels of circulating pro-inflammatory cytokines such as tumor necrosis factor-alpha (TNF-α) and interleukin-6 (IL-6) which lead to increased endothelial permeability and vascular leak (more in *Innate immune response to flavivirus infection)*. [43,48] To help combat the heavy burden of disease, a DENV vaccine, Dengvaxia (CYD-TDV), is currently available in ~20 countries (see section 1.1.4).

Yellow Fever Virus (YFV) is the prototype flavivirus. YFV originated in Africa but spread to the Western world around 1648. [49] YFV has a fascinating history, and was once regarded as the most lethal and feared disease known to humans. The virus reemerged and is once again a disease feared by many. In 1881, Carlos Finlay hypothesized that YF was transmitted to humans by mosquitoes, however, it wasn't until the early 1900's that Walter Reed determined the causative agent of yellow fever was a filterable agent found in the blood of infected individuals that was transmitted by the *Aedes aegypti* mosquito. [50] Due to mosquito control efforts and the success of a YFV vaccine the virus was eradicated from North America and parts of the Caribbean. YFV has since re-emerged and is once again endemic in parts South America and Africa. [50] YFV replicates to high levels in hepatocytes in the liver, resulting in viral hepatitis, renal injury, myocardial injury, hemorrhage, and shock. Viremia is associated with fever, headache, chills, and myalgia. [18,20] In 20-60% of infected individuals, the disease progresses after viral clearance from the serum, in a period known as the period of intoxication. During this late stage, the virus replicates in hepatocytes, and symptoms such as jaundice, kidney failure, and hemorrhaging occur and this disease phase is strongly correlated with highly elevated levels of

pro and anti-inflammatory cytokines. [18,20] The case fatality rate for YFV infection is between 20-50%.[20,51]

Encephalitic flaviviruses

Japanese Encephalitis virus (JEV), first isolated in 1935 from a fatal case of encephalitis is the largest cause of epidemic encephalitis worldwide, affecting individuals that live in Asia, western Pacific countries, and northern Australia. [19,52] The case fatality rate is between 20-30% in humans with neurologic sequelae observed in 30-50% of infected individuals. JEV affects more than just humans: horses can also succumb to JEV encephalitis. Serological surveillance suggests that JEV infects a broad range of animals including pigs, raccoons, dogs, and wild boars. [52] The main transmission vector is *Culex* mosquito species with pigs and wading birds serving as the most common vertebrate hosts. [52] There are four types of approved JEV vaccines currently available which have greatly decreased the JEV disease burden (section 1.1.4).[53]

West Nile virus *(WNV)* is a neurological disease, similar to JEV. Humans are incidental hosts, however, clinical disease can still occur in both humans and horses. [35] Initial infection occurs in Langerhans cells in the skin following a bite from an infected mosquito. The infection then spreads systemically, resulting in primary viremia. WNV can spread to the central nervous system across the blood-brain barrier where it infects neurons in the brain and spinal cord. [35] As with other flaviviruses, most infections are symptomatic however, clinical disease ranges from febrile illness to serious encephalitis. Case mortality rates range from <1 - 17% based on age, with higher fatality rates observed in older individuals. [3] Greater than 50% of symptomatic individuals experience long-term neurological sequelae. [19] WNV is endemic in Africa, Asia,

Europe, and since its introduction to the United States in 1999 it circulates regularly in North America. [35] In the United States, WNV vaccines are currently available for horses however, no vaccine has been approved for human use yet (see section 1.1.4).

Tick-borne encephalitis virus (TBEV) is the most common arthropod-borne viral infection in Europe and central and eastern Asia, transmitted by *Ixodes* and Haemaphysalis *concinna* species of ticks. [23, 54] The main reservoir hosts are small mammals such as rodents, although vector species of ticks also feed on larger mammals such as deer and birds, which may also play a role in the transmission cycle. [23] The majority of infections, 70-98%, are asymptomatic. [55] The clinical spectrum of disease ranges from non-specific symptoms such as fever, headache, myalgia, and arthralgia. Of those who have symptomatic infections, up to 50% develop meningitis to severe meningoencephalitis with or without paralysis, and up to 50% of individuals suffer long-term sequelae. [55] Case fatality rates are subtype-specific, ranging from ~2% to upwards of 40%. [55] There are several TBEV vaccines available for human use including TICOVAC, which is approved in the US for high-risk individuals and laboratory workers. Since the successful induction of vaccine regimes, TBEV has declined substantially. In Australia, rates declined from 5.7 to 0.9 per 100,000 from 1972 to 2011[3] (see section 1.1.4).

Zika Virus (ZIKV) was originally identified in 1947 in the Zika forest in Uganda and is most commonly transmitted by *Aedes* mosquitoes. Historically, infections with ZIKV results in non-specific febrile illness. However, during the recent, explosive epidemic in the Americas (2015-2016), ZIKV infection was associated with more severe disease including congenital malformations and microcephaly in neonates infected in utero. [56] ZIKV can be isolated from the

blood, urine, saliva, and semen, sometimes months after infection. [44] ZIKV infects myeloid lineage cells, epithelial cells, neuroprogenitor cells, ocular tissues, as well as cells in the male and female reproductive tract. As with DENV, many ZIKV infections are asymptomatic. Clinical disease presents with rash, fever, arthralgia, myalgia, conjunctivitis, and fatigue. [57] Rarely, more severe complications have been linked to ZIKV infection, including Guillain-Barre syndrome (GBS), which occurs 1 in every 4000 cases. [44] ZIKV is unique amongst flaviviruses in that it can be transmitted sexually, during or after asymptomatic or symptomatic infection as well as vertically, causing injury to the placenta and developing fetus. [44, 56] Congenital ZIKV infection, which causes abnormalities to the developing fetus was one of the most concerning aspects of the 2015-2016 ZIKV epidemic. There is currently no available ZIKV vaccine, however, several are in development (Table 2).

Innate immune response to flavivirus infection

Host cells recognize and respond to flavivirus infection through several different pathogen recognition receptors (PRRs) including, cell surface, endosomal, and cytosolic sensors. Namely, endosomal PRRs Toll-like receptor 3 (TLR-3) which senses double-stranded RNA, TRL-7 which recognizes single-stranded RNA, and cytosolic sensor retinoic acid-inducible gene 1 (RIG-I) which senses cytosolic RNA. [15] Signaling through these sensors leads to the expression of type I and type III interferon (INF). [15] Type I INF is an important part of the innate immune response to flaviviruses as it induces IFN-stimulated genes (ISGs). INF is needed to restrict viral replication and dissemination *in vivo* and pre-treatment with type I INF inhibits flavivirus replication *in vitro*. [15] Flaviviruses can directly antagonize interferon responses through interactions between NS2A and STAT1 and STAT2. [56] Type I INF knockout mice (*Ifnar1-/-)* exhibit greater morbidly

and mortality than wild-type mice in response to flavivirus infection. [15] The role of cytokines expressed during acute infection have been implicated in vasculopathy observed in severe YFV infections and implicated in severe DENV infection. [22]

Non-structural protein NS1 implicated in tissue tropic pathogenesis

NS1 is conserved across flaviviruses, exhibiting a 60-80% similarity. [58] High levels of secreted NS1 have been associated with more severe disease including vascular leakage and increased endothelial membrane dysfunction (*in vitro*). This phenomenon has been recapitulated with NS1 alone and can be mitigated by treatment with polyclonal immune sera (containing NS1-specific antibodies), NS1-specific mAbs, or prevented by an NS1 vaccination in a mouse model. [31] Data supports that NS1 contributes to pathogenesis by triggering endothelial hyperpermeability, and activates TLR signaling both of which increase proinflammatory cytokines that contribute to vascular leak. [29,31] Additionally, NS1 has been shown to disrupt the endothelial glycocalyx, which correlates with plasma leakage that occurs during severe dengue disease. Tissue-specific barrier disruption has been observed in an *in vitro* model utilizing the trans-endothelial electrical

Table 1 Tissue specific NS1 effects.

Virus specific-NS1	Pulmonary cells	Dermal cells	Umbilical cells	Brain cells	Liver cells
DENV2	++	++	++	++	++
YFV	+	----	--	--	++
ZIKV	--	--	++	++	--
WNV	--	--	--	++	--
JEV	--	--	--	++	--

Based on data from [51] + indicates some level of barrier dysfunction observed following NS1 treatment. ++ indicates a high degree of barrier dysfunction observed following NS1 treatment. – indicates no observed barrier dysfunction following NS1 treatment

resistance (TEER) assay, which measures cell or tissue barrier disruption as a loss of electrical resistance. Physiologically relevant concentrations of NS1 triggered permeability in endothelial tissues associated with viral tropism for each of the following flaviviruses, DENV, YFV, ZIKV, WNV, and JEV (summarized in table 1). These effects can be specifically blocked *in vitro* with NS1-polyclonal immune serum or NS1-specific monoclonal antibodies. Mouse models have shown that NS1-specific antibodies can protect mice from lethal WNV challenge *in vivo*.[35] In addition, NS1 vaccination provided protection in mouse lethal challenge studies pointing out the importance of including NS1 in vaccine platforms. [48]

1.1.3 Flavivirus Adaptive Immunity and Immunopathogenesis

Flavivirus epitopes of importance were first discovered using panels of mostly mouse mAbs following infection or vaccination with E proteins (or E protein fragments), as well as whole virus. [59,60] Later human mAbs were isolated from naturally infected or vaccinated individuals.

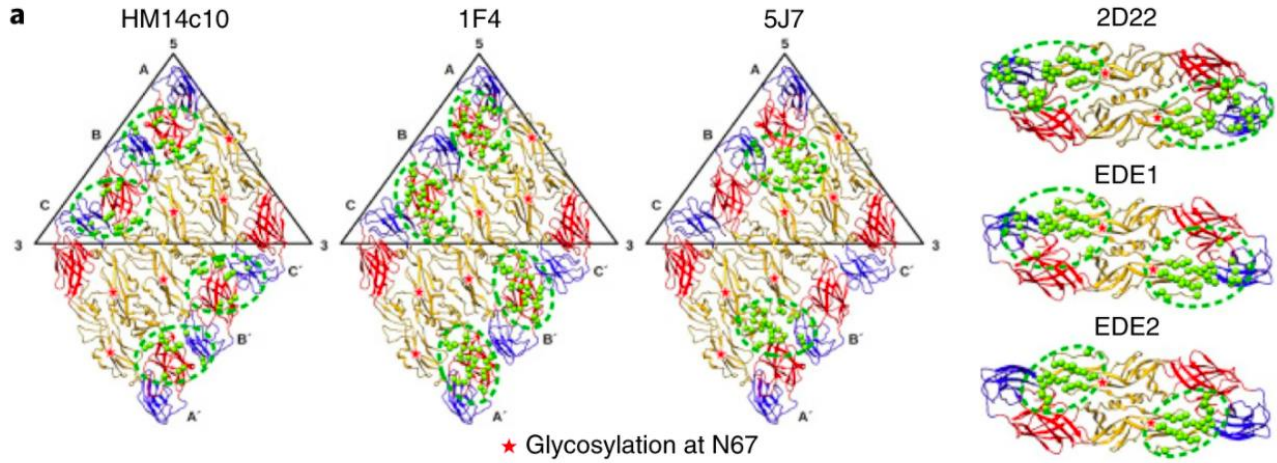

Figure 5 Flavivirus epitopes.

Epitope footprints representing flavivirus monoclonal antibody binding sites The green spheres represent the epitope residues and the dotted green lines outline the monoclonal antibody footprints. [8] Reprinted with permission.

[41,61-68] In order to directly neutralize infectious virus, an antibody must either block receptor

binding or disrupt conformational changes that are needed for membrane fusion. Epitopes identified as important for potent neutralization have been mapped to conformational/quaternary epitopes, that are only present on intact virions comprised of discontinuous segments of the E protein. Properties of neutralizing antibodies are summarized below (Figures 5 and 6).[69,36,62]

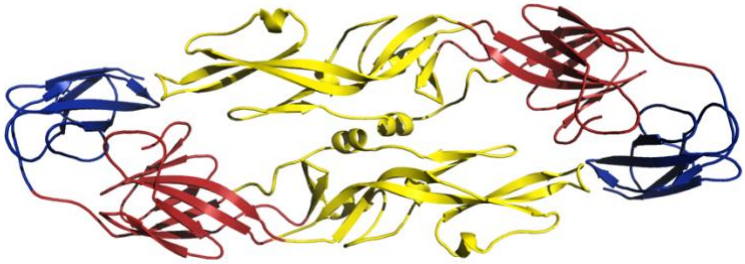

Figure 6 Ribbon diagram of E protein dimer.

EDI in red, EDII in yellow, and EDIII in blue. Ribbon diagram generated by William Messer. Reprinted with permission.

- E-dimer epitope (EDE) antibodies: as the name implies, these antibodies bind epitopes across multiple E dimers. These antibodies are potently neutralizing and can be type-specific or cross-reactive, broadly neutralizing all 4 serotypes of DENV, even providing protective effects outside of the serocomplex, neutralizing closely related flaviviruses such as ZIKV. EDE antibodies can bind to mature and partially mature virions. [8,70] 14C10 is an example of a potent type-specific monoclonal antibody that can bind to a discontinuous epitope that spans adjacent E protein dimers (Figure 5).[71]
- Quaternary epitope antibodies such as 2D22, a DENV-2 type-specific mAb, binds to a quaternary epitope formed by EDIII and EDII on two different monomers on a single E-homodimer.[72,73]
- EDIII antibodies: EDIII contains two main epitopes called the A strand and lateral ridge. In DENV infected mice, the lateral ridge of EDIII is the immunodominant epitope, however, in humans, EDIII antibodies represent a small fraction of the total neutralizing antibody response against DENV and WNV as serum depleted with EDIII beads retains

most of its neutralization potential. [62,74,75] High titers of EDIII antibodies have been identified following ZIKV infection in humans, suggesting that EDIII antibodies play an important role in protection in some flaviviruses, but not others. [76] EDIII antibodies specifically block at a post-attachment stage and are hypothesized to inhibit viral fusion. [35]

- EDI-EDII hinge: 1F4 and 5J7 are highly type-specific neutralizing antibodies that recognize quaternary epitopes on the surface of intact virions, not recombinant E protein. [67] 5J7 epitope footprint spans across three E protein dimers, while the binding site for 1F4 is on a single E monomer, but only present on whole virus. [8,67]
- Fusion loop epitope (FLE) antibodies: The fusion loop is not quaternary, but is the immunodominant antibody target in human immune responses following flavivirus infection. [41] The FLE is hidden within the E dimer on mature virions, but, exposed on the surface of immature or partially mature virions when prM is present. [77] The fusion loop is highly conserved across flaviviruses. FLE antibodies are highly cross-reactive and poorly neutralizing. [8,41]
- Anti-prM antibodies: A substantial proportion of antibodies and MBCs following DENV infection are directed towards prM. These antibodies are highly cross-reactive and poorly neutralizing in vitro and in vivo.[65,66,77]

T-cell responses to flaviviruses

CD4+ cells play a protective role in primary WNV, YFV, ZIKV, and JEV infection in mice. CD4+ cells are not required for controlling DENV infection (primary), but do contribute to viral clearance upon secondary infection or challenge following vaccination in mice. [15] In addition to

controlling primary infection, CD4+ T-cells also provide help to B-cells for improved antibody responses. T-cell epitopes have been mapped to most of the flavivirus proteome. Cytotoxic T-cells (CD8+) preferentially target epitopes within the non-structural proteins NS3, NS5, and NS4B, while CD4+ responses largely target the structural proteins and NS1. [8] This holds true for DENV, JEV, and YFV whereas T-cell responses to ZIKV appear to be directed towards the complete viral proteome, both structural and non-structural proteins, however, the majority of CD4+ and CD8+ cells recognize epitopes on structural proteins. [8] In mice, CD8+ T-cells have been shown to mediate protection against DENV and ZIKV, where depletion of CD8+ T-cells results in increased mortality. [8]

Immune involvement in pathogenesis

The high degree of sequence similarity across DENV serotypes as well as across different flaviviruses can be helpful or harmful, as it can either serve to boost protection or lead to further pathogenesis. Severe dengue, defined by the WHO, occurs in <1% of cases. However, the mechanism behind the development of severe disease remains only partially characterized and controversial. Severe dengue occurs more frequently upon secondary infection with a different serotype, indicating that existing immunity might play a role in disease enhancement. Excessive T-cell infiltration has been associated with increased pathogenesis during YFV and DENV infection in humans and contributes to neuropathogenesis in mouse models of JEV, ZIKV, and WNV infections. [8] Cytotoxic damage, mediated by CD4+ and CD8+ has been described following DENV and YFV infection. [8] CD4+ and CD8+ mediated cytotoxicity is important in early containment and control of flaviviral infection. However, excessive cytotoxicity can lead to tissue damage and cytokine storm that can result in increased disease

severity.[8] For example, during secondary DENV infections, memory T-cells from primary infections mobilize and exhibit higher avidity to the primary serotype of infection and skew the response to secondary infection including increased cytokine production and reduced degranulation. [8] T-cell responses correlate with disease severity in secondary infections in humans in which memory T-cells from the primary infection, can lead to increased pathogenesis through higher levels of inflammatory cytokines upon repeat infection with a different DENV serotype. [15] This has also been observed in mouse studies where mice were challenged with two different serotypes of DENV or DENV-immune CD8+ T-cells were adoptively transferred to mice prior to infection with a different serotype. In both cases, an increase in disease severity was reported. [78]

Infection with one DENV serotype is thought to confer lifelong protection against repeat infections with the same serotype. Early studies conducted by Albert Sabin in the 1950s, as well as more recent studies, concluded that homotypic protection is long-term, while cross-protection against heterotypic infection is only transient, lasting months to 2 years after primary infection. [79] In endemic regions, multiple serotypes often co-circulate, putting individuals at risk of heterologous secondary infection. [62] Repeat infections with different serotypes can lead to broader protection. But, prior flavivirus immunity is the highest risk factor to developing severe disease upon repeat or secondary infection. [80] This implies that the adaptive immune system and possibly waning antibody titers, play an important role. [81] Antibody-dependent enhancement (ADE) has been implicated as a contributing factor. ADE occurs when suboptimal levels of poorly neutralizing antibodies, such as anti-prM antibodies, facilitate viral uptake into non-permissive cells through binding to the Fcγ receptor. This has been recapitulated by adding DENV mAbs or DENV immune sera prior to infection in mouse models, non-human primate

(NHP) models, as well as observed in human cohort studies and babies born to DENV-immune mothers. [82-85] Antibodies that bind to prM or the fusion loop appear to play a large role in enhancing infection, *in vitro* although their role *in vivo* remains controversial and difficult to study. [68] Longitudinal studies in a large pediatric cohort in Nicaragua observed that E-specific antibody binding titers (as determined by inhibition ELISA) between 1:21 and 1:80 come with the greatest risk of severe DENV disease upon secondary infection. [83] The risk was lower in naïve individuals and those with high neutralizing antibody titers. [83] ADE across different flaviviruses is also a concern, especially in light of the recent ZIKV epidemic in the Americas, a region already endemic for DENV. Cross-enhancement between flaviviruses has not been observed in humans but is an ongoing concern. [86] Neutralizing antibodies, or most recently elucidated IgA antibodies, can inhibit enhancement [87,88] and might serve as a promising therapeutic treatment for ADE. IgA is the second most abundant antibody type behind IgG and are incapable of facilitating ADE because they fail to interact with the Fcγ receptor. The presence of neutralizing DENV-specific IgA antibodies has been shown to significantly decrease viral enhancement caused by both DENV immune serum and DENV IgG mAbs.[88] In addition, IgA plasmablasts are highly abundant during DENV primary infection, but not during secondary DENV infection, possibly indicating a protective, anti-inflammatory role for IgA specific antibodies. [88]

1.1.4 Flavivirus vaccines

Licensed vaccines exist for four flaviviruses, including JEV, YFV, TBEV, and DENV. [15] Licensed vaccines, as well as vaccines in clinical trials, are summarized in Table 1-2.

The YFV live-attenuated vaccine (17D) was developed in 1936 and all currently available YFV vaccines today are derived from this strain. [53] The 17-D vaccine is regarded as one of the most successful vaccines against a viral pathogen. [3] It is highly immunogenic, resulting in robust humoral, cellular, and innate immune responses and a single dose leads to robust, durable immunity in most individuals. [3,53] Because of these properties, the YFV backbone has been used as a vector for the expression of prM-E epitopes from other flaviviruses including JEV, DENV, WNV, and ZIKV.

Despite the efficacy of JEV vaccination, several formulations have been discouraged from human use or discontinued. Mouse brain-derived inactivated vaccines that were once largely in use were discontinued in 2005 due to limited immunogenicity and adverse symptoms. These were replaced with cell culture-derived and inactivated vaccines. [53] Live-attenuated vaccines exhibit better immunogenicity than inactivated, but there are concerns of virulence rebound. Chimeric JEV vaccines based on the YFV-17D backbone exhibit decreased immunogenicity. [53] Available vaccines depend on geographical region. These vaccines result in high rates of seroconversion however, vaccine-derived immune response wanes, especially in non-endemic regions where individuals are not subjected to antigen re-exposure (boosting). [89]

There are four available TBEV vaccines depending on geographic region. In all cases, the virus is grown in primary chicken embryo cells and then formalin-inactivated. [3,54] High seroconversion rates and persistence of neutralizing antibodies have been observed for all formulations.

While several WNV vaccines have been approved for horses, a human vaccine remains slow to develop. [90] Several vaccine candidates that are in early clinical testing include inactivated (Formaldehyde and hydrogen peroxide), chimeric (on YFV or DENV4 backbone), and DNA

plasmid expressing prM/E. There are several reasons for a lack of WNV vaccines for humans including safety concerns, difficulty in study design, lack of appropriate animal models and cost. Because of the low incidence rate it is also hard to evaluate vaccine efficacy by field trial. [3, 90] However, the increasing geographical distribution of WNV is putting greater human populations at risk. Therefore, developing a safe and effective WNV vaccine should be prioritized.

The first and only licensed DENV vaccine is Sanofi Pasteur's CYD-TDV (or Dengvaxia®). CYD-TDV has been licensed in approximately 20 countries. [91] CYD-TDV is a tetravalent DENV vaccine, containing prM - E from DENV 1-4 strains cloned into the attenuated YFV-17D background. [92] Because of this construction scheme, CYD-TDV does not contain DENV non-structural proteins. CD8+ specific responses are generated against the non-structural proteins, which in the case of CYD-TDV are YFV. Therefore DENV-specific CD8+ responses are not generated. [53] CYD-TDV failed to generate a balanced tetravalent response, with varied serotype-specific responses. The lowest observed response was against DENV-2, which had an efficacy of 9.2% in Thai school children. [53,91,93] The lowest efficacy and the highest risk of hospitalization was observed in children less than 9 years of age, and the lowest risk was observed in seropositive individuals. Therefore, the WHO determined that CYD-TDV should only be administered in endemic regions with at least an 80% seroprevalence and limited to individuals between 9 and 45 years of age who are DENV seropositive. [53,94-96]

Two additional DENV vaccines are in phase III clinical trials, both of these are live-attenuated tetravalent vaccines. The first was developed by the National Institute of Allergy and Infectious Diseases (NIAID) LATV, and the second was developed by Takeda pharmaceuticals (TAK-003) both vaccines are based on an attenuated DENV backbone. [91] LATV is a single-dose

live-attenuated tetravalent DENV vaccine created by removing a 30 nucleotide span in the 3' untranslated region of DENV. [53] This approach worked for DENV-1, 3, and 4; however, DEN2Δ30 was infectious to mosquitoes, only slightly attenuated in non-human primates, and caused DENV symptoms in naïve individuals (viremia, rash, and neutropenia). [91,97,98] Therefore, rDEN2Δ30 was abandoned as a vaccine antigen but it has since become an attenuated virus used in DENV human challenge studies. [99] Therefore, the DENV-2 component of the vaccine is a chimera with DENV-2 prM and E constructs on the attenuated DENV-4 backbone rDEN4Δ30 known as rDEN2/4Δ30. [91] Two versions of the LATV are currently in clinical trials in both endemic and non-endemic transmission settings. TV003 contains equal amounts of all four serotypes, and TV005 contains a higher amount of the DENV-2 component in an attempt to create a balanced and robust immune response against all 4 serotypes. [91]

TAK-003 is a two-dose live-attenuated tetravalent DENV vaccine on a DENV-2 backbone. DENV-2 16681 was passaged in primary dog kidney cells resulting in viral attenuation, a small plaque morphology, temperature sensitivity, limited replication in mosquito cell culture, and is attenuated in newborn mice. [100] The mutations mapped to regions outside of the structural proteins, the 5' non-coding region, and within NS1, and NS3. [100] This attenuated strain, DENV2-PDK-53, serves as the backbone with the structural proteins prM and E from DENV-1,3, and 4 swapped in to create attenuated chimeric viruses. Immunization with TAK-003 results in the development of a robust humoral and cellular immune response. [101] The lowest antibody titers were detected against DENV-4, which demonstrated a 33-77% seroconversion rate. [102] A second improves seroconversion to DENV-4 and in recent phase III trials in endemic

regions, a high vaccine efficacy was observed, 81% with a promising 95% efficacy against severe DENV disease resulting in hospitalization. [101]

The road to a licensed DENV vaccine has not been without controversy or challenges. Several challenges face vaccine developers, including high degrees of cross-reactivity between

Table 2 Summary of flavivirus vaccines. [3-5]

Virus	Vaccine	Platform	Protection or immune response	Current status
WNV	ChimeriVax	Chimeric with WNV prM-E and YFV backbone	Strong T-cell and neutralizing antibody response (>98% seroconversion), protected mice, hamsters, and NHPs against challenge.	Phase II
	WN/DEN4Delta30	Chimeric prM-E from WNV in attenuated DENV4 backbone	Strong immunogeneic response in mice, geese, and NHPs, seroconversion in >80% humans, 3 doses resulted in 96.5% seroconversion	Phase I
	HydroVax-001	Inactivated using hydrogen peroxide	Strong T-cell and antibody response as well as protected mice in challenge.	Phase I
	VRC-303	DNA plasmid vaccine expressing prM-E	Strong antibody and T-cell response in humans	Phase I
	HBV-002	Recombinant WNV subunit vaccine prM and truncated E	High titers of neutralizing antibodiesand protected mice, hamsters, and NHPs against challenge.	Phase I
DENV	Dengvaxia CYD-TDV	Tetravalent (prM-E from 4 DENV serotypes) on YFV-17D backbone		approved
	TV003	Tetravalent live-attenuated recombinant vaccine 30nt deletion in 3'UTR	Robust antibody and T-cell responses in 74% subjects	Phase III
	TAK003	prM-E of DENV1,3,4 on attenuated DENV2 backbone	Neutralizing antibody titers in naïve and immune individuals	Phase III
	TDENV-PIV	Tetravalent formalin inactivated virus produced in insect cells		Phase I
	DEN1-80E	Monovalent prM and truncated E	Indiced neutralizing antibody response that was modest and waned over time	Phase I
	TVDV	Encodes for prM-E for all 4 DENV serotypes	Induced poor neutralizing antibody response	Phase I
ZIKV	ZPIV	Formalin inactivated	Robust antibody response and protected against challenge in mice and NHPs	Phase I
	VRC-ZKADNA085-00-VP	Plasmid DNA exressing prM-E	against challenge	Phase I
	GLS-5700	Plasmid DNA expressing prM-E		Phase I
	mRNA-1893	mRNA encoding for prM-E	Neutraliing antibody response and protected in challenge in mice and NHPs	Phase II
YFV	17D	Live-attenuated virus (176 passages in chicken embryo tissue)	Highly immunogenic, single dose >98% seroconversion	Approved
	French neurotropic vaccine	Live-attenuated virus		Discontinued 1982
TBEV	FSME-IMMUN	Inactivated whole virus	3 doses plus boosters every 3-5 years, 100% seroconversion after 3rd dose and seropositivity persists for >5 years	Approved
	Encepur	Inactivated whole virus	3 doses plus boosters every 3-5 years, 100% serovonversion after 3 doses, persistant neutralizing antibody titers	Approved
	TBE- Moscow	Inactivated whole virus	2 doses booster after 1 year and every 3 years afterwards, 100% seroconversion after 3 doses, after 2 years 94% remain seropositive	Approved
	Tick-E-Vac	Inactivated whole virus	2 doses booster after 1 year and every 3 years afterwards, 88% seroconversion after 3 doses, after 2 years 84% remain seropositive	Approved
	EnceVir	Inactivated whole virus	2 doses booster after 1 year and every 3 years afterwards	Approved
	SenTaiBao	Inactivated whole virus	2 does okus annual boosters	Approved
JEV		Mouse brain derived	81-95% efficacy discontinued in 2005 due to causing devere acute dissemenated encephalomyelitis	Approved
	IXIARO	Vero cell derived inactivated virus	seroconversion rate that quickly wanes	Approved
	CD.JEVAX	Live-attenuated vaccine	>98% efficacy	Approved
	IMOJEV / THAIJEV	Live-attenuated chimeric on YFV-17D backbone	>95% seroconversion rate	Approved

closely related flaviviruses that share common geographical ranges. This can lead to difficulty in accurately determining flavivirus infection history. Additionally, the presence of cross-reactive antibodies from previous flavivirus exposures can complicate vaccine response and affect disease outcomes. The phenomenon of ADE has been shown mostly in the context of the 4 DENV serotypes, but concerns of the potential for ADE exist for related flaviviruses.

1.2.1 Alphavirus virology

Alphaviruses belonging to the family *Togaviridae* are small (~70nm) spherical, positive sense, single-stranded RNA viruses, enveloped in a host-cell derived lipid membrane containing the viral entry receptor binding proteins.[103] There are more than 40 known alphaviruses belonging to the *Togaviridae* family. Alphaviruses continue to emerge and re-emerge as a public health threat. Similar to flaviviruses, they are commonly transmitted to humans by mosquitoes. Alphaviruses can be classified into seven antigen complexes: including Eastern equine encephalitis (EEE), Western equine encephalitis (WEE), Venezuelan equine encephalitis (VEE), Barmah Forest (BF), Middleburg (MID), Ndumu (NDU), and Semliki Forest (SF) complexes.[104] Alphaviruses can also be broadly divided into two categories based on phylogenetic relatedness and disease manifestations: Old World alphaviruses largely reside in the SF complex and include chikungunya (CHIKV), Mayaro (MAYV), and Ross River (RRV) viruses, which cause arthritic disease; and New World alphaviruses, which include viruses in the EEE, WEE, and VEE

complexes that cause encephalitis in human and animal hosts. [103,104] The viral RNA genome is ~11.5 kb in length, capped on the 5' end and polyadenylated on the 3' end.[103, 105] Two open reading frames encode two polyproteins that are cleaved post-translationally by viral and host proteases into 4 nonstructural proteins, nsP1, 2, 3, and 4 (N-terminal open reading frame) and 3 major structural proteins, Capsid (C) and envelope proteins E1 and E2 as well as small cleavage products/peptides, 6K and E3 (C-terminal open reading frame) (Figure 7). [106] Non-structural proteins are involved in viral replication (see *viral replication*). Structural proteins are required for viral RNA packaging, capsid assembly, and budding, additionally envelope proteins E1 and E2 cover the surface of the virion and serve as the principal neutralizing antibody targets, as well as a target for non-neutralizing, but protective antibodies. [107] E2 is considered to be the major target of neutralizing antibodies; however, E1 also contains conserved, cross-reactive epitopes.[103,105] (see section 1.1.3).

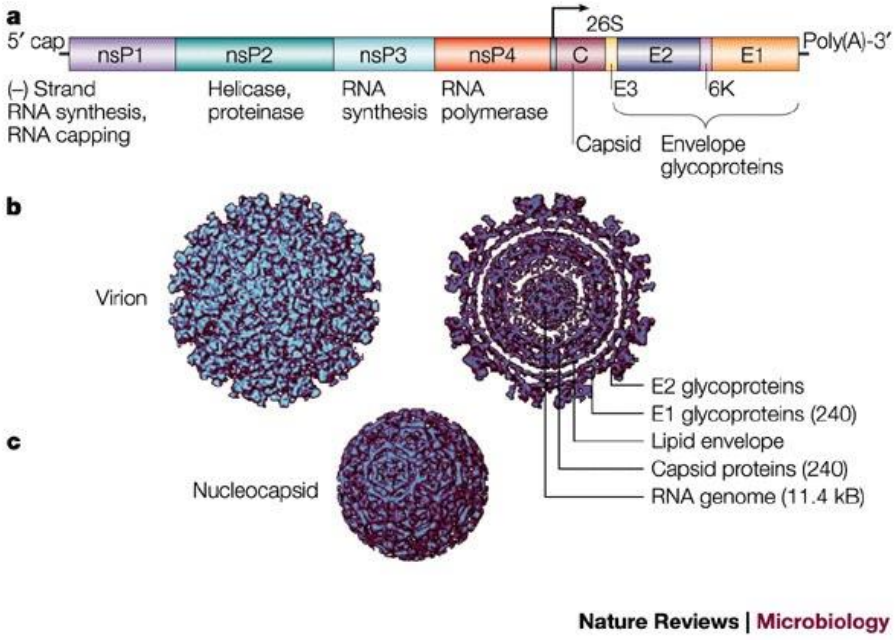

Figure 7 Alphavirus genome and virion structure
Figure reprinted with permission. [2]

Vector Hosts

Many emerging and re-emerging infectious viral diseases are transmitted by insect vectors. [44] Alphaviruses have a broad host range and they have been isolated from every continent except

Antarctica. [108] Similar to flaviviruses, the majority of alphaviruses are arthropod-borne, transmitted by mosquitoes with the ability to replicate in vertebrate and invertebrate hosts. [109, 110] There are some notable exceptions to this rule: salmonid viruses, salmon pancreas disease virus, and sleeping disease virus all affect fish and have evolved with no known vector host. [108,109] Southern Elephant Seal virus affects aquatic mammals, the likely vector is a seal louse, indicating the possibility that lice can also transmit specific alphaviruses. [109,111] Eilat and Tai Forest virus are examples of insect-specific alphaviruses that are unable to replicate in vertebrate cells. Alphaviruses can be maintained through several different transmission cycles.

- Sylvatic transmission cycles occur between non-human primates and tree dwelling mosquitoes with occasional spillover into humans. There is data to suggest a sylvatic cycle for CHIKV exists in Africa between forest mosquitoes and NHPs, although this is not supported in Asia or the Americas. [112] Evidence suggests MAYV exists in a sylvatic cycle in South America, the virus has never been isolated from NHPs; however, a large percentage of vertebrates are seropositive for the virus. [112]
- Enzootic transmission cycles occur between rodents or birds and mosquitoes with occasional spillover into susceptible human hosts. Alphaviruses such as VEE, RRV, and ONNV utilize this cycle for viral maintenance.
- Urban transmission cycles occur between human hosts and peri-domestic mosquitoes that reside nearby. The most common vector mosquitoes are *Aedes* and *Culex*. [108,113] CHIKV is the only currently known alphavirus that can utilize the urban cycle without the need for viral amplification in animal hosts.

Viral replication

Alphaviruses enter host cells through binding interactions between envelope protein, E2, and a host receptor. [110] Receptors that have been identified for alphaviruses include natural resistance-associated macrophage protein (NRAMP2) for Sindbis (SINV), and matrix remodeling associated protein 8 (Mxra8), which has been implicated as a cellular receptor for multiple Old World alphaviruses including CHIKV, MAYV, ONNV, and RRV. [114] Low-density lipoprotein receptor class A domain-containing 3 (LDLRAD3) has been shown to mediate entry for the neurotropic alphavirus VEE. [115] Once the virion enters the endosome the environment becomes more acidic triggering a conformational change that results in E2 being dissociated from the virion. [116] This disassociation allows domain II of E1, the fusion loop, to insert into the host cell membrane, fuse with the endosomal membrane and deposit viral nucleocapsid into the cell.[116] The released viral capsid then disassembles in the cytoplasm releasing the viral genomic RNA. As with flaviviruses, viral replication takes place within the cytoplasm. [110] The alphavirus genome contains two open reading frames (ORFs) are translated from two different mRNAs that are translated at different times during the virus lifecycle. [117] First, the genomic RNA, which encodes for the non-structural proteins (P1234) on the 5' end of the viral genome, is directly translated in a cap-independent manner. [117,118] Initiation occurs at an internal sequence in the 5' untranslated region known as the internal ribosome entry site (IRES). P1234 is cleaved to yield P123 and nsP4, which serve as an initial replication complex, that generates the negative-strand genomic RNA template. [106] Cleavage of P123 into P23 and nsP1 allows P23 to join with nsP4 to form a stable replication complex within membrane invaginations called spherules where negative-strand synthesis and genomic, positive-strand RNA synthesis takes place. [106] After complete cleavage of nsP1, nsP2, nsP3 and nsP4, negative-strand synthesis switches to positive-strand genomic and sub-genomic RNA (26S RNA) synthesis. [118] It is this 26S RNA that is the

template for structural polyprotein synthesis. Capsid (C), is autoproteolytically cleaved from the polyprotein and associates with newly synthesized viral RNA to form the nucleocapsid in the cytoplasm. [106,117] Specific functions of non-structural proteins are summarized below.

- nsP1 is important for capping and methylation of genomic and sub-genomic RNA species. It is also thought to play a role in anchoring replication complexes to the cellular membrane and pore formation. [106]
- nsP2 N-terminal half encodes RNA helicase activity and the C-terminal half contains cysteine protease structure and activity. [106]
- nsP3 contains three domains including an N-terminus macrodomain region that binds to and hydrolyzes ADP ribose moieties; a central alphavirus unique domain (AUD) and a hypervariable domain (HVD) with unknown roles in RNA replication and pathogenesis.[106]
- nsP4 is an RNA-dependent RNA polymerase and serves as the scaffold for other non-structural and host proteins involved in RNA replication.[106]

Structural proteins

The surface of the virion is covered in 240 copies of the E1 and E2 glycoproteins, which are present at a 1:1 ratio, along with the membrane-associated protein 6K. [109] 6K is essential for alphavirus virion assembly, important for transporting structural proteins to the plasma membrane, and promotes viral budding. [117] 6K is incorporated into virions in small amounts and has the ability to form ion channels and alter membrane permeability in mammalian and bacterial cells. [106] E1 is a fusion protein and consists of 3 domains. Domain I is present at the N- terminus located between domains II and III, the C-terminus lies within domain III and the fusion peptide is within the distal end of domain II (Figure 8). E1 monomers form a lattice on the virus surface at the base of the surface spikes. [106,109] E2 is responsible for receptor binding, it is long and thin with an exposed structure on top of the spike followed by a narrower stem region. The receptor attachment site is located near

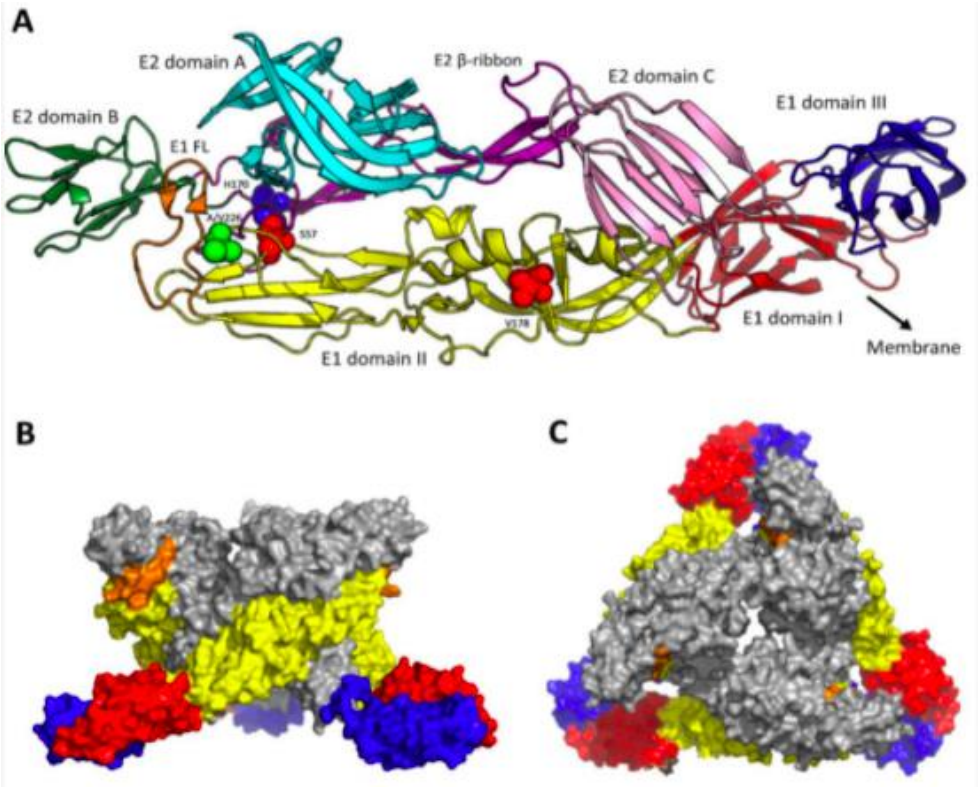

Figure 8 Structure of E1 / E2 heterodimer.

A) Ribbon diagram indicating the different ectodomains of E1 and E2 for CHIKV.B) Side view of one virus spike C) top view of on virus spike. For B and C E1 colors are the same as A, E2 is in gray. [10] Figure not altered, published under Creative Commons licenses.

residue 218. [109] E2 consists of three domains, A, B, and C. Domains A and B are responsible for receptor binding.[116] E3 is responsible for proper particle assembly, mediates spike folding and activation for viral entry and virus maturation.[109] The role for E3 appears to differ between alphaviruses.[106] It is found incorporated into Semliki Forest virus (SFV) virions, but not CHIKV or WEEV.[106]

Virus maturity/egress

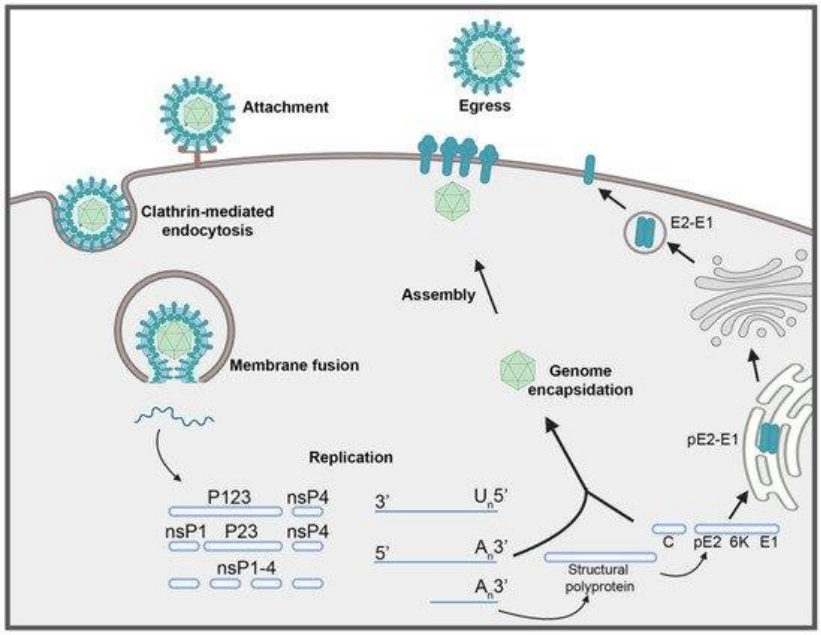

Figure 9 Alphavirus lifecycle

Figure [6] published under Creative Commons license.

During viral replication, E1 and the precursor membrane protein pE2 (precursor to E2 and E3) assembles in the ER. As the immature structural proteins traffic through the secretory pathway, pE2 is cleaved into E2 and E3 by host furin-like protease.[106,109] Low pH induces a conformational change between E1 and E2 that primes the fusion peptide for activation. These E1-E2 heterodimers are then transported to the plasma membrane where they self-assemble into 80 trimeric spikes on the virion surface.[109] Cleavage of E3 is needed for virions to become fusion competent, replacement or mutated pE2 that prevents cleavage results in non-viable virus.[109] Nucleocapsids bud into regions of the host membrane containing the envelope proteins, which promotes virion release (Figure 9).

1.2.2 Alphavirus pathogenesis

Old World alphaviruses cause acute fever, rash, malaise, fatigue, myalgia and arthralgia that may become severe and chronic.[119] Many New World alphaviruses cause severe or even fatal encephalitis. Infection is usually acute and often characterized by high-titer viremia, rash, and fever. Alphaviruses historically circulated in Africa, Asia, Europe, and Oceania.[120] However, human travel, viral adaptations allow for improved transmission, as well as increased range of susceptible vector mosquitos have resulted in outbreaks and the spread of alphaviruses into the Americas. CHIKV has the greatest range, with cases reported in over 100 countries worldwide (Figure 10), while CHIKV's monophyletic relative O'nyong-nyong (ONNV) causes large outbreaks that are limited to regions in Africa. RRV is endemic in Australia and several neighboring Pacific Islands. MAYV is native to and causes outbreaks in South and Latin America. New World alphaviruses circulate in North, South, and Central America. Different from Old World alphaviruses, these encephalitic viruses have a high fatality rate, 30-70% for Eastern Equine Encephalitis. Virus-specific pathogenesis is summarized below.

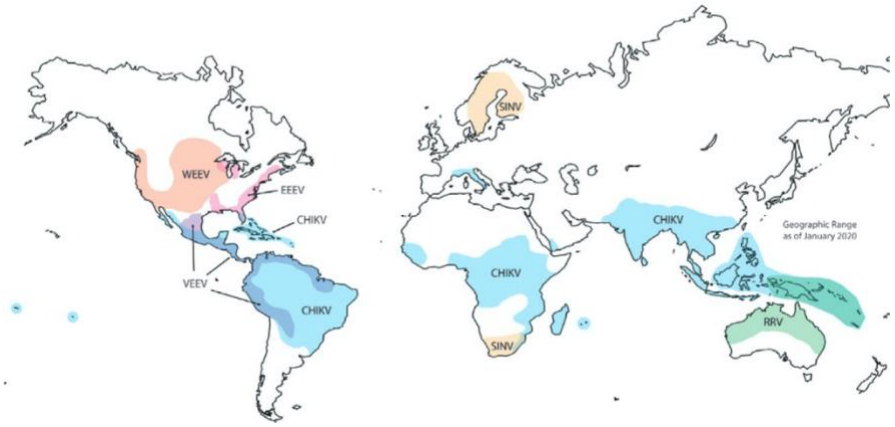

Figure 10 Worldwide distribution of clinically relevant alphaviruses
Figure reprinted with permission. [12]

Arthritogenic alphaviruses

Chikungunya virus (CHIKV) is part of the Semliki Forest virus complex. It was isolated in Tanzania in 1953. [108] Vertebrate hosts consist of humans and non-human primates in the urban cycle, although CHIKV can also be maintained in a sylvatic cycle between monkeys, rodents, birds, and forest mosquitoes in between epidemic periods. [119] The principal CHIKV vectors in the urban cycle are *Aedes aegypti* and *Ae. albopictus* mosquitoes. So far, CHIKV is the only alphavirus to emerge in an urban transmission cycle between humans and domestic mosquitoes with no need for amplification in reservoir hosts. [108] CHIKV historically circulated in regions of Africa and Asia, but in the mid-2000s, CHIKV emerged on a global scale, leading to large outbreaks in Africa and Asia, as well as the Caribbean and North, Central, and South America, resulting in almost 2 million human cases. [121] Chikungunya means "that which bends up" due to the extreme arthralgia this is characteristic of the disease. Acute CHIKV presents with symptoms very similar to DENV (fever, myalgia, rash and headache); however, reoccurring musculoskeletal disease, affecting peripheral joints, can persist for months to years following initial infection. [12, 119]

Unlike flavivirus infections, where most are asymptomatic, many CHIKV infections, upwards of 80% are clinically symptomatic. [12, 119] The very young and elderly are most prone to developing severe disease. High blood pressure, respiratory and cardiac complications are associated with more severe disease severity in adults. [122] Newborns are most susceptible to severe disease-causing myocarditis and meningoencephalitis, with high rates of post-infection neurologic sequelae that persists. [122,123] Overall CHIKV has a low, 0.1%, fatality rate, but the disease itself can lead to chronic disability that has a profound impact on people's lives. Persistent arthralgia has been reported in up to 81% of individuals. [44] Small joints like those in the fingers, wrists, ankles, and knees are most likely to be chronically affected. [12, 119] During

acute infection many pro-inflammatory cytokines are elevated and many of these remain elevated or even increase during convalescence (recovery phase). [12, 119] This suggests that the pathogenesis is mediated by the host immune response rather than directly by the virus. However, viral persistence does occur, with CHIKV detected 44 days post-infection in a monkey model, as well as antigen and RNA detected in macrophages up to 90 days post-infection in a non-human primate. [120] A wide variety of cell types can be infected including, monocytes and macrophages, dendritic cells, fibroblasts, endothelial cells, and muscle cells. [120] Arthritogenic symptoms can persist for up to 40 months. In one large cross-sectional study 1 out of 8 individuals experienced persistent joint pain 3 years after infection. [124]

Mayaro virus (MAYV) was isolated in Trinidad in 1954 and is mainly vectored by *Haemogogus* species of mosquitoes. Sporadic outbreaks are isolated to South America and the Caribbean where MAYV is endemic. [108, 119] MAYV is likely underdiagnosed or misdiagnosed as DENV since many of the symptoms overlap and there is a general lack of molecular diagnostics available to differentiate them. Monkeys are the main reservoir for MAYV, with humans serving as incidental hosts. Human infections occur, commonly in male forest workers, who enter areas where the virus is circulating in a sylvatic cycle. [44,119] Similar to CHIKV infection, clinical disease presents as an acute febrile illness with rash, headache, myalgia, and arthralgia. Persistent joint pain, in up to 80% of infected individuals, largely affects wrists, fingers, ankles, and toes and can persist for up to a year. [44,125] In the Brazilian Amazon, seropositivity rages from 5-60% and no deaths have been reported for MAYV. [44] MAYV is thought to be prone to human (re)emergence due to its ability to replicate in urban-associated mosquito strains as well.

O'nyong-nyong virus (ONNV) was isolated in Uganda in 1959 during a large epidemic that affected 2 million people in East Africa, although no fatalities were reported. [44,119] It was during this large epidemic that the virus was discovered and named after a word that translates to "the joint breaker."[44] Interestingly, it is transmitted by night-feeding mosquitoes *Anopheles funestrus* and *Anopheles gambia*e, which also transmit the malaria parasite. The main vertebrate host for ONNV is humans and outbreaks are currently limited to the continent of Africa and no other natural hosts or vertebrate reservoirs have been identified to date. [108,119] Asymptomatic to symptomatic infection ratio is ~1:2. The main clinical symptoms include fever and arthralgia. As with other arthritogenic alphaviruses discussed, chronic joint pain can persist in up to 80% of affected individuals. [44] ONNV can also cause eye and chest pains, headache, rash, and lymphadenopathy, which is reported in 40-50% of cases and has been suggested as a distinguishing symptom. [44,119] Since the large outbreak in the late 1950s no clinical cases of ONNV were reported until 30 years later, indicating that immunity from prior infection serves to protect against reinfection. Very high infection rates have been observed in susceptible populations of up to 68% of individuals localized in the outbreak areas. [44]

Ross River virus (RRV) is part of the Semliki Forest virus complex, RRV was isolated in Australia in 1959 and is mainly vectored by *Culex* and *Aedes* mosquito species. Rodents, kangaroos, and wallabies serve as the main vertebrate hosts, although horses, possums, and flying foxes can also play a role in maintaining RRV in nature. [119,126] RRV is endemic to Australia and the neighboring Pacific Islands. [108] It is the most common arbovirus that affects humans in Australia, with ~4,600 cases each year. [44,119] Many RRV infections remain asymptomatic, with the asymptomatic to symptomatic ratio between 1.2:1 and 3:1. [126] In rare

cases, RRV can cause splenomegaly, hematuria, glomerulonephritis, neck stiffness, and photophobia. [119] Typical disease presentation includes polyarthralgia or polyarthritis, which usually resolves within 3-6 months with no long-term sequelae. Immunity to RRV appears to be lifelong with no reports of repeat infections. [44] Although adaptive immunity is responsible for protection against repeat infection, it is thought that rheumatic disease can arise from adaptive and innate immune responses to RRV (see section 1.2.3).

Una virus (UNAV) was first isolated in Brazil in 1959. UNAV is most closely related to MAYV. [127] UNAV is widely distributed in South America and is predominantly vectored by *Psorophora* and *Aedes* species of mosquitoes. UNAV can infect humans; however, it is not associated with known clinical disease. UNAV has been isolated from dead or febrile horses in Argentina[108, 125,] and antibodies against UNAV have been detected in birds, horses, and to a small extent humans. [128] Little is known about the transmission cycle or natural hosts both vertebrate and invertebrate. [127]

Encephalitic alphaviruses

Venezuelan equine encephalitis virus (VEEV) was isolated in Venezuela in 1938. [2] It was first recognized as a disease affecting horses, donkeys, and mules. It was not until the 1950's that VEEV was recognized as a causative agent of human disease. [2] VEEV is vectored by *Aedes*, *Culex*, and *Psorophora* mosquito species. The principal vertebrate hosts are rodents, horses, and humans and the virus circulates in South and Central America, with occasional outbreaks in North America. [2,108] Acute symptoms include fever, headache, myalgia, and ocular pain, which can progress to encephalitis with convulsions, seizures, and coma. VEE long-term symptoms

include chronic and reoccurring headaches, depression, seizures, paralysis, and intellectual disabilities.[12] VEEV disease course ranges from asymptomatic to rapid death. The fatality rate in humans is <1%, however, neurological disease presents in 14% of infected individuals. The virus enters the skin via a bite from an infected mosquito where it is taken up by dendritic cells that traffic to the draining lymph node where the virus replicates in lymphoid tissues. [129] Systemic replication and viremia lead to the virus infecting the olfactory neuroepithelium and entering the central nervous tissue. [129]

Eastern equine encephalitis virus (EEEV) was first identified in North American horses in 1831 and in 1938 the first human case was reported. [130] EEEV is mainly transmitted by *Culiseta melanura* mosquitoes and mostly circulates in birds in an enzootic cycle. [131] Transmission to humans usually requires *Culex* or *Aedes* mosquito species to create a "bridge" between infected birds and humans or horses. [131] Humans and horses are considered dead-end hosts, although infection can still lead to clinical disease. EEEV is considered North America's most severe arboviral encephalitic disease, where outbreaks occur sporadically in areas of the Mid-Western United States and along the Atlantic and Gulf coast. [130] EEEV has a high mortality rate of greater than 30%. [131] More than 50% of those that survive the infection suffer from chronic persistent neurological deficits. [12,131]

Western equine encephalitis virus (WEEV) was first identified in North American horses in 1930 and in 1938 the first human case was reported. [130] WEEV is found in both North and South America. The principal hosts are house sparrows and *Culex* mosquitoes. During times of high transmission, WEEV can also utilize *Aedes* species of mosquitos as vectors. [132] Infections are

commonly asymptomatic, although neurological sequelae has been described for individuals recovered from WEEV infections including decreased motor skills, intellectual disabilities, and impaired speech. [12] WEEV causes encephalitis in horses and humans, although they are considered dead-end hosts and this virus appears to be the least fatal of the New World encephalitic alphaviruses to horses, with the case fatality rate ranging from 10-50% in horses and 3-15% in humans. [132] In recent years, there has been a large decrease in confirmed WEEV infections both in terms of human and horse outbreaks as well as detection in mosquito pools. [132]

1.2.3 Alphavirus immunity and immunopathogenesis

Studies of innate immunity to alphaviruses have demonstrated the importance of type I interferon (INF) in promoting viral clearance; however, INF alone is inadequate to completely clear virus from tissues. This observation supports the claim that adaptive immunity plays an important role in complete viral clearance and protection. [133] Studies have shown that antibody-based protection against alphavirus infection in animal models. Passive transfer of CHIKV immune sera protects mice from lethal challenge, CHIKV and MAYV mAbs have been used therapeutically to reduce viral burden and clinical disease, and several CHIKV vaccine candidates induce neutralizing antibody responses that have limited viral burden and clinical disease in mice and NHP models. [121]

Innate immune response

Alphavirus RNA triggers pattern recognition receptors (PPRs) such as Toll-like receptor (TLR) 3 and 7 (endosomal sensors) as well as cytoplasmic sensors (RIG-I and MDA5) which activate downstream adaptor molecules and ultimately induce type-I interferon (INF) antiviral response. [57]

[134,135] Type I INF is associated with control of infection and is the first barrier to viral infection and dissemination. [135,136] IFN induces an antiviral response in infected cells, as well as neighboring cells through the expression of IFN-stimulated genes (ISGs). [135] Mice deficient in INF, are highly susceptible to infection with multiple alphaviruses that result in quick virus-induced demise. [136]

Infected individuals have high levels of circulating cytokines and chemokines, including several pro-inflammatory cytokines such as IFN-α, INF-γ, IL-6, and anti-inflammatory cytokines such as IL-1, IL-4, and IL-10. [136] CCR2+ monocytes have been implicated in footpad swelling in mouse models, and also in preventing excessive inflammatory pathologies and resolving CHIKV-induced inflammation. [136] Infections in CCR2 defective mice leads to neutrophil infiltration and cartilage damage. [136] In response to New World alphavirus infection proinflammatory genes are upregulated as well as upregulation in TLR signaling that correlates with a disruption of the blood-brain barrier. [136]

T-cell response to alphavirus infection

T-cells contribute to alphavirus protection during VEEV, RRV, and CHIKV infection, by mediating viral clearance from the central nervous system and muscle tissues. [12] Both, CD4+ and CD8+ secrete INF-γ locally to help control the virus. [12] Mice lacking CD4+ are able to control viremia and clear CHIKV from infected tissues as well as generate a neutralizing antibody response, albeit with lower titers than WT controls. [137,35,] This suggests that T-cell independent B-cell activation can occur, but whether this response is long-lived remains to be seen. [138,139] Data suggests that CD4+ cells play a protective role in VEEV infection in mice as well as protect against viral infiltration into the central nervous system during SINV infection. [129] Depletion of

CD8+ T-cells, but not CD4+ T cells reversed protection offered by a targeted T-cell CHIKV vaccine in mice. [137] Vaccinating mice with CD8+ T cell epitopes alone prevented CHIKV disease, indicating an important role for CD8+ T-cells in CHIKV protection. [137] This point should not be overlooked during vaccine development.

Antibody-mediated protection and specific important epitopes

The role of protective antibodies has been well studied in animal models as well as in immune individuals. Passive transfer of alphavirus antibodies protects against challenge with WEEV, SINV, VEEV, CHIKV, RRV, and SFV, in various animal models including mice, guinea pigs, and rabbits. [138] Various mouse models that lack B-cells have shown persistent viremia for CHIKV (> 1 years) and SINV, indicating the importance of B-cells and the resulting antibodies in viral clearance from peripheral blood as well as the central nervous system. [138] The receptor-binding envelope protein E2 is the predominant target for anti-CHIKV antibody responses. [105, 140] Neutralizing antibodies against E2 have been identified following Old World and New World alphavirus infections. [138] Non-neutralizing antibodies have been shown to bind to E1, but these more limited responses can also confer protection against disease. [138] The antibody response appears to be targeted towards both linear and complex epitopes. [105] Specific immunodominant protein domains and subunits that contain epitopes recognized by potently neutralizing antibodies are summarized below.

- B domain of E2 (E2B) – The E2B domain is a critical target for neutralizing antibodies in mice and humans. [140] It is a conserved epitope that is recognized by broadly neutralizing antibodies and a primary mediator of neutralizing antibodies. [116]

- Domain II on E1 (EI DII) – This epitope is located within the fusion peptide. Monoclonal antibodies that bind EI DII are protective against Old World (CHIKV and MAYV) and New World (VEEV, EEEV, and WEEV) viruses. Antibodies that bind to this epitope are weakly neutralizing but highly protective by blocking viral egress from cells and inducing phagocytosis in an Fc effector-dependent manner (depending on particular mAb).[116]

Cross-reactive immunity across alphaviruses

There is a high degree of cross-reactivity among alphaviruses within the same antigen complex. This effect is largely due to a high degree of similarity/conservation in the E2 glycoprotein. E2 similarity ranges from 54-82% within alphaviruses in the SF complex, with slightly higher similarity in the E2B domain, a highly conserved region within the SF complex.[125]

A large body of literature indicates cross-reactive neutralizing antibodies may limit the (re)emergence of closely related alphaviruses.[141] CHIKV immune serum and CHIKV-specific mAbs limit MAYV and ONNV disease in mice, CHIKV human immune serum neutralizes MAYV and ONNV virus *in vitro*; neutralizing antibodies alone mediate protection.[141,142] CHIKV immune sera weakly neutralizes distantly related RRV, but even so, can greatly reduce magnitude and duration of RRV-induced musculoskeletal disease in mice, indicating that preexisting alphavirus immunity might mitigate and lessen disease severity during secondary infection.[121]

Immune involvement in pathogenesis

In contrast to flavivirus infections, non-neutralizing antibodies are not broadly thought to cause increased disease pathogenesis through antibody-dependent enhancement (ADE). [143] However, there are several papers describing enhancement during RRV infection, indicating that RRV can enter and replicate within monocytes and macrophages *in vitro*, in the presence of sub-neutralizing concentrations of RRV immune sera, but not related Barmah Forest virus immune sera. [144,145] Another study reported enhancement of CHIKV *in vitro* and in a mouse model. [146] Enhanced attachment was observed in primary human cells (monocytes and B cells) and increased replication was observed in mouse monocytes/macrophages. Blocking Fc gamma receptors negated these effects. Higher viremia and worsened arthritis were observed in mice with passive transfer of sub-neutralizing concentrations of CHIKV-immune sera. [146]

Some studies suggest that T-cells are the cause of persistent arthralgia in CHIKV infection. Others attribute increased pathogenesis and chronic symptoms to viral persistence, persistence of viral RNA that leads to long-term immune activation, and host-specific immune responses that lead to chronic joint pain. [147,148]

Mouse studies using severe combined immunodeficiency (SCID) mice that lack B and T cells have shown improved survival and higher viremia, experiments with nude mice that lack T cells show improved survival and do not develop spinal cord lesions as a result of VEEV infection. [12] Both indicate that T cells play a pathogenic role but individual or combined contributions from CD4+ and CD8+ have not been elucidated. [12] T cells have been observed to play a role in inducing CNS pathology in SINV infection in mice. SCID mice have 100% survival and minimal neuropathology even with high levels of viremia. [12] CD4+ cells have been implicated as a contributor to join inflammation in CHIKV infection in mice and mice lacking CD4+ cells have less inflammation. [137] The same effects have not been observed with CD8+

cells. [137] Why some individuals develop severe disease and persistent joint pain while others do not remains to be fully elucidated.

1.2.4 Alphavirus vaccines

Available vaccines

There are currently no licensed alphavirus vaccines approved for widespread human use. However, there are licensed vaccines approved for horses and humans at high risk of exposure. Combination vaccines for EEEV, WEEV, and VEEV are approved for use in horses; and a live attenuated VEEV vaccine, TC-83, is approved for use in people at high risk of exposure. [12] It is also approved for use in horses in Mexico and Columbia, but not in the US. Vaccination with TC-83 comes at a large environmental risk as the live-attenuated vaccine virus has been isolated in mosquitoes following a large immunization event in the US. [129] In addition, vaccination with TC-83 is reportedly teratogenic, leading to hydrops fetalis and fetal demise if administered during pregnancy. [149] Vaccine response is poor in some individuals, following vaccination, 80% of vaccinees have detectable antibody titers above the limit of detection, however, antibody titers decline rapidly, requiring frequent boosters for antibody maintenance. [129,150] Inactivated VEEV vaccines are also available and approved for use in horses. Formalin inactivated TC-83 called C-84 is approved for use in horses in the US. [129] There are several VEEV vaccines that are currently in pre-clinical or phase I status, including live-attenuated, inactivated, chimeric, and subunit vaccines. [129] No human WEEV vaccine is licensed; however, a formalin-inactivated vaccine is available for horses and is generally administered yearly due to lack of robust and durable immune response. [132] Current means of protection for alphaviruses without available vaccines relies on personal protective measures (long sleeves/pants, mosquito netting, and insect repellant) and mosquito control. There are many alphavirus vaccines currently in early pre-

clinical testing (mouse models) and late pre-clinical testing (NHP models), while a minority are currently in clinical trials with humans. These vaccines will be summarized in Table 3.

The development of alphavirus vaccines

The first attempts at a CHIKV vaccine were in the 1960s following a large epidemic in Thailand. One formulation was derived from a suckling-mouse brain-derived virus inactivated with formalin. This resulted in neutralizing antibody responses in mice. [151] Around the same time a cell culture-derived virus inactivated by UV or formalin was also tested in a monkey model. Both early vaccines resulted in neutralizing antibody responses although studies indicated that UV inactivation of virus preparations lead to a superior immune response, no additional work was reported for this approach. [151] More early work was performed at Walter Reed, where a systematic characterization of vaccine preparations in different cell types was performed. Through this early work, it was determined that growing virus in African green monkey cells provided the highest antibody titers. The virus was formalin-inactivated and found protective against challenge with 4 different CHIKV strains in both mice and monkeys. [151] From this early work, an attenuated vaccine strain 181/25 was developed at Walter Reed in the 1980s.[151] This attenuated strain was developed by 18 plaque to plaque passages of the parent strain (obtained from a human serum sample in Thailand). While this attenuated strain showed reduced viremia in monkey and mice challenge models and was approved for phase 1 clinical trials, development efforts were halted in 1998. The attenuated strain was further studied and has since been deemed unsafe as a vaccine option as only a few mutations are responsible for the attenuation and reversions can happen in mice and humans. [151] Since the reemergence of CHIKV in the early 2000s, developing a safe and effective CHIKV vaccine has once again gained the interest of

vaccine developers. In addition to safety, a CHIKV vaccine should elicit high levels of neutralizing antibodies, provide durable immunity and be easy to produce. Several options are in the pipeline including virus-like particles (VLPs), live-attenuated vaccines, chimeric viruses on several different virus backbones (Measles, vaccinia, adenovirus, VSV, and alphavirus), subunit vaccines, and DNA vaccines. Many CHIKV vaccines are currently in pre-clinical (animal models) and phase I and II clinical trials, these are summarized in Table 3. [104]

Two CHIKV vaccines are in phase II clinical trials. One is a CHIVK VLP vaccine produced from a CHIKV E3-E2-6K-E1 construct inserted into a CMV expression plasmid that is expressed in 293-T cells. [152] The VLP is not infectious and has been shown to induce neutralizing antibody titers. Interestingly, in a phase II trial that followed 400 subjects for 72 weeks post-vaccination, it was determined that 20% of the subjects enrolled were seropositive at baseline. These subjects exhibited a differing immune response to vaccination compared to seronegative subjects. Follow-up studies are being conducted to further investigate this finding. [152]

The most advanced alphavirus vaccine in development so far is the Vero cell culture-derived RRV vaccine, in phase III human trial studies. [138] The vaccine was shown to be safe and induce immunogenicity. Specifically, 3-doses of the vaccine were shown to generate neutralizing antibody titers above the threshold associated with protection. Despite this success, the vaccine was deemed non-financially viable and efforts to further develop the vaccine have stopped. [138] With the emergence and re-emergence of arboviruses in recent years safe and effective vaccines are greatly needed.

Virus	Vaccine	Platform	Protection or immune response	Current status
CHIKV	VLA1553-301	Live-attenuated	Neutralizing antibody response	Phase I
	CHIKV BBV87	Inactivated	Neutralizing antibody response observed in mice	Phase I
	VRC-CHKVLP059-00-VP/PXVX0317 (CHIKV VLP)	VLP	Neutralizing antibody response	Phase II
	VAL-181388	mRNA	Neutralzing antibody response	Phase I
	mRNA-1944	mRNA	Neutralzing antibody response in all subjects	Phase I
	MV-CHIKV	Chimeric measles based	Neutralizing antibody response	Phase II
	CHIK001	Chimeric Adenovirus based	ND	Phase I
RRV	Vero cell culture-derived whole virus RRV vaccine	Inactivated	Neutralizing antibody response, GMT 0-85	Phase III
VEEV	V3526	Live-attenuated	Neutralizing antibody response in NHP	Phase I
	VEEV CO	DNA plasmid	Neutralzing antibody response	Phase I
EEEV	TSI-GSD-104	Formalin inactivated	Neutralizing antibody response (PRNT>40) in 84% individuals after 2-doses	Phase II
WEEV, EEEV, VEEV	VRC-WEVVLP073-00VP	Trivalent VLP	Neutralizing antibody response in NHP	Phase I

Table 3 Summary of alphavirus vaccines currently in clinical trials. [2,7]

1.3.1 Coronavirus virology

Coronaviruses, which belong to the family *coronaviridae*, are named so because of the virion's characteristic fringe-like projections that look like a solar corona. [153] Coronaviruses are enveloped viruses with a large positive-sense RNA genome, the largest RNA genome characterized at ~30 kb (Figure 11). [154] Virions are spherical in shape and approximately 125nm in diameter. [154] This diverse group of viruses can infect a wide variety of animals including pigs, cows, dogs, cats, elk, deer, and camels. Coronaviruses can be grouped into 4 genera based on phylogeny: alpha, beta, delta, and gamma. [154] Four human coronaviruses, including alphacoronaviruses HCoV-229E and HCoV-NL63 and betacoronaviruses HCoV-OC43 and HCoV-HKU1, have circulated globally for decades and are endemic in human populations. These common cold coronaviruses are responsible for 15-30% of respiratory tract infections

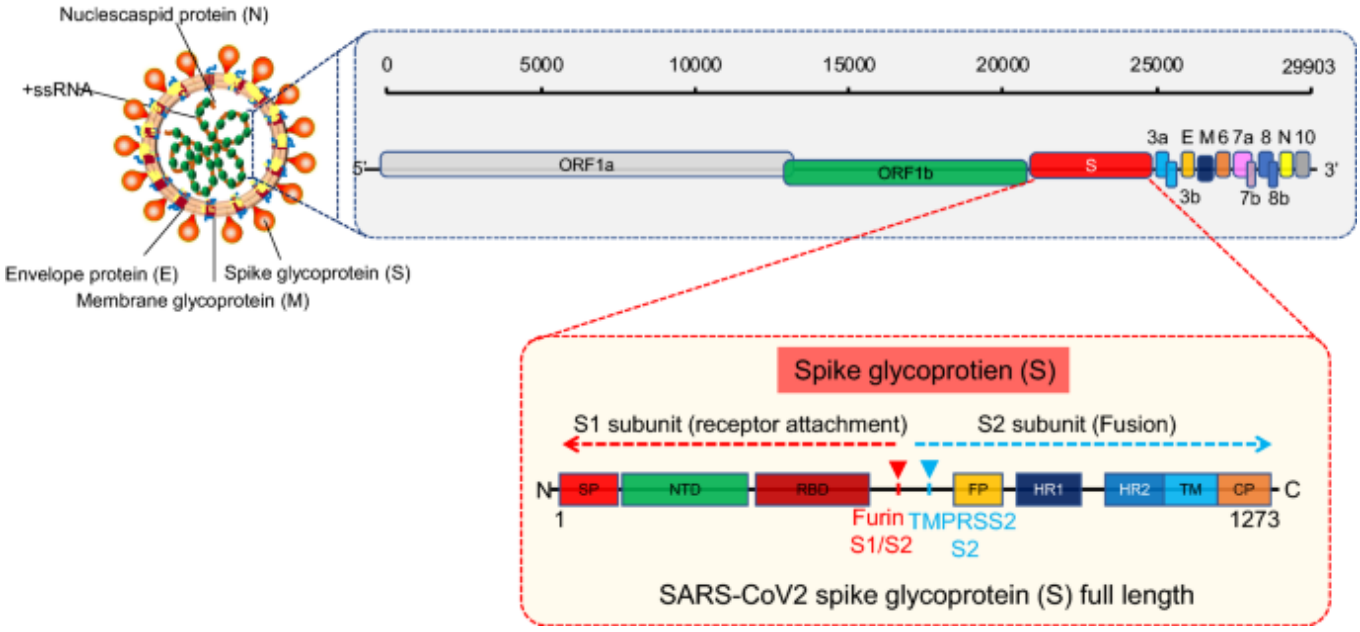

Figure 11 Schematic representation of the SARS-CoV-2 genome, structure, and different domains within the S protein.

Figure from [7] published under Creative Commons licenses.

yearly. [154,155] In certain populations such as the elderly, young children, and immunocompromised, these human coronaviruses can result in severe, life-threatening diseases

such as pneumonia and bronchiolitis. [155] Alpha and betacoronaviruses only affect mammals, causing respiratory disease in humans and gastroenteritis in mammals. [156,157] Gamma and Deltacoronaviruses mainly infect birds. [156]Notable animal coronaviruses include porcine transmissible gastroenteritis virus, porcine enteric diarrhea virus (PEDV), and swine acute diarrhea syndrome coronavirus (SADS-CoV). [156] Several betacoronaviruses have become infamous due to their highly pathogenic nature. For example, severe acute respiratory syndrome coronavirus (SARS-CoV) emerged in 2003, in 2012 Middle East respiratory syndrome coronavirus (MERS-CoV), and most recently, in late 2019 SARS-CoV-2 emerged. SARS-CoV-2 has caused an unrivaled global pandemic, to date causing 355 million infections and 5.6 million deaths (WHO, January 25th, 2022).

Route of transmission

Transmission of human coronaviruses occurs through close contact with infected individuals through respiratory secretions, mostly respiratory droplets, and to lesser extent aerosols, such as through coughing or sneezing. [158,159] In animals, the route of infection can also extend to fecal-oral and foodborne routes. [160] Respiratory secretions enter mucosal surfaces directly or alternately by touching a contaminated surface and then touching the mouth, nose, or eyes. [7, 158,159] Precautions such as social distancing, wearing a mask if unable to socially distance, and washing hands effectively reduce transmission. [158]

Cellular infection

The viral genome encodes 27 proteins and contains a 5’ cap and 3’ poly-A tail that allow for direct translation of replicase proteins. [154] The first two-thirds of the genome encode non-structural proteins, while the remaining one-third encodes structural and accessory proteins. [154]

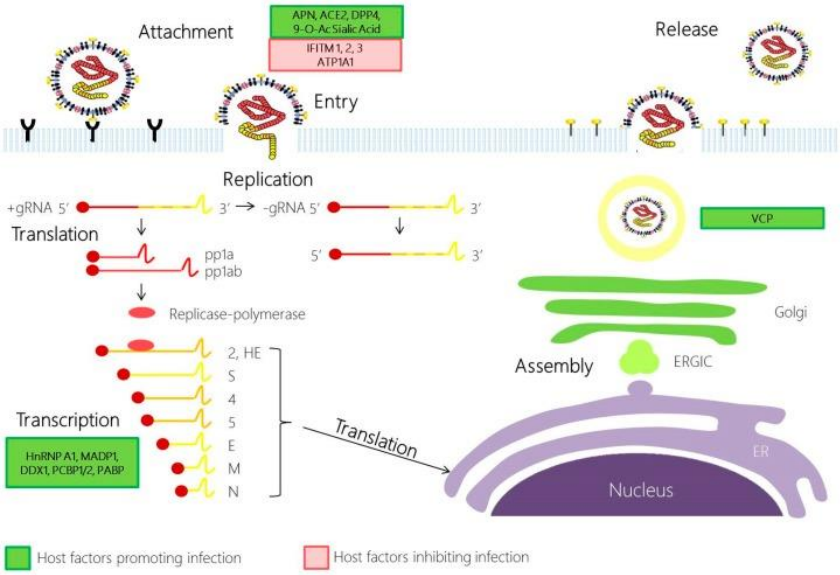

Figure 12 Coronavirus replication cycle.[7]

Published under Creative Commons licenses.

Viral entry occurs through clathrin-mediated endocytosis, facilitated through an interaction between the receptor binding domain (RBD) on the S1 subunit of S protein, and the host angiotensin-converting enzyme 2 (ACE2) receptor (Figure 12). S is cleaved by transmembrane serine protease 2 (TMPRSS) which primes the S protein and allows for fusion to occur between S2 and the endosomal membrane. This fusion leads to viral RNA entering the cytoplasm. [154,161] Replication begins with the cellular ribosomal translation of the replicase gene, which is encoded in two open reading frames (ORFs), rep1a and rep1b. These encode polyproteins, ppla, that contains non-structural proteins 1-11, and pplab which includes non-structural proteins 1-16. [154] The polyprotein is cleaved into individual non-structural proteins by viral encoded papain-like proteases and a serine-type protease. It is these non-structural proteins that assemble the replication complex termed the replicase-transcriptase complex (RTC) where both genomic and sub-genomic RNA synthesis takes place. Following replication, viral structural proteins are translated. [154]

Structural proteins

The coronavirus genome encodes four structural proteins; spike (S), membrane (M), envelope (E), and nucleocapsid (N); all encoded on the 3' end of the genome. [154]

- Spike protein (S) is a class I fusion protein that mediates attachment to the host receptor.[4,] The large (150kD) protein contains 22-N linked glycosylation sites. Homotrimers of S make up the prototypical spikes on the surface of the virion. [154,162] During cellular infection, S is cleaved in the endoplasmic reticulum (ER) by host protease furin or furin-like proprotein convertase in two pieces that generate subunits, S1 and S2. While S1 sits at the top of the spike protein and contains the receptor-binding domain (RBD), S2 forms the stalk of the spike and contains the fusion domain. [154]
- Membrane protein (M) is 25-30 kD and is the most abundant structural protein. M has three domains and is responsible determining the virion shape. [154]
- Envelope protein (E) is 8-12 kD and found in small quantities in the virion. Where it facilitates virus assembly and release. E also has ion channel activity that is not needed for replication but required for pathogenesis. [154]
- Nucleocapsid protein (N) is the only protein present in the nucleocapsid. It contains two domains, each responsible for binding viral RNA through different mechanisms. [154]

Following translation of structural proteins, S, E, and M are inserted into the endoplasmic reticulum (ER) where they move through the secretory pathway. Viral genomes and N protein interact and form the nucleocapsid. The nucleocapsid buds into the membranes of the endoplasmic reticulum-Golgi intermediate compartment which contains S, E, and M, thereby forming a mature virion. [154] S protein is organized into a trimer, giving it a spikey appearance. [163] During the maturation process S protein is cleaved by furin or furin-like proprotein convertase into S1 and S2 subunits which remain associated with one another. [163] Following viral assembly,

mature virions are transported in vesicles and released from the cellular environment by exocytosis. [154]

Viral evolution

Single-stranded RNA viruses, such as coronaviruses, mutate and evolve through rapid changes to the viral genome, partially due to a lack of a proof-reading enzyme and the lack of a second strand template. [164] Unique to RNA viruses, coronaviruses have an RNA proofreading exoribonuclease, nsp-ExoN, that can fix replication errors. [165,166] This lowers the nucleotide point mutation rate, which increases genome stability and viral viability. [167] While this reduces viral adaptation by mutation, coronaviruses also undergo frequent recombination events which can lead to rapid changes in viral genetic diversity. [167] Viral recombination, the exchange of genetic material between genomes, is a normal part of coronavirus replication and has been implicated in the emergence of novel variants. [166] The S gene is considered a recombination hot spot. Changes to viral genome sequence within the S gene allow for adaptations to host range, virulence, and tissue tropism. [167] Researchers have recently found that blocking nsp14-ExoN is not virucidal, but causes recombination events to plummet, inhibiting the virus's ability to repair or escape immune pressure. [166]

Early in the COVID-19 pandemic, a single-point S mutation emerged, D614G. This provided a slight boost in transmissibility and therefore a selective advantage for the virus. [168] Since then, multiple virus variants that differ from the original SARS-CoV-2 sequenced in Wuhan have been documented and identified in the United States and globally. Variants can be classified in several ways:

- A variant of interest (VOI) is defined by the world health organization (WHO) as having genetic changes that are known or predicted to cause an increase in transmissibility, disease severity, immune escape, and identified to cause community outbreaks. [169]
- A variant of concern (VOC) is defined by the WHO as meeting the aforementioned definition of a VOI as well as exhibiting increased transmissibility, increased virulence, or decreased effectiveness of public health measures. The WHO currently recognizes five VOCs discussed in further detail below.[169]

Several naming conventions have been used to name emerging SARS-CoV-2 variants, including the WHO system using letters of the Greek alphabet, and the Pango naming system based on phylogenetic relatedness. [170] The Alpha (B.1.1.7) variant was discovered in the UK in November 2020 and was first isolated in an individual in Oregon in late December 2020. This variant, containing mutations in S, was 50% more transmissible than early lineage strains. [171] Around the same time Beta (B.1.351) emerged in South Africa and Gamma (P.1) in Brazil and Japan. These first three variants of concern (VoC) contained mutations in S protein, notably within RBD, which increased transmissibility by binding more effectively to the host ACE2 receptor. [171] In addition, the mutations led to immune evasion of both serum and monoclonal antibodies. [172] In the spring of 2021, Delta (B.1.617.2) emerged in India and quickly spread around the globe. This variant was highly transmissible and possessed an improved ability to infect and replicate efficiently in host cells. Serum neutralizing antibody titers are reduced against Delta, however, approved therapeutic monoclonal antibodies are still effective. [173] In late November 2021, Omicron (B.1.1.529) emerged and was first isolated in South Africa. The Omicron VOC has 55 mutations spanning the entire genome with 32 mutations in S protein, mostly in the N-terminal domain and RBD. [174] Omicron spreads quickly, has a fitness advantage over Delta, and appears

to evade serum antibodies. Neutralization titers for both post-natural infection and vaccination are dramatically reduced against Omicron and approved therapeutic monoclonal antibodies also show reduced efficiency. [174] Omicron did not directly evolve from previously described VOCs, therefore its emergence suggests a complex evolutionary history.

1.3.2 Coronavirus pathogenesis

Coronaviruses were largely thought to cause mild infections in immunocompetent people until the outbreak of highly pathogenic SARS-CoV in 2003 and MERS-CoV 10 years later emerged as a threat to humans. Since then, research has advanced the understanding of coronavirus pathogenesis, as well as furthered the discovery of animal reservoirs. [156,175] Bats appear to serve as a reservoir host for the majority of alpha and betacoronaviruses. [176]

Severe acute respiratory syndrome coronavirus (SARS-CoV) is the causative agent of SARS. It was discovered in 2003 and is far deadlier than previously identified coronaviruses. The average case fatality rate of 10% increases to 50% in elderly individuals over the age of 60. [154] The SARS outbreak lasted 6 months with no cases detected after 2004. Even though the case fatality rate was high, transmission was largely inefficient as the virus was mostly spread through close contact through large respiratory droplets and to a lesser extent aerosols. Transmission was largely occurred in healthcare and household settings and the virus was effectively controlled with quarantine and isolation. [154] There were just over 8,000 cases and 774 deaths in China and two dozen other countries. [154] SARS-CoV infects lung epithelial cells, utilizing the ACE2 receptor for entry. [155] Although the virus is capable of entering macrophages and dendritic cells it does not replicate efficiently in those cell types. [154] Symptoms include fever, headache, and respiratory symptoms such as cough and pneumonia. Illness can progress into respiratory failure

and acute respiratory distress syndrome (ARDS), which can be fatal. [155] No vaccine is available for SARS-CoV, however, research and development aided the successful development of a SARS-CoV-2 vaccine in 2020 (see section 1.3.4).

Severe acute respiratory syndrome coronavirus 2 (SARS-CoV-2) is the causative agent of COVID-19 which emerged in late 2019 in Wuhan, China, and has since spread to every continent except Antarctica.[177] This novel virus shares 79% genome sequence identity with SARS-CoV. [178] Interestingly, SARS-CoV-2 shares 90% sequence identity with SARS-CoV across the structural proteins, except for S where the sequence diverges. [178] SARS-CoV-2 enters epithelial cells in the respiratory tract via interaction with the ACE2 receptor. There, the virus replicates and disseminates into the respiratory tract, down the airways, and into the lungs where it infects alveolar epithelial cells. [178] The virus rapidly replicates in lung tissue which can trigger a strong immune response, including cytokine storm (more on this in section 1.3.3).[7,178,179] Symptoms include fever, cough, and shortness of breath. Illness can progress to pneumonia, multi-organ failure, ARDS, and even death. [7] Severe disease occurs more commonly in older individuals over 60 years of age compared to children or young healthy adults. [7] Common co-morbidities associated with poor outcomes are hypertension and diabetes mellitus. ACE2 expression is significantly higher in individuals with these conditions as well as those taking ACE inhibitors for hypertension. [7] Three vaccines are currently available in the U.S. to protect against infection with SARS-CoV-2 (see section 1.3.4).

1.3.3 Coronavirus immunity and Immunopathogenesis

Innate immune response

The three main purposes of the innate immune response are to: 1) restrict viral replication, 2) create a localized antiviral state and recruit immune cells to the site of infection, and, 3) prime the adaptive immune response. [180] Host cells detect viruses through innate pattern recognition receptors (PRRs) such as endosomal sensors TLR-3, 7, and 8 and cytosolic sensors retinoic acid-inducible gene 1 (RIG-I) and melanoma differentiation-associated protein 5 (MDA5).[161] Detection of viral RNA results in the upregulation of interferon (IFN) which in turn stimulates downstream antiviral interferon-stimulated genes (ISGs). [181] Rapid IFN responses soon after viral infection can greatly limit viral replication, however, the ongoing antiviral response can lead to a deleterious response that causes tissue damage or cytokine storm. [161] It has been demonstrated that both infectious virus and UV-inactivated SARS-CoV can stimulate a type I IFN response. [181] Infections with SARS-CoV and SARS-CoV-2 are associated with IFN suppression, compared to infection with common cold coronavirus 229E where a rise in type I IFN is observed. [155] At least two mechanisms have been proposed for this IFN suppression, host factors, and antagonism by viral proteins. [182] A large genome-wide screen reported that individuals with severe disease have errors in PRR TLR-3 as well as downstream genes in the IFN pathway. [183] Another group observed the presence of autoantibodies against type I IFN in individuals with more severe disease further supporting the importance of a robust type I IFN response in controlling viremia. Additionally, multiple viral proteins including, nsp1and ORF6, have been shown to modify or block interferon responses in the host, thereby inhibiting an early antiviral immune response. [155,161,184] Regardless, the importance of type I IFN for control of SARS-CoV-2 infection is crucial and an ineffective IFN response is strongly associated with severe or even fatal disease. [180] [185] Low levels of IFN are associated with higher viremia and inflammatory response seen in the more severe disease state. [161, 178]

Response to viral infection can lead to overactivation of the host immune system, which results in the release of an over-abundance of inflammatory cytokines known as a cytokine storm. [161] Controlled cytokine release aids in controlling infection, uncontrolled cytokine response leads to systemic response and tissue damage. [161] During SARS-CoV infection, several cytokines are upregulated, including IL-6, IP-10, IL-8, and monocyte chemoattractant protein (MCP). [181] These factors are associated with poor disease outcomes. [181] During acute SARS-CoV-2 infection, a significant correlation is observed between disease severity and serum concentrations of IL-1, IL-2, IL-6, IL-7, IL-10, and TNF-α. [161, 178] During mild to moderate disease, concentrations of inflammatory cytokines such as TNF-α, IL-6, IL-10 decline over time. In subjects with severe disease these cytokines remain elevated. IL-6 serves as a viable biomarker of disease severity, and a strong correlation between plasma concentration and viral load and lung injury has been observed. [161]

Adaptive T-cell responses

Studies of acute and convalescent individuals indicate that SARS-CoV-2 specific T-cell responses are associated with milder disease, highlighting their importance in control and clearance of infection. [180] Robust T-cell responses have been observed in individuals following natural infection up to 6 months post-infection with SARS-CoV-2 and up to 11 years post-infection with SARS-CoV. [186,187] The magnitude of responses varies by individual, but responses are higher in symptomatic subjects when compared to asymptomatic subjects. [186] CD4+ T-cells predominantly produce IFN-γ and IL-2, a protein signature of Th1 cells. [180,186] CD4+ cells in tissues can also robustly express IL-22, a cytokine associated with lung and gut epithelial tissue repair suggesting a protective effect. [180] The magnitude of the CD4+ T-cell response correlates

with the magnitude of IgG and IgA antibody titers against spike and RBD, suggesting the majority of protective antibody responses are dependent on CD4+ help. [186,188] The CD4+ T cell response was about twice as high as CD8+ SARS-CoV-2 response in convalescent individuals. [180,186] Most CD4+ T-cell responses are directed towards S, M, and N proteins, and to a lesser extent non-structural proteins. [186, 188]

Similarly, the CD8+ T-cell response is directed towards S with N proteins, accounting for the second-highest response. [180] During SARS-CoV infection, S protein was essentially the only target for the CD8+ response. [188] During SARS-CoV-2 infection virus-specific CD8+ T- cells functionally express high levels of IFN-γ, granzyme B, and perforin. [180] Overall, T-cell responses are robust and observed in 70-100% of convalescent subjects following SARS-CoV-2 infection. [186,188] In addition, cross-reactive CD4+ T-cells have been detected in 40-60% of unexposed individuals, indicating that prior infection with common cold coronaviruses generates cross-reactive T-cells that recognize SARS-CoV-2 peptides. [188,189]

Antibody-mediated immunity and specific epitopes of importance

Antibody-mediated protection is short-lived following common cold coronavirus infection, however, SARS-CoV survivors remained seropositive up to at least 17 years following infection. [190,191] For SARS-CoV-2, the highest neutralizing antibody titers have been observed in subjects with more severe disease. The hypothesis for this is prolonged antigen exposure and higher antigen load leads to a more robust humoral immune response. [180] This same observation was made with SARS-CoV. [192] The major target of neutralizing antibodies is RBD, with > 90% of neutralizing antibodies directed against RBD. [180,193] These neutralizing antibodies have little somatic hypermutation, therefore they are hypothesized to develop from naive B-cells instead of pre-existing cross-reactive memory B-cells. [180] Serum neutralizing antibody titers are relatively

low following natural infection, however circulating IgG antibody titers might not be the ideal readout for humoral immunity to a respiratory pathogen.

IgA plays a crucial role in protecting against pathogens at mucosal interfaces and is an important antibody isotype for combating respiratory infections. [194] IgA is mostly expressed in the lamina propria right up against mucosal surfaces in the respiratory and gastrointestinal tracts. Isotype switching from IgG to IgA does not change the binding affinity to RBD but instead affects downstream effector functions. Monomeric IgA is present in the serum and is the second most abundant isotype behind IgG, while dimeric IgA is present at mucosal surfaces. [195] The early SARS-CoV-2 antibody response is dominated by IgA antibodies which can effectively neutralize the virus. [195,196] SARS-CoV-2 IgA neutralizing antibody titers in the serum decrease within the first-month post-infection, however, persist in the saliva for longer. [195,197]An IgA response is critical for clearance and protection against respiratory pathogens, therefore vaccination strategies that elicit an IgA response should be considered.

Cross reactivity across coronaviruses

Amino acid sequence similarities between SARS-CoV and SARS-CoV-2 are 91%, 90%, 95%, and 77% for structural proteins N, M, E, and S respectively. [198] Cross-reactive binding has been observed between convalescent SARS-CoV immune sera and monoclonal antibodies and SARS-CoV-2 S protein and RBD, however, limited to no neutralization is observed. [191,199, 200] Individuals, both adults and children, with no prior history of SARS-CoV-2 infection (pre-pandemic samples), had cross-reactive IgG serum antibodies to N, S2, and RBD, but not S.[201,202] Some of the antibodies bound to conserved epitopes shared between the SARS-CoV-2 immune and naïve sera. [201,202] Contrary to what is observed in serum antibodies, pre-existing T-cell memory, predominantly CD4+, has been observed in 20-50% of individuals never exposed to

SARS-CoV-2. The source of these cross-reactive T-cells is presumably derived from infections with related common cold coronaviruses. [189]

Immune involvement in pathogenesis

Antibodies can be protective or lead to increased pathogenesis in the host. Antibody-dependent enhancement (ADE) occurs by two distinct mechanisms. First, antibodies can facilitate viral entry into FcγRII receptor-bearing phagocytic host cells, usually monocytes/macrophages, through interaction with the Fc portion of IgG antibodies. The result is enhanced viral infection. This has been observed for a variety of viruses including flaviviruses and alphaviruses (see sections 1.1.3 and 1.2.3). For respiratory viruses, another mechanism of ADE can occur via enhanced immune activation. This has been observed in respiratory viruses including RSV and measles. [203] In an Fc-mediated manner, non-neutralizing antibodies can form immune complexes with antigen inside the respiratory tract. This can cause airway obstruction as well as immune cell infiltration, complement activation, and pro-inflammatory cytokine production. [203] ADE has been observed in *in vitro* models of SARS-CoV infection[204-206] as well as reported immunopathology in the lungs, following viral challenge in SARS-CoV vaccinated mice *in vivo.* [206] However in an *in vivo* macaque model of inactivated SARS-CoV vaccination followed by viral challenge, enhancement was not seen by clinical, histopathological, or virological measures. [207] This caused concern for SARS-CoV vaccine trials in humans, however in most animal models including NHPs, vaccination or passive antibody treatment results in protection against challenge for both SARS-CoV and SARS-CoV-2. [208] ADE has not been observed with SARS-CoV-2, although it was a concern early in the pandemic.

1.3.4 Coronavirus vaccines

The journey to a licensed SARS-CoV-2 vaccine has been unprecedentedly expeditious, with over 170 vaccines in the preclinical or clinical test phase a year after the virus had been sequenced. [209] The first wave of vaccines to reach phase III trial and be approved for human use are platforms that allow for quick production on a large scale, such as nucleic acid or virus vectored vaccines while more traditional platforms such as protein subunit or live-attenuated viral vaccines require more time to develop. [209] No live attenuated vaccine has entered Phase III, as it cannot be administered to immunocompromised individuals.

mRNA vaccines are a new technology that, before 2020, had never been approved for use in humans. [209] These mRNA vaccines are quick to develop, can be manufactured on a large scale, and generate a robust cellular and humoral immune response. Therefore, they were an ideal choice to pursue in wake of the COVID-19 crisis. [209] The primary goal for vaccine development is to develop a safe and effective vaccine that prevents serious disease and death from COVID-19 with a secondary goal of preventing SARS-CoV-2 infection. [209]

- mRNA-1273 developed by Moderna and the National Institute of Allergy and Infectious Diseases (NIAID)— This vaccine contains RNA encoding the amino-acid sequence for stabilized pre-fusion S encapsulated in a lipid nanoparticle. [209] Primary vaccination followed by a booster 28 days later was found to induce a strong cellular (CD4+ and CD8+) response as well as neutralizing antibody titers. During clinical trials, the vaccine efficacy was 94% after 2-doses. [209] In December 2020, the FDA approved vaccination of individuals over the age of 18 by emergency use authorization in the United States. [209]
- BNT162b2 developed by Pfizer and BioNTech – This vaccine contains RNA encoding the amino-acid sequence for stabilized full-length spike protein. Vaccination induces

robust CD4+, CD8+ and neutralizing antibody response. [209] Similar to Moderna 1273, the Pfizer vaccine was 95% effective at preventing SARS-CoV-2 infection during the phase III clinical trial. [209,210] In December 2020, the FDA granted emergency use authorization for individuals over the age of 16 in the United States. In May 2021, the EUA was expanded to include children ages 12-15, and in October 2021, children ages 5-11 became eligible to receive the vaccine. [209]

Viral vector vaccines, such as adenovirus-based vaccines, were another platform used to develop a safe and efficacious COVID-19 vaccine. A possible downside includes pre-existing serum antibodies against the vector virus that can affect the robustness of vaccine response. This can be circumvented by using a viral vector that the individual has likely not been exposed to, such as chimpanzee adenovirus ChAdOx1 or Adenovirus 26. [209] For the same reason, boosting may not lead to a robust recall response due to interference with circulating antibody levels. [209]

- Johnson and Johnson (JNJ JNJ-78436735/Ad26.COV2.S) was developed by Janssen—This vaccine is a replication-defective adenoviral vector (Ad26) based vaccine containing DNA encoding the stabilized prefusion S protein from SARS-CoV-2. [209] Cellular and humoral immune responses were observed in phase III trials. The FDA granted emergency use authorization in February 2021 for use in individuals over the age of 18 in the US. [209] JNJ is the first single-dose vaccine currently approved for use. Although the CDC recommends a single dose booster after 2 months, preferably with an mRNA vaccine.

A fourth vaccine candidate and the first recombinant protein subunit vaccine against COVID-19, Novavax, has recently completed phase III trials and has requested approval for emergency use

authorization from the FDA. This protein subunit vaccine contains stabilized prefusion full-length S expressed in a baculovirus system with a Matrix M1 adjuvant. [209] Vaccination induces a robust cellular and humoral immune response and in phase III clinical trials exhibited 90% vaccine efficacy. [209-211]

The rapid vaccine development that took place in 2020 is a huge scientific achievement, however, more work remains to be done. Specifically, developing a vaccine that results in broad protection against newly emerging variants or a prime-boost strategy that provides wide coverage against emerging variants is still highly desired.

1.4. Establishment and maintenance of long-term humoral memory to RNA viruses

The role, development, and structure of B-lymphocytes

B-cells are a specialized type of lymphocyte that when stimulated by an antigen, proliferate and differentiate into antibody-secreting cells. B-cells play important roles in helping to clear infections as well as preventing future infections with the same or similar pathogen. The importance of B-cells in preventing and controlling human disease cannot be underestimated. Many vaccines that protect against pathogens of clinical importance are antibody-mediated. Natural immune responses to infection activate two main types of B-cells, which go on to play a fundamental role in the establishment of immune memory against that infection. Therefore B-cell malignancies or B-cell depleting therapies can have huge impacts on health. The first line of defense against repeat infection are long-lived plasma cells (LLPCs) which are terminally differentiated B-cells that continuously secrete antibodies for months to the lifetime of the individual. [212,213] Memory B-cells (MBCs) make up the second line of defense. These cells do

not secrete antibodies, but instead, respond to repeat infections by rapidly proliferating into a new population of antibody-secreting cells. [214]

B-lymphocytes, bursal or bone marrow-derived cells, begin their development in the fetal liver and continue after birth in the bone marrow. [215,216] B-cells can be simply described as a population of immune cells that express a clonally diverse immunoglobulin (Ig) consisting of paired heavy and light chain receptors that recognize a specific antigen epitope, either on the surface as a membrane-bound immunoglobulin known as a B-cell receptor (BCR) or secreted as an antibody. [216] BCR genes are encoded from germline on three separate genes, variable (V), diversity (D), and joining (J). Site-directed DNA rearrangement of the BCR genes known as VDJ recombination takes place during lymphocyte development in the bone marrow. [215,217] The heavy chain contains constant gene segments (this encodes for antibody isotype further discussed in *Antibody isotype and Fc modifications*), 44 V gene segments, 27 D gene segments, and 6 functional J gene segments. The light chain encodes for kappa or lambda constant chain as well as V and J gene segments. [215] Following rearrangement, the heavy chain has 3 highly variable regions, known as complementarity determining regions (CDRs), which are flanked by less variable regions. The CDR3 is highly unique to each rearrangement and is often used to identify individual B-cell clones. [217] This random process of VDJ rearrangement results in an enormous number of possible gene combinations, up to 10^{16}, resulting in a huge amount of BCR and antibody diversity with the ability to recognize a wide array of pathogens through binding to the BCRs. [214] Following differentiation in the bone marrow, these rare antigen-specific B-cells, 1 in 10^4 to 1 in 10^6 (per naïve B-cell), then exit the bone marrow and enter the peripheral blood where they patrol secondary lymphoid tissues waiting to encounter antigen. [214]

Initial antigen exposure and B-cell proliferation

The lymphatic system is made up of primary lymphoid organs such as the thymus and bone marrow as well as secondary lymphoid tissues such as the spleen, tonsils, and lymph nodes. [215] The lymphatic system puts immune cells such as B-cells in close contact with circulating antigens. [214] Antigen presentation is a crucial step in alerting the immune system to pathogen invasion through an interaction between major histocompatibility class (MHC) I and II molecules and T-cells (a specialized type of lymphocyte-derived from the thymus). [218,219] MHC-I is expressed by all nucleated cells and presents peptides from endogenously derived antigens to CD8+ T-cells. [218] Only professional antigen-presenting cells (APCs) such as dendritic cells, macrophages, or B-cells express MHC-II. [219] Exogenous antigens are taken up by APCs, where the antigen is proteolytically processed and interacts with MHC-II within the endosome. The MHC-II peptide complex is then transported to the plasma membrane where it is presented to CD4+ cells. [219] B-cells can recognize whole unprocessed antigens, such as epitopes on the surface of whole-virus, through binding to the BCR and does not require antigen presentation. [219]

In addition to the BCR-antigen interaction, a second signal is required for B-cell activation. [220] Depending on the nature of the antigen this signal can be in the form of T-cell help, or through a T-cell independent manner where cross-linking of membrane-bound immunoglobulin provides the signal (more on this in *T-cell-independent B-cell activation*). [214,220] Naïve B-cells express on their surface a BCR of isotype IgM and/or IgD. [214] Following activation, a subset of B-cells undergoes class switch recombination (CSR) changing the isotype of their BCR to IgG, IgA, or IgE. [214, 221-223] Isotype-specificity enables functional differences to better respond to the current infection (more in *Antibody isotype and Fc modifications*). Once activated, B-cells will follow one of three different trajectories: 1) differentiation into short-lived extrafollicular plasma

cells, 2) become germinal center independent MBCs, or 3) enter newly formed germinal centers. [220,224] The signals that determine these fates are not entirely elucidated.

Short-lived extrafollicular plasma cells (plasmablasts)

Plasmablasts are B-cells that have been activated by antigen in order to control a current or active infection. These B-cells rapidly respond to infection by proliferating and secreting medium to high-affinity antibodies, both class-switched (IgA and IgG) and not (IgM). These cells have a short lifespan, days to weeks, generally the duration of infection, before undergoing apoptosis. [11,224] This initial burst of antibodies arises early in the course of infection, aiding in the control of the pathogen. [11,225] In a human study of yellow fever virus vaccination, plasmablasts at 14 days post-vaccination encoded for higher affinity antibodies compared to MBCs on the same day post-vaccination. [226] This supports earlier mouse data suggesting that activated B-cells with intermediate to high initial affinity differentiate into short-lived plasma cells to combat the current infection, while the highest binding activated B-cells are recruited to a long-lived plasma cell fate and lower affinity cells towards an MBC fate. [226,227]

Germinal independent MBCs

A subset of MBCs emerge early in infection and do not contain somatic hypermutations or undergo affinity maturation. These MBCs are known as germinal center (GC) independent because they do not undergo positive selection in the GC. Regardless, they are long-lived and capable of producing antibodies upon recall response. [225,228,229]

In GC deficient mice, populations of IgM and IgG MBCs are present, albeit without somatic hypermutations. [224,230] These low-affinity MBCs retain their adaptability potential within the memory pool. [231] These findings support the idea that low-affinity MBCs are an expansion of

the germline repertoire and can emerge independently of GC reactions. It is unclear how germinal center independent MBCs contribute to recall response. See *MBC recall response* for additional discussion.

T-cell-independent B-cell activation

During T-cell independent responses, B-cells are stimulated directly without the need for antigen processing or T-cell help. Non-proteinaceous antigens are usually non-specific mitogenic stimuli that activate pathogen recognition receptors such as Toll-like receptors (TLRs). Examples include lipopolysaccharide (LPS) an endotoxin found in the outer membrane of Gram-negative bacteria that stimulates TLR-4; some flagella present on commensal and pathogenic bacteria that stimulates TLR-5; or unmethylated CpG oligodeoxynucleotides (CpG) is considered a pathogen-associated molecular patterns due to their abundance in microbial genomes, stimulates TLR-9. [232,233] All of these stimuli generate a polyclonal antibody response. [232] Antigens can also consist of large polysaccharides (components of bacterial cell walls) or lipopolysaccharides, made up of repeating sequences, which can bind to the BCR on B-cells resulting in receptor clustering and cross-linking. [234] In order to generate a T-cell independent antibody response BCR clustering must occur. It has been determined that 10-20 BCRs must be cross-linked, prior to BCR clustering, and BCRs are spaced out by about 35nm requiring antigen to be ~500nm in length. [235] Clustering along with a secondary signal, such as LPS which activates TLR signaling, is sufficient to activate B-cells. [234] These types of responses generate short-lived immunity consisting of IgM secretion without affinity maturation, or long-lived memory cells. [234]

T-cell dependent B-cell activation

Humoral response to most antigens requires T-cell help. As previously described (*Initial antigen exposure and B-cell proliferation*), B-cells internalize and proteolytically process antigen that is loaded as peptides onto MHC class I or II on the surface of B-cells. [232] This antigen-MHC complex interacts with the T-cell receptor (TCR) on the surface of T-cells. [214] Following TCR-MHC-II interaction, T-follicular helper cells (T_{FH}) a subset of CD4+ cells provide B-cells with signals that promote survival and proliferation. [11] Interactions between CD40 on B-cells and CD40 ligand on T_{FH} stimulates the NF-kB pathway which activates target genes that promote B-cell survival by inducing expression of Bcl-2 an anti-apoptotic factor. T_{FH} also secrete cytokines such as IL-21 which promote B-cell proliferation and differentiation as well as other cytokines that provide signals which regulate the isotype of antibody that is produced (more on this in *Antibody isotype and Fc modifications*).

Germinal center (GC) reactions

GCs are highly specialized microstructures that transiently form within secondary lymphoid tissues such as lymph nodes, Peyer's patches, and the spleen, and are mostly comprised of proliferating B-cells, with antigen-specific T-cells making up 10% of lymphocytes. [215] Antigens traffic into lymph nodes, either freely as soluble antigens, or cell-associated on antigen-presenting cells, through afferent lymphatic vessels or into the spleen through the blood. [236] During an immune response T and B-cells become activated and follow chemokine gradients to move towards the B-cell follicles where activated T-cells encounter activated B-cells. [224,225] Activated B-cells destined to seed a GC upregulate Bcl6 and migrate to the center of the follicle where they initiate a germinal center response. [231, 11] GC B-cells rapidly proliferate and undergo clonal expansion. During this initial expansion, the GC is divided into two zones (Figure 13). The dark zone (DZ) contains rapidly proliferating germinal center-B-cells that are undergoing

somatic hypermutation (SHM) that leads to affinity maturation, which is the direct result of somatic hypermutation to the BCR on B-cells within the germinal center. [11,231] These mutations occur in the variable region, namely the CDR, and are mediated by activation-induced cytidine deaminase (AID) which converts cytidines to uridines and results in point mutations within the BCR altering binding specificities and affinities of the resulting secreted antibodies. [215] The light zone (LZ) is where germinal center-B-cells undergo selection. The LZ is full of follicular dendritic cells which present antigen to the activated B-cells and T_{FH} cells which are critical for the positive selection of B-cells. [11] If the BCR binds with a high enough affinity in the LZ the B-cell emerges from the germinal center as either a long-lived plasma cell (LLPC) or MBC. If the BCR does not bind antigen with high enough affinity, the B-cell can return to the DZ to further undergo SHM and affinity maturation. [231] Binding affinity appears to play a large role in determining LLPC or MBC fate, as it has been observed that MBCs have a lower affinity to antigen compared to LLPCs. [222] It is not entirely clear what signals determine the fate of germinal center-B-cells; however, up and downregulation of transcription factors plays a role in determining the fate of activated B-cells. IRF4/Blimp-1 is a master regulator of LLPC fate while an MBC specific transcription factor has yet to be identified, although Bach2 has been implicated as a factor in MBC differentiation. [224,231]

Prolonged germinal center responses have been observed *in vivo* in humans following SARS-CoV-2 infection, as well as influenza and yellow fever vaccination. [226,237] This is evident by the increase in antibody affinity, furthered somatic hypermutation, and an increase in neutralization potential over time. Recent studies suggest that germinal centers can persist for 6-12 months following natural infection or vaccination. [226,237]

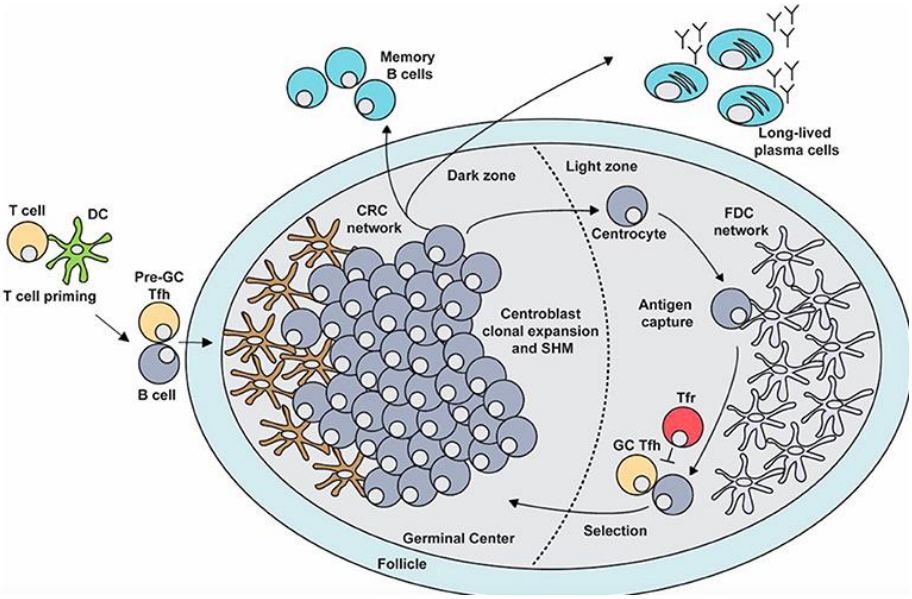

Figure 13 The germinal center within a B-cell follicle of secondary lymphoid tissue that is formed following infection or vaccination.

Figure from [11] published under Creative Commons licenses.

Long-lived plasma cells (LLPCs): are terminally differentiated long-lived B-cells that emerge from germinal centers and traffic to the bone marrow where they reside for years to the lifetime of an individual, regardless of antigen re-exposure. [238, 220,228] The LLPC homing process is mediated by chemotaxis and transcription factors. Upon arrival in the bone marrow, LLPCs undergo a proliferation event and then become quiescent, their survival dependent on cytokines APRIL and IL-6 which are secreted by cells in the bone marrow niche. [220] LLPCs down-regulate MHC-II on their surface, hence disrupting their ability to acquire further CD4+ T-cell help or induce a new antibody response. [239] LLPCs switch from membrane bound BCR to the secreted form and secrete large amounts of a single, high-affinity antigen-specific antibody. [239] LLPC-

derived antibodies are the hallmark of antibody-mediated protection and are regarded as the first line of defense against infections. [220] MBC disruption or depletion of circulating B-cells does not affect serum antibody titers or longevity, therefore LLPCs do not appear to require replenishment from the MBC compartment. [238-242] It is unclear the mechanism behind why LLPCs against some antigens persist for a lifetime while others have a shorter lifespan, some possible reasons are discussed later in this section.

Memory B-cells (MBCs): are long-lived cells that do not secrete antibodies, instead, they patrol peripheral blood, or take up residence in secondary lymphoid organs, looking for their cognate antigen. [225,231] MBCs require antigen activation before they can expand and secrete antibodies to participate in host defense. [228] MBCs are regarded as the second line of defense. They participate in host immune response when pathogens evade serum antibodies, either through waning antibody titers or antibody escape. Therefore, they encode for low-affinity binding BCRs which maintain diversity within the MBC compartment. [243]

MBC recall response

When MBCs encounter their cognate antigen within secondary lymphoid organs, they respond rapidly and have a high sensitivity to low amounts of antigen. [225] Isotype class-switched (IgD-/IgM-) MBCs have a lower activation threshold due to enhanced excitability/signaling differences in the BCR cytoplasmic domain. IgD/IgM have very short cytoplasmic tails whereas IgA, IgG, and IgE have long cytoplasmic tails that amplify the signal and lower the activation threshold. [214, 228] MBCs respond to reinfection by differentiating into plasma cells and secreting antigen-specific antibodies, or by re-entering GCs to become more highly affinity matured to

fight the current infection. [222] This has been observed *in vitro* as well as *in vivo* in mice. [228,244] Mouse studies have informed understanding of MBC recall responses, where it has been reported that IgM MBCs preferentially initiate germinal centers, and IgG MBCs preferentially differentiate into plasma cells. [220,243] It is also known that IgM memory cells with few somatic hypermutations, and therefore little affinity maturation, participated in recall response against a variant antigen (different from the antigen used to prime the immune response). [245] CD80+ MBCs preferentially become plasma cells upon re-infection/challenge (in mice), regardless of isotype. [222] Depending on the type of infection, secondary responses are reportedly dominated by IgG. However, there is a strong research bias towards IgG, and less is known about other isotypes during initial or recall response. IgG MBCs have a lower activation threshold compared to IgM MBCs *in vitro*. Therefore, it has been hypothesized that IgM MBCs might serve as a backup as long as IgG MBCs are present in sufficient numbers. [228, 246]

Using model antigen, phycoerythrin (PE), MBC-transfer experiments in mice indicate that IgM-MBC recall response is inhibited by the presence of antigen-specific antibodies. On the other hand, IgG-MBCs transferred into naïve mice differentiate into a new population of plasma cells upon antigen challenge with very little GC formation, regardless of circulating antibody levels. [228,244] In a mouse model of repeat flavivirus infection, secondary affinity maturation was minimally involved, instead, pre-existing cross-reactive MBCs were involved in recall response. [222] The advantage is a rapid humoral response to pathogen variants compared to a naïve response. [243] It has been hypothesized that one of the most important functions of the MBC compartment is to provide an expanded, heterogeneous pool of long-lived memory cells that can respond to infection with related pathogens. This is especially important in the case of newly

emerging variants and mutating pathogens such as HIV, influenza, dengue virus, and SARS-CoV-2.[247]

The MBC recall response has been well-characterized in animal models compared to humans and it remains challenging to study in humans. It is difficult to get access to primary and secondary lymphoid organs, and instead, peripheral MBCs in the blood are utilized. In addition, humans have more complex infection histories and a broader genetic background that can confound studies. Much of what is known about recall response comes from *in vivo* studies observing humans in response to repeated vaccinations or infections, such as influenza and many questions remain to be answered. [231]

Antibody isotype and Fc modifications

The first antibody produced during initial infection is always IgM. Later in the immune response class switch recombination or isotype switching can occur, through DNA rearrangement that happens in the constant region of the BCR. This process is mediated by activation-induced cytidine deaminase (AID) and regulated by cytokines produced by T_{FH} cells and others during the immune response. [215] Cytokine expression and resulting isotype responses can be summarized as follows: IL-4 induces IgG1 and IgE; IL-5 induces IgA; IFN-γ induces IgG3 and IgG2a; TGF-B induces IgG2b and IgA; and IL-21 induces IgG3, IgG1, and IgA. [215] T-cell help is necessary for the formation of class-switched IgG MBCs and cannot occur in mice lacking CD40. [225] In humans, a condition known as hyper IgM syndrome results in individuals with a genetic deficiency in CD40 ligand that results in a lack of antibodies of classes other than IgM. These individuals are at significant risk of repeated or opportunistic infections. Together this indicates that the CD40-CD40L interaction is crucial for generating a sustained immune response that results in class-switching and affinity maturation. [215]

Pathogens enter the body through various routes including the respiratory tract, digestive tract, or directly into the blood through insect bites or wounds. Antibodies at these sites of infection are important to neutralize or promote the elimination of the pathogen, through other antibody-mediated effector functions, before it makes the host sick. Different antibody isotypes exhibit distinct distribution and specialized functions. [215] IgG is the most common isotype in serum followed by monomeric IgA. At mucosal surfaces, IgA is the most common isotype, with the dimeric form able to transport across epithelial barriers. [215] Infection with mucosal pathogens or mucosal vaccination routes results in an IgA response which can have important consequences. [231] The rarest isotype overall is IgE which has a very short half-life in serum. [214] IgG has the longest half-life in serum, ~26 days, and most infections and vaccinations with a protein antigen generate an IgG response. [248]

Antibodies are dual-functioning molecules, binding directly to pathogens with the antigen-binding fragment (Fab domain) and indirectly with the crystallizable fragment (Fc domain) or constant region by interacting with circulating immune cells that greatly influence innate and adaptive immune responses. [249] The Fc domain engages with Fc receptors (FcγRs), which are broadly expressed on the surface of lymphoid and myeloid cells. The specific distribution of different receptors is unique to particular cell types, and surface expression is mediated by cytokine expression. [250] Differences within the Fc domain determine isotype, subclass, and post-translational modifications such as glycosylation. Fc domain interaction with immune cell receptors will direct different effector functions, such as complement activation (C'), antibody-dependent cellular phagocytosis (ADCP), antibody-dependent cellular cytotoxicity (ADCC), neutrophil activation/NET formation, and the degranulation of mast cells, eosinophils, or basophils. [249] The Fc portion (antibody isotype) determines an antibody's ability

to transport across epithelial barriers and the placenta. [215] The neonatal Fc receptor (FcRn) is responsible for transporting IgG across the placenta, thereby enhancing fetal humoral immunity. [251]

The functionality of the Fc portion is fine-tuned at the genetic level by antibody isotype and subclass, and at the post-translational level by differences in glycosylation. [252] IgE followed by IgM and IgA2 are the most heavily glycosylated. [252] Differences in glycosylation affect stability and half-life as well as secretion, solubility, and biological activity. [253] Antibodies are able to bind and interact with an incredibly broad array of receptors (Fc, complement, and lectin-like receptors) expressed on both immune and non-immune cells. Differences in glycosylation and antibody isotype have different functional implications and have the ability to serve both protective and pathogenic functions. [253]

The role of antigen complexity on durability and quality of immune response

Immune responses to some natural or vaccine antigens are long-lived while others are short-lived. The durability of response appears to be related to the number of antibody binding sites on an antigen referred to as valency, antigen complexity, and antigen structure. [239] Both antigen repetitiveness and antigen load are important parameters in antibody (humoral) responses to infection. If the infection is resolved too quickly, vaccine antigen given at too low a dose, or without sufficient adjuvant (a pharmacological compound that enhances the immune response to an antigen), a sufficient antigen threshold to generate a robust B-cell response might not be met. It is hypothesized that the lifespan of LLPCs is determined during the initial immune response and this lifespan depends on the complexity of the antigen. For example, multivalent or repetitive antigens such as whole virus generate a longer-lived immune response than a monovalent

antigen such as a non-structural protein. This has not been explored in the context of infections such as DENV, where LLPC and MBC responses are generated against both multivalent (whole virus) and monovalent (non-structural protein 1). Another important aspect of immune response duration is antigen threshold. Exposure to some monomeric antigens, such as tetanus toxin, can generate a long-lived and robust humoral immune response if a high enough antigen threshold is met, one that accounts for decay over time. [239]

Correlation between LLPC and MBC populations

Recent work in mice uncovered a hidden repertoire of low-affinity MBCs that are not represented in the LLPC compartment. [222,254] Our group and others have shown that in mice and humans, MBC-derived antibodies are capable of recognizing and responding to a wider variety of antigens compared to their LLPC counterparts. [222,254,255] Previous work has shown a weak correlation between serum antibody levels and MBC frequencies for some vaccine antigens, but for many pathogens, serum antibody levels are a poor predictor of MBC frequencies. [212,255-257] This highlights the importance of evaluating MBCs in addition to evaluating serum antibodies in order to more completely characterize the humoral immune response to a particular antigen. In order to study LLPCs directly, bone marrow aspirates can be isolated and secreted antibodies accessed on a single-cell level. [242] This is often not feasible in human subjects, so serum antibodies are used as a surrogate to studying LLPCs.

As described here, the importance of B-cells in preventing and controlling disease cannot be underestimated. In the proceeding chapters, the establishment and durability of humoral immunity to natural infection or vaccination against RNA viruses of clinical importance (described earlier in this chapter) will be interrogated.

Chapter 2: Interrogating memory B cell founder populations to reveal the memory-derived antibody repertoire in dengue immune individuals with diverse infection histories.

Zoe L. Lyski,[1] Bettie Kareko,[1]Jana Mooster,[1] Brian Booty,[2] Rachel M. Rodriguez, [3] Luisa I Alvarado,[3] Vanessa Rivera-Amill, [3] William B. Messer, William[1,4]

1. Dept. Molecular Microbiology and Immunology, Oregon Health and Science University, Portland, Oregon, United States 2. Oregon Clinical and Translational Research Institute (OCTRI), Portland, Oregon, United States 3. Ponce Health Sciences University, Ponce, Puerto Rico
4. Department of Medicine, Division of Infectious Diseases, Oregon Health and Science University, Portland, Oregon, United States

Author contributions:

Conception of work ZLL and WBM Data collection ZLL, BK. Collection/ management of human samples ZLL, BB, and RRS. Data analysis ZLL and WBM Drafting of the article ZLL. Critical revision of manuscript ZLL and WBM Acquired funding LIA, VRA, and WBM.

Reagents: Fluorescently labeled DENV-1 was graciously provided by Dr. Anuja Mathew

Abstract

Dengue virus (DENV) is one of the most important vector-borne viral pathogens affecting humans worldwide. Following DENV infection, DENV specific naïve host B-cells expand and some immediately produce and secrete DENV-specific antibodies that recognize viral antigens, specifically epitopes of the envelope glycoprotein (E) present on the surface of virions as well as secreted non-structural protein 1 (NS1). After viral clearance, other B-cells become long-lived plasma cells (LLPC), while still others become memory B cells (MBCs) that remain in circulation, poised to expand on repeat infection. This MBC "founder" population is expected to play a critical role in establishing broader DENV immunity upon a repeat DENV infection. Here we quantify DENV-specific MBCs in humans following DENV-1 infection in a cross-sectional manner. Using peripheral blood mononuclear cells (PBMCs) from DENV-1 immune donors from endemic (n=15) and non-endemic (n=24) cohorts with times post-infection ranging from <1-43 years, we use two complementary approaches to quantify the MBC population: flow cytometry and limiting dilution assay. We then sorted single-cell DENV-specific MBCs and stimulated them in culture to become antibody-secreting cells to verify antigen-specificity. Using these approaches, we identified DENV-whole virion envelope and NS1-specific MBCs that remain in circulation decades after infection with varying frequencies in subjects from both boosting (endemic) and non-boosting (non-endemic) transmission settings. These experiments lay the foundation to characterize the DENV-specific MBC repertoire over time and functionally assess the antibodies they are programmed to secrete. The results of this project will provide insight into the MBC founder population following DENV infection in boosting and non-boosting environments.

Introduction

The four antigenically distinct dengue viruses (DENV1-4) are among the most important mosquito-borne viral pathogens affecting humans worldwide, responsible for 100 million symptomatic cases and ~35,000 deaths annually. [16] DENV is an enveloped single-stranded (+) RNA virus. Infection with any of the 4 DENV serotypes causes acute, self-limiting illness that ranges from asymptomatic to severe and sometimes fatal disease. Protection against DENV is thought to require an antibody-mediated immune response, with antibodies that recognize envelope (E) protein on the surface of the virion, leading to virus neutralization. Secreted protein non-structural protein 1 (NS1) plays an important role in pathogenesis and antibodies against NS1 have been shown to be protective *in vitro* and *in vivo* mouse models. [29,48,58]

B-cells are the cell type responsible for antibody-mediated protection. In response to the first or primary (1°) DENV infection, naïve B-cells that recognize DENV differentiate into short-lived plasma cells that proliferate and secrete DENV-specific antibodies to combat the current infection. After viral clearance, Antibody-mediated immunity is maintained in two distinct B-cell compartments. First, through polyclonal antibodies in the sera constitutively secreted by long-lived plasma cells (LLPCs) that reside in the bone marrow. LLPC-derived antibodies have high affinity and are considered the first line of defense against repeat infection with the same or similar virus (or serotype). Second, peripheral memory B-cells (MBCs), quiescent cells, with a B-cell receptor (BCR) on the cell surface that are poised to quickly respond to repeat infection by differentiating into a new population of antibody-secreting short-lived plasma cells. The BCR is a membrane-bound form of the variable portion of antibody the cell is programmed to secrete upon proliferation. The generation of antigen-specific B-cells is the principle behind vaccination with many vaccines striving to achieve antibody-mediated protection through LLPC and MBC populations. The best

way to control DENV would be an effective vaccine, but vaccine development has proved challenging. To date, only one DENV vaccine, CYD-TDV (Dengvaxia®) has been approved for humans, two more live-attenuated vaccines are in phase III clinical trials. [91,92] A striking feature of the CYD-TDV vaccine is the impact of pre-existing DENV immunity on vaccine efficacy: the vaccine was highly effective (78.2%) in vaccinees with prior DENV immunity, but weakly effective (38.1%) in individuals with no DENV infection history. [95] The reasons for this limited vaccine efficacy are not fully understood, but the existence of prior DENV-specific B and T-cell immunity is thought to play a critical role. [36] The specific features of natural DENV immunity, specifically the MBC population that gives rise to broader immunity upon reinfection has not been completely characterized.

On repeat or secondary (2°) infection with a different serotype, primary (1°) MBCs that recognize the invading pathogen can clonally expand and secrete DENV-specific antibodies. Some MBCs rapidly proliferate and become plasmablasts, secreting antibodies, while others can re-enter germinal centers where they will undergo further affinity maturation (AM) through a process of antibody variable region gene rearrangement known as somatic hypermutation (SHM) to better adapt to the infecting virus. Once the current infection has cleared, some of these B-cells will become a new population of MBCs or LLPCs, secreting antibodies that broadly recognize both serotypes of infection or are type-specific to the current infection. [212,258] Many antibodies generated upon recall response are cross-reactive non-neutralizing (CR), recognizing epitopes on E or other viral proteins, but lack protective functions, and some are neutralizing in a type-specific manner (TS) against the serotype of the 1° or 2° infection, and a rare population may be cross-neutralizing, recognizing epitopes shared between multiple serotypes (CN). As such, the 1°MBCs form a critical founder population of future DENV-specific antibody-producing cells and antibody-mediated

protective immunity after repeat infection or vaccination.

Despite their importance in long-term broad antibody-mediated DENV immunity, the relative proportion and contribution of 1° MBCs that give rise to cross-reactive non-neutralizing antibodies, type-specific antibodies, and cross-reactive neutralizing antibody populations are unknown. This lack of knowledge hinders effective vaccine design and underscores important features of natural DENV immunity that remain to be fully understood.

Historically, analysis of the DENV-antibody response in humans has focused on neutralizing serum antibodies secreted by LLPC. While antibody-mediated memory to NS1 and DENV-specific MBCs have been relatively under-characterized. One reason for this is because DENV specific MBCs are rare, estimated at 0.1-0.4% of all MBCs, and hard to interrogate or enumerate in an antigen-specific manner. [63,65,67,259,260] Nevertheless, understanding the DENV-specific MBC founder population is critically important in designing, testing, and deploying DENV vaccines as well as more precisely understanding the basis of DENV immunity following natural infection. Our overarching model is that the relative proportions of TS-MBC, CR-MBC, and CN-MBC present at the time of repeat infection shape the features of broader antibody protection. Here we aim to utilize peripheral blood mononuclear cells (PBMCs), which include MBCs, isolated from cohort individuals with a history of DENV1 infection (Tables 2 and 3), to investigate the DENV-specific MBC-founder population following a single DENV1 infection.

Methods

Human research ethics

The study has been reviewed and approved by the Oregon Health & Science University Institutional Review Board (IRB#10212) for the non-endemic cohort and Ponce Medical School Foundation Review Board (IRB #180321-VR) for the endemic cohort. Informed consent was obtained from subjects upon initiation of their participation in the study.

Non-endemic human-cohort population n=24

DENV immune individuals in this study were enrolled in a larger study of long-term immunity following infection with the arthropod-borne viruses including DENVs, ZIKV, and CHIKV, as well as YFV vaccination. Study subjects with suspected arbovirus infection contacted the long-term immunity study and were offered participation in the study, and following informed consent, provided extensive additional history including other known and suspected arboviral infections, lifetime travel histories, and yellow fever virus (YFV), and Japanese encephalitis virus (JEV) vaccination histories.

Endemic Human-cohort population n=15

DENV immune individuals in this study were enrolled from a larger study of febrile illness in Ponce, Puerto Rico. Study subjects that came to the ER with fever seeking medical attention were approached to enroll in Sentinel Enhanced Dengue Surveillance System (SEDSS) in which they underwent testing for multiple causes of acute febrile illness, including DENV infection. Subjects with PCR confirmed DENV infections were offered to participate in the long-term immunity study and following informed consent, provided additional history including other known and suspected arboviral infections, lifetime travel histories, and vaccination histories. Samples were collected, processed, and shipped to Oregon Health & Science University for further analysis.

Sample collection and storage

On enrollment, subjects provided approximately 80 mL of blood, with 30 mL collected in BD serum vacutainers (Becton-Dickson) for serologic studies and stored at -80°C until used for assays. PBMCs were isolated from 50 mL of whole blood collected in BD EDTA or Heparin vacutainers (Becton-Dickson) and stored in liquid nitrogen.

Virus production

All DENV used in neutralization assays were propagated in Vero cells that over-express furin (generously provided by Fikadu Tafesse). [261] Vero-Furin cells were grown in MEM with 10% FBS, NEAA, anti-anti, and selection antibiotic G418 (InvivoGen) at 37°C and 5% CO_2 DENV used in neutralization assays included DENV1 WestPac'74 (generously provided by Stephen Whitehead, National Institutes of Health), DENV2 16803 (WRCEVA), DENV3 UNC3001, DV4IC.

Neutralization assays - fifty percent foci reduction neutralization test (FRNT50)

$FRNT_{50}$ titers were used to characterize subject sera as previously described. [262] Assays are prepared in duplicate. Subject sera were first heat-inactivated at 56°C for 30 minutes. Sera was diluted four-fold in MEM supplemented with 2% FBS from a starting dilution of 1:10. Serum dilutions were mixed with an equal volume of 50-100 foci-forming units (FFU) of virus giving a final starting serum dilution of 1:20. Virus-dilution mixes without sera were prepared simultaneously as controls for input virus FFUs. After incubation at 37°C for 1 hour, virus mixtures were inoculated into individual wells of 96 well plates, incubated for 1 hour at 37°C 5% CO_2, and overlaid with 1% methylcellulose in Opti-MEM (Gibco) supplemented with NEAA, anti-anti, amphotericin B, and 2% FBS and incubated at 37°C and 5% CO_2 for 48 hours. The overlay was then removed, monolayers were washed with PBS fixed with 0.4% formaldehyde, permeabilized. Cell monolayers were then stained with anti-E monoclonal antibody 4G2 and anti-prM antibody 2H2 followed by secondary antibody and horseradish peroxidase substrate True Blue (KPL). Foci were counted on CTL Immunospot Analyzer. The proportion of virus neutralized per well was calculated, and the serum dilution that neutralizes 50% of input virus ($FRNT_{50}$) was determined by sigmoidal dose-response curve fitting using GraphPad Prism, version 7.0.

Memory B cell Frequency

As previously described[255,263] briefly, PBMCs were thawed and resuspended in LDA media (RPMI 1640 medium (Gibco), 1×Antibiotic-Antimycotic (Corning), 1X non-essential amino acids (HyClone), 20 mM HEPES (Thermo Scientific), 50 μM β-ME, and 10% heat-inactivated fetal bovine serum (VWR). Cells were serially 2-fold diluted (10 wells per dose) starting with 3-5 x 10^5 PBMCs per well at the highest concentration and cultured in in 96-well round-bottom plates in a final volume of 200 μl per well. Cells were stimulated with IL-2 (Prospec) 1000U/ml and R848 (InvivoGen) 2.5μg/mL [264]. To determine background absorbance values, supernatants were used from 8 wells of unstimulated PBMCs only. Plates were incubated at 37°C and 5% CO_2 for 7 days. B cell stimulation and expansion was determined by performing ELISAs detecting total IgG. MBC precursor frequencies were calculated by the semi-logarithmic plot of the percent of negative cultures versus the cell dose per culture, as previously described. [265] Frequencies were calculated as the reciprocal of the cell dilution at which 37% of the cultures were negative for antigen-specific IgG production. Rows that yielded 0% negative wells were excluded since this typically resides outside of the linear range of the curve and artificially reduced the MBC precursor frequency. For subjects with low frequency of antigen-specific antibody-secreting cells frequency was determined by the number of positive wells divided by the total number of IgG positive secreting wells, multiplied by one million, giving a frequency per million PBMCs stimulated.

Antigen-specific ELISAs

Antigen-specific MBC frequencies were calculated by assaying LDA supernatants by antigen-specific ELISAs. [265] Ninety-six half-well ELISA plates (Greiner Bio-one) were coated with 1 μg/mL DENV 1,2,3, and 4 antigens (Microbix Biosystems Inc), or 2 μg/mL recombinant DENV-1 NS1 (Native Antigen) in PBS. Plates were incubated for four days at 4°C, washed with PBS-T

(0.05% Tween), and blocked for 1 hour with 5% milk prepared in PBS-T and then 20µL of LDA supernatants were added to each well and incubated at RT for 1 hour. Plates were washed 4 times with wash buffer, and 50 µL of 1:3,000 dilution of anti-human IgG-HRP (H + L) (Novusbio, NBP1-73319) detection antibody was added and incubated at RT for 1 hour. Plates were washed 4 times with wash buffer, 50 µL of colorimetric detection reagent containing 0.4mg/ml o-phenylenediamine and 0.01% hydrogen peroxide in 0.05M citrate buffer (pH 5) were added and the reaction was stopped after 20 minutes by the addition of 1M HCl. Optical density (OD) at 492nm was measured using a CLARIOstar ELISA plate reader. LDA and NS1 endpoint wells were scored positive at ODs at least 2-fold above background (unstimulated PBMC wells for LDA).

Fluorescently labeling virus

As previously described, [266-268] DENV-1 West Pac 74' was propagated in Vero cells (multiplicity of infection 0.1) in serum-free media. Viral supernatant was concentrated using a 100kD Amicon filter (Millipore) and titrated to determine titer prior to labeling. Sodium bicarbonate (0.2 M) and Alexa Fluor dye (Life Technologies) were added to the concentrated virus (overall pH 8.3) and allowed to incubate for one hour at room temperature while stirring. The reaction was stopped with 1.5 M hydroxylamine and allowed to incubate for an additional hour at room temperature. Free dye was removed using PD-10 columns (GE Health Care Biosciences Corp). The virus was aliquoted and stored at -80 protected from light.

Labeling quantification

Fluorescent labeling and ability of virus prep to bind to anti-E antibody was quantified by flow cytometry as previously described using 3.0-micron beads coated with goat anti-mouse IgG (Fc)

(Spherotech, Inc MPFc-30-5).[268] Beads were incubated with 1mg/mL of mouse anti-dengue 4G2 antibody, washed and resuspended in 1 ml of PBS containing 10%FBS. Control beads were coated with an anti-mouse beta-actin antibody. An aliquot of Alexa fluor-labeled DENV-1 was incubated with coated beads for 1 hour at room temperature while rocking. Beads were washed two times and read on a Guava easyCyte flow cytometer.

Antigen-specific flow cytometry

As previously described, [268] briefly donor PBMCs were thawed from liquid nitrogen and resuspended in RPMI media with 10% FBS and 20 μg/mL DNase (Life Technologies). Cells were pelleted and washed again in PBS. Cells were then labeled with LIVE/DEAD stain (Life Technologies). Cells were rinsed and resuspended in RPMI containing 10% FBS. All further steps were performed at 4°C. PBMC were incubated with a titrated amount of AF-DENV for 30. Cells were washed twice and then labeled with a cocktail of cell surface marker antibodies: CD3-APC-H7, clone SK7; CD14-APC-H7, clone M0P9; CD19-PE-Cy7, clone SJ25C1, CD27-BV785, clone O323, and polyclonal IgD-PE. Cells were washed twice, fixed in 1% Cytofix (BD Biosciences), and analyzed on a FACS Aria II. Data analysis was performed using FlowJo v10.

Single-cell ex vivo stimulations

As described above, LIVE/CD3−CD14-CD19+CD27+IgD-/DENV++ cells were sorted with a BD FACS Aria in single-cell mode into a 96-well plate. The sorted cells were cultured in the presence of CD40L and IL-21 for conversion to antibody-secreting cells. As previously described[269] briefly, cells were sorted into 96-well tissue culture plates containing irradiated 3T3 cells (4500 rad) expressing human CD40L (4.0 × 10^4 cells/well), with RPMI media

supplemented with 20% FBS and recombinant IL-21 (Sino Biologicals) at a final concentration of 50 ng/mL. The plates were incubated at 37 °C, 5% $C0_2$, for 14 days and screened for antibody production by IgG, IgM, and DENV ELISA.

Statistical methods

Non-parametric Spearman correlation was used to determine the correlation between NS1 and DENV-1 antibody and MBC frequencies using GraphPad Prism version 9.1.1.

Results

Study subjects

A total of 39 subjects with a history of DENV-1 infection that occurred between 1975 and 2018 were used for this study. Individual subject sera and peripheral blood mononuclear cells (PBMC) were obtained ranging from 1-43 years post-infection. Fifteen of the subjects are from a larger endemic cohort of arbovirus immune subjects in Ponce, Puerto Rico (Table 4), and twenty-four subjects are from a larger non-endemic cohort of arbovirus exposed individuals based in Portland, Oregon (Table 5). Intake questionnaire and infection history were documented at the time of enrollment.

Subject ID	Age	Time pi (year)	DV1 (WP'74) NT 50	DV2 (16803) NT 50	DV3 (IC2) NT 50	DV4 (IC) NT 50	ZIKV NT 50
51630	21	5.8	1547.2	<1:20	26.0	68.3	<1:20
51653	20	5.8	321.5	53.7	33.0	39.4	<1:20
51665	20	5.3	796.9	<1:20	<1:20	<1:20	<1:20
51618	20	6.3	290.1	<1:20	<1:20	<1:20	<1:20
50209	22	5.5	349.1	<1:20	<1:20	<1:20	<1:20
51743	19	6.3	6229.2	419.8	1067.2	161.4	958.8
51573	32	6.6	354.8	<1:20	<1:20	20.1	<1:20
50183	16	5.5	2485.4	125.5	288.6	173.0	664.4
51556	19	6.8	156.5	<1:20	33.4	48.2	<1:20
51629	20	5.8	803.2	149.8	27.8	20.8	<1:20
50498	21	6.3	1466.6	33.0	113.7	61.3	275.9
51762	16	6.3	4901.8	76.8	320.2	124.4	137.0
51736	14	6.5	1077.1	73.2	29.6	38.5	366.5
51712	15	6.6	873.7	<1:20	56.7	<1:20	<1:20
50159	48	6.3	180.8	<1:20	5462.4	94.7	<1:20

Table 4 Summary demographics and serology from endemic cohort.

All subjects in the endemic cohort have a PCR confirmed DENV infection that occurred in Puerto Rico. <1:20 denotes neutralization titer below the limit of detection. BK generated some of the NT_{50} data in this table. Data analyzed by ZL.

Subject	Age	Country of infection	Time pi (year)	DV1 (WP'74) NT50	DV2 (16803) NT50	DV3 (IC2) NT50	DV4 (IC) NT50	YFV NT90	ZIKV NT50
10107	32	Haiti	2.4	881.7	79.4	125.8	28.9	<1:10	73.4
10266	32	Fiji	3.8	385.9	27.2	55.7	< 1:20	<1:10	<1:20
10395	67	India*	1.7	815.9	117.7	160.4	31.3	<1:10	<1:20
10731	44	Venezuela*	36.7	101.4	< 1:20	< 1:20	< 1:20	<1:10	<1:20
10825	47	Thailand	3.7	962.6	109.3	77.2	87.1	94.0	521.4
11015	73	Vanuata	1.1	1873.0	110.3	279.8	30.5	161.8	<1:20
12497	38	Singapore *	20.6	85.0	<1:20	<1:20	<1:20	<1:10	<1:20
11919	36	India *	8.6	69.9	<1:20	<1:20	<1:20	<1:10	<1:20
14011	20	Mexico	3.7	256.0	34.6	28.9	<1:20	<1:10	<1:20
15453	54	Puerto Rico	10.6	582.5	39.4	74.1	<1:20	<1:10	<1:20
15594	49	Indonesia	20	201.1	< 1:20	37.0	< 1:20	<1:10	<1:20
16155	70	Samoa	43	380.6	< 1:20	< 1:20	< 1:20	<1:10	<1:20
16178	55	Marshall Islands	21	232.2	< 1:20	< 1:20	<1:20	<1:10	<1:20
16534	33	*Phillippines	18	5771.9	30.3	81.2	111.8	<1:10	<1:20
16308	36	India	1.75	390.9	< 1:20	20.8	< 1:20	<1:10	<1:20
12626	73	Mexico	7	281.8	< 1:20	< 1:20	< 1:20	<1:10	< 1:20
10547	30	*Brazil	2.5	87.8	<1:20	<1:20	<1:20	<1:10	<1:20
10735	27	Dominican Republic	8	1116.3	<1:20	32.4	58.7	<1:10	<1:20
11220	27	*Indonesia	0.8	150.3	< 1:20	< 1:20	22.0	<1:10	<1:20
12003	28	French Guiana	6.6	60.9	< 1:20	< 1:20	< 1:20	102.6	<1:20
16303	20	Thailand	0.67	894.7	< 1:20	< 1:20	< 1:20	24.7	<1:20
10994	29	Nicaragua	2	53.1	< 1:20	< 1:20	< 1:20	<1:10	<1:20
14756	33	Vietnam	0.5	329.1	< 1:20	< 1:20	< 1:20	<1:10	<1:20
16247	68	Indonesia	2.5	390.7	< 1:20	< 1:20	86.9	<1:10	<1:20

Table 5 Serology demographics and serology for non-endemic cohort.

*Serology against a panel of flaviviruses for non-endemic cohort based in Portland, Oregon. *denotes born and spent >5 years in an endemic region. <1:20 denotes a neutralization titer below the limit of detection. BK generated some of the NT_{50} data in this table. Data analyzed by ZL.*

Serology by subject

Serum neutralization (NT_{50}) titers were determined for immune serum from thirty-nine subjects with presumed DENV-1 infection history as determined by serology (a neutralization titer of greater than 4-fold higher than any other serotype) or PCR confirmation during acute infection (Tables 2 and 3). Sera were used in neutralization assays against a panel of DENV serotypes 1,2,3,4 as well as closely related flaviviruses Zika (ZIKV) and Yellow Fever (YFV). We conducted foci reduction neutralization titration assays to determine the 50% neutralization titer for each virus (NT_{50}).

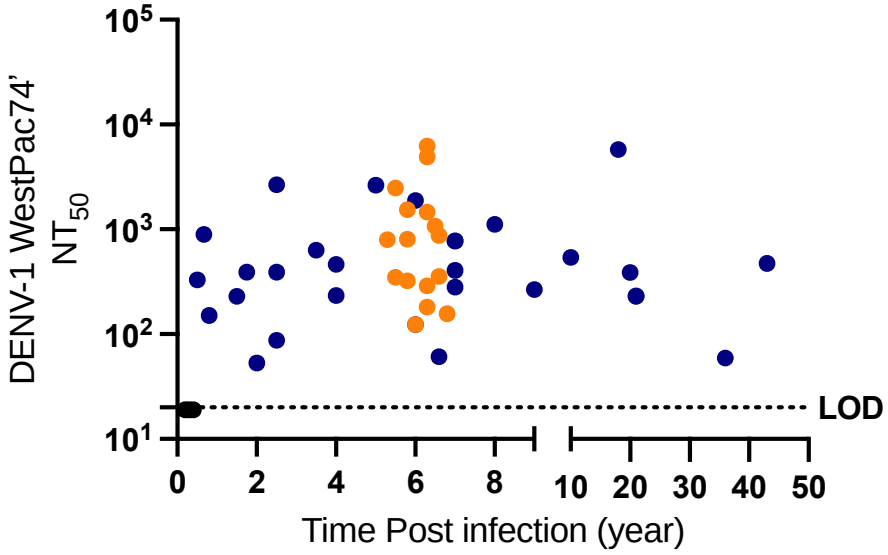

Figure 14 Neutralization titer overtime

DENV-1 NT50 titer against WestPac 74'. Endemic subjects in orange, non-endemic subjects in blue, naïve subjects in black. LOD is 20, samples below the LOD are assigned an arbitrary number of 19.

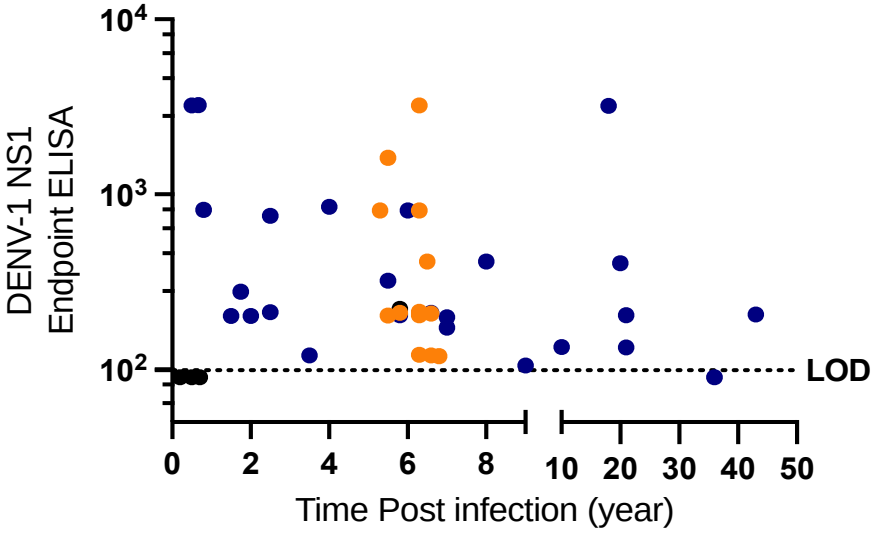

Figure 15 NS1 endpoint ELISA titer overtime

DENV-1 NS1 endpoint ELISA titer. Endemic subjects in orange, non-endemic subjects in blue, naïve subjects in black. LOD is 100, samples below the limit of detection were assigned an arbitrary value of 99.

LLPC-derived antibodies against DENV-1 and NS1

Neutralization assays against DENV-1 WestPac 74' were performed on serum samples from endemic and non-endemic cohorts (Figure 14). The titers were higher in the endemic cohort GMT 798 (156 to 6229) when compared to samples from non-endemic subjects GMT 379 (53 to 5772). With DENV-1 NT50 titers above the limit of detection observed for all subjects, as far out as 43 years post-infection. NS1 endpoint ELISA titers were also determined for all subjects (Figure 15). NS1-specific antibodies were detected in all but one of the subjects (36 years post-infection). Geometric mean endpoint titers were similar between both cohorts, 303 (111 to 3223) for the endemic and 358 (115 to 3234) for non-endemic.

DENV-specific MBC frequency in immune subjects 1 to 43 years post-infection

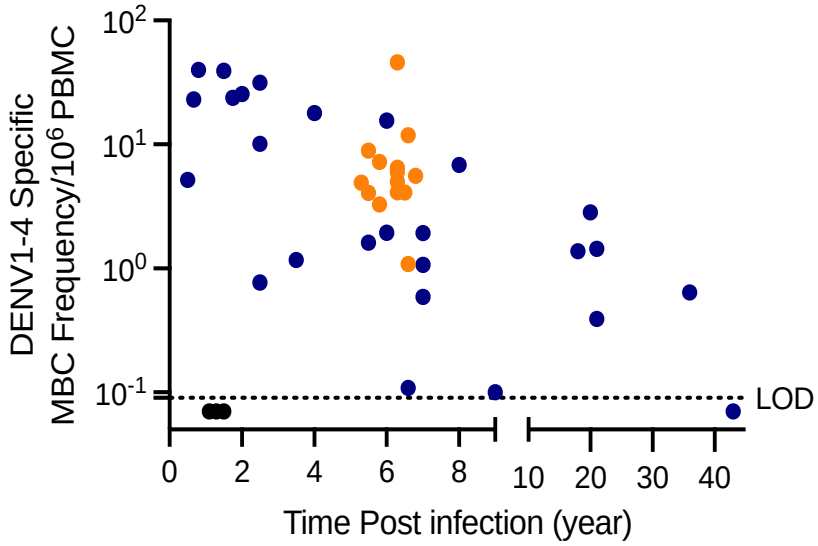

Figure 17 DENV-MBC frequency overtime.

Cross-sectional view of whole virus (DENV 1-4) MBC frequency by limiting dilution assay per 10^6 PBMC. Blue data points are endemic cohort subjects, orange points are endemic subjects, black points are naïve subjects. The limit of detection (LOD) is 0.1 MBC per 10^6 PBMC

To characterize the MBC population in DENV infected subjects, limiting dilution assays and flow cytometry were performed. Following *in vitro* stimulation, DENV-specific MBCs were present in all, but 1 subject, as far out as 37 years post-

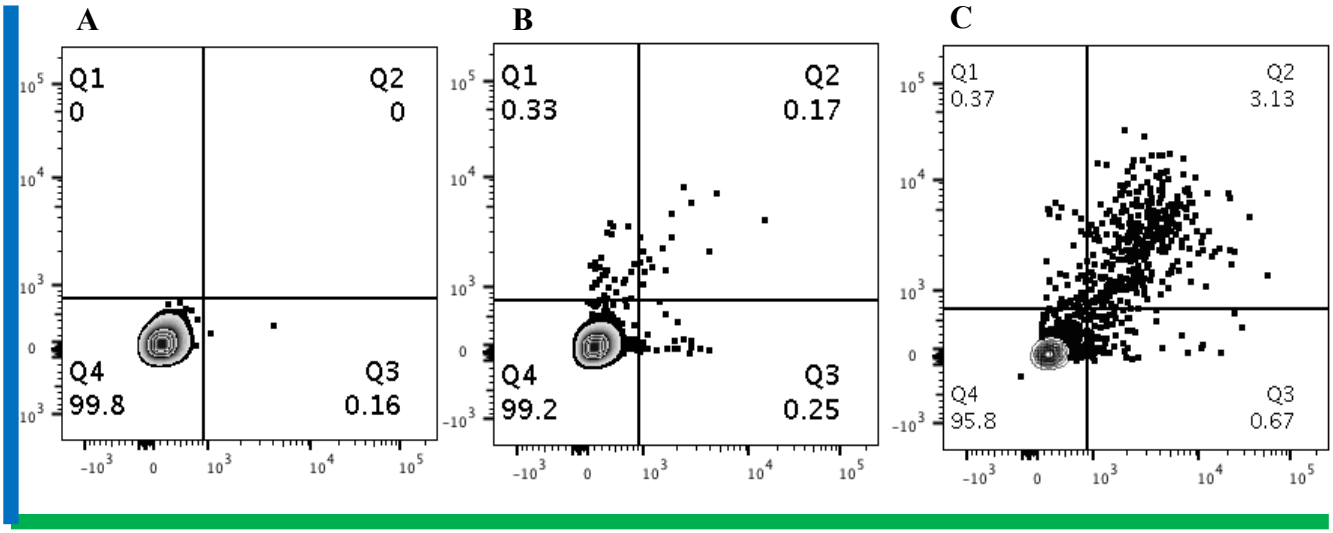

Figure 16 Flow plot depicting gating scheme for DENV + MBCs

Representative flow plots depicting staining to AF647 DENV-1 (blue) and AF488 (green) DENV-1 in MBCs (liveCD14-CD3-CD19+CD27+IgD-) Q2 represents DENV-double positive MBCs. A) Flavivirus naïve donor. B) DENV-1 immune donor 3.8 years post infection. C) DENV-1 immune donor 1.6 years post infection. Experiments performed at RIU with Dr. Anuja Mathew.

infection (Figure 17), although the magnitude differed between individual subjects. Endemic subjects had a geometric mean MBC frequency of 5.8 (1 to 46/10^6 PBMC). Non-endemic subjects had a geometric mean MBC frequency of 3.2 (0.1 to 40/10^6 PBMC). Representative flow plots (Figure 16) depict a DENV-naïve subject as well as two immune subjects. DENV-specific MBCs were identified in all 12 non-endemic subjects analyzed, out to 43 years post-infection (Figure 18) geometric mean frequency 0.146/100 MBC (0.02 to 3.13/100 MBC). A strong correlation (R^2 0.89) was observed between MBC frequency as determined by limiting dilution assay and flow cytometry (Figure 19).

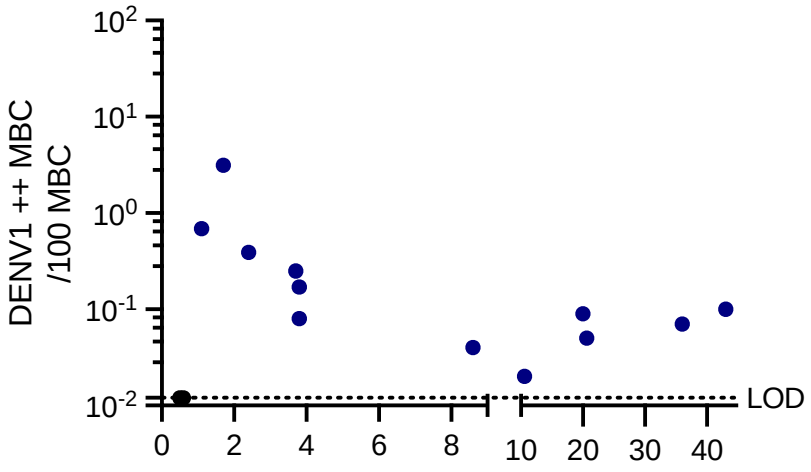

Figure 18 DENV-specific MBC frequency by flow cytometry.

Figure 2-6 DENV-1 specific MBC frequency per MBC determined by flow cytometry with fluorescently labeled DENV-1. Data are shown from 12 subjects from non-endemic cohort. Naïve subjects shown in black.

NS1 specific MBCs frequency in DENV-immune subjects

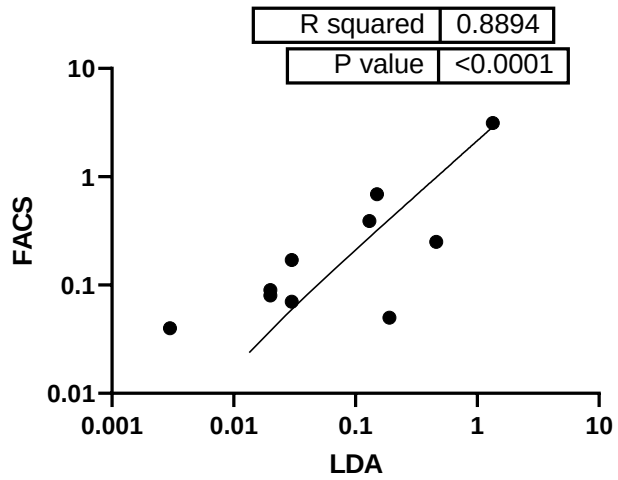

Figure 19 Correlation between LDA and FACS.

Correlation between DENV-specific frequency as determined by limiting dilution assay (LDA) and flowcytometry (FACS).

NS1-specific MBCs were present in all, but 1 subject, as far out as 37 years post-infection (Figure 21), although the magnitude differed between individual subjects. Endemic subjects had a geometric mean MBC frequency of 4.1 (1 to 19/10^6 PBMC) and non-endemic subjects had a geometric mean MBC frequency of 1.6 (0.15 to 42/10^6 PBMC).

Differences between endemic and non-endemic cohorts

The relationship between NS1 and whole DENV MBC frequency was investigated between endemic and non-endemic environments (Figure 20). There was no relationship observed between NS1 and DENV MBC frequency in the endemic cohort (R^2 0.093) compared to the non-endemic

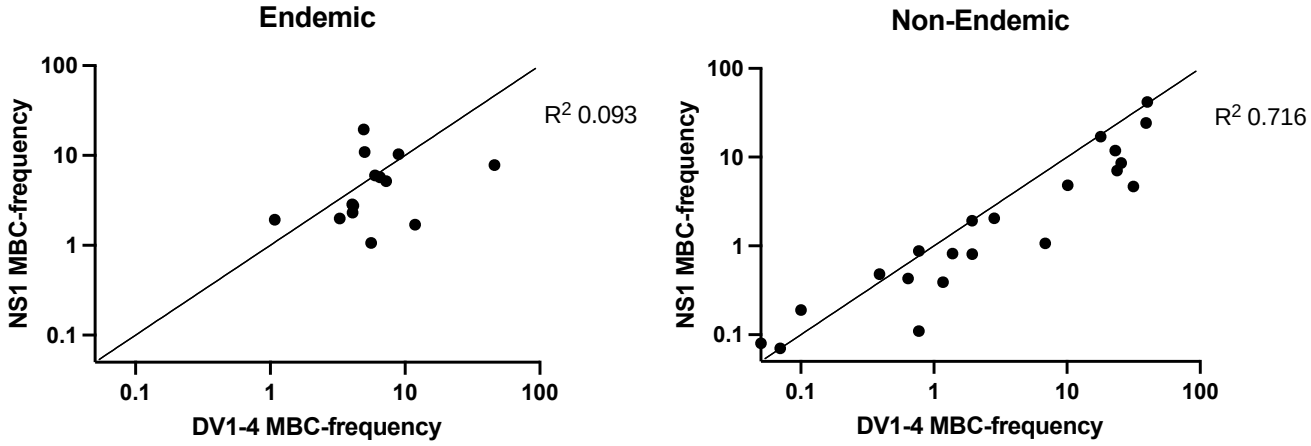

Figure 20 Correlation between DENV and NS1 MBC frequency.

Differences in the relationship between NS1-specific MBC frequency and DENV-specific MBC frequency in endemic and non-endemic cohorts.

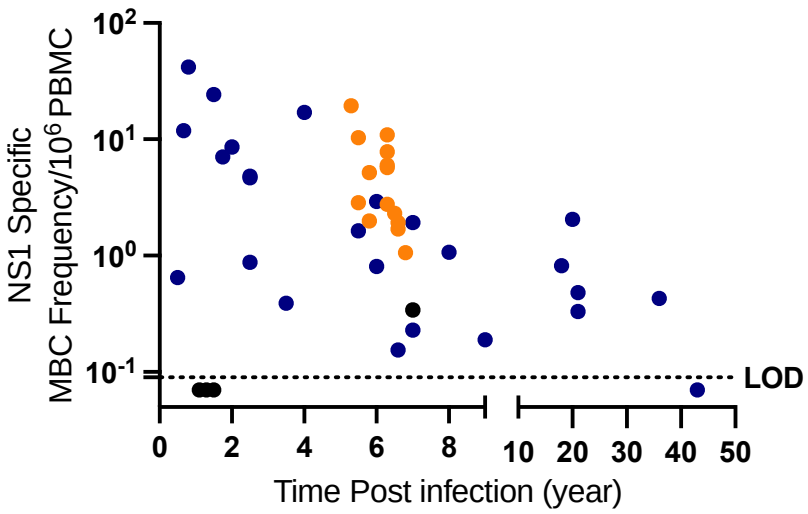

Figure 21 NS1-specific MBC frequency overtime.

Cross-sectional view of DENV-1 NS1 specific MBC frequency by limiting dilution assay per 10^6 PBMC. Blue data points are endemic cohort subjects, orange points are endemic subjects, black points are naïve subjects. The limit of detection (LOD) is 0.1 MBC per 10^6 PBMC.

cohort where we observed a relationship between NS1 and DENV specific MBC frequencies (R^2 0.716). There was no relationship observed between LLPC-derived antibodies (NS1 ELISA titer and NT_{50} titer) in endemic (R^2 0.137) or non-endemic R^2 0.131) cohorts (Figure 22).

Specificity of flow cytometry approach using fluorescently labeled DENV as antigen-bait

To confirm that MBCs that bound to fluorescently labeled DENV by flow cytometry were antigen-specific we employed single-cell sorting of MBCs that bound fluorescently labeled virions both AF488 and AF647 (liveCD14-CD3-CD19+CD27+IgDDENV++) and stimulated them to become

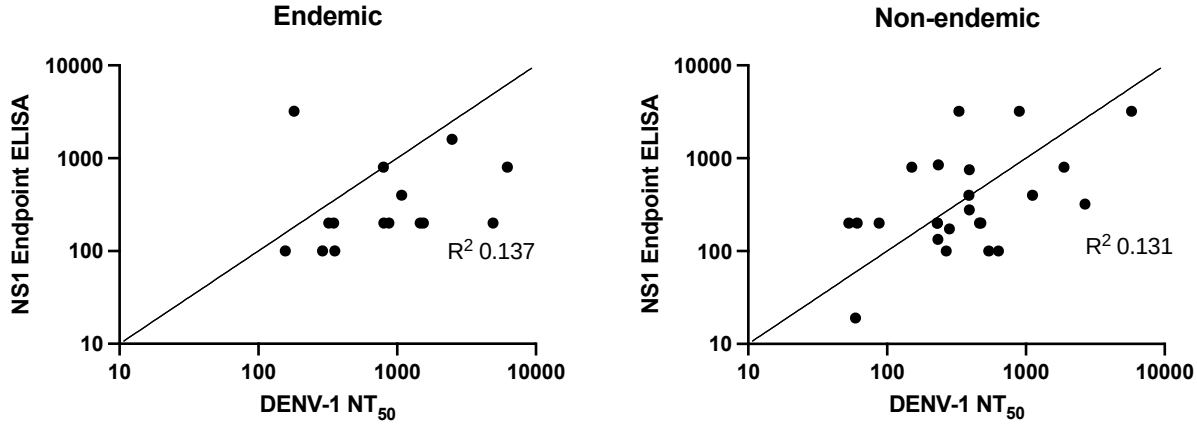

Figure 22 Correlation between LLPC-derived antibodies.

Relationship between LLPC-derived antibodies against NS1 and neutralizing antibodies against DENV-1.

antibody-secreting cells (Table 6). In Summary 160 DENV double-positive MBCs were single-cell sorted into 96-well plates along with 3T3-CD40L feeder cells. Of those, 46 cells (26%) proliferated and differentiated into antibody-secreting cells. Ten (23%) were IgM+, 29 (69%) were IgG+, of IgG+ wells 24 (83%) were also positive by DENV ELISA, and 4 wells (16.6%) were neutralizing against DENV-1. Two wells were positive by DENV ELISA, but negative by IgG and IgM ELISA indicating possible IgA secreting antibodies.

Discussion

Several groups have shown that whole virions are required to display and capture the complete DENV neutralizing antibody epitope repertoire, while E subunits or whole recombinant E antigen alone preferentially capture non-neutralizing cross-reactive antibodies.[67,77,259,260,270,271] Despite this critical observation, prior to this work, whole DENV virions had not been fully

Well	1-A2	1-A10	1-A11	1-A12	1-B3	1-C2	1-C12	1-D2	1-D3	1-D4	1-D9	1-D10	1-E4	1-E6
Ab	IgG (+)	IgG (+)	IgG (+)	IgG (+)	IgG (+)	IgG (+)	IgG (+)	IgG (+)	IgM(+)	IgG (+)	IgG (+)	IgG (+)	pending	IgM
DENV	DV (+)	DV (+)	DV (+)	DV (+)	DV (+)	DV (+)	DV (+)	DV (+)	pending	DV (+)	DV (+)	DV (+)	DV (+)	pending
Neut	No	No	No	Yes	No	No	No	No	No	No	No	No	No	No
Well	1-E10	1-F6	1-F8	1-F10	1-G1	1-G5	1-G10	1-H1	1-H2	1-H3	1-H7	1-H9	1-H10	2-A4
Ab	IgM(+)	IgG (+)	IgG (+)	IgM(+)	IgG (+)	IgM(+)	IgG (+)	IgG (+)	IgG (+)	IgG (+)	IgM(+)	IgG (+)	IgM(+)	IgM(+)
DENV	pending	DV (+)	DV (+)	pending	DV(-)	pending	DV (+)	DV (+)	DV (+)	DV(-)	pending	DV (+)	pending	pending
Neut	No	No	No	No	No	No	No	No	No	No	No	No	No	No
Well	1-E10	1-F6	1-F8	1-F10	1-G1	1-G5	1-G10	1-H1	1-H2	1-H3	1-H7	1-H9	1-H10	2-A4
Ab	IgM(+)	IgG (+)	IgG (+)	IgM(+)	IgG (+)	IgM(+)	IgG (+)	IgG (+)	IgG (+)	IgG (+)	IgM(+)	IgG (+)	IgM(+)	IgM(+)
DENV	pending	DV (+)	DV (+)	pending	DV(-)	pending	DV (+)	DV (+)	DV (+)	DV(-)	pending	DV (+)	pending	pending
Neut	No	No	No	No	No	No	No	No	No	No	No	No	No	No
Well	2-A12	2-B6	2-B7	2-C4	2-D2	2-D4	2-D7	2-D8	2-D9	2-E7	2-E10	2-E11	2-F8	
Ab	IgG (+)	IgG (+)	IgG (+)	IgG (+)	IgG (+)	IgG (+)	IgM(+)	IgG (+)	pending	IgG (+)	IgG (+)	IgM(+)	IgG (+)	
DENV	DV (+)	DV (+)	DV (+)	DV(-)	DV (+)	DV(-)	pending	DV (+)	DV (+)	DV(-)	DV (+)	pending	DV (+)	
Neut	Yes	No	No	No	Yes	No	No	Yes	No	No	No	No	No	

Table 6 DENV++ single cell stimulations.

Qualities of supernatants from DENV specific MBCs single-cell sorted and expanded in tissue culture for 14 days in 96-well plates. Supernatants were assayed by ELISA for total IgG, IgM, and DENV. Blue represents wells that are both IgG+ and DENV+, peach represents IgM wells, green represents wells that were neutralizing by microneutralization assay.

exploited as bait for antigen-specific MBCs. Fluorescently labeled DENV virions have been used

to enumerate individual MBCs in "fluorospot" assays, and for quantification of MBC in human PBMCs but, prior to this work, fluorescently labeled whole virions have not been used to single-cell sort and analyze DENV specific MBCs.[268-272] DENV-specific mAbs have been isolated from humans through the use of MBC-myeloma cell hybridomas or immortalizing MBCs. Both of these methods are time, material, and labor-intensive, require additional screening to identify antigen-specific MBCs and have a low efficacy rate. [259,273-275] Irrespective of approach, MBC-derived mAbs from these studies relied on a handful of immune donors with little or no documented infection history, and many from endemic regions where donors have experienced multiple flavivirus infections. Therefore, to fully elucidate the specificity and breadth of the DENV-specific founder population, MBCs from donors with well-documented infection histories are needed. In this study, we evaluated the DENV immune response in well-characterized endemic and non-endemic cohort subjects with a DENV-1 infection history (Tables 4 and 5). Using two complementary approaches we determined DENV-specific MBC frequencies in a large number of subjects. As a proof of concept, we isolated DENV double-positive MBCs following flow-cytometry with fluorescently labeled antigen bait and observed a high percentage of MBCs that secreted DENV-specific antibodies upon stimulation.

In addition to validating our approaches to elucidate antigen-specific MBCs, we observed neutralizing LLPC-derived antibodies in all of our subjects as well as DENV and NS1-specific MBCs in all but one of our subjects (43 years post-infection). Providing supporting evidence that both populations of antibody-mediated protection, LLPC, and MBC are long-lived, at least several decades following natural infection, for both our endemic as well as our non-endemic subjects. Although the time post-infection is much narrower with our endemic subjects (5.3 to 6.8) compared to a greater than 40-year span for our non-endemic cohort (0.5 to 43). We observed no

relationship between LLPC-antibody titer (ELISA or neutralization) and MBC frequency (data not shown), similar results were previously observed. [212] Providing further evidence that these are two distinct and independent measures of B-cell mediated protection, and points out the importance of interrogating both long-lived compartments of the B-cell response to DENV.

In the current study we observed a relationship between DENV and NS1 MBCs in our non-endemic cohort, but no relationship in our endemic cohort (Figure 23). We hypothesize that this could be due to immune skewing following repeat antigen exposure in our endemic cohort subjects. However, the time span post infection for the endemic cohort is relatively short therefore there is not enough time-dependent variability in the samples to investigate this fully, warranting further longitudinal study.

Regardless of how challenging and complex, studying single MBCs and the mAbs they are programmed to secrete, will provide a comprehensive view of the MBC-founder population and is anticipated to provide much-awaited insight into pre-existing DENV immunity and the development of broader immunity. Based on the success of our preliminary work, our goal for future work is to extend this approach to characterize multiple immune donor repertoires in our cohort. By adapting our approach for DENV we will be poised to contribute substantially to antibody-based protection or immunotherapeutics for emerging pathogens.

Acknowledgments

The work presented in this manuscript was supported by grants from the National Institutes of Health R01AI153434 (WBM), R21AI135537(WBM), UL1TR002369 (WBM), Takeda IISR 2016-101586 (WBM), and the Sunlin and Priscilla Chou foundation (WBM). Centers for Disease Control and Prevention U01CK000437 (VRA) and U01CK000580 (VRA). The funders had no role in study design, data collection and analysis, decision to publish, or preparation of this manuscript.

Chapter 3: Infection with chikungunya virus confers heterotypic cross-neutralizing antibodies and memory B-cells against other arthritogenic alphaviruses predominantly through the B domain of the E2 glycoprotein

This chapter is based on a manuscript under review at PLOS neglected tropical diseases (December 2021)

John M. Powers[1*#], **Zoe L. Lyski[2*]**, Whitney C. Weber [1], Michael Denton [1], Magdalene M. Streblow [1], Adam T. Mayo [1], Nicole N. Haese [1], Chad D. Nix [2], Rachel Rodríguez-Santiago[3], Luisa I. Alvarado[3], Vanessa Rivera-Amill [3], William B. Messer [2,4,5], Daniel N. Streblow [1,6]

[1] Vaccine and Gene Therapy Institute, Oregon Health and Science University, Beaverton, Oregon, USA [2] Department of Molecular Microbiology and Immunology, Oregon Health and Science University, Portland, Oregon, USA [3] Ponce Health Sciences University/ Ponce Research Institute, Ponce, Puerto Rico [4] Department of Medicine, Division of Infectious Disease Oregon Health and Science University, Portland, Oregon, USA [5] OHSU-PSU School of Public Health, Program in Epidemiology, Oregon Health and Science University, Portland, Oregon, USA [6] Division of Pathobiology and Immunology, Oregon National Primate Research Center, Beaverton, Oregon, USA

* Contributed equally to this manuscript

Author contributions: Conception of work JMP, ZLL, WBM, DNS, Data collection, JMP, ZLL, WCW, MD, MMS, ATM, NNH, CDN. Collection/ management of human samples ZLL and RRS. Data analysis JMP, ZLL, WCW, WBM, DNS. Drafting of the article JMP and ZLL. Critical revision of manuscript JMP, ZLL, WCW, WBM, DNS. Acquired funding LIA, VRA, WBM, and DNS.

Abstract

Chikungunya virus is a mosquito-borne alphavirus associated with an acute febrile syndrome often followed by chronic arthritis that persist for months to years post infection. Neutralizing antibodies are the primary immune correlate of protection elicited by infection. Using convalescent blood samples collected from both endemic and non-endemic human subjects with suspected or confirmed chikungunya infection, we identified antibodies with broad neutralizing properties against other alphaviruses within the Semliki Forest complex. Cross-neutralization did not extend to the Venezuelan Equine Encephalitis virus complex, suggesting that the incidence of broadly neutralizing antibodies may be complex restricted. In addition to serology, we also performed memory B-cell analysis, finding chikungunya-specific memory B-cells in all subjects in this study as far out as 24 years post infection. We functionally assessed the ability of memory B-cell derived antibodies to bind to chikungunya virus, the distantly related Mayaro virus, as well as the highly conserved B domain on the viral surface E2 protein thought to contribute to cross-reactivity between related Old World alphaviruses. To specifically assess the role of the E2B domain in cross-neutralization, we depleted Mayaro virus E2 B domain specific antibodies from chikungunya subject convalescent sera, finding E2B depletion significantly decreases Mayaro virus specific cross-neutralizing antibody titers with no significant effect on chikungunya virus neutralization, indicating that the E2 B domain is a key target of cross-neutralizing and potentially cross-protective neutralizing antibodies.

Author summary

The emergence and re-emergence of alphaviruses as important human pathogens raises questions about the durability and breadth of alphavirus immunity following natural infection in humans. In this study, we examine human immune sera from twelve individuals as far back as 24 years post

infection with chikungunya virus and test the sera against a panel of five Old World arthritogenic alphaviruses and one New World encephalitic alphavirus. Both homotypic and cross-reactive memory B-cells were identified in subjects as far out as 24 years post infection indicating a robust and durable humoral immune response. Our results confirm that infection with chikungunya virus can be expected to elicit protective immunity against repeat infection with chikungunya as well as related alphaviruses for years to decades after initial infection. This cross-reactivity might contribute to the restriction of transmission of closely related alphaviruses and indicates the potential for chikungunya candidate vaccines to elicit broad protection against other alphaviruses in the Semliki Forest complex.

Introduction

Alphaviruses, members of the family *Togaviridae*, are a large group of arthropod-borne viruses with worldwide distribution that cause both sporadic infections and epidemics. These predominantly mosquito-borne viruses have a wide host range and can replicate in a variety cell types [276-278]. The alphaviruses are broadly grouped in seven distinct antigenic complexes – Barmah Forest, Eastern Equine Encephalitis, Middleburg, Ndumu, Semliki Forest, Venezuelan Equine Encephalitis, and Western Equine Encephalitis [279]. These viruses can also be divided into two categories, New and Old World, based on phylogenetic relatedness and clinical manifestations of disease. While infections with Old World alphaviruses, such as chikungunya virus (CHIKV) and Semliki Forest virus (SFV) predominantly cause myalgia and arthralgia, New World alphaviruses such as Venezuelan equine encephalitis virus (VEEV) and Eastern equine encephalitis virus (EEEV) infections can cause life-threatening encephalitis.

Of the alphavirus members, CHIKV has the widest global distribution, with cases of CHIKV infection reported in over 40 countries worldwide [280]. Puerto Rico recently experienced a CHIKV

epidemic starting in May 2014 and official surveillance reported 28,327 suspected cases and 31 deaths by the epidemic's end [281]. Other related alphaviruses include O'nyong nyong virus (ONNV), which forms a monophyletic group with CHIKV and is endemic in sub-Saharan Africa and periodically causes outbreaks in West and East Africa [282,283]. Mayaro (MAYV) and Una (UNAV) viruses are closely related alphaviruses that commonly cause disease outbreaks in Central and South America [127]. The most distant member of the SFV complex is Ross River virus (RRV), which is endemic to Australia and several neighboring Pacific Islands [280]. Outside of the SFV complex are the distantly related New World encephalitic alphaviruses that circulate in North, South, and Central America.

In general, alphaviruses are ~70 nm enveloped viruses with an icosahedral capsid of $T = 4$ symmetry that is composed of 240 capsid monomers. Each virus particle contains an ~10 – 12 kb single-stranded, positive sense RNA genome [284-286] that contains two open reading frames, both translated with a 5' cap and 3' polyA tail. The viral genome encodes four nonstructural proteins (nsP1 – nsP4) involved in RNA replication, and five structural proteins (Capsid, E3, E2, 6K, E1) required for viral encapsidation and budding [277,287,288]. Structural E1-E2 heterodimers trimerize to form the surface spikes of the virus envelope responsible for attachment and entry into host cells. Specifically, E2 is responsible for cellular receptor binding, and E1 mediates membrane fusion [289]. The structural proteins E1 and E2 are key targets of the host antibody response. In humans and mice, the antibody response is primarily generated against E2 [290-293]. Previous studies have reported the development of cross-neutralizing antibodies (Abs) in model organisms and humans following infection with SFV complex alphavirus members, and the B domain of the E2 (E2 B) glycoprotein has been implicated as a potential target for broadly cross-neutralizing antibodies due to the disruption of the trimeric spike [121,125,293-295].

Virus-specific antibodies (Abs) are secreted initially by short-lived plasma cells that differentiate in germinal centers of peripheral lymph nodes and then by long-lived plasma cells (LLPCs) that traffic to bone marrow to secrete Abs for months to years post-exposure [296]. LLPC-derived Abs are thought to protect against repeat infections with homologous or closely related pathogens. Memory B-cells (MBCs) also differentiate in germinal centers and circulate in low numbers in peripheral blood. MBCs do not secrete Abs, but instead patrol the periphery for invading pathogens, poised to quickly respond to repeat infection by proliferating and differentiating into Ab secreting plasma cells. It has been reported that MBCs respond to antigenically distinct, but related pathogens that evade preexisting serum Abs [297,298]. Consequently, MBCs have the potential to play a critical role in developing broad immunity especially in the face of waning Ab titers and the emergence of new closely related alphaviruses.

To further characterize the durability, potency, and breadth of cross-reactive anti-alphavirus Abs and MBCs, we evaluated a panel of convalescent samples from subjects enrolled in either a non-endemic cohort based in Portland, Oregon or an endemic cohort based in Ponce, Puerto Rico. Subjects had suspected or confirmed CHIKV infection and samples from three alphavirus naïve subjects were included as controls (Table 6). We evaluated study participants for the presence of CHIKV neutralizing antibodies, cross-alphavirus neutralizing antibodies, and CHIKV-specific and cross-reactive memory B cells. We observed that subjects infected with CHIKV displayed varying levels of neutralizing antibodies against other SFV-complex members, but this breadth did not extend to distantly related VEEV. Similarly, interrogation of the MBC compartment following natural infection identified MBCs capable of recognizing both CHIKV and MAYV. Additionally, we looked for the presence of antibodies and MBCs that recognize the E2 B domain, which has previously been implicated as a potential target for broadly cross-neutralizing antibodies [121,294].

The results of this study indicate that natural infection with CHIKV elicits a robust and durable immune response against repeat infection with CHIKV as well as related Semliki Forest complex alphaviruses for years to decades after initial infection. This cross-reactivity might contribute to the restriction of transmission of closely related alphaviruses in arbovirus endemic regions.

Figure 24 Geographical distribution of infection.

Results

Study subjects

Twelve subjects with a confirmed or suspected history of CHIKV infection that occurred between 1992 and 2016 were used for this study (Table 8). Individual subject sera and peripheral blood mononuclear cells (PBMC)

Subject ID	Age at time of infection	Country of birth	Country of infection	Time post infection (Years)	CHIKV PRNT50	Symptoms
1	40 - 45	Puerto Rico	Puerto Rico	3.2	12673	fever, muscle/joint pain
3	10 - 15	Puerto Rico	Puerto Rico	4.2	8464	fever, muscle/joint pain
8	15 - 20	Puerto Rico	Puerto Rico	2.8	11834	fever, muscle/joint pain, rash
13	10 - 15	Puerto Rico	Puerto Rico	3.4	59931	rash
14	10 - 15	Puerto Rico	Puerto Rico	3.4	14347	fever, muscle/joint pain, rash
16	25 - 30	United States	El Salvador	1.1	17552	fever, muscle/joint pain, rash
17	45 - 50	United States	Papua New Guinea	24.3	82	fever, muscle/joint pain, malaise
18	25 - 30	India	India	9.3	1202	fever, muscle/joint pain, malaise
19	30 - 35	India	India	8.7	1130	fever, muscle/joint pain, malaise, headache
20	25 - 30	India	India	7.9	12565	fever, muscle/joint pain, malaise, headache
21	20 - 25	United States	Haiti	3.5	5996	fever, muscle/joint pain, malaise, headache
22	20 - 25	United States	Haiti	4.0	17924	fever, muscle/joint pain, malaise, headache
Naïve	N/A		N/A	N/A	<1:20	N/A
Naïve	N/A		N/A	N/A	<1:20	N/A
Naïve	N/A		N/A	N/A	<1:20	N/A

Table 8 Summary table of subject demographics

Subjects with confirmed or suspected CHIKV infection enrolled in endemic cohort (orange), a non-endemic cohort (blue), or alphavirus naïve (black). CN generated some of the CHIKV PRNT$_{50}$ data.

were obtained ranging from 1-24 years post-infection. Five of the subjects are from a larger endemic cohort of arbovirus immune subjects in Ponce, Puerto Rico (color coded in orange), were

PCR confirmed cases, and seven subjects are from a larger non-endemic cohort of arbovirus exposed individuals based in Portland, Oregon (color coded in blue) who were identified through clinical history and serum screening neutralization assays against CHIKV (Table 8). The geographical representation of the country of infection for these subjects is depicted in Figure 24.

Alphaviruses specific neutralization and antigenic relationship by subject

Immune serum from twelve subjects with presumed CHIKV infection history and three naive subjects (Table 8) was used in neutralization assays against a panel of five alphaviruses of the SFV antigenic complex including CHIKV, ONNV, MAYV, UNAV, and RRV, as well as VEEV, which is a representative virus from the VEEV antigenic complex. Amino acid sequences for E1, 6K, and E2 were used to generate the phylogenetic tree (Fig 26A) to demonstrate the relatedness of the viruses used in this study. We conducted plaque reduction neutralization titration assays ($PRNT_{50}$) for each of the sera against the panel of alphaviruses to determine the antigenic breadth of the immune response and quantity of antiviral antibodies following alphavirus infection (Fig 26B & C, Supplemental table 8). Serum samples from single time-points from the endemic subjects (coded in orange) and non-endemic subjects (coded in blue) as well as longitudinal samples from two endemic subjects (Fig 26B) obtained at six-month intervals were tested for serum neutralization. All 12 subjects had anti-CHIKV neutralizing antibodies with highest levels of detection observed for endemic Subjects 3 (V2) and 13, which were 5.0 and 3.4 years out from initial infection, respectively, indicating the presence of long-lasting anti-CHIKV immunity following natural infection (Fig 26B and Fig 31D). Anti-CHIKV neutralizing antibody levels were lowest for Subject 17, which demonstrated the highest level of anti-RRV antibodies. As this subject was presumed to be infected in Papua New Guinea, this may represent a primary RRV infection with cross-reactive antibodies against CHIKV (Fig 26C, Tables 8 & 9). Interestingly, this person still had heterotypic immunity even at >20 years post infection. Serum samples from

both Subject 1 and 3 had high anti-CHIKV activity at all time points tested but they also demonstrated a time-dependent reduction in cross-reactive antibody levels (Fig 25B).

We next characterized the antigenic relationship between distinct alphaviruses as determined by

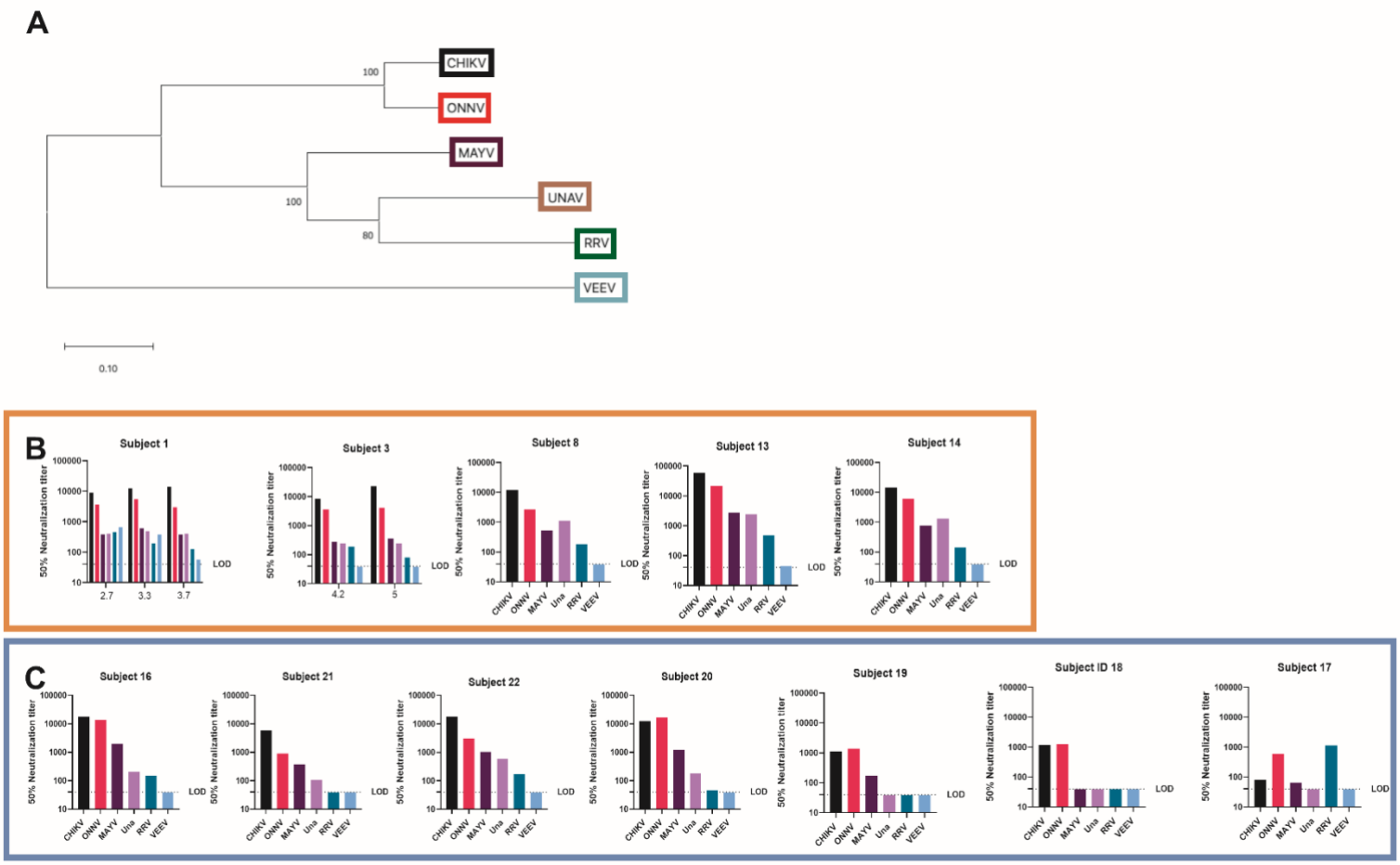

Figure 26 Serology for endemic and non-endemic subjects.

A) Phylogenetic tree produced using the E1, 6k, and E2 AA sequences; viruses are color coded to match serology graphs. B and C) Sera samples from each subject were run, graphs depict NT50 values against CHIKV, ONNV, RRV, MAYV, Una, and VEEV by plaque reduction neutralization titer assays (PRNT) performed on confluent monolayers of Vero cells. Endemic subject serologic profiles are shown in panel B with Subjects 1 and 3 containing multiple longitudinal blood draws, (time represents years post infection. Serology for non-endemic subjects is shown in Panel C. Limit of detection (LOD) is 40, samples below the LOD were assigned an arbitrary value of 39. A) data and figure created by JMP, serology graphs made by ZL. ZL and JMP generated PRNT50 data.

subject serum neutralization titers using antigenic cartography, which has previously been implemented to describe the antigenic relatedness of dengue and influenza viruses [299,300]. Antigenic

maps provide an alternate means of using neutralization titers to evaluate antigenic rather than genetic similarities between viruses. We found that CHIKV and ONNV are the most antigenically similar, consistent with the phylogenetic relationship between these two viruses (Fig 27), suggesting that antibody responses against these viruses share antigenically conserved epitopes; whereas VEEV and RRV are placed at a greater distance from CHIKV, again consistent with the phylogenetic relationships between the viruses (Fig 27). All sera tested cluster around CHIKV and the closely related ONNV, except for Subject 17, which clusters most closely to RRV (Fig 27), consistent with a suspected history of RRV infection. Longitudinal samples from Subjects 1 and 3 clearly demonstrate a shift towards a CHIKV-centric response over time indicating a reduction in cross-neutralizing antibodies.

Dissecting the role of E2 B domain homotypic and heterotypic neutralization

Conservation of the E2 B domain among members of the SFV complex has been shown to correlate with antibody cross reactivity [121,142]. The E2 B domain amino acid sequences for CHIKV,

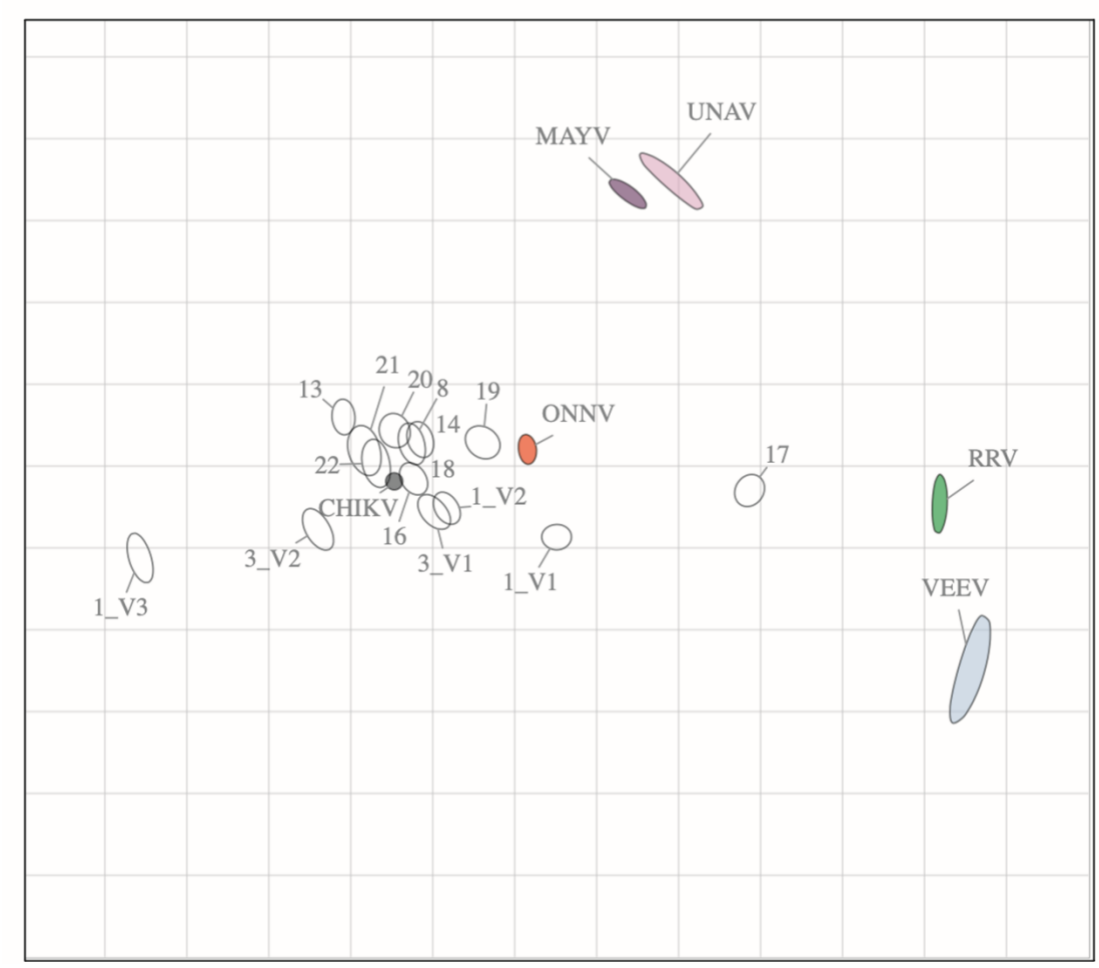

Figure 28 Antigenic cartography

Antigenic map shows the relative antigenic relatedness between CHIKV, ONNV, RRV, MAYV, UNAV, and VEEV. Each unit of antigenic distance (AU), the length of one side of a grid square, is equivalent to a two-fold dilution in a neutralization assay. Sera are shown as open ellipses and labeled by subject number (Fig. 1). Each virus is shown as a color filled ellipse and is colored according to virus strain (Fig. 1). The size and shape of each ellipse is the confidence area of its position. In making the map, each sera is initially plotted on top of the virus it most potently neutralizes and then pairwise distances between each sera:virus combination are calculated as a fold-difference in titer between the most potently neutralized virus and each other virus. The map is then optimized to place each virus relative to the serum samples in a manner that minimizes error between pairwise fold-differences. The closer a virus is to another virus, the more antigenically related the two are. Sera are initially plotted nearest to the virus they most potently neutralize with subsequently increasing distance to other viruses in descending neutralization potency against each virus. Data analyzed and figure made by WBM.

ONNV,MAYV, UNAV, and RRV are highly conserved (ranging from 56 to 88% sequence identity) sharing clusters of amino acids distributed across this region of E2, while VEEV shares only 27%

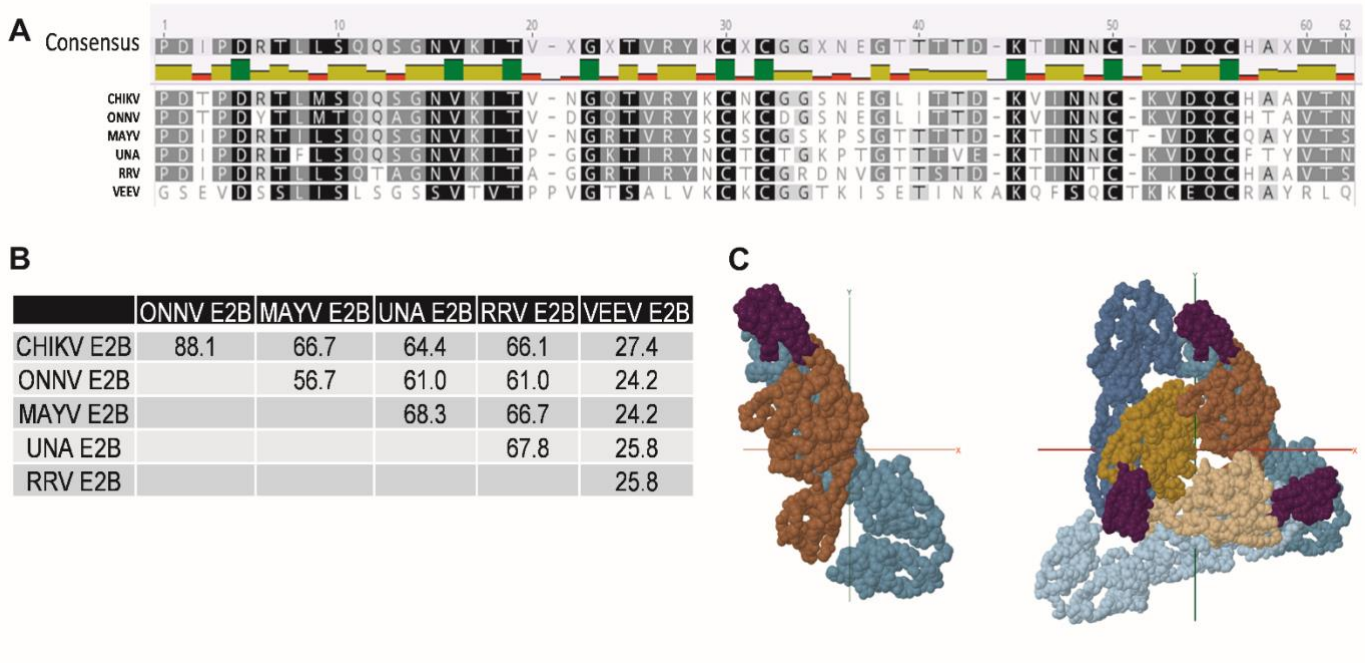

	ONNV E2B	MAYV E2B	UNA E2B	RRV E2B	VEEV E2B
CHIKV E2B	88.1	66.7	64.4	66.1	27.4
ONNV E2B		56.7	61.0	61.0	24.2
MAYV E2B			68.3	66.7	24.2
UNA E2B				67.8	25.8
RRV E2B					25.8

Figure 31 Comparison of alphavirus E2 B domains

Comparison of Alphavirus E2 B domains. A) Amino acid sequence alignment was performed using Geneious software for the E2 B domains of the alphaviruses examined in this study. Regions of 100% homology are highlighted in black, 80-100% similarity is dark grey, 60-80% similarity is light grey, and less than 60% similarity is in white. B) Matrix depicts the amino acid sequence identity as a percentage. C) Top-down view of the organization of the Mayaro Virus E1:E2 monomer (Teal:Brown) shown with the E2 B domain annotated in purple. D) E1:E2 trimer spike organization depicted with the E2 B domain annotated in purple, E1 in shades of teal, and E2 in shades of brown. Data generated and figure made by JMP and WCW.

sequence identity (Fig 31A & B). When viewed in a structural model, the organization of the spike trimer clearly demonstrates the accessibility of antibody binding to the E2B domain (Fig 31C). To explore the cross-neutralizing potential of E2 B domain specific antibodies, we first depleted E2B specific antibodies by adsorbing subject immune sera against magnetic beads coated with purified MAYV E2 B domain polypeptide containing an in-frame C' terminal His tag used for isolation and N' terminal HiBiT tag that was expressed in *E. coli* (Supplemental Fig 33). Serum samples were incubated with E2 B domain bound beads, beads alone, or in the absence of beads. Following

depletion sera were tested by neutralization assays against both CHIKV and MAYV (Fig 32). Depletion with recombinant MAYV E2 B domain protein did not change neutralization titers against serum homotypic CHIKV. However, MAYV neutralization titers decreased for all subjects except for Subject 17, subsequently thought to have had prior RRV infection (Supplemental Table 8). Specifically, heterotypic $PRNT_{50}$ titers against MAYV dropped nearly five –fold (-4.96 ± 2.38) whereas control depleted sera $PRNT_{50}$ titers did not change significantly (-0.46 ± 1.28-fold change) (Fig 34A). Conversely, homotypic CHIKV neutralization assays post bead depletion, showed no

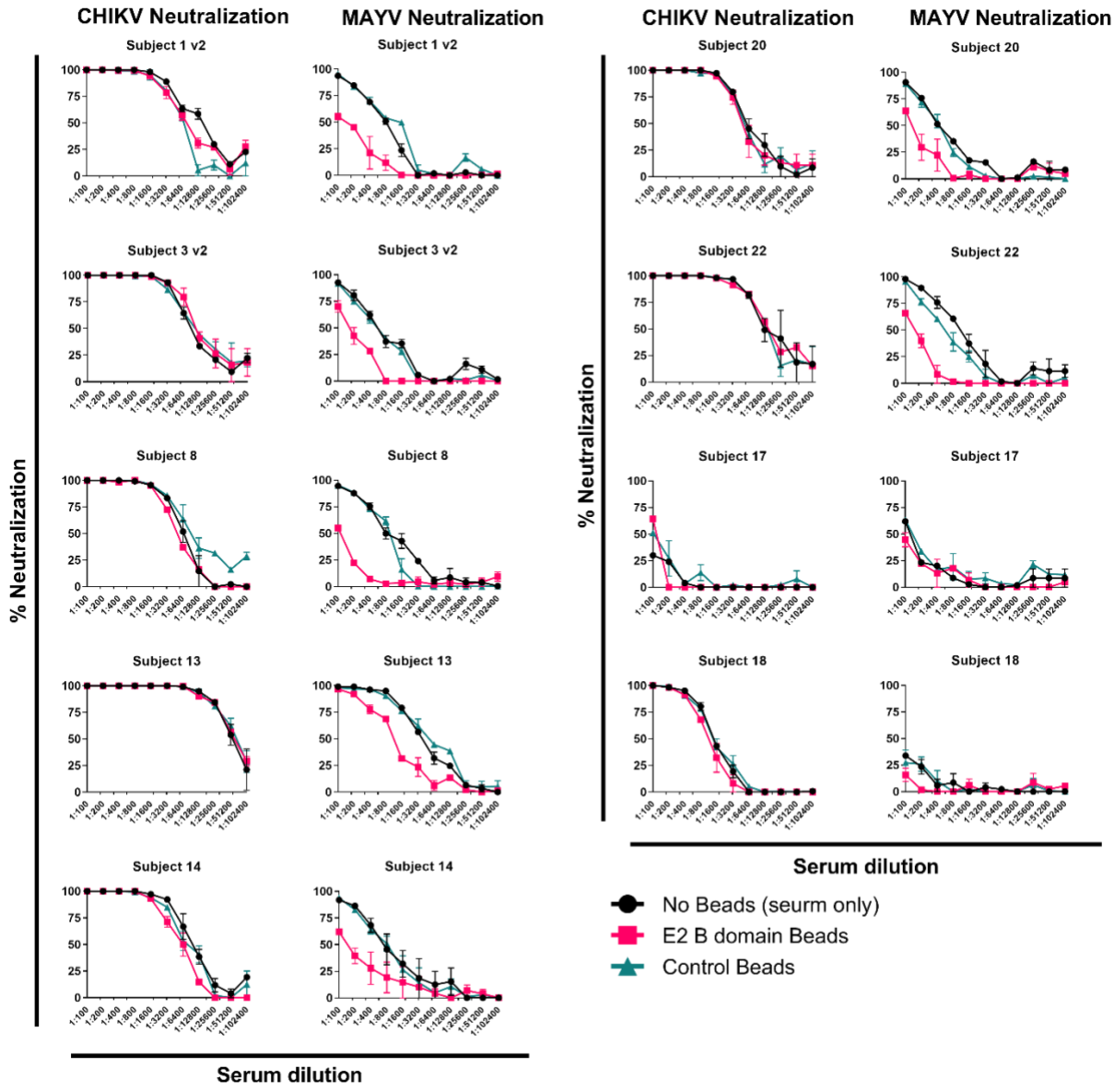

Figure 32 E2B bead depletion

Human sera absorption of the E2 B domain and assessment of neutralization against CHIKV and MAYV. E2 B domain bound to magnetic beads (or control beads alone) was incubated with diluted human serum for 4 hours, the beads were pulled off with a magnet. Following depletion the sera was used in both CHIKV and MAYV neutralization assays. Human sera samples were diluted 1:2 from 1:100 to 1:102,400. "No beads" is diluted serum only in black, E2B absorbed human sera is pink, and control beads bound to diluted human sera is in teal. The data is representative of 3 biological experiments completed with duplicate samples. Data generated and figure created by JMP and WCW.

significant impact on neutralizing antibody titers under either condition compared to the non-adsorbed serum (-0.2 ± 1.47 and 0.14 ± 1.58-fold change, respectively) (Fig 34B).

Homotypic and cross-reactive alphavirus-specific MBC frequency in immune subjects 1 to 24 years post infection

To further characterize homotypic and cross-specific immune response in CHIKV infected subjects, memory B-cell (MBC) limiting dilution assays were performed. PBMCs were serially diluted in 96 well plates and stimulated to expand and secrete Abs. These Abs were then analyzed for antigen specificity by IgG ELISA using whole CHIKV and MAYV virions as bait. All subjects had CHIKV-specific MBCs, as remotely as 24 years post infection (Fig 31A). Cross-reactive MAYV-specific MBCs were present in 10/11 (91%) subjects, with only subject 17 (primary RRV) falling below the limit of detection (Fig 31B). We next looked for MAYV E2B domain specific MBCs, finding 9 of 11 (82%) of subjects had MBCs encoding E2B

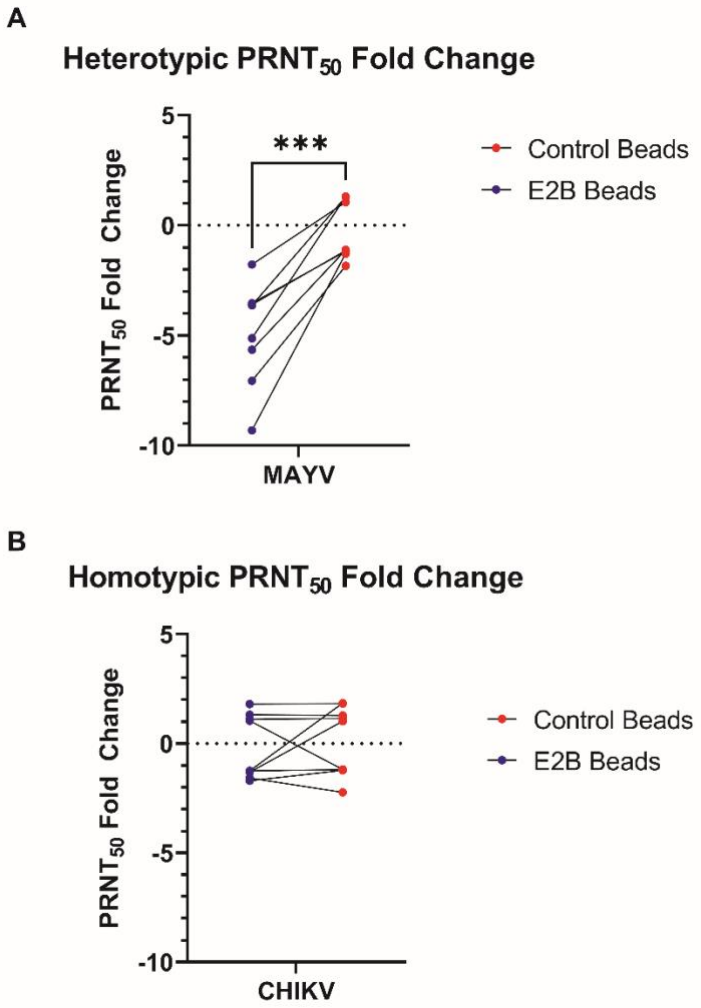

Figure 34 Fold-change in neutralization titers following bead depletion.

Fold change in neutralizing antibody titers following E2B domain adsorption. Fold change in neutralizing antibody titers (nAb) of subject serum samples following adsorption against MAYV E2B domain coated Ni-NTA or control beads was calculated against non-bead-treated serum samples. A) Depletion of E2B domain specific antibodies resulted in significant decreases in nAb titers in heterotypic neutralization assays (-4.96 ± 2.38 and -0.46 ± 1.28-fold change, $p < 0.0005$). B) No significant effect on nAb titer was observed in homotypic neutralization assays when serum samples were adsorbed against E2B domain or control beads (-0.2 ± 1.47 and 0.14 ± 1.58-fold change). Data and figure by JMP.

cross-reactive Abs as remotely as 8.7 years post-infection (Fig 31C). The variability of cross-

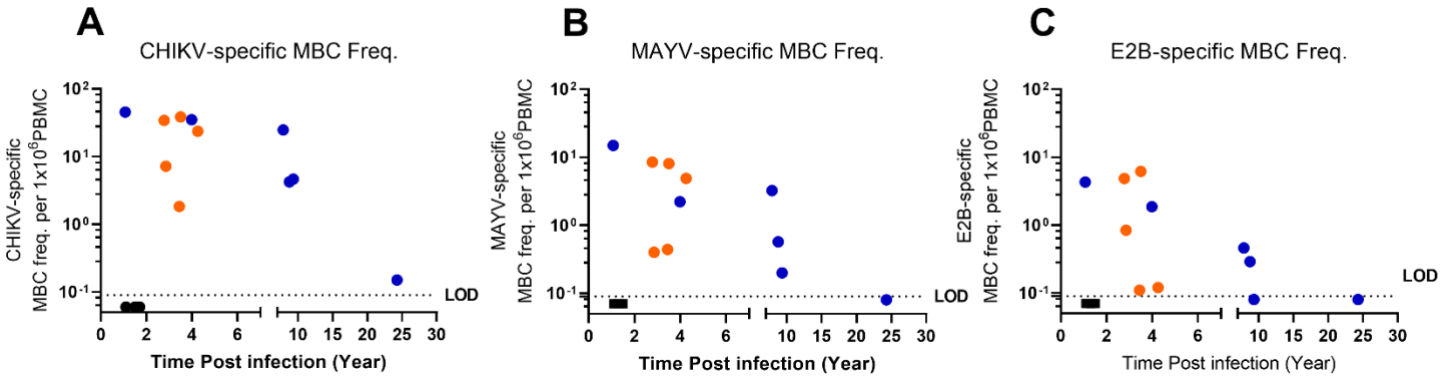

D

Subject ID	Time Post Infection (Years)	Primary Infection by serology	CHIKV MBC Freq.	MAYV MBC Freq.	E2B MBC Freq.	% MAYV MBC attributable to E2B
1	3.3	CHIKV	34.15	8.50	4.85	57.0
3	4.3	CHIKV	23.62	6.93	0.12	1.7
8	2.9	CHIKV	10.37	0.85	0.84	98.1
13	3.4	CHIKV	1.83	0.88	0.11	12.2
14	3.4	CHIKV	38.63	17.99	6.18	34.4
16	1.1	CHIKV	45.36	14.92	4.31	28.9
17	24.3	RRV	0.15	ND	ND	ND
18	9.3	CHIKV	4.64	0.20	ND	ND
19	8.7	CHIKV	4.22	0.57	0.29	50.0
20	7.9	ONNV	24.81	3.24	0.46	14.2
22	4.0	CHIKV	35.15	2.21	1.87	84.7

ND not detectable

Figure 36 Antigen-specific MBC frequency overtime.

MBC frequency per 10^6 PBMC over time in non-endemic cohort (blue n=6), endemic (orange n=5), and naïve subjects (black n=3). A) CHIKV-specific MBC frequency as determined by whole CHIKV-ELISA. B) MAYV-specific MBC frequency determined by whole MAYV-ELISA. C) E2B-specific MBC frequency determined by MAYV-E2B ELISA. Negative samples and those below the limit of detection were assigned an arbitrary value between 0.05 and 0.09 (LOD = 0.1). D) Table summarizes subject sampling time post infection, the alphavirus infection history predicted by serology, MBC frequencies for the three antigens tested, and % MAYV MBC attributable to E2B, determined by E2B MBC frequency divided by total MAYV-MBC frequency, ND = not detected.

reactive MBCs attributable to E2B varied by subject (Fig 31D), ranging from 1.7% to 98% of MAYV-specific MBCs. We found that CHIKV and MAYV-MBC frequencies were highly correlated (R^2=0.747) with a ratio of CHIVK:MAYV of about 10:1 overall (Fig 36 and Supplemental Fig 35). MAYV specific MBC frequency was also highly correlated with MAYV E2B MBC frequency (R^2 0.656) with approximately 1 in 10 MAYV MBCs also being E2B specific (Fig 36D and 39).

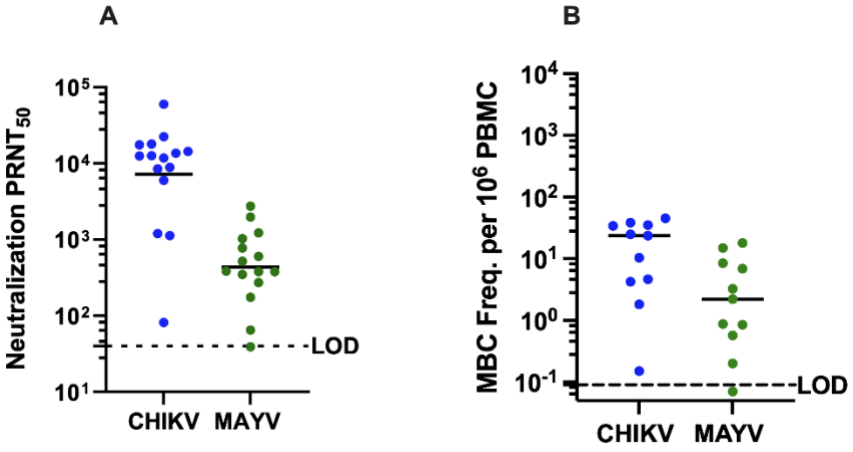

Figure 39 Homotypic verses cross-reactive antibodies

Homotypic verses cross-reactive antibodies. A) Calculated geometric mean $PRNT_{50}$ values between CHIKV and MAYV show a 16-fold difference. B) Antigen-specific MBC frequency between CHIKV and MAYV, less than a 4-fold difference was observed.

Next, we compared fold difference in homotypic (CHIKV) verses heterotypic (MAYV) MBC frequencies, with homotypic and heterotypic geometric mean neutralization titers ($PRNT_{50}$) for all subjects. While overall we found a 16-fold difference (7235.9 compared to 434.9) (Fig 39A) in type specific versus cross-neutralizing PRNT titers, we observed about a four-fold difference in CHIKV versus MAYV MBC frequencies (9.7 compared to 2.5) across all subjects who had detectable MBCs (Fig 39B). Finally, we explored the relationship between MBC frequency and $PRNT_{50}$ titer (Supplemental Figure 34) finding only a very weak correlation (Spearman R^2=0.126) between the two (P value = 0.2862). MAYV MBC frequency and MAYV neutralization titer were also weakly correlated (R^2 =0.318, P= 0.0739).

Discussion

Previous characterization of the durability and breadth of CHIKV specific neutralizing antibodies and virus specific MBCs in humans [125,295,301] and mice [302] have been quite limited, but has shown

broad serum cross reactivity. The majority of characterized cross-neutralizing antibodies recognize E2, with many mapping to the linear epitope E2 B. There have also been reports of non-neutralizing alphavirus antibodies playing a role in protection, but that was not explored in this investigation [107,116]. Here we detected neutralizing antibodies against CHIKV and closely related alphaviruses up to 24 years after infection. Broad neutralization was observed in both endemic and non-endemic subjects with breadth against antigenically distinct viruses declining over time. During this investigation it was determined that one of our CHIKV immune subjects (Subject 17) had a serum neutralization profile consistent with prior RRV infection instead of a CHIKV infection. This is consistent with infection history and by antigenic cartography where the subject clustered most closely to RRV antigenically. This subject was initially identified through a CHIKV specific neutralization assay screen, and we chose to retain the subject in our analyses because their infection history both adds novel information about likely RRV cross-reactive and underscores the breadth of Ab responses within the SFV-complex and illustrates the importance of specific serological tests to determine infection history.

We further determined that much of the cross-neutralization and heterologous binding of both LLPC and MBC-derived Abs was attributed to antibodies that recognize the E2 B domain. Serum antibody absorption to Ni-NTA beads bound to the E2 B domain from MAYV significantly ablated cross-neutralizing effects of immune serum on MAYV without significantly reducing serum potency against CHIKV. As such, this further implicates the E2 B domain as a vaccine antigen for the development of broadly neutralizing alphavirus antibodies and indicates that other antigenic sites are responsible for robust type-specific neutralization. The subjects with the highest percentage of MAYV-specific MBC frequency attributed to the E2 B domain are also the subjects that have the highest fold-change differences in $PRNT_{50}$ following E2B serum depletion. The

representation of specific Abs that bind the E2 B domain in the LLPC and MBC compartments varies greatly by subject; however, it is unclear what mechanisms mediate this difference.

While CHIKV immune serum neutralized other members of the SFV-complex, the difference in geometric mean titers between CHIKV and MAYV differed by 16-fold, compared to the difference in MBC frequencies, which differed by less than 4-fold. This difference observed between serum Abs (a product of long-lived plasma cells) and MBC has been shown before in mice and humans where serum Abs are highly specific for the original antigen of infection, while MBCs recognize a greater breadth of antigens that are similar but antigenically distinct from the original invading pathogen [297,298,303]. Our data expand on previously published data by Zhang *et. al.* that identified that amino acids in the E2 A and B domains were involved in the binding of CHIKV to both mouse and human Mxra8, implicating it as a major target for therapeutic strategies [304]. Our study provides additional evidence of the importance of the E2 B domain following natural CHIKV infection in humans [305,306]. The durability and breadth of the B-cell mediated immune response to CHIKV indicates that regions with high CHIKV seroprevalence constrict the range of closely related alphaviruses as well as point out the importance of specific serologic assays to determine alphavirus infection histories.

Materials and Methods

Human research ethics

The study has been reviewed and approved by the Oregon Health & Science University Institutional Review Board (IRB#10212) for the non-endemic cohort and Ponce Medical School Foundation Review Board (IRB #180321-VR) for the endemic cohort. Informed consent was obtained from subjects upon initiation of their participation in the study.

Non-endemic human-cohort population n=7

CHIKV immune individuals in this study were enrolled in a larger study of long-term immunity following infection with the arthropod-borne viruses including DENVs, ZIKV, and YFV vaccination. Study subjects with suspected arbovirus infection contacted the long-term immunity study and were offered participation in the study, and following informed consent, provided extensive additional history including other known and suspected arboviral infections, lifetime travel histories, and yellow fever virus (YFV) and Japanese encephalitis virus (JEV) vaccination histories.

Endemic Human-cohort population n=5

CHIKV immune individuals in this study were enrolled in a larger study of long-term immunity following infection with the arthropod-borne viruses. Study subjects that came to the ER with fever seeking medical attention were approached to enroll in Sentinel Enhanced Dengue Surveillance System (SEDSS). Subjects with PCR confirmed CHIKV infections were offered to participate in the long-term immunity study and following informed consent, provided additional history including other known and suspected arboviral infections, lifetime travel histories, and vaccination histories. Samples were collected, processed and shipped to Oregon Health & Science University for further analysis.

Sample collection and storage

On enrollment, subjects provided approximately 80 mL of blood, with 30 mL collected in BD serum vacutainers (Becton-Dickson) for serologic studies and stored at -80°C until used for assays. PBMCs were isolated from 50 mL of whole blood collected in BD EDTA or Heparin vacutainers (Becton-Dickson), and stored in liquid nitrogen.

Viruses

$MAYV_{CH}$ was generated from an infectious clone received from Dr. Thomas E. Morrison (UC-Denver). Mayaro $virus_{BeAr505411}$ (NR-49910); Una $virus_{MAC\ 150}$ (NR-49912); RRV_{T48} (NR-51457); $ONNV_{UgMP\ 30}$ (NR-51661); and $VEEV_{TC\text{-}83}$ (NR-63) were obtained through BEI. $CHIKV_{181/25}$ was generated from infectious clones as previously described [307]. Alphaviruses were grown in Vero cells and viral stocks were prepared from clarified supernatants at 72 hours post infection (hpi) by ultracentrifugation over 10% sucrose (SW32Ti, 70 min at 76,755 x g). The virus pellets were resuspended in 1X PBS (Corning) and stored at -80°C. Viral limiting dilution plaque assays using Vero cells were performed on 10-fold serial dilutions of virus stocks. The infected cells were rocked continuously in an incubator at 37°C for 2 hours, and then DMEM (Corning) containing 5% FBS (HyClone), PSG (Gibco), 0.3% high viscosity carboxymethyl cellulose (CMC) (Sigma) and 0.3% low viscosity CMC (Sigma) was added to the cells. At 2 dpi, cells were fixed with 3.7% formaldehyde (Fisher) and stained with 0.2% methylene blue (Fisher). Plaques were visualized under a light microscope and counted.

Neutralization assays - fifty percent plaque reduction neutralization test ($PRNT_{50}$)

$PRNT_{50}$ titers were used to characterize subject sera. Assays are prepared in duplicate (for $CHIKV_{181/25}$). Subject sera were first heat-inactivated at 56°C for 30 minutes. Sera were then diluted four-fold in MEM supplemented with 2% FBS from a starting dilution of 1:10 for $CHIKV_{181/25}$, for the rest ($MAYV_{CH}$, $MAYV_{BeAr}$, Una_{Mac150}, RRV_{T48}, $ONNV_{UgMP30}$, or $VEEV_{TC\text{-}83}$.) 2-fold dilutions were performed in DMEM supplemented with 5% FBS and 1% PSG. Serum dilutions were mixed with an equal volume of 50-100 plaque forming units (PFU) of virus giving a final starting serum dilution of 1:20 for $CHIKV_{181/25}$ and 1:40 for the rest ($MAYV_{CH}$, $MAYV_{BeAr}$, Una_{Mac150}, RRV_{T48}, $ONNV_{UgMP30}$, or $VEEV_{TC\text{-}83}$.). Virus-dilution mixes without sera were

prepared simultaneously as controls for input virus PFUs. After incubation at 37℃ for 2 hours, virus mixtures were inoculated into individual wells of 24 well plates ($CHIKV_{181/25}$) or 12-well plates seeded with Vero cells, incubated for 2 hours at 37℃ 5% CO_2, and overlaid with 1% methylcellulose in Opti-MEM (Gibco) supplemented with NEAA, anti-anti, amphotericin B, and 2% FBS ($CHIKV_{181/25}$) or 5% FBS/DMEM/CMC. Plates were incubated for 2 days ($MAYV_{CH}$, $MAYV_{BeAr}$, Una_{Mac150}, RRV_{T48}, or $VEEV_{TC-83}$) or 3 days ($CHIKV_{181/25}$ and $ONNV_{UgMP30}$) at 37°C and 5% CO_2. The overlay was then removed, monolayers were fixed with 80% methanol ($CHIKV_{181/25}$) or 3.7% formaldehyde and stained with 2% crystal violet ($CHIKV_{181/25}$) or 0.2% methylene blue dye, and plaques were enumerated by visual review of each well. Proportion of virus neutralized per well was calculated, and the serum dilution that neutralizes 50% of control input virus ($PRNT_{50}$) was determined by non-linear regression using GraphPad Prism, version 7.0.

E2 B domain cloning

$MAYV_{BeAr505411}$ was reversed transcribed using SuperScript IV Reverse Transcriptase and cloned into a pcDNA3.1- shuttle vector. The E2 B domain has previously been annotated and was cloned out from the E2 glycoprotein using a forward primer (TGAATTCCATATG-HiBit-CCGGACATTCCGGATAGAAC) and reverse primer (AAGCTTTTAGTGATGGTGATGGTGATGGCTCGTGACGTAAGCCTGACATTTG) [142]. The N-terminal E2 B segment was cloned using the previously mentioned forward primer and a reverse primer (AAGCTTTTAGTGATGGTGATGGTGATGACCGCAAGAGCAGCTGTACCTGACGG). Amplicons were cloned into a pRSET-B bacterial expression vector with NdeI and HindIII restriction enzymes and transformed into Rosetta™(DE3) Competent Cells (Novagen).

E2 B domain expression and binding to Ni-NTA magnetic beads

Rosetta™(DE3) *E.coli* containing the plasmid pRSET-B MAYV E2 B domain were grown in 2X YT broth at 37°C until the OD_{600} reached ~0.6 and then induced with 1 mM final concentration isopropyl β-D-1-thiogalactopyranoside (IPTG) for 10 hours at 37°C. Media was harvested and cells were pelleted at 10,000 x g for 10 min. Pellet was resuspended in a resuspension buffer with 50 mM $NaPO_4^{3-}$ and 300 mM NaCl with 1 mg/mL lysozyme and DNase (5µg/mL) pH 8.0 and sonicated for three thirty second cycles at 84W. Cell lysates were centrifuged at 10,000 x g for 10 min, and inclusion body-containing pellets were resuspended with denaturing buffer (8M urea, 30 mM $NaPO_4$, 300 mM NaCl, and 3mM β-mercaptoethanol). Resuspended pellets were rocked for 10 minutes and then incubated at 65°C for 30 minutes. Supernatants were clarified by centrifugation at 43,725 x g for 15 minutes. Supernatant was added to 1 mL of Superflow™ Ni-NTA resin beads (Qiagen) that had been pre-washed and equilibrated in denaturing buffer and the slurry was rocked for 1 hour at RT. Beads were pelleted at 820 x g for 2 minutes. Pelleted beads were resuspended with a small volume of denaturing buffer and a gravity flow column was packed with the resulting beads. Protein was eluted using 1 wash with 1 mL 50 mM imidazole to remove non-specific proteins and 4 washes with 1 mL of 250 mM imidazole. Elute from the 250 mM imidazole fractions was combined and concentrated to ~750 µL using an Amicon® Ultra-15 Centrifugal Filter Unit (3 kDa cut-off) and this material was filtered through a 0.22 µm filter. Filtered elute was loaded onto a Sephacryl S-100HR column that was equilibrated with gel filtration buffer (8M Urea, 100mM Tris pH 8) and separated using an AKTA Start Liquid Chromatograph (GE Lifesciences). Fractions were analyzed for mobility on a NuPAGE™ 4 – 12% Bis-Tris gel that was visualized following stainig with Coomassie Brilliant Blue R-250. Fractions containing purified E2 B monomer were combined and then dialyzed in 2-fold steps from 8M urea to PBS using a 3.5K MWCO Slide-A-Lyzer™ Dialysis Cassette. Protein was quantified using the

Nano-Glo® HiBiT Lytic Detection System. Dialyzed fractions were then mixed with 300 µl of PBS equilibrated Ni-NTA Magnetic Beads (Pierce) and rocked overnight at 4°C. Control PBS equilibrated Ni-NTA Magnetic Beads were rocked overnight at 4°C in an equivalent volume of 1X PBS.

Human serum antibody absorption to Ni-NTA magnetic beads

E2 B domain loaded or control Ni-NTA magnetic beads were washed 3 times with PBS, followed by a blocking wash with DMEM supplemented with 10% human serum (Sigma Human AB serum #H4522). Beads were resuspended homogenously in 2.1 mL of serum-free DMEM and aliquoted evenly between 2 mL centrifuge tubes for each patient and supernatant was removed. Subject serum samples were diluted 1:100 in serum-free DMEM and 1 mL of diluted serum was incubated with E2 B loaded Ni-NTA magnetic beads, control Ni-NTA magnetic beads, or no beads for 4 hours at 4°C. Following incubation, supernatant was removed to new 2 mL tubes and further diluted for use in neutralization assays.

Neutralization assays with Ni-NTA magnetic bead absorbed human serum

Diluted human serum supernatant following Ni-NTA magnetic bead binding was used in neutralization assays with $MAYV_{BeAr}$ and $CHIKV_{181/25.}$ Serum was diluted 1:2 from 1:100 to 1:102,400 and mixed with media containing 50 PFU of either $MAYV_{BeAr}$ or $CHIKV_{181/25}$. Neutralization assays were then carried out as previously described [308].

Protein modeling of MAYV structural glycoproteins and alphavirus E2 B domain alignment

MAYV 3D structural model 6W2U, deposited by Powell *et al.*, was downloaded from protein data bank [294,309]. Chains A & E were modeled for panel A, and chains A – C & E – G were modeled for panel B. Chains A and E and A – C & E – G were modeled for monomer and trimer orientations,

respectively, using Jmol: an open-source Java viewer for chemical structures in 3D (http://www.jmol.org/). E2 B domain alignment was constructed in Geneious Prime® version 11, using the following GenBank accession numbers: CHIKV (SL15649), ONNV (AF079456), MAYV (KT754168), Una (HM147992), RRV (AEC497521), and VEEV (NC001449). Aligned residues were scored using the BLOSUM62 matrix to compare similarity.

Memory B cell Frequency

PBMCs were thawed and resuspended in LDA media (RPMI 1640 medium (Gibco), 1×Antibiotic-Antimycotic (Corning), 1X non-essential amino acids (HyClone), 20 mM HEPES (Thermo Scientific), 50 μM β-ME, and 10% heat-inactivated fetal bovine serum (VWR). Cells were serially 2-fold diluted (10 wells per dose) starting with 3-5 x 10^5 PBMCs per well at the highest concentration and cultured in in 96-well round-bottom plates in a final volume of 200 μl per well. Cells were stimulated with IL-2 (Prospec) 1000U/ml and R848 (InvivoGen) 2.5μg/mL [264]. To determine background absorbance values, supernatants were used from 8 wells of unstimulated PBMCs only. Plates were incubated at 37°C and 5% CO_2 for 7 days. B cell stimulation and expansion was determined by performing ELISAs detecting total IgG.

MBC precursor frequencies were calculated by the semi-logarithmic plot of the percent of negative cultures versus the cell dose per culture, as previously described [265]. Frequencies were calculated as the reciprocal of the cell dilution at which 37% of the cultures were negative for antigen-specific IgG production. Rows which yielded 0% negative wells were excluded, since this typically resides outside of the linear range of the curve and artificially reduced the MBC precursor frequency. For subjects with low frequency of antigen-specific antibody secreting cells frequency was determined by number of positive wells divided by the total number of IgG positive secreting wells, multiplied by one million, giving a frequency per million PBMCs stimulated.

Antigen-specific ELISAs

Antigen-specific MBC frequencies were calculated by assaying LDA supernatants by antigen-specific ELISAs [265]. Ninety-six half-well ELISA plates (Greiner Bio-one) were coated with 5 x 10^7 PFU/mL CHIKV or 1 x 10^7 PFU/mL MAYV in PBS. Plates were incubated for four days at 4°C, washed with PBS-T (0.05% Tween) and blocked for 1 hour with 5% milk prepared in PBS-T and then 20µL of LDA supernatants were added to each well and incubated at RT for 1 hour. Plates were washed 4 times with wash buffer, and 50 µL of 1:3,000 dilution of donkey anti-human IgG-HRP (H + L) (Novusbio, NBP1-73319) detection antibody was added and incubated at RT for 1 hour. Plates were washed 4 times with wash buffer, 50 µL of colorimetric detection reagent containing 0.4mg/ml o-phenylenediamine and 0.01% hydrogen peroxide in 0.05M citrate buffer (pH 5) were added and the reaction was stopped after 20 minutes by the addition of 1M HCl. Optical density (OD) at 492nm was measured using a CLARIOstar ELISA plate reader. LDA wells were scored positive at ODs at least 2-fold above background (unstimulated PBMC wells).

Antigenic Cartography

The CHIKV antigenic map was constructed as previously described (PMID 26383952 and PMID 15218094) and implemented using the Acmacs Web Cherry platform (https://acmacs-web.antigenic-cartography.org/). Briefly, antigenic maps are constructed by first generating a table of antigenic distances (D_{ij}) between each individual virus (i) and serum (j) using serum titers for each serum-titer pair (N_{ij}). To calculate table distance, the titer against the best neutralized virus for that serum is defined as b_i and the distances for that serum are calculated as $D_{ij} = log_2(b_i) - log(N_{ij})$. For the best neutralized virus for that serum, $N_{ij} = b_i$, and this distance will be equal to 0. For the remaining serum-virus pairs, table distance D_{ij} is equivalent to the fold-difference in titer between b_{ij} and N_{ij}. Euclidean map distance (d_{ij}) for each serum-virus pair is found by minimizing the error between the table distance D_{ij} and map distance, d_{ij}, using the error function E =

$\sum_{ij} e(D_{ij},d_{ij})$, where $e(D_{ij},d_{ij}) = (D_{ij}-d_{ij})^2$ when the neutralization titer is above 1:20. For viruses with neutralization titers <1:20, the error was defined as $e(D_{ij},d_{ij}) = (D_{ij}-1-d_{ij})^2(1/1+e^{-10(Dij-1-dij)})$. To make a map and derive d_{ij} for each serum-virus pair, viruses and sera are assigned random starting coordinates and the error function is minimized using the conjugate gradient optimization method.

Statistical analysis

Statistics and graphs were created with GraphPad Prism 8. Normalized variable slope non-linear regression using upper and lower limits of 100 and 0, respectively, was used to calculate neutralizing antibody titers.

Acknowledgments

The work presented in this manuscript was supported by grants from the National Institutes of Health 1U19AI142790 (DNS), R01AI153434 (WBM), R21AI135537(WBM), UL1TR002369 (WBM), Takeda IISR 2016-101586 (WBM), and the Sunlin and Priscilla Chou foundation (WBM). Centers for Disease Control and Prevention U01CK000437 (VRA) and U01CK000580 (VRA) and T32GM142619 (WCW). The funders had no role in study design, data collection and analysis, decision to publish, or preparation of this manuscript.

Supplemental data

Table 11 Supplemental table PRNT50 titers

Subject ID	CHIKV $PRNT_{50}$	Una $PRNT_{50}$	MAYV $PRNT_{50}$	VEEV $PRNT_{50}$	ONNV $PRNT_{50}$	RRV $PRNT_{50}$
1 V1	8865	404	383	650	3648	458
1 V2	12673	488	601	376	5486	195
1 V3	13612	403	379	56	2925	126
3 V1	8464	243	272	<1:40	3621	183
3 V2	22504	238	348	<1:40	4115	79
8	11834	1124	519	<1:40	2679	182
13	59931	2400	2737	43	21704	479
14	14347	1302	775	<1:40	6157	143
16	17552	203	1977	<1:40	13633	147
17	82	<1:40	65	<1:40	602	1122
18	1202	<1:40	<1:40	<1:40	1265	<1:40
19	1130	39	174	<1:40	1392	<1:40
20	12565	178	1223	<1:40	16996	47
21	5996	105	380	<1:40	907	<1:40
22	17924	588	1025	<1:40	3125	171

Plaque reduction neutralization titer assays were performed to calculate the 50% neutralization titer against a panel of SFV complex alphaviruses and VEEV from the endemic cohort (n=5) and non-endemic cohort (n=7). Data generated by JMP and ZLL.

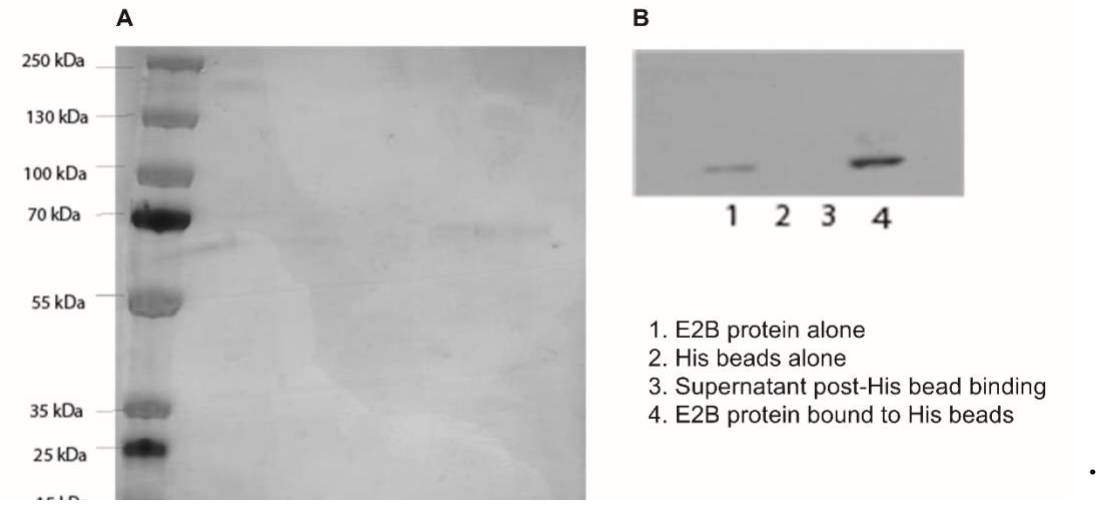

Figure 41 Supplemental figure E2B detection

A) SDS-PAGE and B) western blot for HiBit-tagged protein (~8kDa) to confirm that the E2B protein was indeed bound to the His beads before use in subsequent assays. In A), samples were heated to 95°C for 5 minutes then electrophoresed on a 4-12% Bis-Tris gel for 40min at 160V. Two gels were loaded with the same samples. The first gel was stained using the Coomassie Brilliant Blue Staining Solutions Kit to visualize the protein and confirm the correct protein size of 8 kDa. For western blot in B), the second protein gel was transferred to a polyvinylidene fluoride (PVDF) membrane using a semi-dry transfer system and probed for HiBit using a 1:200 dilution of LgBiT, according to a HiBit Blotting System protocol. The western blot was developed in West Pico Plus by chemiluminescence. For both panels, lane 1 is E2B protein before His bead binding, lane 2 is control His beads only without protein, lane 3 is unbound protein, and lane 4 is E2B protein bound to His beads.

Table 14 Supplementary table E2B domain data

	MAYV PRNT50					CHIKV PRNT50				
	No Beads	E2B Beads	Control Beads	Δ1	Δ2	No Beads	E2B Beads	Control Beads	Δ1	Δ2
Subject 1 v2	709.2	138.2	927.6	-5.13	1.31	14216	8985	6353	-1.58	-2.24
Subject 3 v2	624.4	173.3	549.6	-3.60	-1.14	9988	13159	12761	1.32	1.28
Subject 8	1023	109.9	806.9	-9.31	-1.27	6479	5190	11981	-1.25	1.85
Subject 13	4154	1145	5381	-3.63	1.30	55297	60944	63795	1.10	1.15
Subject 14	814.1	144	731.3	-5.65	-1.11	9856	5768	8028	-1.71	-1.23
Subject 20	477.5	135	404.1	-3.54	-1.18	6742	5386	5605	-1.25	-1.20
Subject 22	1039	147.2	565.3	-7.06	-1.84	17412	18079	14575	1.04	-1.19
Subject 17	122.2	68.84	128.4	-1.78	1.05	56.35	101.7	102.8	1.80	1.82
Subject 18	55.53	<40	42.99	N/A	-1.29	1464	1120	1497	-1.31	1.02

PRNT50 values and Fold Change of E2 B Domain Depleted Serum Relative to Controls. PRNT assays were performed on serum samples incubated with beads alone or beads coupled with E2 B domain protein. PRNT50 values were calculated for each sample using Prism software. Fold change was calculated in Excel and is relative to the appropriate control (Δ1: Fold change in $PRNT_{50}$ titer following E2 B bead treatment relative to non-bead treated serum; Δ2: Fold change in $PRNT_{50}$ titer following control bead treatment relative to non-bead treated serum).

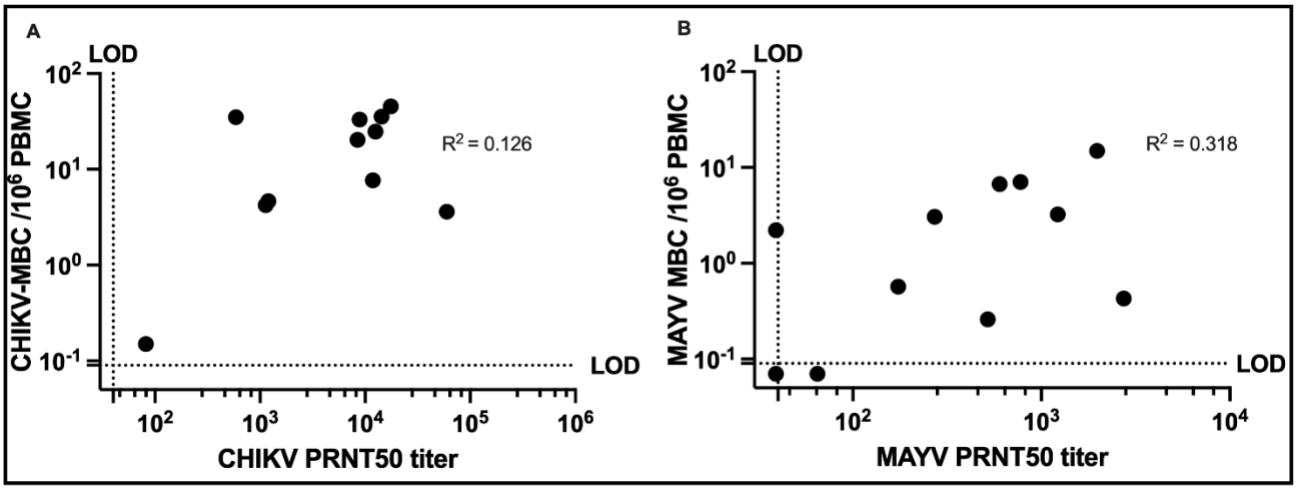

Figure 43 Supplemental figure correlation between MBC frequency and PRNT50 titer

A) CHIKV MBC frequency compared to CHIKV neutralization titer, non-parametric Spearman correlation R^2= 0.126. B) MAYV MBC frequency compared to MAYV neutralization titer non-parametric Spearman correlation R^2 = 0.318.

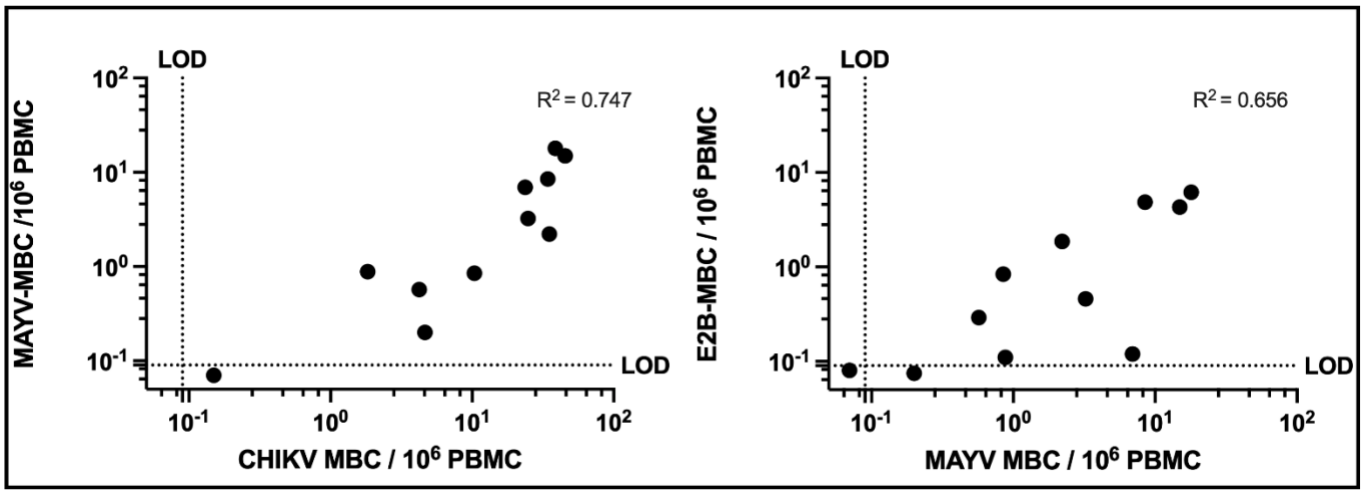

Figure 45 Supplemental figure relationship between antigen-specific MBC frequencies.

A) Relationship between MAYV-MBC frequency and CHIKV-MBC frequency non-parametric Spearman correlation $R^2 = 0.747$. B) E2B-MBC frequency compared to MAYV-MBC frequency non-parametric Spearman correlation $R^2 = 0.656$.

Chapter 4: SARS-CoV-2 specific memory B-cells from individuals with diverse disease severities recognize SARS-CoV-2 variants of concern.

Chapter based on manuscript published at the Journal for Infectious Diseases DOI: 10.1093/infdis/jiab585

Zoe L. Lyski[1], Amanda E. Brunton[2], Matt I. Strnad[2], Peter E. Sullivan[2], Sarah A.R. Siegel[2], Fikadu G. Tafesse[1], Mark K. Slifka[3], and William B. Messer[1, 2, 4]*.

Affiliations 1. Department of Molecular Microbiology & Immunology, Oregon Health & Science University (OHSU), Portland, OR 97239, USA. 2. OHSU-PSU School of Public Health, Portland, OR 97239, USA. 3. Division of Neuroscience, Oregon National Primate Research Center, Oregon Health & Science University, Beaverton, Oregon, USA. 4. Department of Medicine, Division of Infectious Diseases, Oregon Health & Science University (OHSU), Portland, OR 97239, USA.

Author contributions: Conception of work ZLL and WBM. Data collection, ZLL and AEB Collection/ management of human samples ZLL, AEB, MIS, PES, SARS. Data analysis ZLL, AEB, and WBM. Drafting of the article ZLL and WBM. Critical revision of manuscript ZLL, AEB, SARS, MKS, and WBM. Acquired funding WBM.

Abstract

The unprecedented emergence of pandemic SARS-CoV-2 has called for substantial investigations into the human immune system's capacity to protect against reinfection and keep pace with the emergence and evolution SARS-CoV-2 variants of concern (VoCs). Here we characterize the magnitude, breadth, and durability of SARS-CoV-2 specific antibody responses in two distinct B-cell compartments: long-lived plasma cell-derived plasma antibodies and antibodies encoded in SARS-CoV-2 specific memory B-cells in 35 subjects following natural infection with SARS-CoV-2. We found that magnitude of antibody responses varied significantly between individuals, but was the highest overall in hospitalized subjects. VoC RBD-reactive antibodies were found in the plasma of 66% of samples in this investigation, and all but one subject had VoC-RBD-reactive memory B-cells. This finding, that VoC-RBD-reactive MBCs are present in the peripheral blood of 97% of all subjects, including those that experienced asymptomatic or mild disease, provides a reason for optimism regarding the capacity of vaccination, prior infection, and/or both, to elicit immunity that may have the capacity to limit disease severity and transmission of VoCs as they continue to arise and circulate.

Background

Severe acute respiratory syndrome coronavirus-2 (SARS-CoV-2), the causative agent of COVID-19, emerged in 2019, resulting in 249 million cases and 5.03 million deaths worldwide (November 5th, 2021). SARS-CoV-2 infection leads to illness ranging from asymptomatic to severe, requiring hospitalization, mechanical ventilation, and often leading to death. [179] SARS-CoV-2 specific antibodies are a likely correlate of immunity and are thought to protect against repeat infection, [310] and antibody mediated protection has been observed in humans, non-human primate studies, and

in passive transfer of neutralizing antibodies However, SARS-CoV-2 specific serum antibodies decline in the months following natural infection or vaccination, and neutralizing antibody titers have been reported to be low in many convalescent, naturally infected individuals , with even lower titers against emerging SARS-CoV-2 variants of concern (VoC), calling into question both the durability and breadth of antibody-mediated protection against SARS-CoV-2. [180,310,312-316]

When they encounter their cognate antigen, B-cells differentiate in peripheral lymph nodes, where they either become plasma cells that secrete pathogen specific antibodies present in plasma or serum or become memory B cells (MBCs). Short-lived plasma cells/plasmablasts transiently secrete antibodies before undergoing apoptosis, while long-lived plasma cells (LLPCs) traffic to bone marrow and secrete antibodies for months to years' post-infection, protecting against repeat infections with homologous or closely related pathogens. [238] MBCs also differentiate in germinal centers and then circulate in low numbers in peripheral blood. They do not secrete antibodies, instead they survey the periphery for invading pathogens, poised to quickly respond by proliferating and differentiating into a new population of antibody secreting plasma cells/plasmablasts upon repeat infection/vaccination. MBCs have been found to respond to antigenically diverse, pathogens that evade preexisting, plasma antibodies. [222,254]

Consequently, MBCs have the potential to play a critical role in developing host and herd immunity to SARS-CoV-2, especially in the face of waning antibody titers and the emergence of antigenic variants that differ from early lineage SARS-CoV-2.

The emergence of specific CDC-defined SARS-CoV-2 variants of concern (VoC) has led to concerns that some SARS-CoV-2 viruses may evolve to escape human antibody mediated protection. These variants include Alpha (B.1.1.7), Beta (B.1.351), Gamma (P.1), and Delta (B.1.617.2). [317] Mutations, particularly those in the receptor-binding domain (RBD) on the spike

protein, have been shown to increase transmissibility through better binding to the host ACE-2 receptor as well as reduce antibody-mediated neutralization by human convalescent immune, COVID-19 vaccine sera and therapeutic monoclonal antibodies. [171,172,317-322] While SARS-CoV-2 specific MBCs have recently been characterized studies assessing functional binding of MBC-derived antibodies against VoCs have been limited. Such studies would answer the central question of whether the pre-existing SARS-CoV-2 specific MBC antibody repertoire can recognize and quickly respond to VoC reinfection with an antibody milieu that can either protect against or mitigate severity of VoC infection. [313,316,323-325]

To address this question, we undertook a longitudinal study investigates the magnitude, durability and breadth of antibody-mediated immune memory following SARS-CoV-2 infection. We recruited a cohort of 35 COVID-19 convalescent immune subjects from 1-14 months post infection, who tested positive early in the pandemic, March – July 2020. Including 10 subjects who were vaccinated following natural infection. These subjects experienced a range of disease severity ranging from asymptomatic to severe disease. This work provides a framework to define and predict long-lived immunity to SARS-CoV-2 and emerging variants after natural infection and/or vaccination. We non-specifically stimulated study subject peripheral blood mononuclear cells (PBMCs) to become antibody-secreting cells (ASCs) [264,265] and assessed MBC-derived antibody binding to SARS-CoV-2 early lineage strain WA-1 RBD, the only strain circulating in Oregon until alpha (B.1.1.7) was detected December 2020 and a VoC RBD containing the K417N, E484K, and Y501N mutations present in currently circulating VoCs: Y501N is present in the Alpha, Beta, Gamma, and Delta variants and has been shown to increase transmission via enhanced binding to ACE-2 receptor. [326] E484K is present in 15% of strains circulating in the US (CDC reporting 5/21/2021). K417N and E484K are present in the Beta and Gamma strains. [326]

Materials and methods

Human Research Ethics

The study was reviewed and approved by the Oregon Health & Science University Institutional Review Board (IRB# 21230). Informed consent was obtained from subjects on initiation of their participation in the study.

Human subjects

Subjects with PCR confirmed COVID-19 infection were approached as inpatients at Oregon Health and Science (OHSU) hospital, through study recruitment letters sent out by Oregon Health Authority (OHA), or PCR+ individuals who visited occupational health at OHSU. All subjects included in this study tested positive early in the pandemic, March – July 2020.Upon enrollment, a comprehensive medical history was taken in addition to serum, plasma, and peripheral blood mononuclear cells (PBMCs). When possible, one or more follow-up serial sample visits were arranged. Blood samples (n=67) were collected from 35 convalescent subjects with confirmed COVID-19 infection (OHSU IRB# 21230), between 1- and 14-months post infection, as well as banked samples from six pre-2020 healthy controls. Forty mL of whole blood was collected for peripheral blood mononuclear cells (PBMCs) and plasma (BD Vacutainer® Lavender Top EDTA Tubes). Whole blood was centrifuged at 1,000 x g for 10' and the plasma fraction was collected and stored at -80 until use. PBMCs were subsequently isolated using Sepmate tubes (Stemcell) spun at 800 x g for 20', rinsed, counted, aliquoted and stored in liquid nitrogen until needed.

Human MBC limiting dilution analysis

PBMCs were thawed and resuspended in RPMI 1640 (Gibco), 1×Anti-Anti (Corning), 1X non-essential amino acids (HyClone), 20 mM HEPES (Thermo Scientific), 50μMβ-ME, and 10% heat-inactivated FBS (VWR). Cells were cultured in serial 2-fold diluted doses (10 wells per dose), starting with 3-5 x 10^5 PBMCs per well at the highest dose. In 96-well round-bottom

plates in a final volume of 200µl per well. Cells were incubated with 1000U/ml IL-2 (Prospec) and 2.5µg/mL R848 (InvivoGen).[264] To determine background absorbance values, supernatants were used from 8 wells unstimulated PBMCs only. Plates were incubated at 37 °C and 5% CO^2 for 7 days. Stimulation was determined by total IgG ELISA. Antigen-specific MBC frequencies were calculated by assaying LDA supernatants by antigen-specific ELISA.

Antigen-specific ELISA for plasma and LDA

Ninety-six well (plasma, Corning-3590) or half-well ELISA plates (LDA, Greiner Bio-one) were coated with 100mL (plasma) or 50mL (LDA) of 1µg/mL antigen in PBS, recombinant RBD (provided by Dr. David Johnson), recombinant spike subunit 1 (40591-V08H, Sino Biological Inc.), and recombinant VoC-RBD. Plates were incubated overnight at 4ºC, washed with PBS-T (0.05% Tween) and blocked for 1 hour with 5% milk prepared in PBS-T. For plasma, samples were serially 3-fold diluted in dilution buffer and 100uL was added to wells. Plates were incubated at room temperature (RT) for 1 hour. For LDA, following stimulation, 20 mL of LDA supernatants were added to each well and incubated at room temperature (RT) for 1 hour. Plates were washed 4 times with wash buffer, and 100mL (plasma) or 50 mL (LDA) of 1:3000 dilution of anti-human IgG-HRP (BD Pharmingen, 555788) detection antibody was added and incubated at RT for 1 hour. Plates were washed 4 times with wash buffer, 100mL (plasma) or 50 mL (LDA) of colorimetric detection reagent containing 0.4 mg/ml o-phenylenediamine and 0.01% hydrogen peroxide in 0.05 M citrate buffer (pH 5) were added and the reaction was stopped after 20 minutes by the addition of 1 M HCl. Optical density (OD) at 492 nm was measured using a CLARIOstar ELISA plate reader. Plasma Ab endpoint titers were set as the lowest dilution with an OD 4-fold above PBS only wells. LDA wells were scored positive at ODs at least 2-fold above background (unstimulated PBMC wells).

MBC frequency

MBC precursor frequencies were calculated by the semi-logarithmic plot of the percent of negative cultures versus the cell dose per culture, as previously described [265] and frequencies were calculated as the reciprocal of the cell dilution at which 37% of the cultures were negative for antigen-specific IgG production. Rows which yielded 0% negative wells were excluded, since this typically resides outside of the linear range of the curve and artificially reduced the MBC precursor frequency. For subjects with low frequency of antigen-specific antibody secreting cells frequency was determined by number of positive wells divided by the total number of IgG positive secreting wells, multiplied by one million, giving a frequency per million PBMCs stimulated. [327]

Generation of VoC-RBD and protein expression

To generate the triple mutant VoC-RBD we subjected the wild-type RBD encoding nucleotide sequence to site directed mutagenesis to make the following changes: N501Y, E484K, K417N using Q5 site-directed mutagenesis kit (NEB). Purified SARS-CoV-2 VoC-RBD protein was prepared as described previously. [328] Briefly, His-tagged VoC-RBD bearing lentivirus was produced in HEK 293-T cells and used to infect HEK 293-F suspension cells. The suspension cells were allowed to grow for 3 days, shaking at 37°C, 8% CO2. Cells were centrifuged at 4,000 x g for 10', supernatant collected, sterile filtered, and purified by Ni-NTA chromatography. The purified protein was then buffer exchanged into PBS and concentrated.

Statistical methods

Fisher's exact test was used to calculate P-values in table 1. Kruskal Wallis non-parametric tests were used to compare groups based on disease severity. Samples from subjects who were vaccinated prior to subsequent blood sample collections were included in the longitudinal data, but excluded from all statistical analysis. Paired t-test was used to compare ELISA titers between RBD-WA-1 and RBD-VoC as well as used to compare log transformed specific MBC frequencies

against WA-1 and VoC RBD. Spearman's rank-order correlation was performed for all correlation analysis. All analysis was done in GraphPad Prism version 9.1.1.

Univariate and multivariable analyses

We conducted univariate analyses with each pre-determined clinical covariate of interest and MBC frequency was log transformed. Each univariate analysis was conducted as follows: age (continuous), age (categorical, <50 vs. ≥50), disease severity (ordinal), disease severity (categorical, <5 vs. ≥5), and hospitalization status (yes vs. no). For multivariable models our first model included age (continuous), disease severity score (ordinal), and the interaction between age and disease severity. Contrast estimates were evaluated for each disease severity score interaction with age to determine if any effects within each score and mean age existed. Our second model included age, hospitalization status, and the interaction between hospitalization status and age. Student's t-test was used to compare mean S1- IgG MBC frequencies between paired samples and showed no significant difference (20 paired samples, p=0.792) therefore S1-IgG MBC frequency from the initial draw was used for both of the multivariable analysis models.

All analyses are based on the data for the first blood draw, since repeat draws were not available for all subjects. Student t-test was used to compare subjects with two blood draws to determine if there was a significant difference in S1 MBC frequency between time points and it was not statistically significant ($P < 0.05$). All statistical analyses were performed in SAS version 9.4.

Results

COVID-19 cohort population

Thirty-five SARS-CoV-2 PCR positive subjects were recruited in Oregon under an OHSU IRB

	Hospitalized			
	Yes (n=7)	**No (n=28)**	**Total n, % (n=35)**	
Age				
Mean (SD)	66.9 (12.6)	56.1 (13.1)	58.2 (13.6)	p=0.059
Median [range]	65.0 [54, 86]	57.5 [22, 80]	58 [22, 86]	
Gender (n, %)				
Female	1 (14.3)	14 (50.0)	15 (42.9)	p=0.20*
Male	6 (85.7)	14 (50.0)	20 (57.1)	
Ethnicity (n, %)				
Hispanic	1 (14.3)	0 (0)	1 (2.9)	p=0.20*
Non-Hispanic	6 (86.7)	28 (100.0)	34 (97.1)	
Race (n, %)				
White	6 (85.7)	27 (96.4)	33 (94.3)	p=0.36*
Pacific Islander	0 (0)	1 (3.6)	1 (2.9)	p=1.0*
Declined	1(14.3)	0 (0)	1 (2.9)	p=0.20*
Recruitment population (n, %)				
In-patient OHSU	3 (42.9)	0 (0)	3 (8.6)	p<0.01*
Oregon Health Authority	4 (57.1)	20 (71.4)	24 (68.6)	p=0.65*
Occupational Health	0 (0)	8 (28.6)	8 (22.9)	p=0.17*
Admitted to ICU (n, %)				
Yes	3 (42.9)	NA	3 (8.6)	
No	4 (57.1)	NA	4 (11.4)	
Time to first draw post infection, months				
Mean (SD)	5.5 (3.4)	5.5 (2.3)	5.5 (2.5)	p=0.99
Median [range]	6.6 [0.6, 9.9]	5.3 [1.5, 13.5]	5.9 [0.6, 13.5]	

*Fisher's exact

Table 17 Summary of COVID-19 cohort subject demographics

Stratified by hospitalized (n=7) and not-hospitalized (n=28). Age, gender, ethnicity, race, Recruitment population (inpatient subjects hospitalized at OHSU, Oregon Health Authority (OHA), and OHSU occupational health), and further stratifying hospitalized subjects by admitted to the intensive care unit (ICU) n=3 or not (n=4). Data analyzed by AEB.

approved protocol (IRB# 21230) (Table 10). The subjects included in this investigation, tested

positive early in the pandemic, March – July 2020. Time post-infection, defined by months post-PCR diagnosis, ranged from 1-14 months. WHO disease severity scores, [329] ranged from 1 (asymptomatic) to 6 (severe, requiring intubation and mechanical ventilation), with 2 asymptomatic subjects, 26 symptomatic/not hospitalized subjects, and 7 hospitalized subjects. Subjects were 43% female, with a median age of 58 (Table 10). Of the 35 subjects, ten were vaccinated before their final time-point, providing comparator samples for vaccine-elicited boosting vs. natural decay in un-boosted subjects.

The magnitude, durability, and breadth of LLPC-derived antibodies

A total of seventy plasma samples were collected from 35 subjects 21 or more days post-infection, with 26 subjects providing multiple time points. Plasma antibody concentrations were assayed by IgG ELISA using wild-type WA-1 RBD and VoC RBD (Figure 47). Antibody ELISA titers were below our lower-limit of detection for two asymptomatic study subjects at two separate time points (Fig.47 A, B) against full-length S1, RBD and VoC RBD. All but four symptomatic non-hospitalized cases had detectable antibody titers by ELISA against parental WA-1 RBD, but eight symptomatic subjects had S1 ELISA titers at or below the limit of detection (at least one time point), and ten subjects fell below the limit of detection against VoC RBD (at least one time point) (Figure 47A). All of the hospitalized subjects ELISA titers were above the limit of detection against S1, WA-1 RBD and VoC RBD. Overall geometric mean titers (GMT) ELISA titers across antigens were highest for the hospitalized subjects (S1 759, RBD 1178, VoC 500), with symptomatic, non-hospitalized subjects having lower overall GMT ELISA titers vs S1 (315), WA-1-RBD (459) and VoC-RBD (221) compared to hospitalized

*A) Plasma ELISA titers for pre-2020 plasma (black n=6), asymptomatic (blue n=4 from 2 subjects), non-hospitalized green (n=39 from 26 subjects), and hospitalized red (n=14 from 7 subjects).B) Plasma endpoint ELISA titer following mRNA vaccination. Boxed samples indicate draw after 1 dose (11-33 days post 1st dose). Other Samples taken after 2nd dose (16-72 days post 2nd dose). C) Magnitude of antibody responses stratified by disease severity. Geometric mean titers (GMT) are listed above each group. D) Comparison between ELISA titers against RBD-WA1 and VoC-RBD. Samples from subjects who received a vaccination prior to the second draw were excluded from the data analysis. Paired t-test was performed indicating significant differences between the values (p-value <0.0001) significance denoted by ****. Limit of detection (LOD) is set at 50, all samples below the limit of detection are assigned an arbitrary value of 49.*

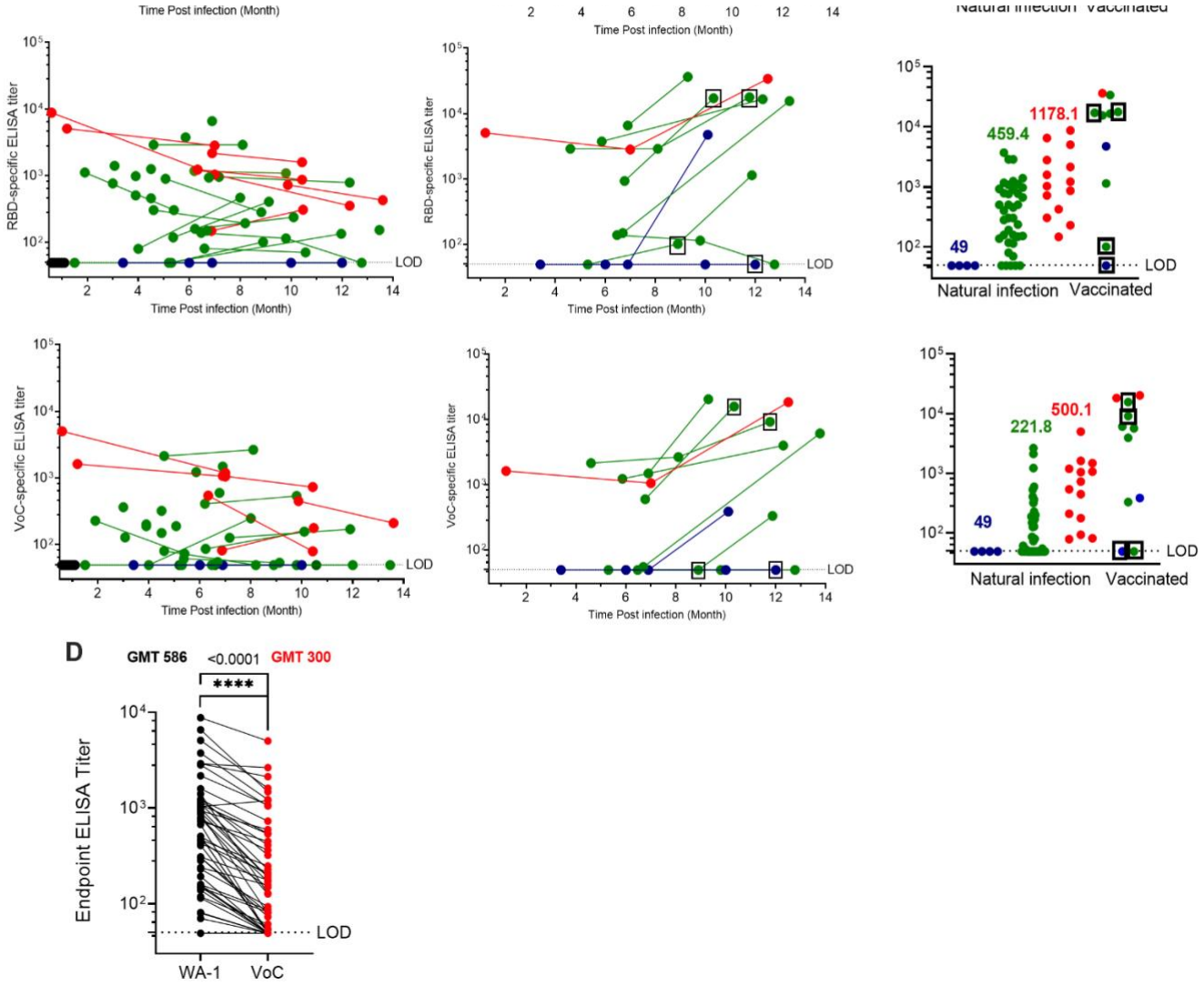

Figure 47 Plasma antibody titers overtime and stratified by disease severity.

subjects (Fig 1C), P= <0.0001. Ten vaccinated subjects are included in the longitudinal data (Figure 4-1B), four samples following a single dose of mRNA vaccine (boxed samples) and seven samples following 2-dose mRNA vaccine series. Most samples showing a boost in ELISA

titer post vaccination, with some achieving the highest ELISA titers against both RBDs in this study. The vaccines were excluded from statistical analyses. There was a significant 1.95-fold decrease in VoC ELISA geometric mean titers when compared to WA-1 (Fig. 36D) across all convalescent samples analyzed.

SARS-CoV-2 specific MBC frequency remains detectable up to 14 months post-infection

Sixty-seven PBMC samples were collected from 35 subjects, with 26 subjects providing multiple time points. In contrast to plasma antibody titers, SARS-CoV-2 S1 and RBD specific MBCs were present above the limit of detection in all subjects in this analysis, even asymptomatic subjects (Figure 37A). Moreover, SARS-COV-2 S1 and RBD-specific MBCs remained detectable for as long as 14 months post-infection (Figure 49A). One subject had a VoC-RBD MBC frequency below the limit of detection. Some subjects experienced an increase in MBC-frequency over time, this is consistent with previous reports of reactive germinal centers persistent for months following infection, leading to further affinity maturation over time in response to SARS CoV-2 infection. [313,316,330] When stratified by disease severity, SARS-CoV specific MBC-frequencies were closely grouped within asymptomatic and hospitalized subjects compared to non-hospitalized subjects whose frequencies spanned the entire range from asymptomatic to hospitalized (Figure 37C) P=0.01. Ten vaccinated subjects were included in the figure (49B) including four samples following a single dose of an mRNA vaccine (boxed samples) and 7 samples following a 2-dose mRNA vaccine series. Most subjects show evidence of post vaccination boost and have high overall SARS-CoV-2 specific MBC frequencies. In contrast to LLPC-derived antibodies RBD-WA-1 and RBD-VoC, MBC–derived antibodies

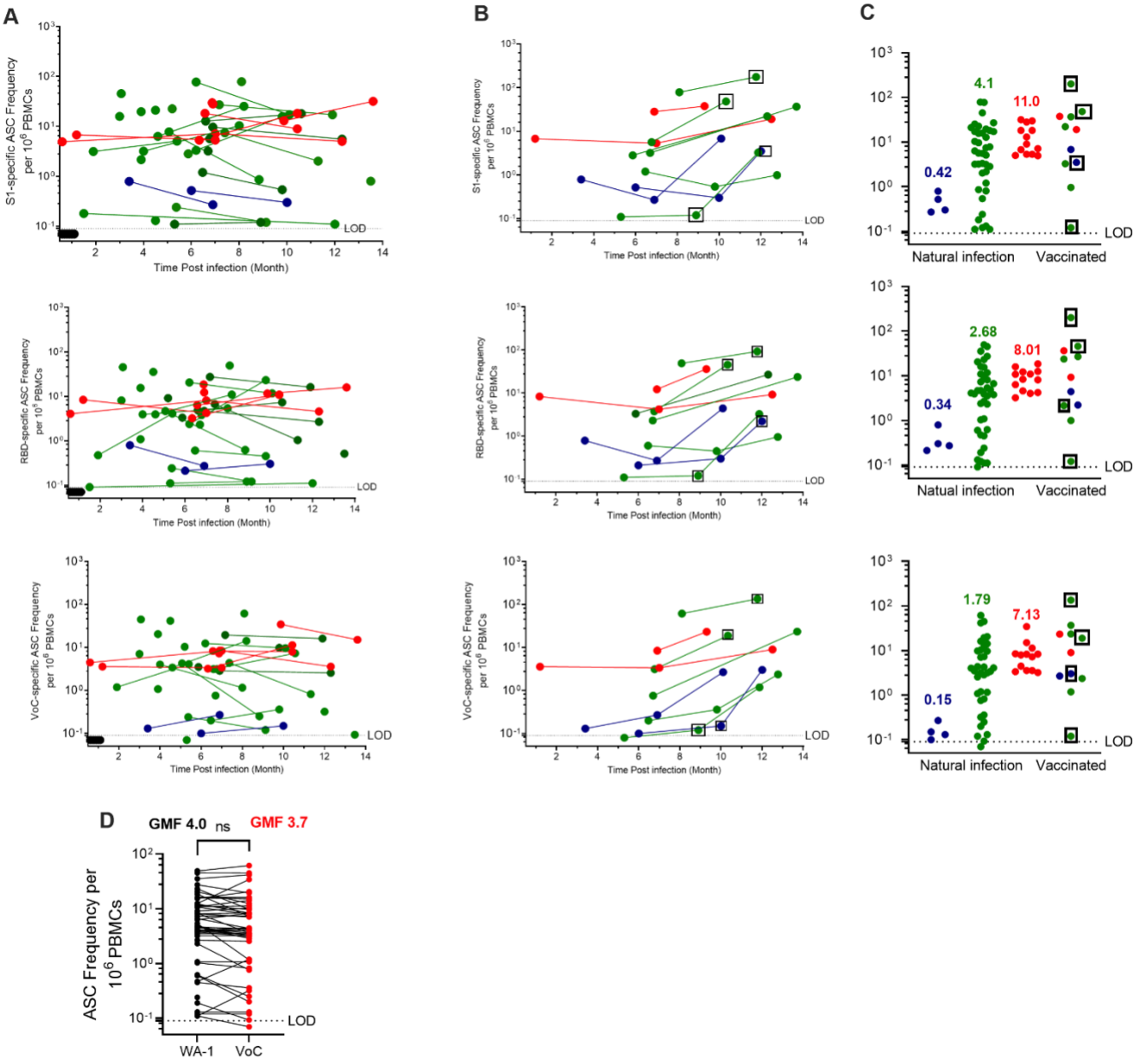

Figure 49 SARS-CoV-2 specific MBC frequency overtime and stratified by disease severity.

A) MBC SARS CoV-2 specific frequency for pre-2020 samples (black n=6), asymptomatic samples (blue n=4 from 2 subjects), non-hospitalized samples, green (n=39 from 26 subjects), and hospitalized red (n=13 from 7 subjects). B) MBC-frequency following mRNA vaccination. Boxed samples indicate draw after 1 dose (11-33 days post 1st dose). Other Samples taken after 2nd dose (16-72 days post 2nd dose). C) Magnitude of MBC-frequencies stratified by disease severity. Geometric mean frequencies (GMF) are listed above each group. D) Comparison between RBD-

showed little variability in their ability to recognize RBD-WA-1 vs RBD-VoC (Figure 49D) with

no significant difference detected between groups.

Relationship between WA-1 and VoC IgG ELISA titer and MBC frequency
We next examined the relationship between RBD-WA-1 specific plasma antibodies and RBD-VoC specific plasma antibodies. We observed a strong linear correlation between WA-1 and VoC RBD specific antibodies, with a Spearman correlation coefficient R^2=0.769 p-value <0.0001, with ELISA titers against RBD-VoC approximately 2-fold lower than RBD-WA-1

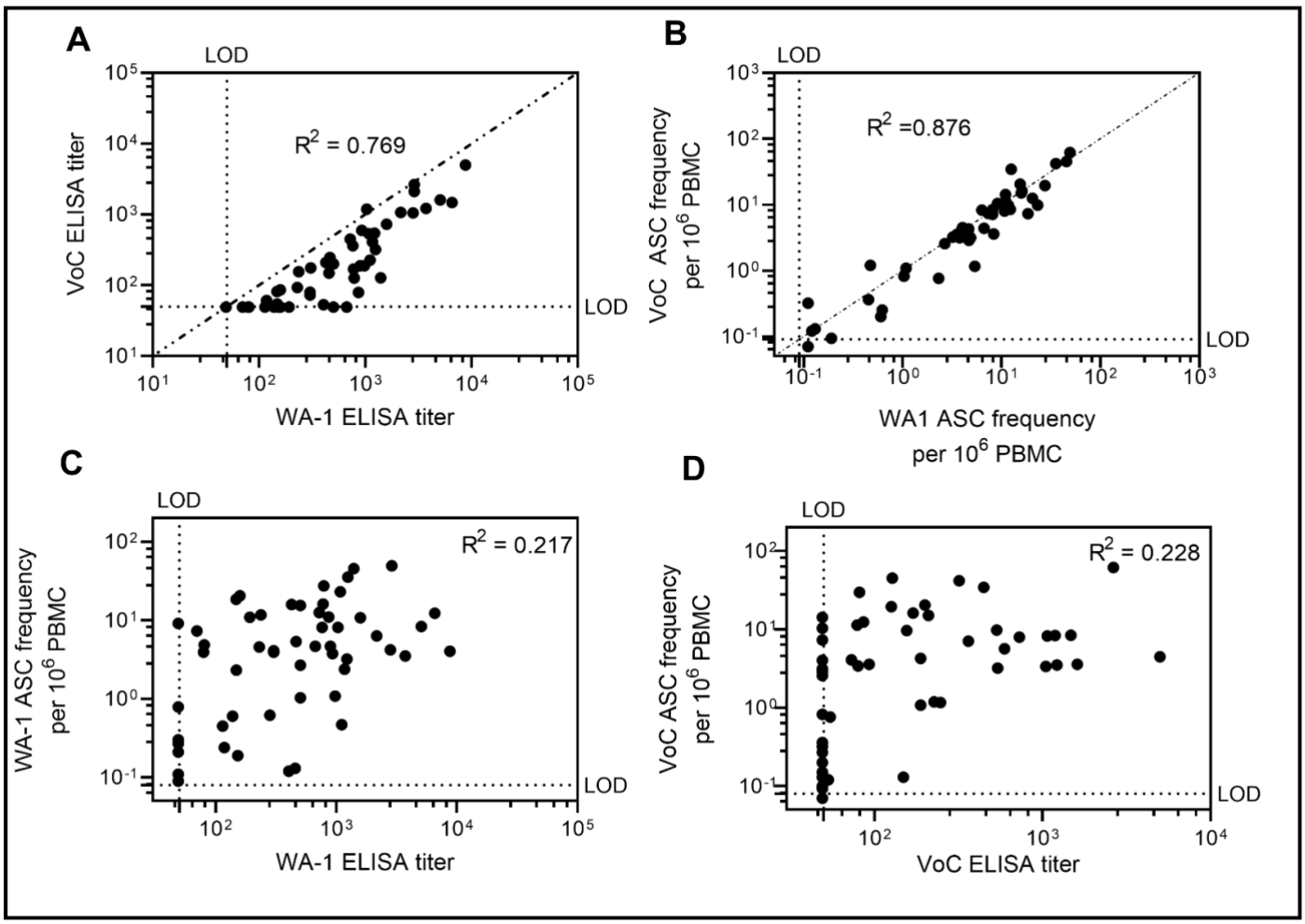

Figure 50 The relationship between WA-1 and VoC antibody binding and MBC frequency as well as the relationship

A) Correlation between RBD-VoC and RBD-WA-1 specific ELISA titers. Spearman correlation coefficient R^2=0.769 p-value <0.0001. B) Correlation between RBD-VoC and RBD-WA-1 specific MBC frequency. Dotted line signifies line of identity. Spearman correlation coefficient R^2=0.876 p-value <0.0001. C) Correlation between WA-1 RBD MBC frequency and ELISA titer (R^2=0.217) and between VoC-RBD MBC frequency and ELISA titer (R^2=0.228).

across all subjects (Figure 36D), WA-1 and VoC RBD specific MBC frequencies were also strongly correlated as well with a Spearman correlation coefficient R^2=0.876 p-value <0.0001, with some samples exhibiting lower frequency to VoC-RBD, but many exhibiting a nearly one to one ratio between both WA-1 and VoC RBDs (Figure 50B). Finally, we noted a much weaker relationship between WA-1 or VoC RBD specific ELISA titers and WA-1 (R^2=0.217, p-value 0.0003) and VoC (R^2=0.228, p-value 0.0004) specific MBC frequency (Figure 50C and D).

The relationship between clinical/disease severity and MBC frequency

	Hospitalized		Total n, %	
Symptoms	**Yes (n=7)**	**No (n=28)**	**(n=35)**	**p-value**
Cough	5 (71)	21 (75)	26 (74)	1.00
Other	6 (86)	17 (61)	23 (66)	0.38
Shortness of breath	6 (86)	16 (57)	22 (63)	0.22
Fever (≥ 100.4F)	3 (43)	15 (54)	18 (51)	0.69
Weakness	5 (71)	12 (43)	17 (49)	0.23
Muscle aches	3 (43)	12 (43)	15 (43)	1.00
Headache	2 (29)	11 (39)	13 (37)	0.69
Chills	3 (43)	7 (25)	10 (29)	0.38
Sore throat	0 (0)	10 (36)	10 (29)	0.08
Loss of taste/smell	2 (29)	8 (29)	10 (29)	1.00
Diarrhea	5 (71)	4 (14)	9 (26)	**0.01**
Runny nose	1 (14)	6 (21)	7 (20)	1.00
Nausea	1 (14)	4 (14)	5 (14)	1.00
Abdominal pain	1 (14)	1 (4)	2 (6)	0.36

Table 19 Summary of reported symptoms experienced during acute illness.

Significance determined by Fisher's exact test, p-values indicated in table. Data and table by AEB.

Outcome: log transformed S1 G MBC				
	Model p-value	**Pt. Estimate**	**Parameter p-value**	**Statistical method used**
Age, continuous	0.79	-0.006	0.79	Linear regression
Age category (<50, 50+)	-	-	0.52	ANOVA
Disease Severity, ordinal	-	-	0.37	ANOVA
Disease Severity (≥5 vs. <5)	-	-	0.69	ANOVA
Hospitalization status	-	-	0.14	ANOVA

Table 20 Univariate analyses

Analysis to determine relationship between MBC frequency, and disease severity score (ordinal or grouped) or age (continuous or grouped).

score, and hospitalization status using ANOVA and simple linear regression models with no significant findings (Table 20). To complete this evaluation, we then analyzed two multivariable models testing the relationship between age and clinical score and MBC frequency. When including an interaction term between age and clinical score, there was no significant relationship (p=0.204, Table 22). Because the distribution of ordinal clinical scores was

Model: S1 G MBC = Age + DS Score + Age*DS Score					
Source	**DF**	**Sum of Squares**	**Mean Square**	**F Value**	**Pr > F**
Model	9	37.792947	4.1992163	1.43	0.2036
Error	46	135.10572	2.9370809		
Corrected Total	55	172.898667			
Source	**DF**	**Type III SS**	**Mean Square**	**F Value**	**Pr > F**
age	1	0.91254217	0.91254217	0.31	0.58
ds_score	3	3.27370958	1.09123653	0.37	0.7739
age*ds_score	3	1.88917146	0.62972382	0.21	0.8859
Model: S1 G MBC = Age + Hosp Status + Age*Hosp Status					
Source	**DF**	**Sum of Squares**	**Mean Square**	**F Value**	**Pr > F**
Model	3	18.5650215	6.1883405	2.09	0.1135
Error	52	154.333646	2.9679547		
Corrected Total	55	172.898667			
Source	**DF**	**Type III SS**	**Mean Square**	**F Value**	**Pr > F**
age	1	3.31508562	3.31508562	1.12	0.2955
hospitalized	1	1.33273145	1.33273145	0.45	0.5058
age*hospitalized	1	0.12151822	0.12151822	0.04	0.8404

Table 22 Multivariate analysis

Two multivariable analyses were run to test whether there was a relationship between age, clinical score and MBC frequency (top). Because the distribution of ordinal clinical scores was largely determined by hospitalization status, we revised the model to test the relationship between age, hospitalization status, and MBC frequency, including an interaction term for age and hospitalization status (bottom). Data and table by AEB.

largely determined by hospitalization status, we revised the model to test the relationship between age, hospitalization status, and MBC frequency, again including an interaction term for age and hospitalization status, and again finding no significant relationship (p=0.114).

Discussion

Breakthrough infections and the emergence of VoCs highlight the limitations of SARS-CoV-2 S specific plasma antibodies alone to recognize and protect against VoCs, and work by our group and others, has shown that serum or plasma antibodies elicited by natural infection have reduced neutralization potency against several VoCs. [319,331] However, serologic studies do not capture the antibodies that will be secreted by MBCs when they are stimulated, expand, and differentiate into a new population of antibody-secreting cells on repeat infection. Here we characterized the SARS-CoV-2 specific MBC derived antibodies, with three critical findings: 1) SARS-CoV-2 RBD specific MBCs can be detected in asymptomatic, seronegative, PCR-positive subjects, 2) MBC populations elicited following primary infection appear relatively stable over time, up to one-year post-infection, and 3), in contrast to plasma antibodies, the antibodies these MBCs are programmed to secrete recognize both parental and VoC RBDs at roughly equivalent frequencies. These results are consistent with MBC studies of other pathogens that show MBCs retain pathogen-specific antibody diversity that is different from LLPC-derived antibodies. [222,254,330] Because of this additional line of antibody defense latent in SARS-CoV-2 specific MBCs, we contend there is reason for optimism regarding the capacity of vaccination, prior infection, and/or both, to limit disease severity and transmission of VoCs as they inevitably emerge in the setting of ongoing transmission. The observation that the high ELISA titers were

seen in previously infected subjects who got vaccinated suggests that vaccines may be particularly effective in previously infected persons, this has been shown previously. [331] While SARS-CoV-2 specific antibodies were detected in 66% of all samples tested and not detected in either of the two asymptomatic subjects in our study, SARS-CoV-2 specific MBCs were detectable in the peripheral blood of all subjects, including asymptomatic subjects. This result supports a recent finding that SARS-CoV-2 specific MBCs are present in the peripheral blood of subjects with no detectable SARS-CoV-2 serum antibodies [332]. In this study, SARS-CoV-2 specific MBC frequency remained stable over time, sometimes even increasing, consistent with other reports and consistent with evidence of extended germinal center activity that remains long after viral clearance, resulting in an increase of MBC frequency as well as an increase in diverse, high affinity MBCs.[313,316,330] As with plasma antibodies, we observed an increase in MBC frequency with an increase in disease severity. We hypothesize that higher and more prolonged antigen load associated with more serious illness correlates with higher antibody titers, similar to what has been shown in Middle Eastern respiratory syndrome (MERS), as well as in SARS-CoV-2 human cohorts. [192,333]

Study limitations include a small number of asymptomatic and hospitalized patients from whom only a subset of longitudinal samples could be collected. Moreover, our LDA approach screened antibodies specific only for S1, RBD and a specific set of known variant mutations in the RBD, while there are VoC associated mutations outside of RBD. Nevertheless, RBD has been widely identified as the most important region for neutralizing antibody epitopes, and while there are likely to be additional RBD mutations that emerge in the future, the principle that MBC-derived antibody diversity extends beyond that seen in circulating antibodies is likely to hold. As more subject antibody responses are studied, more nuanced patterns than those reported here may

emerge. Finally, this study evaluates the specificity of plasma IgG and IgG secreting MBCs. As SARS-CoV-2 is a respiratory pathogen, we expect IgA and MBCs programmed to secrete IgA may also play a role in protection against the variants. Additional studies that address these limitations are critically needed to further our understanding of the multifaceted roles that antibodies continue to play in controlling the COVID-19 pandemic.

Chapter 5: Chronic lymphocytic leukemia: an introduction

5.1.1 Background CLL

Leukemia is a broad category of blood cancer characterized by the uncontrolled growth of leukocytes. Chronic lymphocytic leukemia (CLL) is a heterogenous leukemia characterized by uncontrolled clonal expansion of mature B-cells (CD5+CD23+) in the peripheral blood, lymphoid organs, and bone marrow. [334] The disease is largely considered incurable but has a diverse disease course.

CLL is associated with immune deficits which can be further disrupted by the therapies administered. Interactions between CLL B- cells and the immune system actively create a

supportive environment that allows CLL cells to escape immune pressure. [335] These changes affect more than just the B-cell compartment, such as innate immune responses, impaired natural killer cell function (less cytotoxic), and defects to T-lymphocytes. Including increased numbers of T-cells, such as regulatory T-cells (Tregs) that suppress the cellular immune response. [335-337] Additionally, affected individuals often suffer from hypogammaglobulinemia (low circulating antibody levels) which puts individuals at risk of opportunistic infections. [336,337] In 2021 the estimated number of new CLL cases was 21,250, making up 1.1% of all new cancer cases. CLL deaths made up an estimated 0.7% of all cancer deaths in 2021, although the incidence is relatively low, the global disease burden caused by CLL continues to increase. [338-340] CLL is twice as common in men compared to women, and is typically diagnosed in older adults - 70 years of age is the average age of diagnosis - and is associated with progressive immune defects to both humoral and cellular arms of adaptive immunity. [341] Many affected individuals experience indolent disease progression, with a five-year survival rate of 86%. [342]The leading cause of death in individuals with CLL is disease-related complications such as infections. [337] This is especially concerning in light of the ongoing SARS-CoV-2 pandemic (more in *Infection risk and outcome in individuals with CLL*). [342]

5.1.2 CLL diagnosis and pathogenesis

CLL is derived from mature B-cells that are characterized by weak expression of cell surface markers, CD19, CD20, expression of CD23 (FceRII, the low-affinity IgE receptor), as well as CD200 and CD5. [343] Events leading to the development of CLL are hypothesized to occur in hematopoietic stem cells, through genetic and epigenetic events.

Many CLL diagnoses are made in asymptomatic individuals following routine bloodwork, while others experience signs and symptoms such as night sweats, fatigue, weight

loss, frequent infections, progressive adenopathy, hepatosplenomegaly, or anemia. [341,344] Peripheral blood flow cytometry is the main tool for diagnosis, with greater than 5,000 monoclonal CD5+CD23+ B-cells per microliter of blood for an extended amount of time (3 months), indicating CLL. Another condition, known as monoclonal B-cell lymphocytosis (MBL) is characterized by less than 5000 monoclonal CD5+CD23+ B-cells per microliter of blood for an extended amount of time (3 months), longitudinal studies are required to determine whether MBL progresses to CLL. [345]

5.1.3 Prognosis

There are two standard disease staging systems in place, Rai and Binet, both relying on physical examination and laboratory results (Table 25). [344] The Rai system is most commonly used in the United States and includes five subgroups based on risk (0 – IV). [346] The Binet system utilizes an A, B, C nomenclature to differentiate clinical stages. Five areas of lymphoid involvement include cervical, axillary, and inguinal lymph nodes, as well as the spleen and liver. [347]

Rai						
Stage	**Lymphocytosis: > 15,000/cu mm lymphocytes in the blood with 40% or more lymphocytes in the bone marrow**	**Lymph node enlargement**	**Enlarged liver/spleen**	**Anemia: 11g / 100mL or hematocrit < 33%**	**Thrombocytopenia: platelet count < 100,000 cu/mm**	**Risk**
0	Yes	no	no	no	no	Low
I	Yes	Yes	no	no	no	
II	Yes	Not a requirement	Yes	no	no	Intermediate
III	Yes	Yes	Yes	Yes	no	
IV	Yes	Yes	Yes	With or without	Yes	High
Binet						
A	Yes	Fewer than 3 enlarged lymphoid organs		no	no	Low
B	Yes	Greater than 3 enlarged lymphoid organs		no	no	Intermediate
C	Yes	Irrospective of lymphoid site involvement		Anemia or thrombocytopenia		High

Table 25 Clinical staging by Rai and Binet system. 4-7

Clinicians utilize several clinical, genetic, and molecular tests to allow them to stratify patients based on risk. Studies have shown that this approach can successfully predict average time to

treatment and overall survival in newly diagnosed CLL patients. [342] A prognostic model, CLL international prognostic index (CLL-IPI) was developed with higher discriminatory power compared to clinical staging systems alone. [348] This system takes into account the relative contributions of disease stage as well as disease biology, and patient-specific factors such as age and gender (Table 27). [348] Characteristics that go into the diagnostic index are summarized below:

Useful prognostic serum biomarkers include Beta-2-microglobulin, a ubiquitously

Table 27 CLL International prognostic index criteria.

Risk Category	Score	5-year survival rate
Low	0 to 2	95%
Intermediate	3 to 5	82%
High	6 to 19	68%
Very high	11 to 14	19%
Characteristic	Score	
Del (17p)	6	
Serum thymidine kinase > 10U/L	2	
Serum beta-2-microglobulin. >3.5mg/L	2	
1.7 to 3.5mg/L	1	
Unmutated IgHV status	1	
Eastern Cooperative Oncology Group Performance status >0	1	
Del (11q)	1	
Male	1	
Age > 60 years	1	

expressed protein and a component of MHC-I, and thymidine kinase, a cellular enzyme. Both are highly correlated with disease burden in CLL patients. [349,350] Serum thymidine kinase levels are also useful as a surrogate for IGHV mutational status when sequencing is not available (high levels of thymidine kinase correlate with unmutated IGHV). [351]

The Eastern Cooperative Oncology Group Performance Status is a measurement that describes a patient's ability to function in daily activities and to care for themselves on a scale of 0 (same function as prior to disease diagnosis, without restrictions) to 5 (The subject is dead). [352]

Fluorescence in situ hybridization (FISH), karyotyping, and next-generation sequencing have been useful tools in detecting chromosomal abnormalities and gene mutations, helping clinicians determine treatment options, and stratify risk. [343] The single most important prognostic indicator is a deletion in 17p, determined very high risk due to effects on the tumor suppressor gene p53 which results in the ineffectiveness of certain treatments. [353] Additional chromosomal abnormalities include 11q deletion and 12q trisomy. Patients with 13q deletions (with no other abnormality) have the longest estimated survival times. [353, 343] Gene mutations in NOTCH1 are the most frequent and are associated with poor outcomes in CLL. [343,354] NOTCH1 signaling plays an important role in B-cell survival and apoptosis resistance and is constitutively expressed in CLL B-cells (but not healthy B-cells). [355] Mutations and chromosomal abnormalities can change over the disease course, unlike the mutational status of the IGHV gene which never changes and also serves as an important biomarker in CLL.

It was first observed in the 1990s that CLL patients with a mutated immunoglobulin heavy chain variable region (IGHV) have a longer time to first treatment as well as a longer survival when compared to individuals with an unmutated IGHV gene. [334,356,357] CLL cells with mutations in the IGHV genes likely originate from post-germinal center memory B-cells (CD5+CD27+). Conversely, unmutated IGHV CLL-cells appear to originate from pre-germinal center CD5+CD27- cells which could arise from naïve B-cells in a T-cell independent manner. [358] Mutation status can determine the aggressiveness of disease course, but importantly, IGHV mutational status does not affect the efficacy of targeted treatments. [357]

5.1.4 CLL treatment

CLL is largely considered incurable, with the exception of allogeneic stem cell transplantation, which is generally only recommended when patients have failed to respond or relapsed after treatment with targeted treatments. [359] Therefore, treatment is aimed to control disease and symptoms. [344] Observation without treatment is known as watch and wait and has historically been the gold standard for management of early-stage CLL. [360] The individual is monitored regularly for disease progression and changes in blood cell counts, but no treatments are administered. [344] This is based on previous failed attempts at improving the clinical outcome of CLL treatments with early therapeutic interventions. [361] Survival rates for CLL have improved over time and this can be attributed to better treatment options. [362]

- Chemotherapy: can be used in conjunction with leukapheresis (the removal of lymphocytes from peripheral blood). Chemotherapy was more commonly used prior to the advent of targeted therapy. [356] Alkylating agents (cause DNA damage) such as chlorambucil and purine analogs (inhibits DNA synthesis) such as fludarabine were widely used. [356]
- CD20 monoclonal antibody treatment with rituximab, obinutuzumab, ublituximab, or ofatumumab is often used in conjunction with other therapies such as chemotherapy or targeted therapy. [356] These treatments have seen a decline as newer, more targeted therapy has shown to be much more effective. [356,363] More details below in *anti-CD20 monoclonal antibody treatment*.

- Targeted therapy is the preferred treatment for CLL as it is less harmful to normal healthy cells compared to other more systemic treatments such as chemotherapy. In addition, it

remains effective in patients with 17p deletion or p53 mutation who might not respond to traditional chemotherapy. In addition to improving clinical outcomes, targeted therapies exploit our knowledge of CLL biology. The most common forms of targeted CLL therapy are kinase inhibitors such as Bruton tyrosine kinase (BTK) inhibitors and B-cell lymphoma 2 (BCL2) antagonists. [356,364] These inhibitors are usually taken orally on a daily basis. This will be discussed in more detail in the sections below.

Bruton tyrosine kinase inhibitors

Targeted therapies, small molecule inhibitors, that interfere with B-cell receptor (BCR) signaling are useful as treatments for CLL. Intracellular kinases activate in response to signaling through BCR in response to antigen stimulation leading to B-cell activation. [364, 365] Bruton agammaglobulinemia (X-linked agammaglobulinemia) is a disease caused by a mutation in the gene that encodes for BTK and results in the virtual absence of B-lymphocytes and antibodies. [366] BTK is hence regarded as a critical mediator of BCR signaling, important in the adaptive immune response, and a viable target for CLL treatment. Ibrutinib and second-generation BTK inhibitors such as Acalabrutinib, bind to BTK and inhibit BCR signaling which leads to a decrease in B-cell proliferation. [334] BTK is present on all hematopoietic cells except T-cells. [364] Kinase inhibitors, such as BTK inhibitors, also affect chemokine-signaling which prevents CLL cells from circulating between the peripheral blood and the protective microenvironment within the lymphoid tissue. As such, CLL cells mobilize and move from secondary lymphoid tissues into the peripheral blood, decreasing the size and swelling of lymph nodes and spleen. [356,364,365] Initially this leads to lymphocytosis (increase in lymphocytes in the blood), but over time lymphocyte numbers decrease as CLL cells gradually die off without the pro-survival environment that is afforded in the lymphoid tissues. [365]

BTK can also directly interact with the cytoplasmic domains of most Toll-like receptors (TLR) as well as downstream adaptors such as MYD88 which can play a role in pathogen sensing. [364] TLRs are innate pathogen pattern recognition receptors on the cell surface or within endosomes that recognize highly conserved motifs on the surface of pathogens such as polysaccharides, DNA, or RNA. BTK has a role in sensing pathogens through multiple TLR sensors: TLR2, TLR3, TLR4, TLR 7/8, and TLR 9. [367]Transfer of BTK deficient mice have shown a decreased ability to respond to LPS (a TLR-4 ligand). [364]

BTK signaling also plays a role in the maturation, recruitment, and function of innate immune cells, such as monocytes/macrophages (reduced numbers), neutrophils (immature), dendritic cells (defects in antigen presentation).[367]

Active treatment with BTK inhibitors like ibrutinib has a significant impact on B-cell survival, differentiation, and the development of an antigen-specific antibody response to novel antigen exposure either by natural infection or vaccination. [240,368, 369] However, serum antibodies to previously encountered antigens such as those seen during childhood appear to remain largely intact. [240] Data suggests that cellular immune responses may be preserved in CLL patients on BTK inhibitors. [240,368] The impact of prolonged treatment vs. shorter-term BTK inhibition on immune responses is unknown. However, clinical data suggests some improvement in humoral immunity with prolonged treatment (> 6 months), including a decrease in the number of infections, stable serum IgG levels, and an increase in serum IgA levels over time. [370, 371]

BCL-2 inhibitors

Another form of targeted therapy is a small molecule that works as a BH3 mimic to inhibit BCL-2, a protein regulator of apoptosis. [372] CLL cells express high levels of BCL-2

which helps them avoid spontaneous or drug-induced cell death. [365,372] venetoclax is an FDA-approved oral BCL-2 antagonist and is used for the treatment of CLL. [372] BCL-2 inhibitors are highly effective in high-risk patients, particularly those with 17p deletions. Some patients develop resistance to ventoclax due to mutations in BCL2 that affect inhibitor binding, therefore second-generation BCL-2 inhibitors are in development. [365, 373]

It has been observed that treatment with ventoclax reshapes the immune environment, decreasing immune suppression brought on by CLL. [335] Neutropenia is commonly observed following ventoclax treatment, but is not associated with an increased risk of infection. [335] Treatment with venetoclax decreased numbers of non-CLL lymphocytes, although they generally remained within the normal range and treatment did not appear to reduce the functionality of T-cells or NK cells. [335]

Anti-CD20 monoclonal antibody treatment

Rituximab is a chimeric monoclonal antibody that causes a transient reduction in B-cell count, by binding to CD20 on the surface of B-cells and inducing complement-dependent cytotoxicity and to a lesser extent antibody-dependent cellular cytotoxicity (ADCC). [363,374] Other anti-CD20 monoclonal antibodies are available such as, obinutuzumab, which has been glycoengineered to mediate slightly different effector functions, antibody-dependent phagocytosis and ADCC. [363] In recent years the standard of care has shifted from using anti-CD20 monoclonal antibody treatment in conjunction with chemotherapy to using targeted therapies such as BTK and BCL-2 inhibitors. [363] Because treatment with anti-CD20 monoclonal antibodies depletes circulating B-cells, treatment is correlated with a reduction in

circulating antibody response, however, long-lived plasma cells in the bone marrow appear unaffected. [240]

5.1.5 Infections or vaccinations with CLL

Due to the inherent immune dysfunction caused by CLL itself as well as CLL-targeted treatments described above, individuals with CLL are at an increased risk of infections and are known for being poor vaccine responders. [375]

Infection risk and outcome in individuals with CLL

Individuals with CLL, both on active treatment and treatment naïve, are at high risk of infections, both with pathogenic and non-pathogenic fungi, bacterial, and viral agents that can cause considerable morbidity and mortality. [376] [376]The most commonly documented infections are bacterial (67%), viral (25%), and fungal (7%), of which only 3% were severe. [337,375,377,378] The frequency of particular infections appears to partially depend on treatment. [378,379]

Treatment with alkylating agents results in an increase in Gram-negative bacterial infections due to resulting neutropenia. [379] Treatment with purine analogs results in an increase in fungal and viral infections such as *Aspergillus* and herpesviruses due to resulting T-cell deficits. [379] Treatment with monoclonal antibody treatments results in an increase in fungal and viral infections such as *Aspergillus* and cytomegalovirus reactivation, due to depletion of B lymphocytes. [379] Treatment with BTK inhibitor (ibrutinib) exhibited comparable rates of severe infection (24.0% versus 22.4%) compared to anti-CD20 monoclonal antibody treatment. [379] Treatment with BTK inhibitors resulted in a higher rate of infection during the first 6-months of treatment (16.3 infections per 100-patient months) which reduced to 6.9 after 6 months of

treatment. [380] ventoclax is associated with severe neutropenia, however, rates of infection appear comparable to treatment with BTK inhibitor. [379]

Ways to lower risk of infections

Hypogammaglobinemia, defined as serum IgG less than 600mg/dL, is an important risk factor for developing infections. [375] High-risk individuals with hypogammaglobinemia, who are prone to repeat infections, or infections in which no safe vaccines are available, intravenous immunoglobulin (IVIG), the transfer of intravenous antibodies from a healthy donor, can be beneficial but needs to be administered every 3-4 weeks. [381] *Streptococcus pneumoniae* and *Haemophilus influenzae* are associated with low serum IgG levels which have been shown to correlate with predicting infections. [377,378] Repeat infections occur more often in individuals with serum IgG levels below 600mg/dL however, there are people with low serum IgG who do not suffer from repeat infections indicating that other factors play important roles, such as neutrophil count and the presence of antigen-specific antibodies. [382]

COVID-19 risk in individuals with CLL

Cancer patients represent an especially vulnerable group in light of the ongoing COVID-19 pandemic. [383] Individuals with hematological malignancies who were infected with SARS-CoV-2, the causative agent of COVID-19, had an overall death rate of 34% which further increased in people over the age of 60. [384] Individuals with CLL experienced hospitalization rates as high as 90% with COVID-19, and a case fatality rate of >37%. [385] Given these poor outcomes of disease, vaccines were prioritized in individuals with hematological malignancies, including those with CLL.

Humoral immune response to vaccination in CLL subjects

Because people with CLL are at an increased risk of infection, vaccinations against seasonal infections such as influenza are recommended however, live-attenuated vaccines are not recommended due to the increased risk of infection-mediated complications. [386] Because anti-CD20 monoclonal antibody treatment can ablate circulating B-cells, vaccination is not recommended within 6 months of receiving treatment. [379] Vaccine response in CLL patients is suboptimal, due to defects in antigen presentation, innate signaling, and adaptive immune responses already described. [375,387] Antibody responses following vaccination are impaired in patients with hematologic malignancies. [240,336,368,387-389] Often attributed to a lack of functional B-cells and T-cell help combined contribute to poor vaccine responses. [240,389] Protein antigens such as tetanus-diphtheria toxoid protein and conjugate vaccine antigens such as *Haemophilus influenzae* b, are much better at eliciting an antibody response than polysaccharide-only (Pneumococcal polysaccharide) which is ineffective in CLL patients. [390,391, 392] Poor seroconversion was also observed following seasonal influenza vaccination with rates ranging from 0 to 26%, the lowest responders being those on active treatment with BTK inhibitors. [393, 394] Following mRNA COVID-19 vaccination, the overall seroconversion rate was 60%, when stratified by treatment none of the patients on active or previous treatment seroconverted while 72% of treatment-naive subjects had detectable RBD-specific antibodies. [395]

Overall rates of seroconversion appear to be significantly influenced by disease status, immunoglobulin (IgG) levels, and active or recent therapies. [396-399] In particular, treatment with anti-CD20 directed monoclonal antibodies and BTK inhibitors are associated with poor vaccine responses. [336,369,388]

Cellular immune response

The antibody-specific response to vaccination in CLL patients has been much more extensively explored than the cellular immune response. However, overall the cellular immune response appears to be much less impaired than the humoral immune response after vaccination. [240,389,400] Following 2-dose COVID-19 mRNA vaccination, 35-80% of CLL subjects, with diverse treatment history, generated a functional cellular response, compared to 100% of healthy controls. [401, 395, 240] In one study, Forty percent of CD4+ responders seroconverted, providing supporting evidence for the importance of CD4+ T-cell help in generating a B-cell response. [240] In response to recombinant varicella-zoster vaccination 78% of CLL subjects observed a CD4+ specific response. [386] The robust cellular responses seen post-vaccination are consistent with results seen after natural infection in CLL patients, with recent studies observing 82% of subjects developed spike-specific T cell responses following SARS-CoV-2 infection. [402]

Antibody-mediated immune memory and memory B-cell recall response

Immune memory, serum antibodies to previously experienced antigens, are less disrupted than antibody response to novel vaccine antigens. In a vaccine study, 41.5% compared to only 3.8% of patients on BTK inhibitors were seropositive. For treatment naïve subjects the seropositivity rate was 59.1% for previously experienced antigens compared to 28.1% for novel antigens. [369] This indicates that BTK inhibitors disrupt the generation of a novel immune response, but don't necessarily significantly interfere with immune memory (long-lived plasma-derived antibodies in the serum). In another investigation, the authors explored long-lived antibody-mediated immunity to measles virus, a common childhood antigen exposed to either through vaccination or natural infection. [403] Eighty-one percent of subjects were seropositive for measles. Of three seronegative subjects, two were on active treatment and one subject was treatment

naïve. This is a slightly higher response rate than was observed in a recent cross-sectional study of 959 patients which detected an overall 63% measles seropositivity rate in cancer patients with hematological malignancies. [403] Overall, the antibody response to measles seems largely unaffected in CLL subjects, indicating that certain populations of long-lived plasma cells responsible for maintaining circulating serum antibodies remain stable throughout CLL immune dysfunction and treatment. These findings may have clinical implications, especially in the setting of vaccines that are not associated with durable antibodies where the combination of circulating B-cell depletion (anti-CD20) and diminishing antibody response may abrogate viral-specific humoral immunity**.**

Chapter 6: Cellular and humoral Immune response to mRNA COVID-19 vaccination in subjects with chronic lymphocytic leukemia

Zoe L.Lyski,[1] Myung S. Kim,[2] David Xthona Lee,[1] Hans-Peter Raué,[3] Vikram Raghunathan,[2] Janet Griffin,[2] Debbie Ryan,[2] Amanda E. Brunton,[4] Marcel E. Curlin,[5] Mark K. Slifka,[3] William B. Messer,[1,4,5] Stephen E. Spurgeon[2*]

Affiliations
1. Department of Molecular Microbiology & Immunology, Oregon Health & Science University (OHSU), Portland, OR 97239, USA. 2. Knight Cancer Institute, Oregon Health & Science University (OHSU), Portland, OR 97239, USA 3. Division of Neuroscience, Oregon National Primate Research Center, Oregon Health & Science University, Beaverton, Oregon, USA. 4. OHSU-PSU School of Public Health, Portland, OR 97239, USA. 5. Department of Medicine, Division of Infectious Diseases, Oregon Health & Science University (OHSU), Portland, OR 97239, USA

Author contributions: Conception of work ZLL, MSK, WBM, and SES. Data collection, ZLL,

MSK, DXL, HPR, and AEB. Collection/ management of human samples ZLL, AEB, JG, DR, and

MEC. Data analysis ZLL, MSK, DXL, HPR, and AEB. Drafting of the article ZLL, MSK, and SES. Critical revision of manuscript ZLL, HPR, MEC, MKS, and SES. Acquired funding WBM and SES.

Introduction

Severe acute respiratory syndrome coronavirus 2 (SARS-CoV-2) is of special concern to patients with chronic lymphocytic leukemia (CLL).[385,404] Over time individuals with CLL experience impaired B-cell function and antibody production, leaving patients at increased risk of severe infection or death. Patients with CLL suffer immune dysregulation from the disease, which is further disrupted by the effects of CLL specific treatments. There are now three vaccines for SARS-CoV-2 approved in the United States[405], with high immunogenicity in immunocompetent subjects.[210,406,407]

The post-immunization dynamics in CLL patients is different than that observed in healthy subjects. Attenuated humoral responses to vaccination have been previously documented.[408-411] Patients with CLL have among the lowest immune responses, influenced by disease status, immunoglobulin (IgG) levels and active or recent therapies.[396-399] In particular, treatment with anti-CD20 monoclonal antibodies (mAbs) or Bruton tyrosine kinase inhibitors (BTKi) is associated with poor vaccine response.[369,411]

In this longitudinal cohort study, we interrogated the cellular and humoral immune response to novel vaccine antigen, BNT162b2 (Pfizer-BioNTech) or mRNA-1273 (Moderna), as well as the humoral recall response to measles in 16 subjects with CLL. In response to vaccination, immunocompetent individuals generate an antigen-specific response that results in cellular and humoral memory that persists long after vaccination[212] including CD4+ T-cells, CD8+ T-cells, and

two distinct long-lived populations of B-cells, long-lived plasma cells (LLPCs) and memory B-cells (MBCs). LLPCs, traffic to the bone marrow and continuously secrete the antibodies that comprise polyclonal immune serum and MBCs, which do not secrete antibodies, circulate in peripheral blood surveying for invading pathogens. MBCs are especially important in the face of waning antibody titers or the emergence of new variants that might escape neutralization by serum antibodies.[303]

Results

We enrolled subjects 18 years and older without a known history of COVID-19 infection, prior to receiving, the Moderna or Pfizer-BioNTech 2-dose SARS-CoV-2 mRNA vaccine series. This study reports the presence and magnitude of humoral and cellular immune responses including quantitative receptor-binding domain (RBD)-specific antibody titers, RBD-specific MBC frequency following *in vitro* stimulation and functional, TNF-α and INF-γ secreting spike peptide-specific CD4+ and CD8 T-cells at baseline (prior to vaccination) and around one-month (24-103 days) following two-dose mRNA vaccination series.

We observed a 25% seroconversion rate. Four patients with vaccine-mediated antibody responses were diverse with 1 treatment naïve, 1 on current treatment with bcl-2 inhibitor and 2 under observation. For patients under observation, 1 was in remission while the other had relapsed disease. When stratified by treatment, 50% of subjects currently on observation following treatment seroconverted compared to 12.5% currently on active treatment (Figure 39A, and Table 16 and 17). Of the responders (4/16), one had never received anti-CD20 mAb treatment and three had over 12 months prior, consistent with previous studies.[412] In an attempt to identify potential predictors of response, we evaluated a number of clinical factors as well as immune profiling. Although no significant differences were appreciated, responders had overall higher IgG serum levels, and lower ALC, mean B-cell percentage, class switched MBCs, and B1-B-

ID	Age	Vaccine	Response to mRNA COVID-19 vaccine				Response to Measles		Treatment	CD20 Ab	ALC	IgG	CD19+	IgD-CD27+	CD4	CD8 (%)
	/Sex		Ab	CD4	CD8	MBC	Ab	MBC			1-4.8	700 - 1600 mg/dL	4-17 (%)	5-21 (%)	30-60 (%)	10-30%
1	62/M	P	-	-	-	-	-	-	N	N	48.00	85	96.00	3.60	2.00	0.70
2	63/F	P	-	-	+	-	+	+	N	N	21.00	-	76.00	59.00	9.30	10.00
3	48/M	?	+	+	-	-	-	-	C	Y(≤12)	1.00	-	2.10	17.00	39.00	33.00
4	77/F	M	-	-	-	-	+	-	N	N	87.00	573	-	-	-	-
5	81/F	P	-	-	+	-	+	+	C	Y(>12)	5.80	-	-	-	19.00	3.80
6	67/M	M	-	+	+	-	+	+	C	N	2.90	918	30.00	2.30	41.00	19.00
7	60/F	P	-	+	+	-	+	-	O(6)	Y(>12)	1.60	-	0.00	0.00	86.00	8.00
8	66/M	P	-	-	-	-	+	-	C	Y(>12)	0.43	526	3.00	22.00	35.00	47.00
9	65/F	?	-	+	+	-	+	-	C	Y(≤12)	1.30	-	0.07	0.00	62.00	21.00
10	62/F	P	-	+	-	-	-	-	C	Y(>12)	30.00	262	65.00	2.40	23.00	8.00
11	63/M	P	+	+	+	-	+	+	N	N	17.00	780	83.00	0.21	13.00	2.10
12	61/M	P	+	+	+	+	+	-	O(6-12)	Y(>12)	0.75	593	8.00	3.80	42.00	15.00
13	70/M	P	-	+	-	-	+	-	C	Y(>12)	5.80	101	45.00	1.50	20.00	20.00
14	65/M	P	-	+	-	-	+	-	O(>12)	Y(>12)	0.33	405	-	-	77.00	9.30
15	64/M	M	-	-	+	-	+	-	C	Y(>12)	1.70	100	0.41	0.94	26.00	42.00
16	75/M	P	+	+	+	-	+	-	O(>12)	Y(>12)	0.29	547	0.10	0.00	22.00	19.00

Table 29 Summary table of subject immune responses to mRNA COVID-19 vaccination

+ indicates a response above the limit of detection, a - indicates a response below the limit of detection. For T-cell specific responses, a + indicates an increase in spike specific T-cells compared to baseline, a – indicates no change (or decrease) in spike specific T-cells following vaccination. Current treatment status, CD20 Ab treatment as well as clinical values taken at baseline (time of enrollment) when available. A dash for clinical values indicates that baseline values are not available. For clinical values, the normal range is indicated. N: Treatment Naïve, C: Currently on treatment, O (6): Observation, last treatment within 6 months, O (6-12): Observation, 6-12 months since last treatment, O (>12): Observation, more than 12 months since last treatment.

cells when compared to non-responders (Tables 29 and 30). Interestingly, only one subject, currently in disease remission, with bcl-2 inhibitor treatment occurring > 6 months prior to vaccination in combination with an anti-CD20 mAb treatment given > 12 months prior to vaccination, exhibited an RBD-specific memory B-cell response (Subject 12). The observation that 3 of 4 patients with an RBD-specific antibody response did not have detectable RBD-specific MBCs is notable (Figure 51B). All subjects who had an RBD-specific antibody response also had a spike (S)-specific CD4+ T-cell response, indicating that a population of T-helper cells was available for B-cell priming. SARS-CoV-2 S reactive T-cells were present at baseline in some of the subjects (Figure 51C and table 29). Subjects 5 and 8, and Subjects 3 and 13 exhibited no expansion of S-responsive CD4+ T-cells and or and S-reactive CD8+ T-cells respectively following vaccination. This is consistent with previous reports of S-reactive T-cells in naïve individuals without prior antigen exposure.[413] The cellular immune response appeared to be fairly robust in these CLL subjects compared to humoral immune response, consistent with previous

studies.[400,414] We observed a 62.5% CD4+ and 56% CD8+ T-cell response. Four subjects had a S-specific CD4+ response alone, 3 had a S-specific CD8+ response alone, and 6 subjects had both a CD4+ and CD8+ response. Four of the 10 CD4+ responders seroconverted, providing supporting evidence for the importance of CD4+ T-cell help in generating a B-cell response. Active treatment with BTKi has a significant impact on B-cell survival, differentiation and the development of an antigen-specific antibody response to novel antigen exposure. B-cells are dependent on BTK signaling, for differentiation and proliferation signals, and immune response to novel antigens, either by natural infection or vaccination is severely limited in these subjects,[369] however recall to previously encountered antigens remain largely intact (Figure 51D). Seventy-one percent of subjects on BTKi had cellular immune response with CD4+ and/or CD8+ T-cells. Whether this finding translates to an effective T-cell response associated with a clinical benefit is of interest. Given BTKi are administered daily, further studies that evaluate timing of vaccines, or interruption of ongoing BTKi therapy in an attempt to enhance vaccine response are warranted. This approach has shown success in patients with rheumatologic disease on immunosuppressive therapies.[415] Bcl-2 is a protein regulator of apoptosis and preclinical data suggests bcl-2 inhibition affects T-cell function.[416] The impact of ongoing bcl-2 inhibition with venetoclax remains an unanswered question worthy of additional study. A recent study[369] reports impaired vaccine response to novel antigens in CLL patients, resulting in seroconversion in 28.1% of treatment naïve subjects and only 3.8% of patients on BTKi. When compared to humoral response to previously vaccinated antigens, the response was 41.5% in subjects on BTKi and 59.1% for treatment naïve subjects indicating that BTKi disrupt the generation of novel immune response, but don't necessarily interfere with recall. We explored recall response to measles, where we observed that 81% of subjects were seropositive for measles serum antibodies, two

subjects (Subject 3 and 10) are currently on active treatment with bcl-2 inhibitor and BTKi respectively and one is treatment naïve. This is a slightly higher response rate than was observed in a recent cross-sectional study of 959 patients[403] which detected a 63% measles seropositivity rate in subjects with hematological malignancies. The antibody response to measles seems largely unaffected in CLL subjects, indicating that LLPCs responsible for maintaining circulating serum antibodies remain stable throughout CLL immune dysfunction and treatment. However, the MBC recall response to measles was highly disrupted in these subjects. Only 25% retained a detectable population of measles-specific MBCs, of these four subjects, two were on active treatment (Subject 5 and 6) and two were treatment naïve. Even though a population of measles specific MBCs was detected in these subjects, the frequencies were lower than those observed in age/gender matched healthy controls (geometric mean frequency 78.4).

Conclusion

In summary, the results of this study provide a thorough evaluation of the humoral and cellular immune response to initial 2-dose mRNA COVID-19 vaccine series in CLL patients. Our results highlight the limitations of serology studies alone in defining vaccine-mediated immune responses, particularly in this immune-dysregulated patient population. Larger longitudinal studies, incorporating clinical outcomes in vaccinated CLL patients as well as the impact of a third, booster or heterologous vaccine are needed.

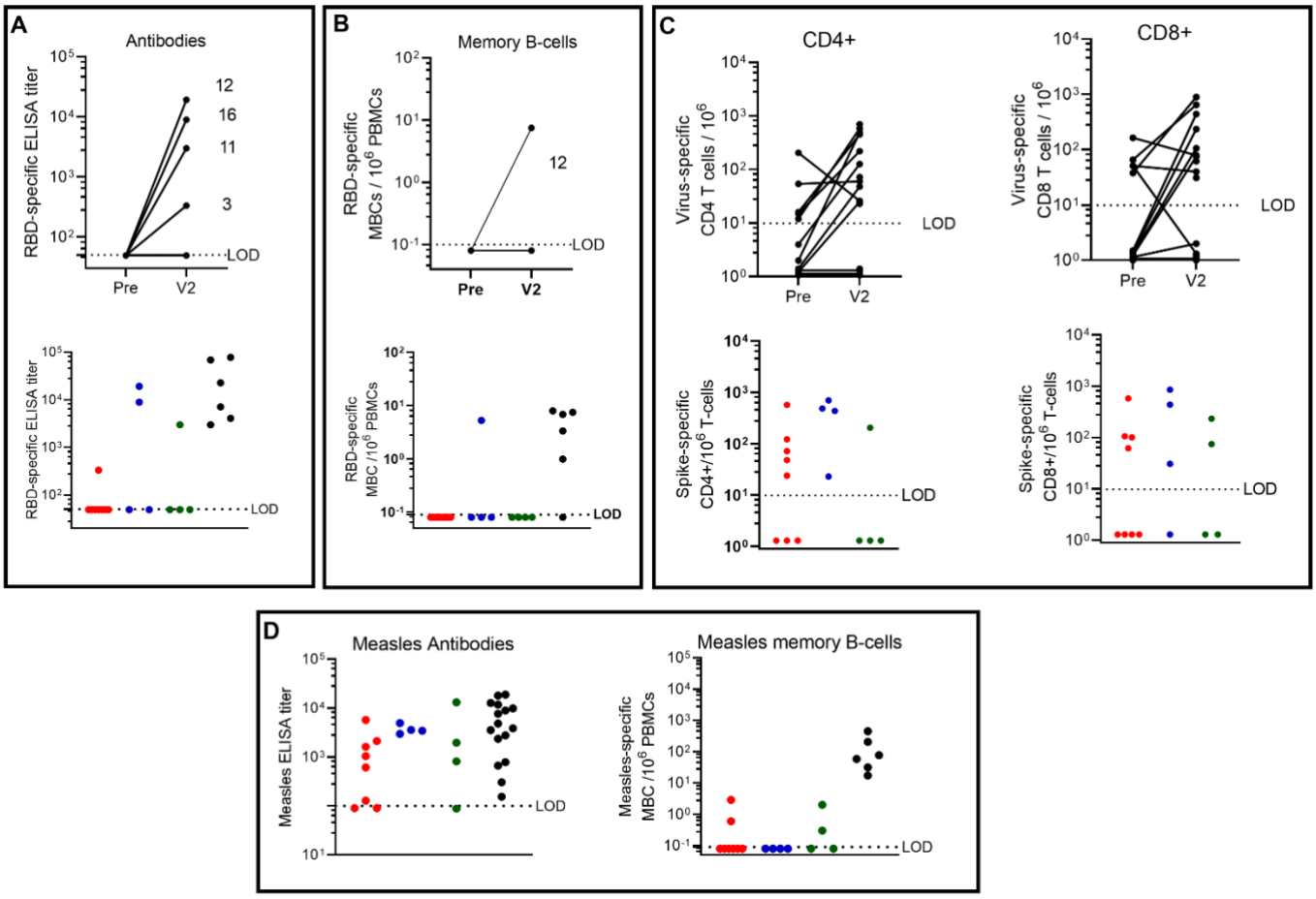

Figure 51 Humoral and cellular immune response to mRNA COVID-19 vaccination.

A) Antibodies- RBD-specific endpoint ELISA titer following COVID-19 mRNA vaccination. Top) Pre bleed prior to vaccination and V2 following 2-dose vaccination series (24-103 days). Bottom) RBD-specific ELISA titer stratified by treatment group, geometric mean titer (GMT) of responders shown above graph. The limit of detection, LOD, is set at 50, samples below the LOD were given an arbitrary value of 49. Healthy subject samples were taken (13-28 days) following 2-dose vaccination series. B) RBD-specific memory B-cell frequency per 10^6 PBMCs following COVID-19 mRNA vaccination. Top) Pre bleed prior to vaccination and V2 (24-103) days following 2-dose vaccination series. Bottom) RBD-specific MBC frequency stratified by treatment group. Geometric mean titer of responders shown above graph. Healthy subject samples, (247-264) post 2-dose vaccine series. Limit of detection, LOD = 0.1, an arbitrary number 0.08 was assigned to samples below the limit of detection. C) Spike-specific CD4 and CD8 T-cell frequency per 10^6 T-cells following COVID-19 mRNA vaccination. Top) Pre bleed prior to vaccination and V2 following 2-dose vaccination series (24-103 days). Bottom) Spike-specific CD4+ and CD8+ response to vaccination, the increase in T-cell expansion from baseline, stratified by treatment group. Geometric mean of responders shown above graph. Limit of detection (LOD =10), for subjects without vaccine specific response, an arbitrary value between 1.1- 1.5 was assigned. D). Humoral immune recall response to a childhood antigen, measles, in CLL subjects and age-gender matched healthy controls. Antibodies) Measles-specific endpoint ELISA titer stratified by treatment group. Limit of detection (LOD = 100) Samples below the limit of detection assigned an arbitrary value of 80. Geometric mean titer (GMT) of responders shown above the graph for each group. Memory B-cells) Measles-specific MBC frequency stratified by treatment group, geometric mean frequency of responders shown above graph. Limit of detection, LOD = 0.1 an arbitrary number between .05 and .1 was assigned to those samples. Red = active treatment, blue = observation after treatment, green = treatment naïve, and black = healthy age/gender matched controls.

Methods

Study Design

This study was conducted at a single site at Oregon Health and Science University. The protocol was approved by the Oregon Health and Science University Institutional Review Board (OHSU IRB# 21230). All participants gave written informed consent before enrolling in the study. This vaccine arm of the cohort is part of a larger biobank study on human immune response during and following acute viral infection and vaccination against novel viruses. SARS-CoV-2 vaccines were administered through standard procedures as part of the Oregon's COVID-19 Vaccination Plan and not as part of the study. On initial enrollment, demographics, CLL disease characteristics, and treatment details were collected (Table 1), and baseline laboratory values were obtained (Table 2), including SARS-CoV-2 spike antibody titer, serum IgG, a complete blood count, and multicolor flow cytometry measuring immune cell populations (Table 2). One-month following completion of 2-dose mRNA vaccination series, follow up draws were completed and vaccine-specific immune response was evaluated. Study protocol includes additional serology studies at 3 months, 6 months, and 1 year following vaccine.

Participants

Eligible participants were adults 18 years or older with confirmed diagnosis of CLL or small lymphocytic lymphoma (SLL) who did not have a history of previous SARS-CoV-2 infection or vaccination. Subjects were excluded if they had received anti-CD20 therapy within 6 months of enrollment. Prior intravenous immune globulin (IVIG) therapy was not an exclusion criterion.

Healthy subject controls

Age and gender matched controls who received a two-dose mRNA (Pfizer-BioNTech) vaccine in January – February 2021were enrolled in a vaccine study approved by the Oregon Health and Science University Institutional Review Board. Serum from twelve age/gender matched controls (13 – 28 days following 2nd dose) and PBMCs (247 – 267 days following 2nd dose) from six

age/gender matched controls were used for determining RBD and measles specific antibody responses in immunocompetent subjects.

Statistical Analysis

Mean and median lymphocyte panel laboratory findings were determined for each positive and negative antibody response, cellular immune response, and MBC frequency. Group means were compared using an independent t-test, except where applicable and noted, the Satterthwaite test statistic was used instead. Mean, median, and independent group t-tests were also calculated for IgG and ALC values collected at the time of vaccination. The relationship between prior CD20 mAB treatment and current treatment status with antibody, MBC frequency, and cellular immune responses were similarly assessed using a chi-square test, or Fisher's exact, where applicable. All statistical analyses were performed in SAS version 9.4.

Sample processing

After obtaining informed consent, at the time points indicated, 10mL of whole blood was collected for serum (BD Vacutainer® Red Top Serum Tubes) and 40mL of whole blood was collected for PBMCs and plasma (BD Vacutainer® Lavender Top EDTA Tubes). Plasma and serum samples were centrifuged for 10 minutes at 1000 x G, heat inactivated and stored at -20C. PBMCs were isolated and stored in liquid nitrogen until needed.

Antigen-specific plasma endpoint ELISA:

ELISAs were performed as previously described[417], Briefly, ninety-six well ELISA plates (3590, Corning) were coated with 100 µL recombinant RBD protein (Provided by Dr. David Johnson) at a concentration of 0.5 µL/mL or 50 µL of measles virus antigen (MyBioSource, MBS239121) at a concentration of 4 µg/mL prepared in PBS and the plates were incubated overnight at 4°C. Coating antigen was removed, plates were washed once with PBS-T containing 0.05% Tween (wash buffer) and blocked for 1 hour at RT with 5% milk prepared in PBS-T containing 0.05% Tween (dilution buffer). Plasma in dilution buffer, 100 µL of 1:50 (RBD) or 1:30 (measles)

dilution was added to each well. Plasma samples were serially 3-fold diluted in dilution buffer. Plates were incubated at RT for 1 hour. The plates were washed 3 times with wash buffer and 100 µL of 1:3000 dilution of anti-human IgG (H+L) HRP (Novus, NBP1-73319) detection antibody was added and incubated at RT for 1 hour. After rinsing (3X) with wash buffer, 100 µL of colorimetric detection reagent containing 0.4 µg/ml o-phenylenediamine and 0.01% hydrogen peroxide in 0.05 M citrate buffer (pH 5) were added and the reaction was stopped after 20 minutes by the addition of 100 µL 1 M HCl. Optical density (OD) at 492 nm was measured using a CLARIOstar ELISA plate reader. Antibody titers were determined by logarithmic transformation of the linear portion of the curve with an endpoint of 0.1 optical density units.

MBC limiting dilution analysis:

PBMCs were thawed and resuspended in LDA media, RPMI 1640 (Gibco), 1×Anti-Anti (Corning), 1X non-essential amino acids (HyClone), 20 mM HEPES (Thermo Scientific), 50µMβ-ME, and 10% heat-inactivated FBS (VWR). Cells were cultured in serial 2-fold diluted doses (10 wells per dose), starting with 3-5 x 10^5 PBMCs per well at the highest dose. In 96-well round-bottom plates in a final volume of 200µl per well[263]. Cells were incubated with IL-2 (Prospec) 1000U/ml and R848 (InvivoGen) 2.5ug/m.[264] To determine background absorbance values, supernatants were used from 8 wells unstimulated PBMCs only. Plates were incubated at 37 °C and 5% CO^2 for 7 days. Stimulation was determined by running total IgG ELISAs. Antigen-specific MBC frequencies were calculated by assaying LDA supernatants by antigen-specific ELISAs. MBC precursor frequencies were calculated by the semi-logarithmic plot of the percent of negative cultures versus the cell dose per culture, as previously described [265] and frequencies were calculated as the reciprocal of the cell dilution at which 37% of the cultures were negative for antigen-specific IgG production. Cell doses which yielded 0% negative wells were excluded, since this typically resides outside of the linear range of the curve and artificially

reduced the MBC precursor frequency. For subjects with low frequency of antigen-specific antibody secreting cells frequency was determined by number of positive wells divided by the total number of IgG positive secreting wells, multiplied by one million, giving a frequency per million PBMCs stimulated.

Antigen-specific ELISA for LDA:

Ninety-six well half-well ELISA plates (Greiner Bio-one) were coated with 50uL of 0.5 µg/mL antigen in PBS, recombinant RBD protein (provided by Dr. David Johnson) and measles virus antigen (MyBioSource, MBS239121). Plates were incubated overnight at 4°C, washed once with PBS-T containing 0.05% Tween (wash buffer) and blocked for 1 hour with 5% milk prepared in PBS-T containing 0.05% Tween (dilution buffer). 20 uL of LDA supernatants were added to each well. Plates were incubated at room temperature (RT) for 1 hour, washed 4 times with wash buffer, and 50 uL of 1:3000 dilution of anti-human IgG-HRP (BD Pharmingen, 555788) detection antibody was added and incubated at RT for 1 hour. Plates were washed 4 times with wash buffer, 50 uL of colorimetric detection reagent containing 0.4 mg/ml o-phenylenediamine and 0.01% hydrogen peroxide in 0.05 M citrate buffer (pH 5) were added and the reaction was stopped after 20 minutes by the addition of 50 uL 1 M HCl. Optical density (OD) at 492 nm was measured using a CLARIOstar ELISA plate reader. Positive wells were determined as wells 2-fold above background (unstimulated PBMC wells).

Spike-specific simulation and intracellular cytokine staining

PBMCs were thawed at 37°C, washed and resuspended in RPMI1640 (Corning) supplemented with 5% FBS (Hyclone), Glutamine (Corning), HEPES (Lonza) and Pen Strep (Gibco). Cells were stimulated at 1 million cells/well in 200 µl in 96 well round bottom plates (Corning) at 37°C/6% CO_2 with 2 peptide pools (peptides 1-90 and 91-181 at 0.5 µg/ml of each peptide) of overlapping (10AA) 17mers representing the SARS-CoV-2 Spike protein (BEI Resources). All

conditions contain a final DMSO concentration of 0.045%. Positive control wells were stimulated with 0.04 µg/ml anti-CD3 (HIT3a NA/LE, BD Biosciences) in media containing 0.045% DMSO or incubated with 0.045% DMSO media alone to assess spontaneous production of cytokines. After 1 hour, Brefeldin A (Sigma) was added to a final concentration of 2 µg/ml and stimulations were continued for 5 hours. Intracellular cytokine staining was performed as described previously.[418,419] After stimulation, cells were stained overnight at 4°C with anti-CD8, anti-CD4+ (2ST8.5H10 and L200 BD Biosciences) and Aqua live/dead stain (InVitrogen) in PBS + 1% FBS + 0.1 mg/ml MsIgG. Following overnight incubation, cells were fixed with 2% formaldehyde in PBS. After staining with anti-IFNγ and anti-TNFα (4S.B3 and Mab11 from eBioscience)) in PermWash cells were washed with PermWash, PBS + 1% FBS and fixed with 2% formaldehyde in PBS. Data was acquired on an LSR Fortessa (Becton Dickenson) and analyzed using FlowJo software (Becton Dickenson). Cytokine expression in medium +DMSO alone cultures was subtracted from peptide-stimulated cultures to calculate peptide-specific cytokine expression. Responses to both peptide pools were added together to yield the total frequency of SARS-CoV-2-specific cytokine producing CD4+ and CD8+ T cells.

Supplemental data

	N= 16 (median, IQR)
Age	64.5 (60-75)
Sex	
Male	10
Female	6
Race	
White	15
Asian/White	1
Treatment status	
Treatment naive	4
Active treatment	8
Observation after prior treatment	4
Previous lines of treatment (n=12)	1 (0-4)
Current treatment (n=8)	
BCL2 inhibitor + anti-CD20	1
BCL2 inhibitor + BTK inhibitor	1
BTK inhibitor	6
Time since previous anti-CD20 (n=11)	
6-12 months	2
>12 months	9
Previous IVIG (n=6)	
≤ 6 months	0
>6 months	6
IGHV (n=8)	
Mutated	5
Unmutated	3
Baseline IgG (n=10)	466 (85-918)
Baseline ALC (n=14)	2.91 (0.33-87)
Rai stage at diagnosis	
0	9
I	5
II	1
III	0
IV	1

Table 31 Supplemental table of subject demographics

			TNFa+IFNg+ Spike-specific response cells per 10^6 T-cells	
Subject ID	Treatment	Visit	CD4	CD8
1	N	Pre	0	0
		Post vaccination	0	0
2	N	Pre	0	0
		Post vaccination	0	**235**
3	C	Pre	**4**	164
		Post vaccination	**126**	79
4	N	Pre	0	**51**
		Post vaccination	0	0
5	C	Pre	**54**	0
		Post vaccination	**60**	**106**
6	C	Post vaccination	**72**	**62**
7	O (6)	Pre	**2**	0
		Post vaccination	**488**	**440**
8	C	Pre	**205**	0
		Post vaccination	**26**	2
9	C	Pre	**12**	**66**
		Post vaccination	**583**	**647**
10	C	Pre	1	0
		Post vaccination	**25**	0
11	N	Pre	**15**	0
		Post vaccination	**220**	**75**
12	O (6-12)	Pre	16	38
		Post vaccination	**451**	**894**
13	C	Pre	0	**51**
		Post vaccination	**48**	40
14	O (>12)	Post vaccination	**701**	0
15	C	Post vaccination	0	101
16	O (>12)	Post vaccination	**23**	**31**
	BOLD	2 fold background		

Table 32 Supplemental table T-cell specific responses

T-cell specific response per subject, pre and post vaccine. CD4 and CD8 spike-specific T-cell response per subject per 10^6 T-cells. N: Treatment Naïve, C: Currently on treatment, O (6): Observation, last treatment within 6 months, O (6-12): Observation, 6-12 months since last treatment, O (>12): Observation, more than 12 months since last treatment.

Table 34 *Clinical markers at baseline, stratified by antibody,*

	Response										
	Antibody			CD4			CD8			MBC	
	Pos (n=4)	Neg (n=11)		Pos (n=10)	Neg (n=5)		Pos (n=8)	Neg (n=7)		Pos (n=1)	Neg (n=14)
B-cells (CD19+) %											
Mean (SD)	23.3 (39.9)	34.4 (36.2)	p=0.6	23.3 (31.0)	47.5 (43.6)	p=0.2	32.4 (36.0)	30.2 (39.0)	p=0.9	8.01 (NA)	33.1 (36.8)
Median [min, max]	5.1 [0.1, 82.9]	30.3 [0, 96.2]		5.1 [0, 82.9]	61.6 [0.4, 96.2]		19.2 [0.004, 82.9]	3.0 [0, 96.2]		8.01 (NA)	16.7 [0, 96.2]
B-cells (CD19+) #, log[a]											
Mean (SD)	5.6 (3.5)	6.4 (3.9)	p=0.7	5.9 (3.7)	6.6 (4.1)	p=0.7	6.4 (3.8)	6.0 (3.9)	p=0.9	4.09 (NA)	6.4 (3.8)
Median [min, max]	4.1 [3.0, 9.6]	7.9 [0, 10.7]		6.8 [0, 9.9]	8.2 [1.9, 10.7]		7.5 [0, 9.7]	5.5 [1.9, 10.7]		4.09 (NA)	7.9 [0, 10.7]
IGD+27-naive B-cells of B-cell %											
Mean (SD)	29.9 (42.9)	24.6 (32.1)	p=0.8	24.2 (34.4)	29.7 (35.8)	p=0.8	17.1 (31.5)	36.2 (35.7)	p=0.3	93.6 (NA)	21.2 (29.1)
Median [min, max]	10.9 [4.1, 93.6]	11.4 [0, 91.5]		7.5 [0, 93.6]	21.3 [0.09, 91.5]		7.1 [0, 93.6]	24.1 [0, 91.5]		93.6 (NA)	10.7 [0, 91.5]
IGD+27+non-switched B of B-cell %											
Mean (SD)	45.3 (43.8)	40.8 (43.3)	p=0.9	44.9 (44.1)	36.4 (41.4)	p=0.7	49.8 (48.7)	33.2 (34.1)	p=0.5	1.48 (NA)	44.9 (41.9)
Median [min, max]	42.1 [1.5, 95.7]	19.8 [0, 100]		41.4 [0, 100]	19.8 [0.09, 87.8]		52.2 [0, 100]	19.8 [0, 73.2]		1.48 (NA)	43.0 [0, 100]
IGD-27+Switched Memory B of B-cell %											
Mean (SD)	5.3 (8.1)	8.4 (18.0)	p=0.7	2.8 (5.3)	17.3 (25.1)	p=0.3[c]	8.2 (20.6)	6.9 (9.1)	p=0.9	3.77 (NA)	7.9 (16.3)
Median [min, max]	2.0 [0, 17.3]	1.5 [0, 59.2]		0.9 [0, 17.3]	3.6 [0.5, 59.2]		0.3 [0, 59.2]	2.4 [0, 22.5]		3.77 (NA)	1.2 [0, 59.2]
B1 B-cells(CD5+CD19+) %											
Mean (SD)	19.5 (37.7)	32.8 (35.1)	p=0.5	20.5 (28.2)	46.9 (43.6)	p=0.2	30.5 (35.3)	28.0 (37.4)	p=0.9	0.8 (NA)	31.3 (35.4)
Median [min, max]	0.96 [0.08, 76.2]	30.4 [0.006, 95.9]		1.0 [0.006, 76.2]	60.0 [0.2, 95.9]		15.6 [0.007,76.2]	2.2 [0.006, 95.9]		0.8 (NA)	16.3 [0.006, 95.9]
B1 B-cells(CD5+CD19+) #, log[b]											
Mean (SD)	4.6 (4.3)	7.1 (3.5)	p=0.3	6.3 (3.4)	6.4 (4.3)	p=0.96	7.2 (3.2)	5.7 (4.2)	p=0.5	1.79 (NA)	6.8 (3.5)
Median [min, max]	2.4 [1.8, 9.5]	8.0 [1.4, 10.7]		7.3 [1.8, 9.6]	8.2 [1.4, 10.7]		8.2 [1.8, 9.7]	5.1 [1.4, 10.7]		1.79 (NA)	8.0 [1.4, 10.7]

[a]Sample size: antibody (n=3, 9), CD4 (n=7, 5), CD8 (n=6, 6), MBC (n=11)

[b]Sample size: antibody (n=3, 8), CD4 (n=6, 5), CD8 (n=5, 6), MBC (n=10)

[c]Satterthwaite test statistic

Table 35 Specific B-cell populations (%) stratified by antibody, CD4, CD8, and MBC responders and non-responders

	Response											
	Antibody			CD4			CD8			MBC		
	Pos (n=4)	Neg (n=12)		Pos (n=10)	Neg (n=6)		Pos (n=8)	Neg (n=8)		Pos (n=1)	Neg (n=15)	
Prior CD20 mAB, n (col %)[a]	3 (75.0)	8 (66.7)	p=1.0	8 (80.0)	3 (50.0)	p=0.3	5 (62.5)	6 (75.0)	p=1.0	0 (0.0)	11 (73.3)	p=0.31
Treatment, n (col %)												
Naïve[a]	1 (25.0)	3 (25.0)	p=1.0	1 (10.0)	3 (50.0)	p=0.12	2 (25.0)	2 (25.0)	p=1.0	0 (0.0)	4 (26.7)	p=1.0
Active[a]	1 (25.0)	7 (58.3)	p=0.57	5 (50.0)	3 (50.0)	p=1.0	3 (37.5)	5 (62.5)	p=0.62	0 (0.0)	8 (53.3)	p=1.0
Observation[a]	2 (50.0)	2 (16.7)	p=0.24	4 (40.0)	0 (0.0)	p=0.23	3 (37.5)	1 (12.5)	p=0.57	1 (100.0)	3 (20.0)	p=0.25
IgG mg/dL, log[b]												
Mean (SD)	6.4 (0.19)	5.6 (0.92)	p=0.15	6.1 (0.76)	5.4 (1.03)	p=0.27	6.5 (0.24)	5.4 (0.84)	**p=0.03**	6.4 (NA)	5.8 (0.90)	
Median [min, max]	6.4 [6.3, 6.7]	5.8 [4.4, 6.8]		6.3 [4.6, 6.8]	5.4 [4.4, 6.4]		6.5 [6.3, 6.8]	5.6 [4.4, 6.4]		6.4 (NA)	6.1 [4.4, 6.8]	
ALC												
Mean (SD)	4.8 (8.17)	17.2 (26.6)	p=0.38	6.1 (9.81)	27.3 (34.3)	p=0.19[c]	6.3 (8.07)	21.8 (31.7)	p=0.22[c]	0.75 (NA)	14.9 (24.3)	
Median [min, max]	0.9 [0.3, 17.0]	4.4 [0.3, 87.0]		1.5 [0.3, 30.0]	13.4 [0.4, 87.0]		2.3 [0.3, 21.0]	3.8 [0.3, 87.0]		0.75 (NA)	2.9 [0.3, 87.0]	

[a]Fisher's exact

[b]IgG sample size: antibody (n=3, 8), CD4 (n=7, 4), CD8 (n=4, 7), MBC (n=1, 10)

[c]Satterthwaite

Table 36 Clinical markers at baseline, stratified by antibody, CD4, CD8, and MBC responders and non-responders.

.

Chapter 7: Conclusions and future directions

In Chapter 2, we identified long-lived humoral immunity to DENV, including both LLPC and MBCs in our endemic and non-endemic cohorts up to 43 years post-infection. We observed no relationship between neutralizing antibody titers and NS1 ELISA titers in either cohort, indicating that they might serve as independent correlates of protection. I predict that different infection courses result in different antigen loads for NS1 and whole virus, therefore we could hypothesize that more severe cases of dengue result in higher loads of secreted NS1 and therefore a higher titer of LLPC-derived NS1 antibodies. We could test this hypothesis by enrolling subjects during acute infection and following them overtime to determine if serum NS1 levels are correlated with a more robust NS1 antibody response. Longitudinal data from a large endemic cohort in Nicaragua has provided some insight into antibody titers that are necessary to prevent severe disease or hospitalization. [81] What is unclear is what role NS1-specific antibodies play in protection and how the durability of NS1 antibodies might be different from E-specific (whole virion) antibodies. For this initial analysis a cross-sectional approach was taken, with single samples from a large number of subjects interrogated. For future experiments I would like to apply the techniques developed here to interrogate samples longitudinally, this would inform us as to how LLPC and MBC populations change over time in boosting (endemic) and non-boosting environments. Next steps would be to look at whole-virus-specific antibodies as well as NS1.

Slifka and Amanna [239] developed an imprinted lifespan model describing four principles of immune durability. 1) Lifespan is imprinted at the time of antigen exposure. 2) The bone marrow environment is space limited therefore LLPCs have varying lifespans based on the probability that the antigen is relevant and protective. By this tenet, soluble epitopes are more likely to represent self-antigens or T-cell independent antigens, whereas complex antigens capable of generating a T-cell dependent response have a high probability of being more long-lived. 3) Within T-cell dependent responses, antigens can be further divided into monovalent and multivalent. Complex antigens on the surfaces of viruses and bacteria are highly repetitive (multivalent) compared to internal proteins such as nonstructural proteins which are more likely to be monomeric. It is hypothesized that monomeric responses have a lower probability of being protective, therefore they are shorter lived, years to decades, compared to multivalent responses which can last the lifespan of an individual. 4) In order to achieve long-term immunity a certain antigenic threshold must be met. Based on these principles, I hypothesize that with longitudinal follow-up we will see antibodies specific to NS1 (monomeric, less complex) decay at a faster rate that E-specific (whole virion, complex) antibodies. I also hypothesize that we will see differences between our non-endemic (non-boosting) and out endemic (boosting) cohorts, providing evidence that repeat antigen exposure, even if it doesn't result in clinical disease, maintains LLPC and MBC populations.

In chapter 2, we utilized two independent, highly correlated methods, LDA and flow cytometry to interrogate DENV-specific MBCs. By LDA we identified functional, DENV-1 specific antibodies in all subjects except the farthest out from infection (43 years), all 12 immune-subjects interrogated by flow cytometry were positive for the presence of DENV++

MBCs, even as long as 43 years post-infection. We provided supporting evidence for the use of fluorescently labeled whole virus as bait in flow cytometry by sorting cells and confirming their antigen-specificity. This sets the stage for future experiments interrogating antigen-specific MBCs in our large cohorts of endemic and non-endemic subjects. This approach should allow us to identify DENV-specific, or cross-reactive MBCs of interest at the single cell level and clonally track MBCs of interest overtime. In addition, this approach allows us to clone individual MBC-derived monoclonal antibodies to better understand the antibody repertoire that is formed after a single DENV infection.

Using longitudinal samples from our unique human cohorts we can ask some exciting questions about MBC recall response. With the techniques developed here, the next steps would be to map the MBC" founder" population after initial infection and determine what MBCs expand after subsequent challenge, either natural infection or vaccination (DENV or closely related flavivirus YFV). I hypothesize that a new population of serotype-specific B-cells, specific to the infecting virus will be generated. As well as a population of broad, unmutated MBCs from the initial infection that will respond quickly by clonally expanding into a new population of antibody-secreting cells. These experiments have the potential to uncover questions of original antigen sin and how primary DENV immunity effects subsequent infections.

In chapter 3 we observed breadth in alphavirus antibody responses that extend to all members of the SFV complex but not beyond. Antibody breadth was greatest in individuals with recent infection and became more CHIKV-specific with time. We observed that a specific linear peptide (E2B) on the E2 protein is important for cross-neutralization, and when we deplete E2B antibodies from serum we lose the ability to neutralize heterotypic virus. For some subjects the effects of E2B bead depletion were great (10-fold) and in others small (less than 2-fold). We

also observed long-lived populations of alphavirus-specific MBCs, as far as 24 years post-infection, including MBCs specific to CHIKV, MAYV, and E2B. Similar to what we observed with serum antibodies, the fraction of cross-reactive antibodies that are attributable to E2B vary amongst individuals. The mechanism behind this is not understood at this time, but warrants further investigation. The next steps would be following these subjects longitudinally as well as recruiting more subjects, at varying times post infection, so that we can further investigate differences in cross-reactivity overtime. Due to the principles of immune imprinting summarized above, I hypothesize that cross-reactive E2B antibodies which recognize a linear epitope on E2 (E2B) are not as long-lived and will decay faster than antibodies that recognize more complex epitopes. Additionally, it would be interesting to apply these techniques to interrogating CHIKV vaccine responses to see if the same cross-reactive responses are generated. According to the 4th principle of immune imprinting, a sufficient antigen load must be reached in order to generate a robust and long-lived response, therefore I hypothesize that replicating vaccine platforms would be able to generate a robust humoral response.

In chapter 4 we once again used limiting dilution assays to interrogate antigen-specific MBCs to a newly emerged respiratory pathogen, SARS-CoV-2, highlighting the versatility of our approach. Here, we interrogated the magnitude, breadth, and durability of SARS-CoV-2 specific LLPC-derived and MBC-derived antibodies. Much like we have observed in chapters 2 and 3, the magnitude varies between subjects. Interestingly, when we stratified our SARS-CoV-2 subjects by disease severity, none of our asymptomatic subjects had a detectible antibody titer above our limit of detection. However, they did have detectable S1 and RBD-specific MBCs representing an expanded population of antigen-specific MBCs, poised to respond in the event of

SARS-CoV-2 infection or vaccination. Populations of LLPC-antibodies and MBCs appeared durable out to 13 months post-infection, however further longitudinal analysis is warranted. Future studies dedicated to further understanding the differences in humoral immune responses and disease severity are needed, specifically what clinical features of disease determine the best responders. I hypothesize that because the immunodominant epitope, RBD, is multivalent epitope on the surface of the virion, a high enough antibody threshold must be met in order to account for decay overtime. Future studies to understand how antibody breadth to emerging variants develops are also of great importance. Longitudinal studies can help elucidate whether vaccination or repeat infection is leading to new populations of antigen specific B-cells or further affinity maturation of existing B-cell populations. One limitation of our work is that we only interrogated IgG-specific responses. IgG is an important antibody isotype for systemic infections as it protects from viremia, however IgA present at mucosal surfaces is important as the first line of defense. Therefore, IgA might be a better correlate of protection and warrants future investigation in our cohort.

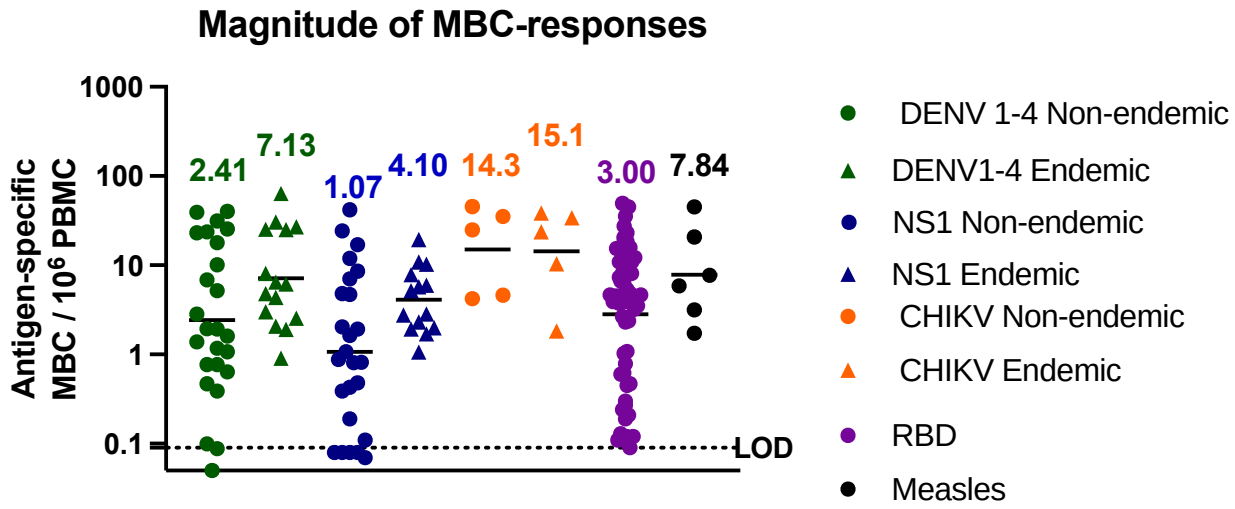

Figure 52 Summary of antigen-specific MBC responses observed in our cohorts irrespective of time post-infection. Geometric mean frequencies are shown above each population of antigen-specific MBCs.

In chapters 2,3, 4, and 6 using different antigens we observed robust populations of antigen-specific MBCs (Figure 40), as well as differences between LLPC-derived antibodies and MBC frequency, highlighting the importance of studying both arms of the humoral immune response. Often immune response to vaccination or natural infection is based on serum antibody titers alone, here we have shown, for multiple antigens that the LLPC-derived antibody response does not correlate strongly with the antigen-specific MBC response from the same infection/vaccination, therefore it is important to study both arms of the humoral immune response, as they are independent measurements. In chapters 3 and 4 we observed greater antibody breadth in MBC-derived antibodies compared to LLPC-derived antibodies, providing further supporting evidence that these are two independently formed B-cell populations that serve distinct purposes in immune protection. We are optimistic that the increased breadth within the MBC-population plays an important role in protection against newly emerging viruses and viral variants that escape serum antibodies.

In chapter 6 we showed a poor humoral immune response to mRNA COVID-19 vaccination in our CLL cohort. This is not surprising, given the immune disruptions that are associated with CLL disease and treatment, however there is potential to utilize this disruption to better understand the basic immunology behind immune responses to vaccination. Of the 16 subjects, 25% seroconverted, however only 25% of those subjects had a detectable SARS-CoV-2-specific MBC response. Future studies will allow us to follow these subjects longitudinally to see if an antigen-specific MBC response develops overtime, or if the seroconversion we are observing is the product of short-lived plasma cells only and true memory (LLPC and MBC) responses are not being generated. The cellular response was much less impaired; however, it remains to be seen if a T-cell response alone is protective in these individuals. In appendix 2 we

reported our findings for two subjects who received a 3rd heterologous dose of a COVID-19 vaccine. Here one subject seroconverted and was positive for the presence of RBD-specific B-cells, and spike-specific CD4+ and CD8+T-cells. Future studies will be aimed at determining if more of our CLL cohort subjects respond to a third (or 4th dose of COVID-19 vaccination) and if this response can be predicted based on available clinical data such as serum IgG levels, ALC, or numbers of circulating B-cells.

Because the poorest responders are those on active treatment, consideration should be given to timing of treatment in regard to vaccination schedule. Further experiments could be dedicated to investigating the timing, or interruption of treatment with vaccine response. Most interestingly, I think this system allows us to better understand the requirements of a successful vaccine response.

Appendix I: Approaches to Interrogating the Human Memory B-Cell and Memory-Derived Antibody Repertoire Following Dengue Virus Infection

Zoe L. Lyski and William B. Messer
Department of Molecular Microbiology and Immunology, Oregon Health and Sciences University, Portland, OR, United States

Adapted from a review paper published in Frontiers in Immunology June 2019 DOI: 10.3389/fimmu.2019.01276

Abstract

Memory B-cells (MBCs) are potential antibody-secreting immune cells that differentiate and mature following host exposure to a pathogen. Following differentiation, MBCs remain in peripheral circulation after recovery and are poised to secrete antigen-specific antibodies if and when they are re-exposed to their cognate antigen. Consequently, MBCs form the founder population and provide one of the first lines of pathogen-specific defense against reinfection. The role MBCs play is complicated for viruses that are heterologous, such as dengue virus (DENV), which exist as antigenically different serotypes. On second infection with a different serotype, MBCs from initial dengue infection rapidly proliferate and secrete antibodies: many of these MBC derived antibodies will be cross-reactive and weakly neutralizing, while some antibodies may recognize epitopes conserved across serotypes and have the capacity to broadly neutralize 2 or more serotypes. It is also possible that a new population of MBCs and antibodies specific for the

second virus serotype need to arise for long-term broader immunity to develop. Methods to interrogate and track memory B cell responses are important for evaluating both natural immunity and vaccine response. However, the low abundance of MBCs for any specific pathogen makes it challenging to interrogate frequency, specificity, and breadth for the pathogen of interest. This review discusses current approaches that have been used to interrogate the memory B cell immune response against viral pathogens in general and DENV specifically. Including strengths, limitations, and future directions. Single-cell approaches could help uncover the DENV specific MBC antibody repertoire, and improved methods for isolating DENV specific monoclonal antibodies from human peripheral blood cells would allow for functional analysis of the anti-DENV repertoire.

Introduction

Neutralizing antibody responses play a critical role in anti-viral immunity–controlling and preventing infection, and are an important aim of vaccination. During initial infection, naive host B-cells, specific to the infecting antigen, proliferate and differentiate into short-lived plasmablasts that secrete antibodies at a high rate to combat the existing infection. Following viral clearance two distinct layers of humoral immunity remain to protect against repeat infection with the same antigen—antibodies in the sera, constitutively produced by long lived plasma cells (LLPCs) and memory B-cells (MBC) primed to expand and secrete antibodies upon antigen re-exposure. LLPCs, are terminally differentiated, non-dividing cells that reside in the bone marrow and produce antibodies for years to decades providing protection against repeat infections with the same antigen. [213,238,420-422] These antibodies are typically assessed by in vitro neutralization and binding assays, and in many cases regarded as correlates of protection against viral pathogens. [212] MBCs make up the second line of antibody-mediated defense, providing protection by rapidly activating, proliferating, and secreting antibodies in response to cognate

antigen. Once regarded as a backup to LLPC-derived antibodies, the specificity and breadth of potential MBC responses are increasingly appreciated, especially with regard to protection against heterogeneous but antigenically related viral pathogens, such as influenza, different serotypes of DENV, and viral escape mutants. [212,254,421] Naive B-cells, MBC precursors, originate in the bone marrow before migrating to the spleen where they undergo further differentiation, redistribute to lymph nodes, and await antigen encounter. Recent work in mice suggests that MBCs originate in low-affinity germinal center compartments within peripheral lymph nodes, which might contribute to more broadly reactive Ig receptors and increase the breadth of recall responses MBCs form a heterogeneous population, and it is thought that they preferentially differentiate upon reinfection. [254,421] Specifically, IgG MBCs favor differentiating into plasmablasts whereas IgM MBCs preferentially re-enter germinal centers to undergo further rounds of affinity maturation. [228,421,423,424] MBCs can be identified by their B-cell receptor (BCR), a membrane-bound immunoglobulin (Ig) identical to the antibody they secrete upon activation. Upon reinfection, the recall response is rapid, dominated by high-affinity isotype switched antibodies, IgG, IgA, or IgE, depending on pathogen. This recall response leads to the generation of new antigen-specific LLPCs and MBCs. [421] Although human MBCs have been characterized for many important viral pathogens, including HIV, RSV, influenza, human DENV MBC derived antibodies were not fully characterized until 2010. [41,425-428] Mosquito-transmitted DENV is responsible for ∼100 million symptomatic cases and 35,000 deaths annually making it the most common and serious vector-borne disease affecting humans. DENV is an enveloped positive sense RNA virus, that circulates as four distinct serotypes (DENV 1-4), with 60–85% shared sequence homology. [16,429] Repeat infections often occur in DENV endemic regions–Asia, Latin America, Africa, and parts of Oceana. Population growth, increased global travel, and

spread of the vector have led to increasing epidemics. DENV infection causes symptoms that include high fever and rash. A portion of patients (~500,000 per year) develop severe dengue—referred to as dengue shock syndrome (DSS) or dengue hemorrhagic fever (DHF)—which can further progress to organ failure and death. First (1^0) infection with one serotype is thought to provide life-long protection against that serotype, but only short-lived protection against heterologous infection. [258] Secondary (2^0) infection with a different serotype can lead to broader protection, up to all four serotypes, but comes at a greater risk of serious disease during acute infection, through a process of antibody-dependent enhancement, which occurs when sub-neutralizing antibodies bind to virus and facilitate uptake into cells via Fc receptors. [271,430] The mechanism by which subsequent broader immunity develops is incompletely understood: while it is known that immediately following second infection the antibody response contains a large proportion of cross-reactive antibodies that can neutralize both viruses the relative contribution of type-specific, weakly cross-neutralizing and broadly neutralizing antibodies to long-term immunity is unclear, and may depend on virus maturation state. [36,431] Further complicating the hypothesized role of broadly cross-neutralizing antibodies is the recent finding by Raut et al. that in vitro neutralization assays using mature and partially mature tissue-culture derived DENV1 over-estimated by almost 15-fold the potency of heterotypic neutralizing antibodies when compared to neutralizing potency against the same fully mature DENV1 circulating in humans. [261] Deeper understanding of the diversity and epitope-specificity of 1◦ MBCs could lead to the development of subunit vaccines that preferentially elicit potently neutralizing antibodies against all 4 DENV serotypes while avoiding potentially enhancing antibodies. Analyses of human antibody response to DENV infection have traditionally characterized serum antibodies, a product of LLPCs through virus neutralization, binding, and enhancement assays. [62] More

recently, greater focus has been put on characterizing B-cells that produce these antibodies. Historically, methods to interrogate antigen-specific B-cells, particularly in humans, have been challenging to develop. [268,432] However, complex, studying individual and population MBCs and the monoclonal antibodies (mAbs) they produce is an area of critical importance. Such studies allow for better understanding of the nature of human immune response to pathogens such as DENV and are expected to lead to more rationally designed vaccines. Over several decades, methods to interrogate antigen-specific MBCs have had several useful functions: identifying subset of MBCs available to respond to repeat infections, tracking MBCs prior to and after vaccination or booster, isolating and characterizing human mAbs following natural infection or vaccination, and analyzing memory-derived antibody repertoires. Only recently have these methods been employed in the DENV field. [64,65,272] Here we review the leading approaches for characterizing human DENV MBCs, evaluating their strengths, limitations, and potential for further contribution to the field (summarized in Table 22).

Limiting Dilution Assay (LDA)

The LDA was first used to detect virus-specific MBCs in mice over 20 years ago. [433] This approach allows the frequency and specificity of rare antigen-specific MBCs in circulation to be enumerated. PBMCs or enriched B-cells are stimulated *ex vivo* with a mitogen cocktail along with non-proliferating feeder cells. With this approach, MBCs become antigen-secreting cells. The cells can be enumerated by ELISpot (described later) or secreted antibodies assayed by antigen-specific ELISA. This approach has been used to determine the frequency of viral-specific MBCs in humans following vaccination or natural infection

Strengths and Limitations

Non-specific stimulation of human MBCs allows for the characterization of multiple antigen-specific MBC derived antibodies from a single PBMC sample. [212] Antibody-containing supernatant or MBCs can be used for a wide range of assays including: ELISpot, ELISA, and neutralization. The major limitations of this approach are that the cells are not immortalized therefore longevity is limited, surface BCR is down-regulated, and single antigen-specific MBCs clones cannot be identified and subjected to downstream sequencing and cloning.

Enzyme-Linked Immunosorbent Spot Assay (ELISpot)

Provides a sensitive and specific tool to detect antigen-specific MBCs. First described over 35 years ago as a method for quantifying rare B and T cells and is still widely used today, as it is sensitive enough to detect a single antigen-specific cell. [434] Plasmablasts can be studied directly *ex vivo*, but MBCs must be stimulated to become antibody-secreting cells. Membrane-bound antigen enables binding of mAbs secreted by B-cells. Bound antibody is detected using a secondary antibody and a colorimetric substrate, resulting in colored spots on the membrane that can be easily enumerated using imaging software. Advances in ELISpot technology have allowed researchers to detect different isotypes of MBCs that recognize multiple epitopes and multiple antigens. [435] Recently developed multifunctional FluoroSpot assays allow enumeration of cross-reactive and type-specific DENV and Zika MBCs following natural infection and vaccination. [270,271] This allows researchers to determine serotype specificity on a single-cell basis, rather than polyclonal level.

Strengths and Limitations

ELISpot is highly sensitive and allows for the enumeration of rare cells of interest—frequency, specificity, and antibody isotype can be determined. The major limitation is that it does not allow

for isolation and downstream analysis—Functional properties of antibodies, such as neutralization cannot be assessed, and cells' BCRs of interest cannot be sequenced or cloned for mAb production.

Hybridoma Approaches

The use of hybridomas to immortalize MBCs was first described over 40 years ago. [436] Hybridomas are made by fusing a myeloma cell with a B-cell from an immunized or naturally infected individual, the resulting hybrid cell secretes mAbs specific to their antigen. Technical advances have made it feasible to generate hybridomas from human peripheral blood MBCs. [274] These advances include expanding B-cells prior to fusion, finding new human myeloma cells to fuse with, and improved fusion techniques including electrical cytofusion. [275] Using optimized techniques Yu et al. [275], fusion efficiency improved from 0.001 [274] to 0.43% [275] which enabled them to isolate neutralizing mAbs against RSV and influenza from human peripheral MBCs. Hybridoma technology is a well-established and indispensable platform for generating high-quality mAbs and has been used to produce mAbs against a wide range of viral antigens including DENV.

Strengths and Limitations

Major advantages of this approach include pairing of BCR heavy and light chains, native constant region of the mAb expressed allowing Fc-mediated effector functions, such as enhancement to be accessed. [274,437] Finally, the hybridoma products are stable in culture and can be frozen for future use.

One major limitation of this approach is extremely low fusion efficiency. Consequently, traditional hybridoma strategies are not as well suited for identifying rare antigen-specific MBCs

that circulate in low numbers in the periphery of immune donors, as overall only a small amount of the total B cell repertoire is captured.

The second major limitation has been the challenge of making human, rather than mouse, derived hybridomas. Work by Wahala et al. [438] found that humans and mice recognize distinct and different epitopes on the DENV virion following immunization in mice or natural infection in humans. Nearly all neutralizing antibodies found in humans after natural infection recognize complex quaternary epitopes on the surface of whole virions, in contrast to the DENV neutralizing antibody response in mice, where the majority of neutralizing antibodies recognize a single domain region, domain III, on the envelope glycoprotein. [67,260,438]

B-Cell Immortalization

MBC immortalization can be achieved through transforming peripheral MBCs using Epstein Barr Virus (EBV), or through expression of BCL-6, and BCL-XL. This results in stable cell lines that express BCR on the surface and secrete antibodies, making them a useful tool in the generation of human mAbs and has become a leading approach in characterizing DENV-specific MBCs in humans.

EBV transformation for B-cell cultures was developed in the 1970's Steinitz et al. [439] when normal human B-cells were infected with EBV, a lymphotropic herpesvirus, transforming MBCs into stable antibody-secreting cell lines. Supernatants can be screened for specificity to antigen of choice and serial dilution down to a single cell enables this method to be applied to mAb production. Many groups have utilized and continue to utilize EBV immortalization to isolate human mAbs against a wide variety of human pathogens, including HIV[439], SARS coronavirus [440], Influenza [441], RSV [442], and DENV. [41,428,430,443]

Another technique employed to immortalize MBCs is through forced expression of BCL-6 (required for GC formation) and BCL-XL (anti-apoptotic Bcl-2 protein family). Both are expressed in GC B-cells, and by introducing these genes into peripheral blood MBCs and culturing with CD40L and IL-21, they become highly proliferating with surface and secreted Ig. [444] BCL-6 + BCL-XL transduced cells express *AICDA*, encoding the enzyme activation-induced cytidine deaminase (AID), at the same levels as isolated tonsil derived GC B-cells, but not normally expressed in peripheral MBCs or plasma cells. AID mediates somatic hypermutation (SHM) and class-switch recombination (CSR) and therefore increases diversity of the BCR. AID is functional in these cells and low levels of SHM is observed in the Ig genes of expanded B-cells. These cells can be maintained for prolonged periods of time in culture to allow for mAb production. [445]Using this approach, researchers have identified neutralizing mAbs in humans that recognize RSV [444], Hepatitis C virus [446], influenza [447], and DENV [448].

Strengths and Limitations

Immortalized B-cells have a plasmablast-like phenotype, with secretory and membrane-bound Ig, which makes them a powerful tool for discovery and characterization of mAbs. Probes that bind to BCRs of interest enable the isolation of antigen-specific B-cells from a polyclonal population. Immortalized cells are stable and can be frozen for future use. The presence of AID and the potential for SHM can be utilized to generate clones that have higher or lower affinities than the parental clone, allowing for a method of affinity maturation in culture. [445]

Transformation efficiency for BCL-6+BCL-XL is 60–80% in humans [445], and EBV transformation have improved from 10 to >30% with the addition of TLR agonists, typically CpG or R848. [442,449] This approach requires significant numbers of cells to yield few cells of

interest. Because cells proliferate with this approach, frequency of particular antigen-specific MBCs cannot be enumerated.

Using EBV-transformed human B-cells to generate human hybridomas can increase efficiency by as much as 25-fold compared to that of using untransformed PBMCs. Therefore, Investigators often utilize a combination approach of EBV immortalization followed by fusion to isolate human DENV-specific mAbs from naturally infected or vaccinated donors. [272,447]

Antigen—Specific Flow Cytometry

Flow cytometry-based approaches have been used to enumerate antigen-specific MBCs against model antigens in mice [450] and humans. [263] However, viral antigen-specific flow cytometry has been utilized more recently, Weitkamp et al. [441] identified human rotavirus specific B-cells, Scheid et al. [451] characterized low-frequency HIV specific MBCs in humans and Woda et al. [452] characterized DENV-specific MBCs in human immune donors. Recognizing the complex and quaternary nature of DENV neutralizing epitopes [260]Authors Woda and Mathew [268] and Appanna et al. [272] used fluorescently labeled whole DENV virus [267] as a probe to detect DENV-specific MBCs in immune donors while Cox et al. [432] used biotinylated DENV envelope protein as a probe along with dual labeled streptavidin antibodies to identify DENV envelope-specific MBCs. This method enabled researchers to isolate 8 DENV-neutralizing mAbs from a single donor (Table 1).

Strengths and Limitations

Antigen choice is important, DENV neutralizing epitopes are comprised of complex conformational structures and not recapitulated by simple linear peptides or recombinant proteins. [260] However, whole viruses are inherently sticky and adheres to host cells. To tackle this non-specific binding [268,443] utilized fluorescently labeled Vero cell supernatant as well as

dual labeled probes to decrease background. [453] A major strength of this approach is the possibility of tracking multiple serotypes of DENV- specific MBCs prior to and post-infection or vaccination [452] as well as the potential for single-cell sorting antigen-specific MBCs for downstream assays such as immortalization, sequencing, or cloning. [432]

References	Method	Efficiency	#Donors	mAbs isolated	Key findings
Schieffelin et al.(15)	B-cell immortalization (EBV)	N/A	1 > 2 years post infection	3	DENV-specific MBCs were in circulation >2 years post exposure 2% of cultures were DENV2 specific All isolated mAbs were IgG1
Beltramello et al.(14)	B-cell immortalization (EBV) with CpG screened and cloned by limiting dilution	6.5–14%	5 3-1° 2-2° 200 days to >8 years post-infection.	70	All of the isolated mAbs were IgG: 68 IgG1, 1 IgG3, 1 IgG4 13 mAbs recognized EDIII and were the most potently neutralizing of all the mAbs isolated (5 serotype specific, 8 cross reactive) 34 mAbs recognized DI/DII they were highly cross reactive and less neutralizing, 6 mAbs recognized PrM, 11 mAbs recognized non-structural proteins, and 1 recognized capsid
Smith et al.(27)	B cells immortalized (EBV) with CpG and CHK2. Screened by ELISA. Positive wells fused to generate hybridomas.	>10-fold increase in the # of successful human hybridomas generated	12 6–1° 6–2° 4–24 years post infection	37	29/37 isolated mAbs recognized E protein, 26 were IgG1 and 3 were IgG2 26/37 isolated mAbs were cross reactive, most bound to EDI/II 5- isolated mAbs EDIII specific (1C7, 1M23, 2J20, 1B23, 1M19) all cross reactive 3-mAbs had moderate to strong neutralizing potency against at least one serotype (2D22, 5J7, 2J20) 8- isolated mAbs PrM specific, mAbs exhibited enhancing properties
Smith et al.(30)	B-cell immortalization (EBV) CpG and CHK2. Screened by ELISA and neutralization then fused to generate hybridomas.	N/A	3 2–1° 1–2° 1-9 years post-infection	50	Most potently neutralizing mAbs bound to EDIII (1M7) or complex (1F4) epitopes on intact virions. DENV specific MBC frequency similar between primary and secondary donors at 14–18 DENV specific MBC per thousand B cells. 15 of the isolated mAbs were non-neutralizing, and bound to rE or PrM.
Cox et al.(25)	FACS using E (DENV2-80E) and dual labeled secondary antibodies. Isolated double positive MBCs.	20 million PBMCs, 148 DENV E+ MBCs sorted.	1 from an endemic region Serum neutralized all 4 serotypes	9	DENV E specific MBCs are present in naturally infected donors. Authors isolated and characterized DENV neutralizing mAbs from MBCs against envelope domain I and the fusion loop. Of the sorted MBCs following 2 week stimulation in culture 64% were positive for IgG, 20% were positive for DENV by ELISA, 8% secreted DENV2 specific mAbs Of the 9 mAbs isolated 1-non-neutralizing, 3-serotype-specific, 2-neutralized 2–3 serotypes 3-neutralized 4 serotypes.
Appanna et al.(28)	FACS using fluorescently labeled DENV3. Isolated DENV positive MBCs	N/A	4 2°	19	40–60% of the DENV-specific MBCs sorted bound to DENV Most mAbs isolated bound to complex epitopes, 24.4% bound to PrM and 17.8% bound to rE Majority were cross reactive and weakly neutralizing
Nivarthi et al.(50)	B-cell immortalization (EBV) CpG and CHK2 followed by fusion	N/A	2 1° DENV-4	8	Frequency of DENV-specific B-cells in circulation 0.19–0.2%. Of the 8 mAbs isolated, 2 neutralized DENV-4 and recognize regions on EDI/EDII hinge.

Table 37 Summary of human DENV-specific monoclonal antibodies isolated from immune donors

Future Directions

An important early advancement in the field of human mAb generation was the advent of single-cell RT-PCR approaches that allow for sequencing, cloning, and characterization of each BCR from individually sorted MBCs. [454] This approach remains useful when the population of interest represents a large proportion of total cells in the population (plasmablasts during acute infection), or when a valid probe or screening approach exists to identify MBCs of interest prior to sequencing. In addition to generating mAbs, sequencing of the BCR provides information about B-cell clonal evolution during infection. While groundbreaking, this single-cell approach is time and resource-intensive as it requires heavy and light chains to undergo PCR, sequencing, and cloning independently and remain correctly paired for transfection into expression plasmids.

This single-cell approach provides a glimpse into the overall antibody repertoire, which has a potential diversity of more than 1×10^{13} in humans, but high throughput methods that capture the entire antigen-specific MBC repertoire recently developed with other pathogens would be expected to advance the DENV field as well. High-throughput droplet microfluidic approaches allow for individual partitioning of single B-cells, that are individually barcoded and allow for paired sequencing of Ig heavy and light chains from a single B cell captured within a droplet. [455] From this, a complete Ig library can be generated, as well this approach allows for simultaneous sequencing of barcoded Ig genes with the possibility of co-expressed functional genes to fully understand the pathogen-specific MBC repertoire. MAbs that are generated from these antibody gene sequences allow for functional analysis of the repertoire.

Another high throughput approach recently used to isolate mAbs from humans involves using microfluidics to partition individual cells then physically link heavy and light mRNAs and perform overlap extension PCR to generate a continuous heavy-light chain amplicon for cloning

into a yeast display system for Fab or IgG which allows screening for antigen specificity and affinity by FACS. [456,457] Through this approach researchers were able to isolate broadly neutralizing antibodies against HIV, Ebola, and influenza.

The ability to fully interrogate the MBC response established after natural infection to viral antigens will allow researchers to durably and comprehensively interrogate vaccine responses to further understand the differences between natural and vaccine-derived immunity.

Acknowledgments

We thank Dr. Ann Hessell for critically reading the manuscript and providing helpful input.

Funding. This work was supported by federal funds from the National Institute of Allergy and Infectious Diseases R21 AI135537-01 (to WM) and the National Center for Advancing Translational Science CTSA UL1 TR000128, Oregon Clinical and Translational Research Institute, Takeda Vaccines IISR 2016-101586 (to WM), the Sunlin and Priscilla Chou Foundation (to WM), and the Tartar Trust Fellowship, Oregon Health and Sciences University, School of Medicine (to ZL).

Appendix 2: Immunogenicity of Pfizer mRNA COVID-19 vaccination followed by J&J adenovirus COVID-19 vaccination in two patients with chronic lymphocytic leukemia.

Zoe L. Lyski,[1] Myung Sun Kim,[2] David Xthona Lee,[1] David Sampson,[2] Hans P. Raué,[4] Vikram Raghunathan,[2] Debbie Ryan,[2] Amanda E. Brunton,[3] Mark K. Slifka,[4] William B. Messer,[1,3,5] Stephen E. Spurgeon.[2]*

Affiliations

1. Department of Molecular Microbiology & Immunology, Oregon Health & Science University (OHSU), Portland, OR 97239, USA. 2. Knight Cancer Institute, Oregon Health & Science University (OHSU), Portland, OR 97239, USA 3. OHSU-PSU School of Public Health, Portland, OR 97239, USA. 3. Division of Neuroscience, Oregon National Primate Research Center, Oregon Health & Science University, Beaverton, Oregon, USA.4. Department of Medicine, Division of Infectious Diseases, Oregon Health & Science University (OHSU), Portland, OR 97239, USA.

Author contributions: Conception of work ZLL, MSK, WBM, and SES. Data collection, ZLL, MSK, DXL, HPR, and AEB. Collection/ management of human samples ZLL, AEB, JG, DR. Data analysis ZLL, MSK, DXL, HPR, and AEB. Drafting of the article ZLL, MSK, and SES. Critical revision of manuscript ZLL, HPR, MEC, MKS, and SES. Acquired funding WBM and SES.

Acknowledgments

The authors would like to thank the subjects for participating in this research study.
This work was funded in part by National Institute of Allergy and Infectious Diseases NIAID 1R01AI145835 (WBM), by US National Institute of Health grant P51 OD011092 (MKS), and endowed funds from the Knight Cancer Institute's Scholar Award for Leukemia and Lymphoma Research (SES). The funders had no involvement in study design; in the collection, analysis and interpretation of data; in the writing of the report; or in the decision to submit the article for publication.

Abstract

Individuals with Chronic Lymphocytic Leukemia (CLL) have significant immune disfunction, often further disrupted by treatment. While currently available COVID-19 vaccinations are highly effective in immunocompetent individuals, they are often poorly immunogenic in CLL patients. It is important to understand the role heterologous boost would have in patients who did not respond to the initial two-dose mRNA vaccine series. SARS-CoV-2 specific immune response, including antibodies, memory B-cells, CD4 and CD8 T-cells were assessed prior to vaccination, as well as post initial vaccination series and post third dose in two subjects. One subject seroconverted, had RBD-specific memory B-cells and spike-specific CD4 T-cells while the other did not. Both subjects had a spike-specific CD8 T-cell response after original mRNA vaccination series that was further boosted after third dose, or remained stable. The results of this study, however small, is especially promising to CLL individuals who did not seroconvert following initial mRNA vaccination series.

Introduction

Chronic Lymphocytic Leukemia (CLL) is characterized by monoclonal proliferation of dysfunctional B-cells, leading to a broad range of immune defects. CLL patients face significant risk of morbidity and mortality from infections [458], including from SARS-CoV-2, the causative agent of COVID-19 [459]. Vaccines can be instrumental in mitigating the risk of infections in CLL; however, responses to vaccination is highly variable and significantly influenced by CLL disease status, baseline characteristics, types of vaccine and active CLL therapy [387].

Although current COVID-19 vaccines elicit robust immunity in immunocompetent hosts [210], the antibody response in CLL patients is highly variable [398,460,461] and particularly poor in patients with low total immunoglobulin levels, those that have had anti-CD20 monoclonal antibodies within the past year, or are undergoing active therapy with agents such as Bruton's Tyrosine

Kinase inhibitors (BTKi). The best responses to date have been in CLL patients who are in remission and/or years out from active treatment.

Given decreased vaccine efficacy in CLL, an additional dose of vaccine may be beneficial in CLL patients, especially given rise of variants of concern (VoCs). Initial data from solid organ transplant recipients on immunosuppression as well as individuals with solid tumors on active therapy showed a role for additional vaccination [462,463]. This led to the FDA extending the EUA for Pfizer-BioNTech and Moderna mRNA vaccines to include additional doses in immunocompromised patients. However, these results may not be generalizable to CLL, and additional studies are needed to better define vaccine responses in the CLL patient population, including the role of mixing mRNA vaccination with other vaccine formulations, such as the adenovirus vectored vaccine Ad26COV2.s, commonly known as Johnson and Johnson (J&J) vaccine.

Case Report

Here we describe two CLL patients who "self-referred" to outside pharmacies for an additional vaccination with J&J COVID-19 vaccine following 2 doses of the BNT162b2 vaccine (Pfizer-BioNTech). Both patients had previously enrolled as study subjects in an IRB approved observational study, (OHSU IRB# 21230) to investigate immune response following COVID-19 vaccination. The additional J&J dose was subsequently self-reported to the study team. On initial enrollment, demographics, CLL disease characteristics, and treatment details were collected (Table 1), and baseline laboratory values were obtained, included semi-quantitative SARS-CoV-2 spike antibody titer, serum IgG, a complete blood count, and multicolor flow cytometry measuring immune cell populations (Table 23). Whole blood was collected for additional serologic and cellular studies.

Subject ID	Age	Gender	Year of diagnosis	Current Treatment	Prior Treatment	IgG mg/dL	Absolute Lymphocyte Count K/mm3	B-cells (CD19+) %	Naïve B-cells (IgD+CD27-) %	Memory B-cells (IgD-CD27+) %	B1 B-cells (CD5+CD19+) %
						(768 - 1632)	(1.00 - 4.80)	(4-17)	(50-80)	(5-21)	(<6)
1	60's	F	2014	None	None	834	21.09	76	0.092	59.1	76.18
2	80's	F	2014	Ibrutinib (2017)	Obinutuzumab x 6 cycles (completed 2015)	510	5.93	61	11.37	0.45	59.96

Table 38 Baseline characteristics and demographics for subjects included in the study.

SARS-CoV-2 spike receptor binding domain (RBD)-specific antibody levels were tested by ELISA and endpoint titers were calculated as previously described [417]. In addition, baseline PBMC samples were functionally tested for the presence of SARS-CoV-2 spike RBD-specific memory B-cells (MBCs) by limiting dilution assay as previously described [265,303]. Briefly, PBMCs were serially diluted and incubated with a stimulation cocktail in which the MBCs present within PBMCs differentiate and become antibody-secreting cells. The supernatants were collected 7 days later and assayed for antigen specificity by RBD-ELISA. This allows one to functionally test MBC- derived antibodies and back-calculate a frequency of total IgG secreting MBCs as well as RBD-specific MBCs (12, 13). In addition, CD4+ and CD8+ T-cells were also functionally assessed for the presence of IFNγ and TNFα secretion following spike protein derived peptide stimulation. Briefly, PBMCs were stimulated with 2 peptide pools of overlapping (10AA) 17mers representing the SARS-CoV-2 Spike protein (BEI Resources). Following stimulation, cells were stained as previously described [418,419]. Data was acquired on an LSR Fortessa (Becton Dickenson) and analyzed using FlowJo software. Cytokine expression in medium alone cultures was subtracted from peptide-stimulated cultures to calculate peptide-specific cytokine expression. Responses to both peptide pools were added together to yield the total frequency of SARS-CoV-2-specific cytokine producing CD4+ and CD8+ T cells.

Neither subject had pre-vaccination B-cell responses as measured by RBD-specific antibodies or MBCs. Neither had a virus-specific CD8+ response at baseline. While Subject 2 had spike

peptide-reactive CD4+ T-cells at baseline these cells were unresponsive and did not expand following vaccination. In contrast, CD8+ responses were observed after mRNA vaccination in both subjects (Fig. 41). It has previously been reported that SARS-CoV-2 naïve individuals may have preexisting cross-reactivity to SARS-COV-2 peptides through prior infection by common cold coronaviruses: SARS-CoV-2 specific CD4+ T-cells have been identified in 20-50% of people without SARS-CoV-2 exposure or vaccination [464].

Approximately four weeks after initial vaccination neither subject had detectable RBD-specific SARS-CoV-2 antibodies or MBCs. Both had measurable vaccine-induced CD8+ T-cell responses following mRNA vaccination, although CD4+ responses did not appear to increase above baseline (Fig. 41).

Subject 1 received the J&J vaccine 104 days and Subject 2- 81 days after completion of the BNT162b2 vaccine series. Following J&J vaccination additional samples were obtained, Subject 1, 30 days after third vaccine, and Subject 2, 27 days following third vaccine. Interestingly, Subject 1 had undetectable RBD-specific antibodies, RBD-specific MBCs, and virus-specific CD4+ T-cells after initial vaccination series. However, following an additional vaccination, all three measures increased above the limit of detection, RBD ELISA titer of 625, RBD-specific MBC frequency of 3.6 / 10^6 B-cells, and 166 spike-specific CD4+ T-cells / 10^6, and a spike-specific CD8+ T-cell response that remained stable and did not boost appreciably following 3rd vaccination (Fig. 41). Subject 2 did not seroconvert or have detectable virus specific MBCs after their primary mRNA vaccination series however they had a spike-specific CD8+ T-cell response

that further boosted after a 3rd dose and a virus-specific CD4+ response that didn't change following original vaccine series or 3rd dose of J&J.

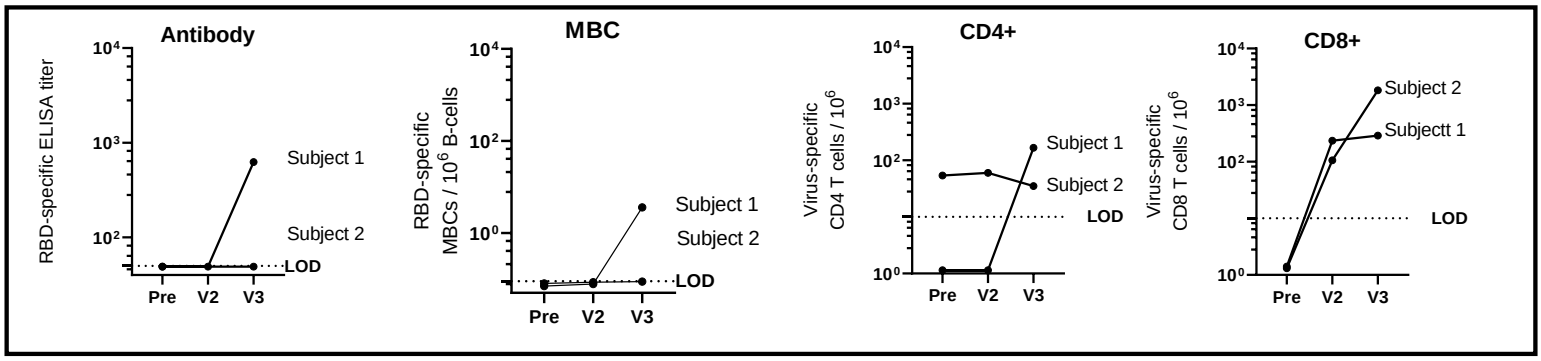

Figure 53 Immune response to COVID-19 vaccination in CLL subjects. with J&J.

RBD-specific antibody titer. Subjects without a detectable antibody titer (< 1:50 serum dilution) were assigned a value of 49. Limit of detection (LOD) is 50. Frequency of RBD-specific MBCs per 10^6 CD19+ B-cells following ex vivo stimulation. Subjects who did not have a detectable response were assigned a value between 0.07 and 0.09. Limit of detection (LOD) is 0.1. SARS-CoV-2 spike peptide-reactive CD4 and CD8 T-cells are defined as double-positive for IFNγ and TNFα cytokine secretion. Patients who did not have a detectable T-cell response were assigned an arbitrary number between less than 2. Limit of detection (LOD) is 10. Visit 1 (pre) blood draw was taken 21 and 40 days prior Pfizer vaccine series (2-doses). Visit 2 (V2) blood draw was taken 33 and 24 days post-vaccination, and visit 3 (V3) was drawn 30 and 27 days after 3rd vaccination. DXL generated data for antibody graph, HPR generated data from T-cell graphs, ZLL analyzed data, generated data for MBC graph, and created figure.

Discussion

Other than subject age (60s vs 80s), the most notable difference between the subjects' baseline characteristics (Table 23) is that Subject 1 was treatment naive, while Subject 2 had undergone previous treatment (6 years ago) with obinutuzumab an anti-CD20 mAb and is currently on active treatment with Ibrutinib, since 2017. Both had baseline B-cell frequencies outside of the normal range, with Subject 1 exhibiting a low percentage of naïve B-cells (0.092) and a high percentage of MBCs (59.1), while Subject 2 had a low percentage of naïve B-cells (11.37) and MBCs (0.45). Although Subject 2 had mild hypogammaglobulinemia, neither had a history of recurring infections or need for IgG supplementation. Levels of baseline CD4+ and CD8+ T-

cells (absolute values) were also normal, in each subject prior to vaccination (data not shown). Both had very low percentages of naïve B cells which could explain the initial poor response to vaccination. The significance of the increased percentage of MBCs in Subject 1 is unclear but does suggest some broader preservation of normal B cell maturation and immune function. Although Subject 1 did have an immune response, antibody levels were relatively low as compared to some of the levels observed in immunocompetent post-vaccine populations [465] and certain CLL populations (5). The clinical significance of specific antibody levels remains unknown.

Active treatment with Bruton's Tyrosine Kinase (BTK) inhibitors like ibrutinib may have a profound impact on B-cell survival, differentiation, and production of antibodies as the absence of intact BTK–dependent B-cell receptor mediated signaling prevents B-cells from differentiating into mature peripheral B-cells. Immune response following vaccination or natural infection is limited in these patients [369]. Recall to antigens encountered prior to treatment appears to remain largely intact, however response to novel antigens encountered during treatment seems to be abrogated. Subject 2 has been on ibrutinib for over four years. The impact of prolonged treatment vs. shorter-term BTK inhibition on immune responses is unknown. However, clinical data [466] suggest some improvement in humoral immunity with prolonged (> 6 months) treatment. T-cells are also disrupted in individuals with CLL and even further disrupted with BTK treatment [467]. In the cases presented here both subjects did have an increase in virus specific CD8+ T-cells however the significance is unclear in terms of protection as neutralizing antibodies are often viewed as the correlate of protection against COVID-19.

Conclusion

The results of this study, however small, provide initial evidence that a 3rd vaccination against COVID-19 with the heterotypic vaccine Ad26COV2.s results in an immune response that was

not observed following the recommended 2-dose mRNA vaccination series. This is especially promising news to subjects who are treatment naïve, not currently in active treatment, or who may consider vaccination before beginning active treatment.

References

1 van den Elsen, K., Quek, J. P. & Luo, D. Molecular Insights into the Flavivirus Replication Complex. *Viruses* **13**, 956, doi:10.3390/v13060956 (2021).

2 Weaver, S. C. & Barrett, A. D. Transmission cycles, host range, evolution and emergence of arboviral disease. *Nat Rev Microbiol* **2**, 789-801, doi:10.1038/nrmicro1006 (2004).

3 Ishikawa, T., Yamanaka, A. & Konishi, E. A review of successful flavivirus vaccines and the problems with those flaviviruses for which vaccines are not yet available. *Vaccine* **32**, 1326-1337, doi:10.1016/j.vaccine.2014.01.040 (2014).

4 Kubinski, M. *et al.* Tick-Borne Encephalitis Virus: A Quest for Better Vaccines against a Virus on the Rise. *Vaccines* **8**, 451, doi:10.3390/vaccines8030451 (2020).

5 Scherwitzl, I., Mongkolsapaja, J. & Screaton, G. Recent advances in human flavivirus vaccines. *Curr Opin Virol* **23**, 95-101, doi:10.1016/j.coviro.2017.04.002 (2017).

6 Rangel, M. V. & Stapleford, K. A. Alphavirus Virulence Determinants. *Pathogens* **10**, 981 (2021).

7 Kumar, M. & Al Khodor, S. Pathophysiology and treatment strategies for COVID-19. *Journal of Translational Medicine* **18**, 353, doi:10.1186/s12967-020-02520-8 (2020).

8 Slon Campos, J. L., Mongkolsapaya, J. & Screaton, G. R. The immune response against flaviviruses. *Nature immunology* **19**, 1189-1198, doi:10.1038/s41590-018-0210-3 (2018).

9 Wahala, W. M. P. B. & De Silva, A. M. The Human Antibody Response to Dengue Virus Infection. *Viruses* **3**, 2374-2395 (2011).

10 Van Duijl-Richter, M. K. S., Hoornweg, T. E., Rodenhuis-Zybert, I. A. & Smit, J. M. Early Events in Chikungunya Virus Infection—From Virus CellBinding to Membrane Fusion. *Viruses* **7**, 3647-3674 (2015).

11 Stebegg, M. *et al.* Regulation of the Germinal Center Response. *Frontiers in Immunology* **9**, doi:10.3389/fimmu.2018.02469 (2018).

12 Baxter, V. K. & Heise, M. T. Immunopathogenesis of alphaviruses. *Advances in virus research* **107**, 315-382, doi:10.1016/bs.aivir.2020.06.002 (2020).

13 in *Virus Taxonomy* (eds Andrew M. Q. King, Michael J. Adams, Eric B. Carstens, & Elliot J. Lefkowitz) 1003-1020 (Elsevier, 2012).

14 Mukhopadhyay, S., Kuhn, R. J. & Rossmann, M. G. A structural perspective of the flavivirus life cycle. *Nature Reviews Microbiology* **3**, 13-22, doi:10.1038/nrmicro1067 (2005).

15 Pierson, T. C. & Diamond, M. S. The continued threat of emerging flaviviruses. *Nature Microbiology* **5**, 796-812, doi:10.1038/s41564-020-0714-0 (2020).

16 Bhatt, S. *et al.* The global distribution and burden of dengue. *Nature* **496**, 504-507, doi:10.1038/nature12060 (2013).

17 Halabi, K. & Mayrose, I. Mechanisms Underlying Host Range Variation in Flavivirus: From Empirical Knowledge to Predictive Models. *Journal of Molecular Evolution* **89**, 329-340, doi:10.1007/s00239-021-10013-5 (2021).

18 Douam, F. & Ploss, A. Yellow Fever Virus: Knowledge Gaps Impeding the Fight Against an Old Foe. *Trends in microbiology* **26**, 913-928, doi:10.1016/j.tim.2018.05.012 (2018).

19 Weaver, S. C. & Barrett, A. D. T. Transmission cycles, host range, evolution and emergence of arboviral disease. *Nat Rev Microbiol* **2**, 789-801, doi:10.1038/nrmicro1006 (2004).
20 Gardner, C. L. & Ryman, K. D. Yellow fever: a reemerging threat. *Clin Lab Med* **30**, 237-260, doi:10.1016/j.cll.2010.01.001 (2010).
21 Huang, Y.-J. S., Higgs, S., Horne, K. M. & Vanlandingham, D. L. Flavivirus-mosquito interactions. *Viruses* **6**, 4703-4730, doi:10.3390/v6114703 (2014).
22 Quaresma, J. A., Pagliari, C., Medeiros, D. B., Duarte, M. I. & Vasconcelos, P. F. Immunity and immune response, pathology and pathologic changes: progress and challenges in the immunopathology of yellow fever. *Reviews in medical virology* **23**, 305-318 (2013).
23 Michelitsch, A., Wernike, K., Klaus, C., Dobler, G. & Beer, M. Exploring the Reservoir Hosts of Tick-Borne Encephalitis Virus. *Viruses* **11**, 669, doi:10.3390/v11070669 (2019).
24 Laureti, M., Narayanan, D., Rodriguez-Andres, J., Fazakerley, J. K. & Kedzierski, L. Flavivirus Receptors: Diversity, Identity, and Cell Entry. *Frontiers in Immunology* **9**, doi:10.3389/fimmu.2018.02180 (2018).
25 Smit, J. M., Moesker, B., Rodenhuis-Zybert, I. & Wilschut, J. Flavivirus cell entry and membrane fusion. *Viruses* **3**, 160-171, doi:10.3390/v3020160 (2011).
26 Romero-Brey, I. & Bartenschlager, R. Membranous replication factories induced by plus-strand RNA viruses. *Viruses* **6**, 2826-2857, doi:10.3390/v6072826 (2014).
27 Aktepe, T. E. & Mackenzie, J. M. Shaping the flavivirus replication complex: It is curvaceous! *Cell Microbiol* **20**, e12884-e12884, doi:10.1111/cmi.12884 (2018).
28 Leier, H. C., Messer, W. B. & Tafesse, F. G. Lipids and pathogenic flaviviruses: An intimate union. *PLoS Pathog* **14**, e1006952, doi:10.1371/journal.ppat.1006952 (2018).
29 Rastogi, M., Sharma, N. & Singh, S. K. Flavivirus NS1: a multifaceted enigmatic viral protein. *Virology journal* **13**, 131, doi:10.1186/s12985-016-0590-7 (2016).
30 Young, P. R., Hilditch, P. A., Bletchly, C. & Halloran, W. An antigen capture enzyme-linked immunosorbent assay reveals high levels of the dengue virus protein NS1 in the sera of infected patients. *Journal of clinical microbiology* **38**, 1053-1057, doi:10.1128/JCM.38.3.1053-1057.2000 (2000).
31 Beatty, P. R. *et al.* Dengue virus NS1 triggers endothelial permeability and vascular leak that is prevented by NS1 vaccination. *Sci Transl Med* **7**, 304ra141, doi:10.1126/scitranslmed.aaa3787 (2015).
32 Mazeaud, C., Freppel, W. & Chatel-Chaix, L. The Multiples Fates of the Flavivirus RNA Genome During Pathogenesis. *Frontiers in Genetics* **9**, doi:10.3389/fgene.2018.00595 (2018).
33 Bollati, M. *et al.* Structure and functionality in flavivirus NS-proteins: perspectives for drug design. *Antiviral Res* **87**, 125-148, doi:10.1016/j.antiviral.2009.11.009 (2010).
34 Fanunza, E. *et al.* Zika virus NS2A inhibits interferon signaling by degradation of STAT1 and STAT2. *Virulence* **12**, 1580-1596, doi:10.1080/21505594.2021.1935613 (2021).
35 Samuel, M. A. & Diamond, M. S. Pathogenesis of West Nile Virus Infection: a Balance between Virulence, Innate and Adaptive Immunity, and Viral Evasion. *Journal of Virology* **80**, 9349-9360, doi:doi:10.1128/JVI.01122-06 (2006).

36 Gallichotte, E. N., Baric, R. S. & de Silva, A. M. The Molecular Specificity of the Human Antibody Response to Dengue Virus Infections. *Adv Exp Med Biol* **1062**, 63-76, doi:10.1007/978-981-10-8727-1_5 (2018).
37 Barnard, T. R., Abram, Q. H., Lin, Q. F., Wang, A. B. & Sagan, S. M. Molecular Determinants of Flavivirus Virion Assembly. *Trends in Biochemical Sciences* **46**, 378-390, doi:10.1016/j.tibs.2020.12.007 (2021).
38 Nicholls, C. M. R., Sevvana, M. & Kuhn, R. J. Structure-guided paradigm shifts in flavivirus assembly and maturation mechanisms. *Advances in virus research* **108**, 33-83, doi:10.1016/bs.aivir.2020.08.003 (2020).
39 Pierson, T. C. & Diamond, M. S. Degrees of maturity: the complex structure and biology of flaviviruses. *Curr Opin Virol* **2**, 168-175, doi:10.1016/j.coviro.2012.02.011 (2012).
40 Raut, R. *et al.* Dengue type 1 viruses circulating in humans are highly infectious and poorly neutralized by human antibodies. *Proceedings of the National Academy of Sciences* **116**, 227-232, doi:10.1073/pnas.1812055115 (2019).
41 Beltramello, M. *et al.* The human immune response to Dengue virus is dominated by highly cross-reactive antibodies endowed with neutralizing and enhancing activity. *Cell Host Microbe* **8**, 271-283, doi:10.1016/j.chom.2010.08.007 (2010).
42 Diamond, M. S. & Pierson, T. C. Molecular Insight into Dengue Virus Pathogenesis and Its Implications for Disease Control. *Cell* **162**, 488-492, doi:10.1016/j.cell.2015.07.005 (2015).
43 Screaton, G., Mongkolsapaya, J., Yacoub, S. & Roberts, C. New insights into the immunopathology and control of dengue virus infection. *Nature Reviews Immunology* **15**, 745-759, doi:10.1038/nri3916 (2015).
44 Endy, T. P. Viral Febrile Illnesses and Emerging Pathogens. *Hunter's Tropical Medicine and Emerging Infectious Diseases*, 325-350, doi:10.1016/B978-0-323-55512-8.00036-3 (2020).
45 Bente, D. A. & Rico-Hesse, R. Models of dengue virus infection. *Drug Discov Today Dis Models* **3**, 97-103, doi:10.1016/j.ddmod.2006.03.014 (2006).
46 Yacoub, S. & Farrar, J. in *Manson's Tropical Infectious Diseases (Twenty-third Edition)* (eds Jeremy Farrar *et al.*) 162-170.e162 (W.B. Saunders, 2014).
47 Michael, B. *et al.* (Switzerland: WHO press, 2009).
48 Beatty, P. R. *et al.* Dengue virus NS1 triggers endothelial permeability and vascular leak that is prevented by NS1 vaccination. *Science Translational Medicine* **7**, 304ra141-304ra141, doi:doi:10.1126/scitranslmed.aaa3787 (2015).
49 Hindle, E. Yellow Fever: an Epidemiological and Historical Study of its Place of Origin. *Nature* **130**, 646-647, doi:10.1038/130646a0 (1932).
50 REED, W., CARROLL, J. & AGRAMONTE, A. THE ETIOLOGY OF YELLOW FEVER.: AN ADDITIONAL NOTE. *Journal of the American Medical Association* **XXXVI**, 431-440, doi:10.1001/jama.1901.52470070017001f (1901).
51 Tomori, O. Yellow fever: the recurring plague. *Crit Rev Clin Lab Sci* **41**, 391-427, doi:10.1080/10408360490497474 (2004).
52 Wang, H. & Liang, G. Epidemiology of Japanese encephalitis: past, present, and future prospects. *Ther Clin Risk Manag* **11**, 435-448, doi:10.2147/TCRM.S51168 (2015).

53 Araujo, S. C. *et al.* Anti-Flavivirus Vaccines: Review of the Present Situation and Perspectives of Subunit Vaccines Produced in Escherichia coli. *Vaccines (Basel)* **8**, doi:10.3390/vaccines8030492 (2020).
54 Heinz, F. X. *et al.* Vaccination and tick-borne encephalitis, central Europe. *Emerg Infect Dis* **19**, 69-76, doi:10.3201/eid1901.120458 (2013).
55 Bogovic, P. & Strle, F. Tick-borne encephalitis: A review of epidemiology, clinical characteristics, and management. *World J Clin Cases* **3**, 430-441, doi:10.12998/wjcc.v3.i5.430 (2015).
56 Miner, J. J. & Diamond, M. S. Zika Virus Pathogenesis and Tissue Tropism. *Cell host & microbe* **21**, 134-142, doi:10.1016/j.chom.2017.01.004 (2017).
57 Musso, D. & Gubler, D. J. Zika Virus. *Clin Microbiol Rev* **29**, 487-524, doi:10.1128/CMR.00072-15 (2016).
58 Puerta-Guardo, H. *et al.* Flavivirus NS1 Triggers Tissue-Specific Vascular Endothelial Dysfunction Reflecting Disease Tropism. *Cell reports* **26**, 1598-1613.e1598, doi:10.1016/j.celrep.2019.01.036 (2019).
59 Roehrig, J. T., Bolin, R. A. & Kelly, R. G. Monoclonal antibody mapping of the envelope glycoprotein of the dengue 2 virus, Jamaica. *Virology* **246**, 317-328, doi:10.1006/viro.1998.9200 (1998).
60 Hiramatsu, K., Tadano, M., Men, R. & Lai, C. J. Mutational analysis of a neutralization epitope on the dengue type 2 virus (DEN2) envelope protein: monoclonal antibody resistant DEN2/DEN4 chimeras exhibit reduced mouse neurovirulence. *Virology* **224**, 437-445, doi:10.1006/viro.1996.0550 (1996).
61 Dowd, K. A. & Pierson, T. C. Antibody-mediated neutralization of flaviviruses: a reductionist view. *Virology* **411**, 306-315, doi:10.1016/j.virol.2010.12.020 (2011).
62 Wahala, W. M. & Silva, A. M. The human antibody response to dengue virus infection. *Viruses* **3**, 2374-2395, doi:10.3390/v3122374 (2011).
63 Smith, S. A. *et al.* Isolation of dengue virus-specific memory B cells with live virus antigen from human subjects following natural infection reveals the presence of diverse novel functional groups of antibody clones. *J Virol* **88**, 12233-12241, doi:10.1128/jvi.00247-14 (2014).
64 Smith, S. A. *et al.* Human monoclonal antibodies derived from memory B cells following live attenuated dengue virus vaccination or natural infection exhibit similar characteristics. *J Infect Dis* **207**, 1898-1908, doi:10.1093/infdis/jit119 (2013).
65 Smith, S. A. *et al.* Persistence of circulating memory B cell clones with potential for dengue virus disease enhancement for decades following infection. *J Virol* **86**, 2665-2675, doi:10.1128/jvi.06335-11 (2012).
66 de Alwis, R. *et al.* In-depth analysis of the antibody response of individuals exposed to primary dengue virus infection. *PLoS Negl Trop Dis* **5**, e1188, doi:10.1371/journal.pntd.0001188 (2011).
67 de Alwis, R. *et al.* Identification of human neutralizing antibodies that bind to complex epitopes on dengue virions. *Proc Natl Acad Sci U S A* **109**, 7439-7444, doi:10.1073/pnas.1200566109 (2012).

68 de Alwis, R. *et al.* Dengue viruses are enhanced by distinct populations of serotype cross-reactive antibodies in human immune sera. *PLoS Pathog* **10**, e1004386-e1004386, doi:10.1371/journal.ppat.1004386 (2014).
69 Rey, F. A., Stiasny, K., Vaney, M.-C., Dellarole, M. & Heinz, F. X. The bright and the dark side of human antibody responses to flaviviruses: lessons for vaccine design. *EMBO reports* **19**, 206-224, doi:https://doi.org/10.15252/embr.201745302 (2018).
70 Barba-Spaeth, G. *et al.* Structural basis of potent Zika-dengue virus antibody cross-neutralization. *Nature* **536**, 48-53, doi:10.1038/nature18938 (2016).
71 Teoh, E. P. *et al.* The structural basis for serotype-specific neutralization of dengue virus by a human antibody. *Sci Transl Med* **4**, 139ra183, doi:10.1126/scitranslmed.3003888 (2012).
72 Gallichotte, E. N. *et al.* A New Quaternary Structure Epitope on Dengue Virus Serotype 2 Is the Target of Durable Type-Specific Neutralizing Antibodies. *mBio* **6**, e01461-01415, doi:10.1128/mBio.01461-15.
73 Fibriansah, G. *et al.* DENGUE VIRUS. Cryo-EM structure of an antibody that neutralizes dengue virus type 2 by locking E protein dimers. *Science (New York, N.Y.)* **349**, 88-91, doi:10.1126/science.aaa8651 (2015).
74 Wahala, W. M. P. B., Kraus, A. A., Haymore, L. B., Accavitti-Loper, M. A. & de Silva, A. M. Dengue virus neutralization by human immune sera: role of envelope protein domain III-reactive antibody. *Virology* **392**, 103-113, doi:10.1016/j.virol.2009.06.037 (2009).
75 Throsby, M. *et al.* Isolation and characterization of human monoclonal antibodies from individuals infected with West Nile Virus. *Journal of virology* **80**, 6982-6992, doi:10.1128/JVI.00551-06 (2006).
76 Robbiani, D. F. *et al.* Recurrent Potent Human Neutralizing Antibodies to Zika Virus in Brazil and Mexico. *Cell* **169**, 597-609.e511, doi:10.1016/j.cell.2017.04.024 (2017).
77 Dejnirattisai, W. *et al.* Cross-reacting antibodies enhance dengue virus infection in humans. *Science (New York, N.Y.)* **328**, 745-748, doi:10.1126/science.1185181 (2010).
78 Talarico, L. B. *et al.* The Role of Heterotypic DENV-specific CD8(+)T Lymphocytes in an Immunocompetent Mouse Model of Secondary Dengue Virus Infection. *EBioMedicine* **20**, 202-216, doi:10.1016/j.ebiom.2017.04.033 (2017).
79 Anderson, K. B. *et al.* A shorter time interval between first and second dengue infections is associated with protection from clinical illness in a school-based cohort in Thailand. *J Infect Dis* **209**, 360-368, doi:10.1093/infdis/jit436 (2014).
80 Halstead, S. B. Dengue. *Lancet* **370**, 1644-1652, doi:10.1016/s0140-6736(07)61687-0 (2007).
81 Katzelnick, L. C. *et al.* Antibody-dependent enhancement of severe dengue disease in humans. *Science (New York, N.Y.)* **358**, 929-932, doi:10.1126/science.aan6836 (2017).
82 Bhatt, P., Sabeena, S. P., Varma, M. & Arunkumar, G. Current Understanding of the Pathogenesis of Dengue Virus Infection. *Curr Microbiol* **78**, 17-32, doi:10.1007/s00284-020-02284-w (2021).
83 Katzelnick, L. C. *et al.* Antibody-dependent enhancement of severe dengue disease in humans. *Science (New York, N.Y.)* **358**, 929-932, doi:10.1126/science.aan6836 (2017).

84 Balsitis, S. J. *et al.* Lethal antibody enhancement of dengue disease in mice is prevented by Fc modification. *PLoS Pathog* **6**, e1000790-e1000790, doi:10.1371/journal.ppat.1000790 (2010).
85 Kliks, S. C., Nimmanitya, S., Nisalak, A. & Burke, D. S. Evidence that maternal dengue antibodies are important in the development of dengue hemorrhagic fever in infants. *The American journal of tropical medicine and hygiene* **38**, 411-419, doi:10.4269/ajtmh.1988.38.411 (1988).
86 Masel, J. *et al.* Does prior dengue virus exposure worsen clinical outcomes of Zika virus infection? A systematic review, pooled analysis and lessons learned. *PLoS neglected tropical diseases* **13**, e0007060-e0007060, doi:10.1371/journal.pntd.0007060 (2019).
87 Williams, K. L. *et al.* Therapeutic efficacy of antibodies lacking Fcγ receptor binding against lethal dengue virus infection is due to neutralizing potency and blocking of enhancing antibodies [corrected]. *PLoS Pathog* **9**, e1003157, doi:10.1371/journal.ppat.1003157 (2013).
88 Wegman, A. D. *et al.* Monomeric IgA Antagonizes IgG-Mediated Enhancement of DENV Infection. *Frontiers in Immunology* **12**, doi:10.3389/fimmu.2021.777672 (2021).
89 Hegde, N. R. & Gore, M. M. Japanese encephalitis vaccines: Immunogenicity, protective efficacy, effectiveness, and impact on the burden of disease. *Human vaccines & immunotherapeutics* **13**, 1-18, doi:10.1080/21645515.2017.1285472 (2017).
90 Ulbert, S. West Nile virus vaccines - current situation and future directions. *Human vaccines & immunotherapeutics* **15**, 2337-2342, doi:10.1080/21645515.2019.1621149 (2019).
91 Pinheiro-Michelsen, J. R. *et al.* Anti-dengue Vaccines: From Development to Clinical Trials. *Frontiers in immunology* **11**, 1252-1252, doi:10.3389/fimmu.2020.01252 (2020).
92 Henein, S. *et al.* Dissecting Antibodies Induced by a Chimeric Yellow Fever-Dengue, Live-Attenuated, Tetravalent Dengue Vaccine (CYD-TDV) in Naive and Dengue-Exposed Individuals. *J Infect Dis* **215**, 351-358, doi:10.1093/infdis/jiw576 (2017).
93 Sabchareon, A. *et al.* Protective efficacy of the recombinant, live-attenuated, CYD tetravalent dengue vaccine in Thai schoolchildren: a randomised, controlled phase 2b trial. *Lancet* **380**, 1559-1567, doi:10.1016/s0140-6736(12)61428-7 (2012).
94 WHO. Dengue vaccines:WHO position paper September 2018. *Weekly epidemiological record* **36**, 457-476 (2018).
95 Hadinegoro, S. R. *et al.* Efficacy and Long-Term Safety of a Dengue Vaccine in Regions of Endemic Disease. *The New England journal of medicine* **373**, 1195-1206, doi:10.1056/NEJMoa1506223 (2015).
96 Sridhar, S. *et al.* Effect of Dengue Serostatus on Dengue Vaccine Safety and Efficacy. *The New England journal of medicine* **379**, 327-340, doi:10.1056/NEJMoa1800820 (2018).
97 Larsen, C. P., Whitehead, S. S. & Durbin, A. P. Dengue human infection models to advance dengue vaccine development. *Vaccine* **33**, 7075-7082, doi:10.1016/j.vaccine.2015.09.052 (2015).
98 Blaney, J. E., Jr., Hanson, C. T., Hanley, K. A., Murphy, B. R. & Whitehead, S. S. Vaccine candidates derived from a novel infectious cDNA clone of an American genotype dengue virus type 2. *BMC infectious diseases* **4**, 39-39, doi:10.1186/1471-2334-4-39 (2004).

99 Kirkpatrick, B. D. *et al.* The live attenuated dengue vaccine TV003 elicits complete protection against dengue in a human challenge model. *Sci Transl Med* **8**, 330ra336, doi:10.1126/scitranslmed.aaf1517 (2016).
100 Huang, C. Y. H. *et al.* Dengue 2 PDK-53 virus as a chimeric carrier for tetravalent dengue vaccine development. *Journal of virology* **77**, 11436-11447, doi:10.1128/jvi.77.21.11436-11447.2003 (2003).
101 Biswal, S. *et al.* Efficacy of a Tetravalent Dengue Vaccine in Healthy Children and Adolescents. *The New England journal of medicine* **381**, 2009-2019, doi:10.1056/NEJMoa1903869 (2019).
102 Rupp, R. *et al.* Safety and immunogenicity of different doses and schedules of a live attenuated tetravalent dengue vaccine (TDV) in healthy adults: A Phase 1b randomized study. *Vaccine* **33**, 6351-6359, doi:10.1016/j.vaccine.2015.09.008 (2015).
103 Powers, A. M. *et al.* Evolutionary relationships and systematics of the alphaviruses. *Journal of virology* **75**, 10118-10131, doi:10.1128/JVI.75.21.10118-10131.2001 (2001).
104 Reyes-Sandoval, A. 51 years in of Chikungunya clinical vaccine development: A historical perspective. *Human vaccines & immunotherapeutics* **15**, 2351-2358, doi:10.1080/21645515.2019.1574149 (2019).
105 Kam, Y.-W. *et al.* Longitudinal analysis of the human antibody response to Chikungunya virus infection: implications for serodiagnosis and vaccine development. *Journal of virology* **86**, 13005-13015, doi:10.1128/JVI.01780-12 (2012).
106 Leung, J. Y.-S., Ng, M. M.-L. & Chu, J. J. H. Replication of alphaviruses: a review on the entry process of alphaviruses into cells. *Adv Virol* **2011**, 249640-249640, doi:10.1155/2011/249640 (2011).
107 Earnest, J. T. *et al.* The mechanistic basis of protection by non-neutralizing anti-alphavirus antibodies. *Cell Rep* **35**, 108962, doi:10.1016/j.celrep.2021.108962 (2021).
108 Forrester, N. L. *et al.* Genome-scale phylogeny of the alphavirus genus suggests a marine origin. *Journal of virology* **86**, 2729-2738, doi:10.1128/JVI.05591-11 (2012).
109 Jose, J., Snyder, J. E. & Kuhn, R. J. A structural and functional perspective of alphavirus replication and assembly. *Future Microbiol* **4**, 837-856, doi:10.2217/fmb.09.59 (2009).
110 Schmaljohn, A. L. & McClain, D. in *Medical Microbiology* Vol. 4th edition (ed Baron S) Ch. 54, (1996).
111 Nowee, G. *et al.* A Tale of 20 Alphaviruses; Inter-species Diversity and Conserved Interactions Between Viral Non-structural Protein 3 and Stress Granule Proteins. *Frontiers in Cell and Developmental Biology* **9**, doi:10.3389/fcell.2021.625711 (2021).
112 Valentine, M. J., Murdock, C. C. & Kelly, P. J. Sylvatic cycles of arboviruses in non-human primates. *Parasites & Vectors* **12**, 463, doi:10.1186/s13071-019-3732-0 (2019).
113 Lim, E. X. Y., Lee, W. S., Madzokere, E. T. & Herrero, L. J. Mosquitoes as Suitable Vectors for Alphaviruses. *Viruses* **10**, 84, doi:10.3390/v10020084 (2018).
114 Kim, A. S. *et al.* An Evolutionary Insertion in the Mxra8 Receptor-Binding Site Confers Resistance to Alphavirus Infection and Pathogenesis. *Cell Host & Microbe* **27**, 428-440.e429, doi:https://doi.org/10.1016/j.chom.2020.01.008 (2020).
115 Ma, H. *et al.* LDLRAD3 is a receptor for Venezuelan equine encephalitis virus. *Nature* **588**, 308-314, doi:10.1038/s41586-020-2915-3 (2020).

116 Kim, A. S. *et al.* Pan-protective anti-alphavirus human antibodies target a conserved E1 protein epitope. *Cell* **184**, 4414-4429.e4419, doi:10.1016/j.cell.2021.07.006 (2021).
117 Carrasco, L., Sanz, M. A. & González-Almela, E. The Regulation of Translation in Alphavirus-Infected Cells. *Viruses* **10**, 70, doi:10.3390/v10020070 (2018).
118 Abdelnabi, R. & Delang, L. Antiviral Strategies against Arthritogenic Alphaviruses. *Microorganisms* **8**, 1365 (2020).
119 Lwande, O. W. *et al.* Global emergence of Alphaviruses that cause arthritis in humans. *Infect Ecol Epidemiol* **5**, 29853-29853, doi:10.3402/iee.v5.29853 (2015).
120 Suhrbier, A., Jaffar-Bandjee, M.-C. & Gasque, P. Arthritogenic alphaviruses—an overview. *Nature Reviews Rheumatology* **8**, 420-429, doi:10.1038/nrrheum.2012.64 (2012).
121 Fox, J. M. *et al.* A cross-reactive antibody protects against Ross River virus musculoskeletal disease despite rapid neutralization escape in mice. *PLoS pathogens* **16**, e1008743, doi:10.1371/journal.ppat.1008743 (2020).
122 Constant, L. E. C. *et al.* Overview on Chikungunya Virus Infection: From Epidemiology to State-of-the-Art Experimental Models. *Front Microbiol* **12**, doi:10.3389/fmicb.2021.744164 (2021).
123 van Ewijk, R. *et al.* Neurologic sequelae of severe chikungunya infection in the first 6 months of life: a prospective cohort study 24-months post-infection. *BMC Infectious Diseases* **21**, 179, doi:10.1186/s12879-021-05876-4 (2021).
124 Tritsch, S. R. *et al.* Chronic joint pain 3 years after chikungunya virus infection largely characterized by relapsing-remitting symptoms. *The Journal of Rheumatology*, jrheum.190162, doi:10.3899/jrheum.190162 (2019).
125 Martins, K. A. *et al.* Neutralizing Antibodies from Convalescent Chikungunya Virus Patients Can Cross-Neutralize Mayaro and Una Viruses. *The American journal of tropical medicine and hygiene* **100**, 1541-1544, doi:10.4269/ajtmh.18-0756 (2019).
126 Harley, D., Sleigh, A. & Ritchie, S. Ross River virus transmission, infection, and disease: a cross-disciplinary review. *Clin Microbiol Rev* **14**, 909-932, doi:10.1128/CMR.14.4.909-932.2001 (2001).
127 Powers, A. M. *et al.* Genetic relationships among Mayaro and Una viruses suggest distinct patterns of transmission. *The American journal of tropical medicine and hygiene* **75**, 461-469 (2006).
128 Diaz, L. A., Spinsanti, L. I., Almiron, W. R. & Contigiani, M. S. UNA virus: first report of human infection in Argentina. *Rev Inst Med Trop Sao Paulo* **45**, 109-110, doi:10.1590/s0036-46652003000200012 (2003).
129 Sharma, A. & Knollmann-Ritschel, B. Current Understanding of the Molecular Basis of Venezuelan Equine Encephalitis Virus Pathogenesis and Vaccine Development. *Viruses* **11**, 164, doi:10.3390/v11020164 (2019).
130 Corrin, T., Ackford, R., Mascarenhas, M., Greig, J. & Waddell, L. A. Eastern Equine Encephalitis Virus: A Scoping Review of the Global Evidence. *Vector Borne Zoonotic Dis* **21**, 305-320, doi:10.1089/vbz.2020.2671 (2021).
131 Lindsey, N. P., Staples, J. E. & Fischer, M. Eastern Equine Encephalitis Virus in the United States, 2003-2016. *The American journal of tropical medicine and hygiene* **98**, 1472-1477, doi:10.4269/ajtmh.17-0927 (2018).

132 Bergren, N. A. *et al.* "Submergence" of Western equine encephalitis virus: Evidence of positive selection argues against genetic drift and fitness reductions. *PLoS Pathog* **16**, e1008102, doi:10.1371/journal.ppat.1008102 (2020).
133 Teo, T. H. *et al.* A pathogenic role for CD4+ T cells during Chikungunya virus infection in mice. *Journal of immunology (Baltimore, Md. : 1950)* **190**, 259-269, doi:10.4049/jimmunol.1202177 (2013).
134 Fox, J. M. & Diamond, M. S. Immune-Mediated Protection and Pathogenesis of Chikungunya Virus. *The Journal of Immunology* **197**, 4210-4218, doi:10.4049/jimmunol.1601426 (2016).
135 Felipe, V. L. J., Paula A, V. & Silvio, U.-I. Chikungunya virus infection induces differential inflammatory and antiviral responses in human monocytes and monocyte-derived macrophages. *Acta Tropica* **211**, 105619, doi:https://doi.org/10.1016/j.actatropica.2020.105619 (2020).
136 Burt, F. J. *et al.* Chikungunya virus: an update on the biology and pathogenesis of this emerging pathogen. *The Lancet. Infectious diseases* **17**, e107-e117, doi:10.1016/s1473-3099(16)30385-1 (2017).
137 Broeckel, R. M. *et al.* Vaccine-Induced Skewing of T Cell Responses Protects Against Chikungunya Virus Disease. *Frontiers in Immunology* **10**, doi:10.3389/fimmu.2019.02563 (2019).
138 Torres-Ruesta, A., Chee, R. S.-L. & Ng, L. F. P. Insights into Antibody-Mediated Alphavirus Immunity and Vaccine Development Landscape. *Microorganisms* **9**, 899 (2021).
139 Poo, Y. S. *et al.* Multiple immune factors are involved in controlling acute and chronic chikungunya virus infection. *PLoS Negl Trop Dis* **8**, e3354, doi:10.1371/journal.pntd.0003354 (2014).
140 Weger-Lucarelli, J., Aliota, M. T., Kamlangdee, A. & Osorio, J. E. Identifying the Role of E2 Domains on Alphavirus Neutralization and Protective Immune Responses. *PLOS Neglected Tropical Diseases* **9**, e0004163, doi:10.1371/journal.pntd.0004163 (2015).
141 Webb, E. M. *et al.* Effects of Chikungunya virus immunity on Mayaro virus disease and epidemic potential. *Sci Rep* **9**, 20399, doi:10.1038/s41598-019-56551-3 (2019).
142 Fox, J. M. *et al.* Broadly Neutralizing Alphavirus Antibodies Bind an Epitope on E2 and Inhibit Entry and Egress. *Cell* **163**, 1095-1107, doi:10.1016/j.cell.2015.10.050 (2015).
143 Earnest, J. T. *et al.* The mechanistic basis of protection by non-neutralizing anti-alphavirus antibodies. *Cell Reports* **35**, 108962, doi:https://doi.org/10.1016/j.celrep.2021.108962 (2021).
144 Linn, M. L., Aaskov, J. G. & Suhrbier, A. Antibody-dependent enhancement and persistence in macrophages of an arbovirus associated with arthritis. *J Gen Virol* **77 (Pt 3)**, 407-411, doi:10.1099/0022-1317-77-3-407 (1996).
145 Lidbury Brett, A. & Mahalingam, S. Specific Ablation of Antiviral Gene Expression in Macrophages by Antibody-Dependent Enhancement of Ross River Virus Infection. *Journal of Virology* **74**, 8376-8381, doi:10.1128/JVI.74.18.8376-8381.2000 (2000).
146 Lum, F.-M. *et al.* Antibody-mediated enhancement aggravates chikungunya virus infection and disease severity. *Sci Rep* **8**, 1860, doi:10.1038/s41598-018-20305-4 (2018).

147 Hawman, D. W. *et al.* Chronic joint disease caused by persistent Chikungunya virus infection is controlled by the adaptive immune response. *J Virol* **87**, 13878-13888, doi:10.1128/jvi.02666-13 (2013).
148 Amdekar, S., Parashar, D. & Alagarasu, K. Chikungunya Virus-Induced Arthritis: Role of Host and Viral Factors in the Pathogenesis. *Viral Immunol* **30**, 691-702, doi:10.1089/vim.2017.0052 (2017).
149 Casamassima, A. C., Hess, L. W. & Marty, A. TC-83 Venezuelan equine encephalitis vaccine exposure during pregnancy. *Teratology* **36**, 287-289, doi:https://doi.org/10.1002/tera.1420360303 (1987).
150 Pittman, P. R. *et al.* Long-term duration of detectable neutralizing antibodies after administration of live-attenuated VEE vaccine and following booster vaccination with inactivated VEE vaccine. *Vaccine* **14**, 337-343, doi:10.1016/0264-410x(95)00168-z (1996).
151 Powers, A. M. Vaccine and Therapeutic Options To Control Chikungunya Virus. *Clin Microbiol Rev* **31**, e00104-00116, doi:10.1128/CMR.00104-16 (2017).
152 Chen, G. L. *et al.* Effect of a Chikungunya Virus–Like Particle Vaccine on Safety and Tolerability Outcomes: A Randomized Clinical Trial. *JAMA* **323**, 1369-1377, doi:10.1001/jama.2020.2477 (2020).
153 Virology: Coronaviruses. *Nature* **220**, 650-650, doi:10.1038/220650b0 (1968).
154 Fehr, A. R. & Perlman, S. Coronaviruses: an overview of their replication and pathogenesis. *Methods in molecular biology (Clifton, N.J.)* **1282**, 1-23, doi:10.1007/978-1-4939-2438-7_1 (2015).
155 Lim, Y. X., Ng, Y. L., Tam, J. P. & Liu, D. X. Human Coronaviruses: A Review of Virus-Host Interactions. *Diseases* **4**, 26, doi:10.3390/diseases4030026 (2016).
156 Cui, J., Li, F. & Shi, Z.-L. Origin and evolution of pathogenic coronaviruses. *Nature Reviews Microbiology* **17**, 181-192, doi:10.1038/s41579-018-0118-9 (2019).
157 Woo, P. C. Y. *et al.* Discovery of seven novel Mammalian and avian coronaviruses in the genus deltacoronavirus supports bat coronaviruses as the gene source of alphacoronavirus and betacoronavirus and avian coronaviruses as the gene source of gammacoronavirus and deltacoronavirus. *Journal of virology* **86**, 3995-4008, doi:10.1128/JVI.06540-11 (2012).
158 Zhou, L., Ayeh, S. K., Chidambaram, V. & Karakousis, P. C. Modes of transmission of SARS-CoV-2 and evidence for preventive behavioral interventions. *BMC Infectious Diseases* **21**, 496, doi:10.1186/s12879-021-06222-4 (2021).
159 Seto, W. H. *et al.* Effectiveness of precautions against droplets and contact in prevention of nosocomial transmission of severe acute respiratory syndrome (SARS). *The Lancet* **361**, 1519-1520, doi:10.1016/S0140-6736(03)13168-6 (2003).
160 Parkhe, P. & Verma, S. Evolution, Interspecies Transmission, and Zoonotic Significance of Animal Coronaviruses. *Frontiers in Veterinary Science* **8** (2021).
161 Ricci, D. *et al.* Innate Immune Response to SARS-CoV-2 Infection: From Cells to Soluble Mediators. *Int J Mol Sci* **22**, doi:10.3390/ijms22137017 (2021).
162 Watanabe, Y., Allen Joel, D., Wrapp, D., McLellan Jason, S. & Crispin, M. Site-specific glycan analysis of the SARS-CoV-2 spike. *Science (New York, N.Y.)* **369**, 330-333, doi:10.1126/science.abb9983 (2020).

163 Jackson, C. B., Farzan, M., Chen, B. & Choe, H. Mechanisms of SARS-CoV-2 entry into cells. *Nature Reviews Molecular Cell Biology* **23**, 3-20, doi:10.1038/s41580-021-00418-x (2022).
164 Holland, J. *et al.* Rapid Evolution of RNA Genomes. *Science (New York, N.Y.)* **215**, 1577-1585, doi:10.1126/science.7041255 (1982).
165 Denison, M. R., Graham, R. L., Donaldson, E. F., Eckerle, L. D. & Baric, R. S. Coronaviruses: an RNA proofreading machine regulates replication fidelity and diversity. *RNA Biol* **8**, 270-279, doi:10.4161/rna.8.2.15013 (2011).
166 Gribble, J. *et al.* The coronavirus proofreading exoribonuclease mediates extensive viral recombination. *PLoS Pathog* **17**, e1009226, doi:10.1371/journal.ppat.1009226 (2021).
167 Goldstein, S. A., Brown, J., Pedersen, B. S., Quinlan, A. R. & Elde, N. C. Extensive recombination-driven coronavirus diversification expands the pool of potential pandemic pathogens. *bioRxiv*, 2021.2002.2003.429646, doi:10.1101/2021.02.03.429646 (2021).
168 Volz, E. *et al.* Evaluating the Effects of SARS-CoV-2 Spike Mutation D614G on Transmissibility and Pathogenicity. *Cell* **184**, 64-75.e11, doi:https://doi.org/10.1016/j.cell.2020.11.020 (2021).
169 Organization, W. H. *Tracking SARS-CoV-2 Variants* 2022).
170 Rambaut, A. *et al.* A dynamic nomenclature proposal for SARS-CoV-2 lineages to assist genomic epidemiology. *Nature Microbiology* **5**, 1403-1407, doi:10.1038/s41564-020-0770-5 (2020).
171 Davies Nicholas, G. *et al.* Estimated transmissibility and impact of SARS-CoV-2 lineage B.1.1.7 in England. *Science (New York, N.Y.)* **372**, eabg3055, doi:10.1126/science.abg3055 (2021).
172 Wang, P. *et al.* Antibody Resistance of SARS-CoV-2 Variants B.1.351 and B.1.1.7. *bioRxiv*, 2021.2001.2025.428137, doi:10.1101/2021.01.25.428137 (2021).
173 Edara, V.-V. *et al.* Infection and vaccine-induced neutralizing antibody responses to the SARS-CoV-2 B.1.617.1 variant. *bioRxiv*, 2021.2005.2009.443299, doi:10.1101/2021.05.09.443299 (2021).
174 Planas, D. *et al.* Considerable escape of SARS-CoV-2 variant Omicron to antibody neutralization. *bioRxiv*, 2021.2012.2014.472630, doi:10.1101/2021.12.14.472630 (2021).
175 Vlasova, A. N., Kenney, S. P., Jung, K., Wang, Q. & Saif, L. J. Deltacoronavirus Evolution and Transmission: Current Scenario and Evolutionary Perspectives. *Frontiers in Veterinary Science* **7**, doi:10.3389/fvets.2020.626785 (2021).
176 Ruiz-Aravena, M. *et al.* Ecology, evolution and spillover of coronaviruses from bats. *Nature Reviews Microbiology*, doi:10.1038/s41579-021-00652-2 (2021).
177 Galanti, M. & Shaman, J. Direct Observation of Repeated Infections With Endemic Coronaviruses. *The Journal of Infectious Diseases* **223**, 409-415, doi:10.1093/infdis/jiaa392 (2020).
178 Hu, B., Guo, H., Zhou, P. & Shi, Z.-L. Characteristics of SARS-CoV-2 and COVID-19. *Nature Reviews Microbiology* **19**, 141-154, doi:10.1038/s41579-020-00459-7 (2021).

179 Huang, C. *et al.* Clinical features of patients infected with 2019 novel coronavirus in Wuhan, China. *Lancet (London, England)* **395**, 497-506, doi:10.1016/S0140-6736(20)30183-5 (2020).
180 Sette, A. & Crotty, S. Adaptive immunity to SARS-CoV-2 and COVID-19. *Cell* **184**, 861-880, doi:10.1016/j.cell.2021.01.007 (2021).
181 Frieman, M., Heise, M. & Baric, R. SARS coronavirus and innate immunity. *Virus Res* **133**, 101-112, doi:10.1016/j.virusres.2007.03.015 (2008).
182 Wong, L.-Y. R. & Perlman, S. Immune dysregulation and immunopathology induced by SARS-CoV-2 and related coronaviruses — are we our own worst enemy? *Nature Reviews Immunology* **22**, 47-56, doi:10.1038/s41577-021-00656-2 (2022).
183 Zhang, Q. *et al.* Inborn errors of type I IFN immunity in patients with life-threatening COVID-19. *Science (New York, N.Y.)* **370**, eabd4570, doi:10.1126/science.abd4570 (2020).
184 Setaro, A. C. & Gaglia, M. M. All hands on deck: SARS-CoV-2 proteins that block early anti-viral interferon responses. *Current Research in Virological Science* **2**, 100015, doi:https://doi.org/10.1016/j.crviro.2021.100015 (2021).
185 Bastard, P. *et al.* Autoantibodies against type I IFNs in patients with life-threatening COVID-19. *Science (New York, N.Y.)* **370**, eabd4585, doi:10.1126/science.abd4585 (2020).
186 Zuo, J. *et al.* Robust SARS-CoV-2-specific T cell immunity is maintained at 6 months following primary infection. *Nature immunology* **22**, 620-626, doi:10.1038/s41590-021-00902-8 (2021).
187 Ng, O.-W. *et al.* Memory T cell responses targeting the SARS coronavirus persist up to 11 years post-infection. *Vaccine* **34**, 2008-2014, doi:https://doi.org/10.1016/j.vaccine.2016.02.063 (2016).
188 Grifoni, A. *et al.* Targets of T Cell Responses to SARS-CoV-2 Coronavirus in Humans with COVID-19 Disease and Unexposed Individuals. *Cell* **181**, 1489-1501.e1415, doi:10.1016/j.cell.2020.05.015 (2020).
189 Mateus, J. *et al.* Selective and cross-reactive SARS-CoV-2 T cell epitopes in unexposed humans. *Science (New York, N.Y.)* **370**, 89-94, doi:10.1126/science.abd3871 (2020).
190 Wu, L. P. *et al.* Duration of antibody responses after severe acute respiratory syndrome. *Emerg Infect Dis* **13**, 1562-1564, doi:10.3201/eid1310.070576 (2007).
191 Anderson, D. E. *et al.* Lack of cross-neutralization by SARS patient sera towards SARS-CoV-2. *Emerging Microbes & Infections* **9**, 900-902, doi:10.1080/22221751.2020.1761267 (2020).
192 Sariol, A. & Perlman, S. Lessons for COVID-19 Immunity from Other Coronavirus Infections. *Immunity* **53**, 248-263, doi:10.1016/j.immuni.2020.07.005 (2020).
193 Premkumar, L. *et al.* The receptor binding domain of the viral spike protein is an immunodominant and highly specific target of antibodies in SARS-CoV-2 patients. *Sci Immunol* **5**, doi:10.1126/sciimmunol.abc8413 (2020).
194 Chao, Y. X., Rötzschke, O. & Tan, E.-K. The role of IgA in COVID-19. *Brain Behav Immun* **87**, 182-183, doi:10.1016/j.bbi.2020.05.057 (2020).
195 Quinti, I., Mortari, E. P., Fernandez Salinas, A., Milito, C. & Carsetti, R. IgA Antibodies and IgA Deficiency in SARS-CoV-2 Infection. *Front Cell Infect Microbiol* **11**, 257 (2021).

196 Burgess, S., Ponsford, M. J. & Gill, D. Are we underestimating seroprevalence of SARS-CoV-2? *BMJ* **370**, m3364, doi:10.1136/bmj.m3364 (2020).
197 Wang, Z. *et al.* Enhanced SARS-CoV-2 neutralization by dimeric IgA. *Science Translational Medicine* **13**, eabf1555, doi:10.1126/scitranslmed.abf1555 (2021).
198 Bates, T. A. *et al.* Cross-reactivity of SARS-CoV structural protein antibodies against SARS-CoV-2. *Cell Rep* **34**, 108737, doi:10.1016/j.celrep.2021.108737 (2021).
199 Lv, H. *et al.* Cross-reactive Antibody Response between SARS-CoV-2 and SARS-CoV Infections. *Cell reports* **31**, 107725-107725, doi:10.1016/j.celrep.2020.107725 (2020).
200 Yuan, M. *et al.* A highly conserved cryptic epitope in the receptor binding domains of SARS-CoV-2 and SARS-CoV. *Science (New York, N.Y.)* **368**, 630-633, doi:10.1126/science.abb7269 (2020).
201 Fraley, E. *et al.* Cross-reactive antibody immunity against SARS-CoV-2 in children and adults. *Cellular & Molecular Immunology* **18**, 1826-1828, doi:10.1038/s41423-021-00700-0 (2021).
202 Shrock, E. *et al.* Viral epitope profiling of COVID-19 patients reveals cross-reactivity and correlates of severity. *Science (New York, N.Y.)* **370**, eabd4250, doi:10.1126/science.abd4250 (2020).
203 Lee, W. S., Wheatley, A. K., Kent, S. J. & DeKosky, B. J. Antibody-dependent enhancement and SARS-CoV-2 vaccines and therapies. *Nature Microbiology* **5**, 1185-1191, doi:10.1038/s41564-020-00789-5 (2020).
204 Wang, S.-F. *et al.* Antibody-dependent SARS coronavirus infection is mediated by antibodies against spike proteins. *Biochem Biophys Res Commun* **451**, 208-214, doi:10.1016/j.bbrc.2014.07.090 (2014).
205 Jaume, M. *et al.* Anti-severe acute respiratory syndrome coronavirus spike antibodies trigger infection of human immune cells via a pH- and cysteine protease-independent FcγR pathway. *Journal of virology* **85**, 10582-10597, doi:10.1128/JVI.00671-11 (2011).
206 Tseng, C.-T. *et al.* Immunization with SARS coronavirus vaccines leads to pulmonary immunopathology on challenge with the SARS virus. *PloS one* **7**, e35421-e35421, doi:10.1371/journal.pone.0035421 (2012).
207 Luo, F. *et al.* Evaluation of Antibody-Dependent Enhancement of SARS-CoV Infection in Rhesus Macaques Immunized with an Inactivated SARS-CoV Vaccine. *Virol Sin* **33**, 201-204, doi:10.1007/s12250-018-0009-2 (2018).
208 Arvin, A. M. *et al.* A perspective on potential antibody-dependent enhancement of SARS-CoV-2. *Nature* **584**, 353-363, doi:10.1038/s41586-020-2538-8 (2020).
209 Kyriakidis, N. C., López-Cortés, A., González, E. V., Grimaldos, A. B. & Prado, E. O. SARS-CoV-2 vaccines strategies: a comprehensive review of phase 3 candidates. *npj Vaccines* **6**, 28, doi:10.1038/s41541-021-00292-w (2021).
210 Polack, F. P. *et al.* Safety and Efficacy of the BNT162b2 mRNA Covid-19 Vaccine. *New England Journal of Medicine* **383**, 2603-2615, doi:10.1056/NEJMoa2034577 (2020).
211 Heath, P. T. *et al.* Safety and Efficacy of NVX-CoV2373 Covid-19 Vaccine. *New England Journal of Medicine* **385**, 1172-1183, doi:10.1056/NEJMoa2107659 (2021).
212 Amanna, I. J., Carlson, N. E. & Slifka, M. K. Duration of Humoral Immunity to Common Viral and Vaccine Antigens. *New England Journal of Medicine* **357**, 1903-1915, doi:10.1056/NEJMoa066092 (2007).
232

213 Amanna, I. J. & Slifka, M. K. Mechanisms that determine plasma cell lifespan and the duration of humoral immunity. *Immunol Rev* **236**, 125-138, doi:10.1111/j.1600-065X.2010.00912.x (2010).
214 Cyster, J. G. & Allen, C. D. C. B Cell Responses: Cell Interaction Dynamics and Decisions. *Cell* **177**, 524-540, doi:10.1016/j.cell.2019.03.016 (2019).
215 Janeway CA Jr., T. P., Walport M. in *Immunobiology: THe immune system in Health and Disease* Ch. 7, (Garland Science, 2017).
216 LeBien, T. W. & Tedder, T. F. B lymphocytes: how they develop and function. *Blood* **112**, 1570-1580, doi:10.1182/blood-2008-02-078071 (2008).
217 Li, A. *et al.* Utilization of Ig heavy chain variable, diversity, and joining gene segments in children with B-lineage acute lymphoblastic leukemia: implications for the mechanisms of VDJ recombination and for pathogenesis. *Blood* **103**, 4602-4609, doi:10.1182/blood-2003-11-3857 (2004).
218 Hewitt, E. W. The MHC class I antigen presentation pathway: strategies for viral immune evasion. *Immunology* **110**, 163-169, doi:10.1046/j.1365-2567.2003.01738.x (2003).
219 Roche, P. A. & Furuta, K. The ins and outs of MHC class II-mediated antigen processing and presentation. *Nature Reviews Immunology* **15**, 203-216, doi:10.1038/nri3818 (2015).
220 Ripperger, T. J. & Bhattacharya, D. Transcriptional and Metabolic Control of Memory B Cells and Plasma Cells. *Annu Rev Immunol* **39**, 345-368, doi:10.1146/annurev-immunol-093019-125603 (2021).
221 Roco, J. A. *et al.* Class-Switch Recombination Occurs Infrequently in Germinal Centers. *Immunity* **51**, 337-350.e337, doi:10.1016/j.immuni.2019.07.001 (2019).
222 Wong, R. *et al.* Affinity-Restricted Memory B Cells Dominate Recall Responses to Heterologous Flaviviruses. *Immunity* **53**, 1078-1094.e1077, doi:10.1016/j.immuni.2020.09.001 (2020).
223 Xu, Z., Zan, H., Pone, E. J., Mai, T. & Casali, P. Immunoglobulin class-switch DNA recombination: induction, targeting and beyond. *Nature Reviews Immunology* **12**, 517-531, doi:10.1038/nri3216 (2012).
224 Akkaya, M., Kwak, K. & Pierce, S. K. B cell memory: building two walls of protection against pathogens. *Nature Reviews Immunology* **20**, 229-238, doi:10.1038/s41577-019-0244-2 (2020).
225 Takemori, T., Kaji, T., Takahashi, Y., Shimoda, M. & Rajewsky, K. Generation of memory B cells inside and outside germinal centers. *European journal of immunology* **44**, 1258-1264, doi:10.1002/eji.201343716 (2014).
226 Wec, A. Z. *et al.* Longitudinal dynamics of the human B cell response to the yellow fever 17D vaccine. *Proceedings of the National Academy of Sciences* **117**, 6675-6685, doi:10.1073/pnas.1921388117 (2020).
227 Baumgarth, N. How specific is too specific? B-cell responses to viral infections reveal the importance of breadth over depth. *Immunological reviews* **255**, 82-94, doi:10.1111/imr.12094 (2013).
228 Wienands, J. & Engels, N. The Memory Function of the B Cell Antigen Receptor. *Current topics in microbiology and immunology* **393**, 107-121, doi:10.1007/82_2015_480 (2016).

229 Inamine, A. *et al.* Two waves of memory B-cell generation in the primary immune response. *Int Immunol* **17**, 581-589, doi:10.1093/intimm/dxh241 (2005).
230 Toyama, H. *et al.* Memory B cells without somatic hypermutation are generated from Bcl6-deficient B cells. *Immunity* **17**, 329-339, doi:10.1016/s1074-7613(02)00387-4 (2002).
231 Palm, A.-K. E. & Henry, C. Remembrance of Things Past: Long-Term B Cell Memory After Infection and Vaccination. *Frontiers in Immunology* **10**, doi:10.3389/fimmu.2019.01787 (2019).
232 Obukhanych, T. V. & Nussenzweig, M. C. T-independent type II immune responses generate memory B cells. *The Journal of experimental medicine* **203**, 305-310, doi:10.1084/jem.20052036 (2006).
233 in *Immunology Guidebook* (eds Julius M. Cruse, Robert E. Lewis, & Huan Wang) 17-45 (Academic Press, 2004).
234 MacLennan, I. C. Germinal centers. *Annu Rev Immunol* **12**, 117-139, doi:10.1146/annurev.iy.12.040194.001001 (1994).
235 Bennett, K. M. *et al.* Hybrid flagellin as a T cell independent vaccine scaffold. *BMC Biotechnol* **15**, 71-71, doi:10.1186/s12896-015-0194-0 (2015).
236 Hirosue, S. & Dubrot, J. Modes of Antigen Presentation by Lymph Node Stromal Cells and Their Immunological Implications. *Frontiers in Immunology* **6**, doi:10.3389/fimmu.2015.00446 (2015).
237 Andrews, S. F. *et al.* Activation Dynamics and Immunoglobulin Evolution of Pre-existing and Newly Generated Human Memory B cell Responses to Influenza Hemagglutinin. *Immunity* **51**, 398-410.e395, doi:10.1016/j.immuni.2019.06.024 (2019).
238 Slifka, M. K., Antia, R., Whitmire, J. K. & Ahmed, R. Humoral immunity due to long-lived plasma cells. *Immunity* **8**, 363-372 (1998).
239 Slifka, M. K. & Amanna, I. J. Role of Multivalency and Antigenic Threshold in Generating Protective Antibody Responses. *Frontiers in Immunology* **10**, 956 (2019).
240 Lyski, Z. *et al.* Cellular and humoral Immune response to mRNA COVID-19 vaccination in subjects with chronic lymphocytic leukemia. *Blood Advances*, bloodadvances.2021006633, doi:10.1182/bloodadvances.2021006633 (2021).
241 Hammarlund, E. *et al.* Plasma cell survival in the absence of B cell memory. *Nat Commun* **8**, 1781, doi:10.1038/s41467-017-01901-w (2017).
242 Hammarlund, E. *et al.* Plasma cell survival in the absence of B cell memory. *Nature Communications* **8**, 1781, doi:10.1038/s41467-017-01901-w (2017).
243 White, H. N. B-Cell Memory Responses to Variant Viral Antigens. *Viruses* **13**, 565, doi:10.3390/v13040565 (2021).
244 Pape, K. A., Taylor, J. J., Maul, R. W., Gearhart, P. J. & Jenkins, M. K. Different B cell populations mediate early and late memory during an endogenous immune response. *Science (New York, N.Y.)* **331**, 1203-1207, doi:10.1126/science.1201730 (2011).
245 Burton, B. R. *et al.* Variant proteins stimulate more IgM+ GC B-cells revealing a mechanism of cross-reactive recognition by antibody memory. *eLife* **7**, e26832, doi:10.7554/eLife.26832 (2018).

246 Pape, K. A., Taylor, J. J., Maul, R. W., Gearhart, P. J. & Jenkins, M. K. Different B cell populations mediate early and late memory during an endogenous immune response. *Science (New York, N.Y.)* **331**, 1203-1207, doi:10.1126/science.1201730 (2011).
247 Viant, C. *et al.* Antibody Affinity Shapes the Choice between Memory and Germinal Center B Cell Fates. *Cell* **183**, 1298-1311.e1211, doi:10.1016/j.cell.2020.09.063 (2020).
248 Mankarious, S. *et al.* The half-lives of IgG subclasses and specific antibodies in patients with primary immunodeficiency who are receiving intravenously administered immunoglobulin. *J Lab Clin Med* **112**, 634-640 (1988).
249 Lu, L. L., Suscovich, T. J., Fortune, S. M. & Alter, G. Beyond binding: antibody effector functions in infectious diseases. *Nature Reviews Immunology* **18**, 46-61, doi:10.1038/nri.2017.106 (2018).
250 Bournazos, S., Gupta, A. & Ravetch, J. V. The role of IgG Fc receptors in antibody-dependent enhancement. *Nature Reviews Immunology* **20**, 633-643, doi:10.1038/s41577-020-00410-0 (2020).
251 Pyzik, M. *et al.* The Neonatal Fc Receptor (FcRn): A Misnomer? *Frontiers in Immunology* **10**, doi:10.3389/fimmu.2019.01540 (2019).
252 Irvine, E. B. & Alter, G. Understanding the role of antibody glycosylation through the lens of severe viral and bacterial diseases. *Glycobiology* **30**, 241-253, doi:10.1093/glycob/cwaa018 (2020).
253 Alter, G., Ottenhoff, T. H. M. & Joosten, S. A. Antibody glycosylation in inflammation, disease and vaccination. *Semin Immunol* **39**, 102-110, doi:10.1016/j.smim.2018.05.003 (2018).
254 Purtha, W. E., Tedder, T. F., Johnson, S., Bhattacharya, D. & Diamond, M. S. Memory B cells, but not long-lived plasma cells, possess antigen specificities for viral escape mutants. *The Journal of experimental medicine* **208**, 2599-2606, doi:10.1084/jem.20110740 (2011).
255 Lyski, Z. L. *et al.* SARS-CoV-2 specific memory B-cells from individuals with diverse disease severities recognize SARS-CoV-2 variants of concern. *J Infect Dis*, doi:10.1093/infdis/jiab585 (2021).
256 Goel, R. R. *et al.* Distinct antibody and memory B cell responses in SARS-CoV-2 naïve and recovered individuals following mRNA vaccination. *Science immunology* **6**, eabi6950, doi:10.1126/sciimmunol.abi6950 (2021).
257 Nivarthi, U. K. *et al.* Mapping the Human Memory B Cell and Serum Neutralizing Antibody Responses to Dengue Virus Serotype 4 Infection and Vaccination. *J Virol* **91**, doi:10.1128/jvi.02041-16 (2017).
258 Katzelnick, L. C., Coloma, J. & Harris, E. Dengue: knowledge gaps, unmet needs, and research priorities. *The Lancet. Infectious diseases* **17**, e88-e100, doi:10.1016/s1473-3099(16)30473-x (2017).
259 Lyski, Z. L. & Messer, W. B. Approaches to Interrogating the Human Memory B-Cell and Memory-Derived Antibody Repertoire Following Dengue Virus Infection. *Front Immunol* **10**, 1276, doi:10.3389/fimmu.2019.01276 (2019).
260 Dejnirattisai, W. *et al.* A new class of highly potent, broadly neutralizing antibodies isolated from viremic patients infected with dengue virus. *Nature immunology* **16**, 170-177, doi:10.1038/ni.3058 (2015).

261 Raut, R. *et al.* Dengue type 1 viruses circulating in humans are highly infectious and poorly neutralized by human antibodies. *Proc Natl Acad Sci U S A* **116**, 227-232, doi:10.1073/pnas.1812055115 (2019).
262 Nix, C. D. *et al.* Potency and breadth of human primary ZIKV immune sera shows that Zika viruses cluster antigenically as a single serotype. *PLoS neglected tropical diseases* **14**, e0008006-e0008006, doi:10.1371/journal.pntd.0008006 (2020).
263 Amanna, I. J. & Slifka, M. K. Quantitation of rare memory B cell populations by two independent and complementary approaches. *J Immunol Methods* **317**, 175-185, doi:10.1016/j.jim.2006.09.005 (2006).
264 Pinna, D., Corti, D., Jarrossay, D., Sallusto, F. & Lanzavecchia, A. Clonal dissection of the human memory B-cell repertoire following infection and vaccination. *European Journal of Immunology* **39**, 1260-1270, doi:10.1002/eji.200839129 (2009).
265 Amanna, I. J. & Slifka, M. K. Quantitation of rare memory B cell populations by two independent and complementary approaches. *Journal of immunological methods* **317**, 175-185, doi:10.1016/j.jim.2006.09.005 (2006).
266 Zhang, S., Tan, H. C. & Ooi, E. E. Visualizing dengue virus through Alexa Fluor labeling. *Journal of visualized experiments : JoVE*, e3168, doi:10.3791/3168 (2011).
267 Zhang, S. L., Tan, H. C., Hanson, B. J. & Ooi, E. E. A simple method for Alexa Fluor dye labelling of dengue virus. *Journal of virological methods* **167**, 172-177, doi:10.1016/j.jviromet.2010.04.001 (2010).
268 Woda, M. & Mathew, A. Fluorescently labeled dengue viruses as probes to identify antigen-specific memory B cells by multiparametric flow cytometry. *J Immunol Methods* **416**, 167-177, doi:10.1016/j.jim.2014.12.001 (2015).
269 Cox, K. S. *et al.* Rapid isolation of dengue-neutralizing antibodies from single cell-sorted human antigen-specific memory B-cell cultures. *mAbs* **8**, 129-140, doi:10.1080/19420862.2015.1109757 (2016).
270 Adam, A. *et al.* Multiplexed FluoroSpot for the Analysis of Dengue Virus- and Zika Virus-Specific and Cross-Reactive Memory B Cells. *Journal of immunology (Baltimore, Md. : 1950)* **201**, 3804-3814, doi:10.4049/jimmunol.1800892 (2018).
271 Andrade, P., Coloma, J. & Harris, E. ELISPOT-Based "Multi-Color FluoroSpot" to Study Type-Specific and Cross-Reactive Responses in Memory B Cells after Dengue and Zika Virus Infections. *Methods in molecular biology (Clifton, N.J.)* **1808**, 151-163, doi:10.1007/978-1-4939-8567-8_13 (2018).
272 Appanna, R. *et al.* Plasmablasts During Acute Dengue Infection Represent a Small Subset of a Broader Virus-specific Memory B Cell Pool. *EBioMedicine* **12**, 178-188, doi:10.1016/j.ebiom.2016.09.003 (2016).
273 Kwakkenbos, M. J. *et al.* Generation of stable monoclonal antibody–producing B cell receptor–positive human memory B cells by genetic programming. *Nature medicine* **16**, 123-128, doi:10.1038/nm.2071 (2010).
274 Smith, S. A. & Crowe, J. E., Jr. Use of Human Hybridoma Technology To Isolate Human Monoclonal Antibodies. *Microbiology spectrum* **3**, Aid-0027-2014, doi:10.1128/microbiolspec.AID-0027-2014 (2015).

275 Yu, X., McGraw, P. A., House, F. S. & Crowe, J. E., Jr. An optimized electrofusion-based protocol for generating virus-specific human monoclonal antibodies. *J Immunol Methods* **336**, 142-151, doi:10.1016/j.jim.2008.04.008 (2008).
276 Chen, R. *et al.* ICTV Virus Taxonomy Profile: Togaviridae. *Journal of General Virology* **99**, 761-762, doi:10.1099/jgv.0.001072 (2018).
277 La Linn, M. *et al.* Arbovirus of Marine Mammals: a New Alphavirus Isolated from the Elephant Seal Louse, Lepidophthirus macrorhini. *Journal of Virology* **75**, 4103-4109, doi:10.1128/jvi.75.9.4103-4109.2001 (2001).
278 Weston, J. *et al.* Comparison of Two Aquatic Alphaviruses, Salmon Pancreas Disease Virus and Sleeping Disease Virus, by Using Genome Sequence Analysis, Monoclonal Reactivity, and Cross-Infection. *Journal of virology* **76**, 6155-6163, doi:10.1128/jvi.76.12.6155-6163.2002 (2002).
279 Fields, B. N., Knipe, D. M. & Howley, P. M. Fields virology. (2013).
280 Baxter, V. K. & Heise, M. T. in *Advances in Virus Research* Vol. 107 (eds John P. Carr & Marilyn J. Roossinck) 315-382 (Academic Press, 2020).
281 Freitas, A. R. R., Donalisio, M. R. & Alarcón-Elbal, P. M. Excess Mortality and Causes Associated with Chikungunya, Puerto Rico, 2014-2015. *Emerg Infect Dis* **24**, 2352-2355, doi:10.3201/eid2412.170639 (2018).
282 Rezza, G. in *Emerging Infectious Diseases* (eds Önder Ergönül, Füsun Can, Lawrence Madoff, & Murat Akova) 163-174 (Academic Press, 2014).
283 Weaver, S. C. & Lecuit, M. Chikungunya virus and the global spread of a mosquito-borne disease. *The New England journal of medicine* **372**, 1231-1239, doi:10.1056/NEJMra1406035 (2015).
284 Caspar, D. L. & Klug, A. Physical principles in the construction of regular viruses. *Cold Spring Harb Symp Quant Biol* **27**, 1-24, doi:10.1101/sqb.1962.027.001.005 (1962).
285 Jose, J., Snyder, J. E. & Kuhn, R. J. A structural and functional perspective of alphavirus replication and assembly. *Future Microbiol* **4**, 837-856, doi:10.2217/fmb.09.59 (2009).
286 Zheng, Y. & Kielian, M. Imaging of the alphavirus capsid protein during virus replication. *Journal of virology* **87**, 9579-9589, doi:10.1128/JVI.01299-13 (2013).
287 Leung, J. Y.-S., Ng, M. M.-L. & Chu, J. J. H. Replication of Alphaviruses: A Review on the Entry Process of Alphaviruses into Cells. *Advances in Virology* **2011**, 1-9, doi:10.1155/2011/249640 (2011).
288 Kim, D. Y. *et al.* New World and Old World Alphaviruses Have Evolved to Exploit Different Components of Stress Granules, FXR and G3BP Proteins, for Assembly of Viral Replication Complexes. *PLoS pathogens* **12**, e1005810, doi:10.1371/journal.ppat.1005810 (2016).
289 Haese, N., Powers, J. & Streblow, D. N. Small Molecule Inhibitors Targeting Chikungunya Virus. *Curr Top Microbiol Immunol*, doi:10.1007/82_2020_195 (2020).
290 Kam, Y. W. *et al.* Longitudinal analysis of the human antibody response to Chikungunya virus infection: implications for serodiagnosis and vaccine development. *Journal of virology* **86**, 13005-13015, doi:10.1128/jvi.01780-12 (2012).
291 Smith, S. A. *et al.* Isolation and Characterization of Broad and Ultrapotent Human Monoclonal Antibodies with Therapeutic Activity against Chikungunya Virus. *Cell Host Microbe* **18**, 86-95, doi:10.1016/j.chom.2015.06.009 (2015).

292 Weber, C., Büchner, S. M. & Schnierle, B. S. A small antigenic determinant of the Chikungunya virus E2 protein is sufficient to induce neutralizing antibodies which are partially protective in mice. *PLoS Negl Trop Dis* **9**, e0003684, doi:10.1371/journal.pntd.0003684 (2015).
293 Weger-Lucarelli, J., Aliota, M. T., Kamlangdee, A. & Osorio, J. E. Identifying the Role of E2 Domains on Alphavirus Neutralization and Protective Immune Responses. *PLoS Negl Trop Dis* **9**, e0004163, doi:10.1371/journal.pntd.0004163 (2015).
294 Powell, L. A. *et al.* Human mAbs Broadly Protect against Arthritogenic Alphaviruses by Recognizing Conserved Elements of the Mxra8 Receptor-Binding Site. *Cell Host Microbe* **28**, 699-711.e697, doi:10.1016/j.chom.2020.07.008 (2020).
295 Quiroz, J. A. *et al.* Human monoclonal antibodies against chikungunya virus target multiple distinct epitopes in the E1 and E2 glycoproteins. *PLoS pathogens* **15**, e1008061, doi:10.1371/journal.ppat.1008061 (2019).
296 Slifka, M. K., Antia, R., Whitmire, J. K. & Ahmed, R. Humoral Immunity Due to Long-Lived Plasma Cells. *Immunity* **8**, 363-372, doi:10.1016/s1074-7613(00)80541-5 (1998).
297 Purtha, W. E., Tedder, T. F., Johnson, S., Bhattacharya, D. & Diamond, M. S. Memory B cells, but not long-lived plasma cells, possess antigen specificities for viral escape mutants. *Journal of Experimental Medicine* **208**, 2599-2606, doi:10.1084/jem.20110740 (2011).
298 Wong, R. *et al.* Affinity-Restricted Memory B Cells Dominate Recall Responses to Heterologous Flaviviruses. *Immunity* **53**, 1078-1094.e1077, doi:10.1016/j.immuni.2020.09.001 (2020).
299 Katzelnick, L. C. *et al.* Dengue viruses cluster antigenically but not as discrete serotypes. *Science* **349**, 1338-1343, doi:10.1126/science.aac5017 (2015).
300 Smith, D. J. *et al.* Mapping the Antigenic and Genetic Evolution of Influenza Virus. *Science* **305**, 371-376, doi:10.1126/science.1097211 (2004).
301 Henss, L. *et al.* Analysis of Humoral Immune Responses in Chikungunya Virus (CHIKV)-Infected Patients and Individuals Vaccinated With a Candidate CHIKV Vaccine. *The Journal of infectious diseases* **221**, 1713-1723, doi:10.1093/infdis/jiz658 (2019).
302 Earnest, J. T. *et al.* Neutralizing antibodies against Mayaro virus require Fc effector functions for protective activity. *J Exp Med* **216**, 2282-2301, doi:10.1084/jem.20190736 (2019).
303 Lyski, Z. L. *et al.* SARS-CoV-2 specific memory B-cells from individuals with diverse disease severities recognize SARS-CoV-2 variants of concern. *medRxiv*, 2021.2005.2028.21258025, doi:10.1101/2021.05.28.21258025 (2021).
304 Zhang, R. *et al.* Mxra8 is a receptor for multiple arthritogenic alphaviruses. *Nature* **557**, 570-574, doi:10.1038/s41586-018-0121-3 (2018).
305 Powell, L. A. *et al.* Human mAbs Broadly Protect against Arthritogenic Alphaviruses by Recognizing Conserved Elements of the Mxra8 Receptor-Binding Site. *Cell Host Microbe* **28**, 699-711 e697, doi:10.1016/j.chom.2020.07.008 (2020).
306 Henss, L. *et al.* Analysis of Humoral Immune Responses in Chikungunya Virus (CHIKV)-Infected Patients and Individuals Vaccinated With a Candidate CHIKV Vaccine. *J Infect Dis* **221**, 1713-1723, doi:10.1093/infdis/jiz658 (2020).

307 Broeckel, R. M. *et al.* Vaccine-Induced Skewing of T Cell Responses Protects Against Chikungunya Virus Disease. *Front Immunol* **10**, 2563, doi:10.3389/fimmu.2019.02563 (2019).
308 Powers, J. M. *et al.* Non-replicating adenovirus based Mayaro virus vaccine elicits protective immune responses and cross protects against other alphaviruses. *PLoS Negl Trop Dis* **15**, e0009308, doi:10.1371/journal.pntd.0009308 (2021).
309 Berman, H. M. *et al.* The Protein Data Bank. *Nucleic acids research* **28**, 235-242, doi:10.1093/nar/28.1.235 (2000).
310 Rydyznski Moderbacher, C. *et al.* Antigen-Specific Adaptive Immunity to SARS-CoV-2 in Acute COVID-19 and Associations with Age and Disease Severity. *Cell* **183**, 996-1012.e1019, doi:10.1016/j.cell.2020.09.038 (2020).
311 Bates, T. A. *et al. Neutralization of SARS-CoV-2 variants by convalescent and vaccinated serum* (Cold Spring Harbor Laboratory, 2021).
312 Zost, S. J. *et al.* Rapid isolation and profiling of a diverse panel of human monoclonal antibodies targeting the SARS-CoV-2 spike protein. *Nature medicine* **26**, 1422-1427, doi:10.1038/s41591-020-0998-x (2020).
313 Gaebler, C. *et al.* Evolution of antibody immunity to SARS-CoV-2. *Nature* **591**, 639-644, doi:10.1038/s41586-021-03207-w (2021).
314 Rudberg, A.-S. *et al.* SARS-CoV-2 exposure, symptoms and seroprevalence in healthcare workers in Sweden. *Nature Communications* **11**, 5064, doi:10.1038/s41467-020-18848-0 (2020).
315 Madariaga, M. L. L. *et al.* Clinical predictors of donor antibody titre and correlation with recipient antibody response in a COVID-19 convalescent plasma clinical trial. *J Intern Med* **289**, 559-573, doi:10.1111/joim.13185 (2021).
316 Dan, J. M. *et al.* Immunological memory to SARS-CoV-2 assessed for up to 8 months after infection. *Science (New York, N.Y.)* **371**, doi:10.1126/science.abf4063 (2021).
317 Stamatatos, L. *et al.* mRNA vaccination boosts cross-variant neutralizing antibodies elicited by SARS-CoV-2 infection. *Science (New York, N.Y.)*, doi:10.1126/science.abg9175 (2021).
318 Tegally, H. *et al.* Detection of a SARS-CoV-2 variant of concern in South Africa. *Nature* **592**, 438-443, doi:10.1038/s41586-021-03402-9 (2021).
319 Bates, T. A. *et al.* Neutralization of SARS-CoV-2 variants by convalescent and BNT162b2 vaccinated serum. *Nature Communications* **12**, 5135, doi:10.1038/s41467-021-25479-6 (2021).
320 Cele, S. *et al.* Escape of SARS-CoV-2 501Y.V2 from neutralization by convalescent plasma. *Nature* **593**, 142-146, doi:10.1038/s41586-021-03471-w (2021).
321 Hajjo, R., Sabbah, D. A. & Bardaweel, S. K. Emerging SARS-CoV-2 Lineages in Middle Eastern Jordan with Increasing Mutations Near Antibody Recognition Sites. *medRxiv*, 2021.2002.2009.21251052, doi:10.1101/2021.02.09.21251052 (2021).
322 Stadlbauer, D. *et al.* SARS-CoV-2 Seroconversion in Humans: A Detailed Protocol for a Serological Assay, Antigen Production, and Test Setup. *Curr Protoc Microbiol* **57**, e100, doi:10.1002/cpmc.100 (2020).

323 Chen, R. E. *et al.* Resistance of SARS-CoV-2 variants to neutralization by monoclonal and serum-derived polyclonal antibodies. *Nature medicine* **27**, 717-726, doi:10.1038/s41591-021-01294-w (2021).
324 Hartley Gemma, E. *et al.* Rapid generation of durable B cell memory to SARS-CoV-2 spike and nucleocapsid proteins in COVID-19 and convalescence. *Science Immunology* **5**, eabf8891, doi:10.1126/sciimmunol.abf8891 (2020).
325 Sokal, A. *et al.* Maturation and persistence of the anti-SARS-CoV-2 memory B cell response. *Cell* **184**, 1201-1213.e1214, doi:10.1016/j.cell.2021.01.050 (2021).
326 Jangra, S. *et al.* SARS-CoV-2 spike E484K mutation reduces antibody neutralisation. *Lancet Microbe* **2**, e283-e284, doi:10.1016/s2666-5247(21)00068-9 (2021).
327 Amanna, I. J. & Slifka, M. K. Quantitation of rare memory B cell populations by two independent and complementary approaches. *Journal of Immunological Methods* **317**, 175-185, doi:https://doi.org/10.1016/j.jim.2006.09.005 (2006).
328 Bates, T. A. *et al.* Cross-reactivity of SARS-CoV structural protein antibodies against SARS-CoV-2. *Cell Reports* **34**, 108737, doi:https://doi.org/10.1016/j.celrep.2021.108737 (2021).
329 Organization, W. H. *Novel coronavirus COVID-19 therapeutic trial synopsis*, <https://www.who.int/publications/i/item/covid-19-therapeutic-trial-synopsis> (2020).
330 Rodda, L. B. *et al.* Functional SARS-CoV-2-Specific Immune Memory Persists after Mild COVID-19. *Cell* **184**, 169-183.e117, doi:10.1016/j.cell.2020.11.029 (2021).
331 Leier, H. C. *et al.* Previously infected vaccinees broadly neutralize SARS-CoV-2 variants. *medRxiv*, 2021.2004.2025.21256049, doi:10.1101/2021.04.25.21256049 (2021).
332 Winklmeier, S. *et al. Persistence of functional memory B cells recognizing SARS-CoV-2 variants despite loss of specific IgG* (Cold Spring Harbor Laboratory, 2021).
333 Robbiani, D. F. *et al.* Convergent antibody responses to SARS-CoV-2 in convalescent individuals. *Nature* **584**, 437-442, doi:10.1038/s41586-020-2456-9 (2020).
334 Bosch, F. & Dalla-Favera, R. Chronic lymphocytic leukaemia: from genetics to treatment. *Nature Reviews Clinical Oncology* **16**, 684-701, doi:10.1038/s41571-019-0239-8 (2019).
335 de Weerdt, I. *et al.* Distinct immune composition in lymph node and peripheral blood of CLL patients is reshaped during venetoclax treatment. *Blood advances* **3**, 2642-2652, doi:10.1182/bloodadvances.2019000360 (2019).
336 Benjamini, O. *et al.* Safety and efficacy of BNT162b mRNA Covid19 Vaccine in patients with chronic lymphocytic leukemia. *Haematologica*, doi:10.3324/haematol.2021.279196 (2021).
337 Forconi, F. & Moss, P. Perturbation of the normal immune system in patients with CLL. *Blood* **126**, 573-581, doi:10.1182/blood-2015-03-567388 (2015).
338 Institute., N. C. *Cancer stat facts: leukemia — chronic lymphocytic leukemia (CLL).* , <https://seer.cancer.gov/statfacts/html/clyl.html> (2021).
339 Siegel, R. L., Miller, K. D., Fuchs, H. E. & Jemal, A. Cancer Statistics, 2021. *CA: A Cancer Journal for Clinicians* **71**, 7-33, doi:https://doi.org/10.3322/caac.21654 (2021).
340 Yao, Y., Lin, X., Li, F., Jin, J. & Wang, H. The global burden and attributable risk factors of chronic lymphocytic leukemia in 204 countries and territories from 1990 to 2019: analysis based on the global burden of disease study 2019. *BioMedical Engineering OnLine* **21**, 4, doi:10.1186/s12938-021-00973-6 (2022).
240

341 Beusterien, K. M. *et al.* Population preference values for treatment outcomes in chronic lymphocytic leukaemia: a cross-sectional utility study. *Health Qual Life Outcomes* **8**, 50-50, doi:10.1186/1477-7525-8-50 (2010).
342 Wang, Y. *et al.* Cause of death in patients with newly diagnosed chronic lymphocytic leukemia (CLL) stratified by the CLL-International Prognostic Index. *Blood Cancer Journal* **11**, 140, doi:10.1038/s41408-021-00532-1 (2021).
343 Yun, X., Zhang, Y. & Wang, X. Recent progress of prognostic biomarkers and risk scoring systems in chronic lymphocytic leukemia. *Biomarker Research* **8**, 40, doi:10.1186/s40364-020-00222-3 (2020).
344 Bell, R. Developing a Clinical Program Based on the Needs of Patients With Chronic Lymphocytic Leukemia: Preparing for Illness Episodes. *J Adv Pract Oncol* **8**, 462-473 (2017).
345 Marti, G. E. *et al.* Diagnostic criteria for monoclonal B-cell lymphocytosis. *Br J Haematol* **130**, 325-332, doi:10.1111/j.1365-2141.2005.05550.x (2005).
346 Rai, K. R. *et al.* Clinical staging of chronic lymphocytic leukemia. *Blood* **46**, 219-234 (1975).
347 Rai KR, K. M. in *Holland-Frei Cancer Medicine* (ed Pollock RE Kufe DW, Weichselbaum RR, et al.,) (Holland-Frei Cancer Medicine., 2003).
348 Pflug, N. *et al.* Development of a comprehensive prognostic index for patients with chronic lymphocytic leukemia. *Blood* **124**, 49-62, doi:10.1182/blood-2014-02-556399 (2014).
349 Moreno, C. *et al.* Beta-2 Microglobulin Is a Strong Prognostic Marker in Patients with Chronic Lymphocytic Leukemia Submitted to Allogeneic Stem Cell Transplantation. *Blood* **114**, 1244-1244, doi:10.1182/blood.V114.22.1244.1244 (2009).
350 Hallek, M. *et al.* Serum beta(2)-microglobulin and serum thymidine kinase are independent predictors of progression-free survival in chronic lymphocytic leukemia and immunocytoma. *Leuk Lymphoma* **22**, 439-447, doi:10.3109/10428199609054782 (1996).
351 Magnac, C. *et al.* Predictive value of serum thymidine kinase level for Ig-V mutational status in B-CLL. *Leukemia* **17**, 133-137, doi:10.1038/sj.leu.2402780 (2003).
352 Oken, M. M. *et al.* Toxicity and response criteria of the Eastern Cooperative Oncology Group. *Am J Clin Oncol* **5**, 649-655 (1982).
353 Döhner, H. *et al.* Genomic Aberrations and Survival in Chronic Lymphocytic Leukemia. *New England Journal of Medicine* **343**, 1910-1916, doi:10.1056/NEJM200012283432602 (2000).
354 Rosati, E. *et al.* NOTCH1 Aberrations in Chronic Lymphocytic Leukemia. *Frontiers in oncology* **8**, 229-229, doi:10.3389/fonc.2018.00229 (2018).
355 Rosati, E. *et al.* Constitutively activated Notch signaling is involved in survival and apoptosis resistance of B-CLL cells. *Blood* **113**, 856-865, doi:10.1182/blood-2008-02-139725 (2009).
356 Burger, J. A. Treatment of Chronic Lymphocytic Leukemia. *New England Journal of Medicine* **383**, 460-473, doi:10.1056/NEJMra1908213 (2020).
357 Giudice, I. D. & Foà, R. Another step forward in the 20-year history of IGHV mutations in chronic lymphocytic leukemia. *Haematologica* **104**, 219-221, doi:10.3324/haematol.2018.207399 (2019).

358 Klein, U. *et al.* Gene expression profiling of B cell chronic lymphocytic leukemia reveals a homogeneous phenotype related to memory B cells. *The Journal of experimental medicine* **194**, 1625-1638, doi:10.1084/jem.194.11.1625 (2001).
359 Gribben, J. G. How and when I do allogeneic transplant in CLL. *Blood* **132**, 31-39, doi:10.1182/blood-2018-01-785998 (2018).
360 Herling, C. D. *et al.* Early treatment with FCR versus watch and wait in patients with stage Binet A high-risk chronic lymphocytic leukemia (CLL): a randomized phase 3 trial. *Leukemia* **34**, 2038-2050, doi:10.1038/s41375-020-0747-7 (2020).
361 Hoechstetter, M. A. *et al.* Early, risk-adapted treatment with fludarabine in Binet stage A chronic lymphocytic leukemia patients: results of the CLL1 trial of the German CLL study group. *Leukemia* **31**, 2833-2837, doi:10.1038/leu.2017.246 (2017).
362 Alrawashdh, N. *et al.* Survival trends in chronic lymphocytic leukemia in the era of oral targeted therapies in the United States: SEER database analyses (1985 to 2017). *Journal of Clinical Oncology* **39**, 7524-7524, doi:10.1200/JCO.2021.39.15_suppl.7524 (2021).
363 Shah, H. R. & Stephens, D. M. Is there a role for anti-CD20 antibodies in CLL? *Hematology* **2021**, 68-75, doi:10.1182/hematology.2021000234 (2021).
364 Hendriks, R. W., Yuvaraj, S. & Kil, L. P. Targeting Bruton's tyrosine kinase in B cell malignancies. *Nature Reviews Cancer* **14**, 219-232, doi:10.1038/nrc3702 (2014).
365 Kipps, T. J. & Choi, M. Y. Targeted Therapy in Chronic Lymphocytic Leukemia. *Cancer J* **25**, 378-385, doi:10.1097/PPO.0000000000000416 (2019).
366 Mattsson, P. T., Vihinen, M. & Smith, C. I. X-linked agammaglobulinemia (XLA): a genetic tyrosine kinase (Btk) disease. *Bioessays* **18**, 825-834, doi:10.1002/bies.950181009 (1996).
367 Weber, A. N. R. *et al.* Bruton's Tyrosine Kinase: An Emerging Key Player in Innate Immunity. *Frontiers in Immunology* **8**, doi:10.3389/fimmu.2017.01454 (2017).
368 Lyski, Z. L. *et al.* Immunogenicity of Pfizer mRNA COVID-19 vaccination followed by J&J adenovirus COVID-19 vaccination in two CLL patients. *medRxiv*, doi:10.1101/2021.09.02.21262146 (2021).
369 Pleyer, C. *et al.* Effect of Bruton tyrosine kinase inhibitor on efficacy of adjuvanted recombinant hepatitis B and zoster vaccines. *Blood* **137**, 185-189, doi:10.1182/blood.2020008758 (2021).
370 Pleyer, C. *et al.* Reconstitution of humoral immunity and decreased risk of infections in patients with chronic lymphocytic leukemia treated with Bruton tyrosine kinase inhibitors. *Leuk Lymphoma* **61**, 2375-2382, doi:10.1080/10428194.2020.1772477 (2020).
371 Barrientos, J. C. *et al.* Improvement in Parameters of Hematologic and Immunologic Function and Patient Well-being in the Phase III RESONATE Study of Ibrutinib Versus Ofatumumab in Patients With Previously Treated Chronic Lymphocytic Leukemia/Small Lymphocytic Lymphoma. *Clin Lymphoma Myeloma Leuk* **18**, 803-813.e807, doi:10.1016/j.clml.2018.08.007 (2018).
372 Kapoor, I., Bodo, J., Hill, B. T., Hsi, E. D. & Almasan, A. Targeting BCL-2 in B-cell malignancies and overcoming therapeutic resistance. *Cell Death & Disease* **11**, 941, doi:10.1038/s41419-020-03144-y (2020).

373 Stilgenbauer, S. *et al.* Venetoclax in relapsed or refractory chronic lymphocytic leukaemia with 17p deletion: a multicentre, open-label, phase 2 study. *Lancet Oncol* **17**, 768-778, doi:10.1016/s1470-2045(16)30019-5 (2016).
374 Maloney, D. G. Mechanism of action of rituximab. *Anticancer Drugs* **12 Suppl 2**, S1-4 (2001).
375 Morrison, V. A. Infectious complications of chronic lymphocytic leukaemia: pathogenesis, spectrum of infection, preventive approaches. *Best Pract Res Clin Haematol* **23**, 145-153, doi:10.1016/j.beha.2009.12.004 (2010).
376 Williams, A. M. *et al.* Analysis of the risk of infection in patients with chronic lymphocytic leukemia in the era of novel therapies. *Leukemia & Lymphoma* **59**, 625-632, doi:10.1080/10428194.2017.1347931 (2018).
377 Steingrímsson, V. *et al.* A nationwide study on inpatient opportunistic infections in patients with chronic lymphocytic leukemia in the pre-ibrutinib era. *Eur J Haematol* **106**, 346-353, doi:10.1111/ejh.13553 (2021).
378 Nosari, A. Infectious complications in chronic lymphocytic leukemia. *Mediterr J Hematol Infect Dis* **4**, e2012070-e2012070, doi:10.4084/MJHID.2012.070 (2012).
379 Teh, B. W., Tam, C. S., Handunnetti, S., Worth, L. J. & Slavin, M. A. Infections in patients with chronic lymphocytic leukaemia: Mitigating risk in the era of targeted therapies. *Blood Rev* **32**, 499-507, doi:10.1016/j.blre.2018.04.007 (2018).
380 Sun, C. *et al.* Partial reconstitution of humoral immunity and fewer infections in patients with chronic lymphocytic leukemia treated with ibrutinib. *Blood* **126**, 2213-2219, doi:10.1182/blood-2015-04-639203 (2015).
381 Perez, E. E. *et al.* Update on the use of immunoglobulin in human disease: A review of evidence. *Journal of Allergy and Clinical Immunology* **139**, S1-S46, doi:https://doi.org/10.1016/j.jaci.2016.09.023 (2017).
382 Gamm, H. *et al.* Intravenous immune globulin in chronic lymphocytic leukaemia. *Clin Exp Immunol* **97 Suppl 1**, 17-20 (1994).
383 Kuderer, N. M. *et al.* Clinical impact of COVID-19 on patients with cancer (CCC19): a cohort study. *Lancet* **395**, 1907-1918, doi:10.1016/s0140-6736(20)31187-9 (2020).
384 Vijenthira, A. *et al.* Outcomes of patients with hematologic malignancies and COVID-19: a systematic review and meta-analysis of 3377 patients. *Blood* **136**, 2881-2892, doi:10.1182/blood.2020008824 (2020).
385 Mato, A. R. *et al.* Outcomes of COVID-19 in patients with CLL: a multicenter international experience. *Blood* **136**, 1134-1143, doi:10.1182/blood.2020006965 (2020).
386 Zent, C. S. *et al.* Short term results of vaccination with adjuvanted recombinant varicella zoster glycoprotein E during initial BTK inhibitor therapy for CLL or lymphoplasmacytic lymphoma. *Leukemia* **35**, 1788-1791, doi:10.1038/s41375-020-01074-4 (2021).
387 Whitaker, J. A. *et al.* The humoral immune response to high-dose influenza vaccine in persons with monoclonal B-cell lymphocytosis (MBL) and chronic lymphocytic leukemia (CLL). *Vaccine* **39**, 1122-1130, doi:10.1016/j.vaccine.2021.01.001 (2021).
388 Molica, S. *et al.* A Clue to Better Select Chronic Lymphocytic Leukemia Patients with Optimal Response to BNT162b2 mRNA COVID-19 Vaccine. *Blood* **138**, 3740-3740, doi:10.1182/blood-2021-149104 (2021).

389 Muchtar, E. *et al.* Humoral and cellular immune responses to recombinant herpes zoster vaccine in patients with chronic lymphocytic leukemia and monoclonal B cell lymphocytosis. *Am J Hematol* **97**, 90-98, doi:10.1002/ajh.26388 (2022).
390 Sinisalo, M. *et al.* Response to vaccination against different types of antigens in patients with chronic lymphocytic leukaemia. *Br J Haematol* **114**, 107-110, doi:10.1046/j.1365-2141.2001.02882.x (2001).
391 Sinisalo, M., Aittoniemi, J., Käyhty, H. & Vilpo, J. Vaccination against infections in chronic lymphocytic leukemia. *Leuk Lymphoma* **44**, 649-652, doi:10.1080/1042819031000063408 (2003).
392 Svensson, T. *et al.* Pneumococcal conjugate vaccine triggers a better immune response than pneumococcal polysaccharide vaccine in patients with chronic lymphocytic leukemia A randomized study by the Swedish CLL group. *Vaccine* **36**, 3701-3707, doi:10.1016/j.vaccine.2018.05.012 (2018).
393 Douglas, A. P. *et al.* Ibrutinib may impair serological responses to influenza vaccination. *Haematologica* **102**, e397-e399, doi:10.3324/haematol.2017.164285 (2017).
394 Sun, C. *et al.* Seasonal Influenza Vaccination in Patients With Chronic Lymphocytic Leukemia Treated With Ibrutinib. *JAMA Oncology* **2**, 1656-1657, doi:10.1001/jamaoncol.2016.2437 (2016).
395 Haydu, J. E. *et al.* Humoral and cellular immunogenicity of SARS-CoV-2 vaccines in chronic lymphocytic leukemia: a prospective cohort study. *Blood Advances*, bloodadvances.2021006627, doi:10.1182/bloodadvances.2021006627 (2022).
396 Roeker, L. E. *et al.* COVID-19 vaccine efficacy in patients with chronic lymphocytic leukemia. *Leukemia* **35**, 2703-2705, doi:10.1038/s41375-021-01270-w (2021).
397 Agha, M., Blake, M., Chilleo, C., Wells, A. & Haidar, G. Suboptimal response to COVID-19 mRNA vaccines in hematologic malignancies patients. *medRxiv*, 2021.2004.2006.21254949, doi:10.1101/2021.04.06.21254949 (2021).
398 Herishanu, Y. *et al.* Efficacy of the BNT162b2 mRNA COVID-19 vaccine in patients with chronic lymphocytic leukemia. *Blood* **137**, 3165-3173, doi:10.1182/blood.2021011568 (2021).
399 Greenberger, L. M. *et al.* Antibody response to SARS-CoV-2 vaccines in patients with hematologic malignancies. *Cancer Cell* **39**, 1031-1033, doi:10.1016/j.ccell.2021.07.012 (2021).
400 Malard, F. *et al.* Weak immunogenicity of SARS-CoV-2 vaccine in patients with hematologic malignancies. *Blood Cancer Journal* **11**, 142, doi:10.1038/s41408-021-00534-z (2021).
401 Mellinghoff, S. C. *et al.* SARS-CoV-2 specific cellular response following COVID-19 vaccination in patients with chronic lymphocytic leukemia. *Leukemia* **36**, 562-565, doi:10.1038/s41375-021-01500-1 (2022).
402 Blixt, L. *et al.* Covid-19 in patients with chronic lymphocytic leukemia: clinical outcome and B- and T-cell immunity during 13 months in consecutive patients. *Leukemia*, doi:10.1038/s41375-021-01424-w (2021).
403 Marquis, S. R. *et al.* Seroprevalence of Measles and Mumps Antibodies Among Individuals With Cancer. *JAMA Network Open* **4**, e2118508-e2118508, doi:10.1001/jamanetworkopen.2021.18508 (2021).

404 Roeker, L. E. *et al.* COVID-19 in patients with CLL: improved survival outcomes and update on management strategies. *Blood* **138**, 1768-1773, doi:10.1182/blood.2021011841 (2021).
405 Different COVID-19 Vaccines. Center for Disease Control and Prevention. Updated August 19, 2021. Accessed August 30, 2021. https://www.cdc.gov/coronavirus/2019-ncov/vaccines/different-vaccines.html
406 Baden, L. R. *et al.* Efficacy and Safety of the mRNA-1273 SARS-CoV-2 Vaccine. *New England Journal of Medicine* **384**, 403-416, doi:10.1056/NEJMoa2035389 (2020).
407 Sadoff, J. *et al.* Safety and Efficacy of Single-Dose Ad26.COV2.S Vaccine against Covid-19. *New England Journal of Medicine* **384**, 2187-2201, doi:10.1056/NEJMoa2101544 (2021).
408 Mauro, F. R. *et al.* Response to the conjugate pneumococcal vaccine (PCV13) in patients with chronic lymphocytic leukemia (CLL). *Leukemia* **35**, 737-746, doi:10.1038/s41375-020-0884-z (2021).
409 Hartkamp, A., Mulder, A. H., Rijkers, G. T., van Velzen-Blad, H. & Biesma, D. H. Antibody responses to pneumococcal and haemophilus vaccinations in patients with B-cell chronic lymphocytic leukaemia. *Vaccine* **19**, 1671-1677, doi:10.1016/s0264-410x(00)00409-6 (2001).
410 van der Velden, A. M. *et al.* Influenza virus vaccination and booster in B-cell chronic lymphocytic leukaemia patients. *Eur J Intern Med* **12**, 420-424, doi:10.1016/s0953-6205(01)00149-2 (2001).
411 Parry, H. *et al.* Antibody responses after first and second Covid-19 vaccination in patients with chronic lymphocytic leukaemia. *Blood Cancer Journal* **11**, 136, doi:10.1038/s41408-021-00528-x (2021).
412 Marchesi, F. *et al.* Impact of anti-CD20 monoclonal antibodies on serologic response to BNT162b2 vaccine in B-cell Non-Hodgkin's lymphomas. *Leukemia*, doi:10.1038/s41375-021-01418-8 (2021).
413 Mateus, J. *et al.* Selective and cross-reactive SARS-CoV-2 T cell epitopes in unexposed humans. *Science* **370**, 89-94, doi:doi:10.1126/science.abd3871 (2020).
414 Bilich, T. *et al.* T cell and antibody kinetics delineate SARS-CoV-2 peptides mediating long-term immune responses in COVID-19 convalescent individuals. *Science Translational Medicine* **13**, eabf7517, doi:10.1126/scitranslmed.abf7517 (2021).
415 Park, J. K. *et al.* Effect of methotrexate discontinuation on efficacy of seasonal influenza vaccination in patients with rheumatoid arthritis: a randomised clinical trial. *Ann Rheum Dis* **76**, 1559-1565, doi:10.1136/annrheumdis-2017-211128 (2017).
416 Farsaci, B. *et al.* Effect of a small molecule BCL-2 inhibitor on immune function and use with a recombinant vaccine. *International Journal of Cancer* **127**, 1603-1613, doi:https://doi.org/10.1002/ijc.25177 (2010).
417 Thomas, A. *et al.* Establishment of Monoclonal Antibody Standards for Quantitative Serological Diagnosis of SARS-CoV-2 in Low-Incidence Settings. *Open Forum Infectious Diseases* **8**, doi:10.1093/ofid/ofab061 (2021).
418 Raué, H. P. & Slifka, M. K. Pivotal advance: CTLA-4+ T cells exhibit normal antiviral functions during acute viral infection. *J Leukoc Biol* **81**, 1165-1175, doi:10.1189/jlb.0806535 (2007).

419 Raué, H. P. & Slifka, M. K. CD8+ T cell immunodominance shifts during the early stages of acute LCMV infection independently from functional avidity maturation. *Virology* **390**, 197-204, doi:10.1016/j.virol.2009.05.021 (2009).
420 Bernasconi, N. L., Traggiai, E. & Lanzavecchia, A. Maintenance of serological memory by polyclonal activation of human memory B cells. *Science (New York, N.Y.)* **298**, 2199-2202, doi:10.1126/science.1076071 (2002).
421 Inoue, T., Moran, I., Shinnakasu, R., Phan, T. G. & Kurosaki, T. Generation of memory B cells and their reactivation. *Immunol Rev* **283**, 138-149, doi:10.1111/imr.12640 (2018).
422 Yoshida, T. *et al.* Memory B and memory plasma cells. *Immunol Rev* **237**, 117-139, doi:10.1111/j.1600-065X.2010.00938.x (2010).
423 Seifert, M. *et al.* Functional capacities of human IgM memory B cells in early inflammatory responses and secondary germinal center reactions. *Proc Natl Acad Sci U S A* **112**, E546-555, doi:10.1073/pnas.1416276112 (2015).
424 Shinnakasu, R. & Kurosaki, T. Regulation of memory B and plasma cell differentiation. *Curr Opin Immunol* **45**, 126-131, doi:10.1016/j.coi.2017.03.003 (2017).
425 Moir, S. & Fauci, A. S. B-cell responses to HIV infection. *Immunol Rev* **275**, 33-48, doi:10.1111/imr.12502 (2017).
426 Cortjens, B. *et al.* Broadly Reactive Anti-Respiratory Syncytial Virus G Antibodies from Exposed Individuals Effectively Inhibit Infection of Primary Airway Epithelial Cells. *J Virol* **91**, doi:10.1128/jvi.02357-16 (2017).
427 Wrammert, J. *et al.* Rapid cloning of high-affinity human monoclonal antibodies against influenza virus. *Nature* **453**, 667-671, doi:10.1038/nature06890 (2008).
428 Schieffelin, J. S. *et al.* Neutralizing and non-neutralizing monoclonal antibodies against dengue virus E protein derived from a naturally infected patient. *Virology journal* **7**, 28, doi:10.1186/1743-422x-7-28 (2010).
429 Vasilakis, N. & Weaver, S. C. The history and evolution of human dengue emergence. *Advances in virus research* **72**, 1-76, doi:10.1016/s0065-3527(08)00401-6 (2008).
430 Halstead, S. B. & O'Rourke, E. J. Antibody-enhanced dengue virus infection in primate leukocytes. *Nature* **265**, 739-741, doi:10.1038/265739a0 (1977).
431 Tsai, W. Y. *et al.* Potent Neutralizing Human Monoclonal Antibodies Preferentially Target Mature Dengue Virus Particles: Implication for Novel Strategy for Dengue Vaccine. *J Virol* **92**, doi:10.1128/jvi.00556-18 (2018).
432 Cox, K. S. *et al.* Rapid isolation of dengue-neutralizing antibodies from single cell-sorted human antigen-specific memory B-cell cultures. *mAbs* **8**, 129-140, doi:10.1080/19420862.2015.1109757 (2015).
433 Slifka, M. K. & Ahmed, R. Limiting dilution analysis of virus-specific memory B cells by an ELISPOT assay. *J Immunol Methods* **199**, 37-46, doi:10.1016/s0022-1759(96)00146-9 (1996).
434 Czerkinsky, C. C., Nilsson, L. A., Nygren, H., Ouchterlony, O. & Tarkowski, A. A solid-phase enzyme-linked immunospot (ELISPOT) assay for enumeration of specific antibody-secreting cells. *J Immunol Methods* **65**, 109-121, doi:10.1016/0022-1759(83)90308-3 (1983).

435 Sasaki, S. *et al.* Comparison of the influenza virus-specific effector and memory B-cell responses to immunization of children and adults with live attenuated or inactivated influenza virus vaccines. *J Virol* **81**, 215-228, doi:10.1128/jvi.01957-06 (2007).
436 Köhler, G. & Milstein, C. Continuous cultures of fused cells secreting antibody of predefined specificity. *Nature* **256**, 495-497, doi:10.1038/256495a0 (1975).
437 Liu, J. K. The history of monoclonal antibody development - Progress, remaining challenges and future innovations. *Annals of medicine and surgery (2012)* **3**, 113-116, doi:10.1016/j.amsu.2014.09.001 (2014).
438 Wahala, W. M., Kraus, A. A., Haymore, L. B., Accavitti-Loper, M. A. & de Silva, A. M. Dengue virus neutralization by human immune sera: role of envelope protein domain III-reactive antibody. *Virology* **392**, 103-113, doi:10.1016/j.virol.2009.06.037 (2009).
439 Robinson, J. E., Holton, D., Pacheco-Morell, S., Liu, J. & McMurdo, H. Identification of conserved and variant epitopes of human immunodeficiency virus type 1 (HIV-1) gp120 by human monoclonal antibodies produced by EBV-transformed cell lines. *AIDS research and human retroviruses* **6**, 567-579, doi:10.1089/aid.1990.6.567 (1990).
440 Traggiai, E. *et al.* An efficient method to make human monoclonal antibodies from memory B cells: potent neutralization of SARS coronavirus. *Nature medicine* **10**, 871-875, doi:10.1038/nm1080 (2004).
441 Simmons, C. P. *et al.* Prophylactic and therapeutic efficacy of human monoclonal antibodies against H5N1 influenza. *PLoS medicine* **4**, e178, doi:10.1371/journal.pmed.0040178 (2007).
442 Corti, D. & Lanzavecchia, A. Efficient Methods To Isolate Human Monoclonal Antibodies from Memory B Cells and Plasma Cells. *Microbiology spectrum* **2**, doi:10.1128/microbiolspec.AID-0018-2014 (2014).
443 Friberg, H. *et al.* Analysis of human monoclonal antibodies generated by dengue virus-specific memory B cells. *Viral Immunol* **25**, 348-359, doi:10.1089/vim.2012.0010 (2012).
444 Kwakkenbos, M. J. *et al.* Generation of stable monoclonal antibody-producing B cell receptor-positive human memory B cells by genetic programming. *Nature medicine* **16**, 123-128, doi:10.1038/nm.2071 (2010).
445 Kwakkenbos, M. J., van Helden, P. M., Beaumont, T. & Spits, H. Stable long-term cultures of self-renewing B cells and their applications. *Immunol Rev* **270**, 65-77, doi:10.1111/imr.12395 (2016).
446 Merat, S. J. *et al.* Hepatitis C virus Broadly Neutralizing Monoclonal Antibodies Isolated 25 Years after Spontaneous Clearance. *PloS one* **11**, e0165047, doi:10.1371/journal.pone.0165047 (2016).
447 Ekiert, D. C. *et al.* A highly conserved neutralizing epitope on group 2 influenza A viruses. *Science (New York, N.Y.)* **333**, 843-850, doi:10.1126/science.1204839 (2011).
448 Nivarthi, U. K. *et al.* Longitudinal analysis of acute and convalescent B cell responses in a human primary dengue serotype 2 infection model. *EBioMedicine* **41**, 465-478, doi:10.1016/j.ebiom.2019.02.060 (2019).
449 Lanzavecchia, A. Dissecting human antibody responses: useful, basic and surprising findings. *EMBO molecular medicine* **10**, doi:10.15252/emmm.201808879 (2018).

450 Kodituwakku, A. P., Jessup, C., Zola, H. & Roberton, D. M. Isolation of antigen-specific B cells. *Immunology and cell biology* **81**, 163-170, doi:10.1046/j.1440-1711.2003.01152.x (2003).
451 Scheid, J. F. *et al.* A method for identification of HIV gp140 binding memory B cells in human blood. *J Immunol Methods* **343**, 65-67, doi:10.1016/j.jim.2008.11.012 (2009).
452 Woda, M. *et al.* Dynamics of Dengue Virus (DENV)-Specific B Cells in the Response to DENV Serotype 1 Infections, Using Flow Cytometry With Labeled Virions. *J Infect Dis* **214**, 1001-1009, doi:10.1093/infdis/jiw308 (2016).
453 Moody, M. A. & Haynes, B. F. Antigen-specific B cell detection reagents: use and quality control. *Cytometry A* **73**, 1086-1092, doi:10.1002/cyto.a.20599 (2008).
454 Tiller, T. *et al.* Efficient generation of monoclonal antibodies from single human B cells by single cell RT-PCR and expression vector cloning. *J Immunol Methods* **329**, 112-124, doi:10.1016/j.jim.2007.09.017 (2008).
455 Wen, N. *et al.* Development of Droplet Microfluidics Enabling High-Throughput Single-Cell Analysis. *Molecules (Basel, Switzerland)* **21**, doi:10.3390/molecules21070881 (2016).
456 Adler, A. S. *et al.* Rare, high-affinity anti-pathogen antibodies from human repertoires, discovered using microfluidics and molecular genomics. *MAbs* **9**, 1282-1296, doi:10.1080/19420862.2017.1371383 (2017).
457 Wang, B. *et al.* Functional interrogation and mining of natively paired human V(H):V(L) antibody repertoires. *Nature biotechnology* **36**, 152-155, doi:10.1038/nbt.4052 (2018).
458 Wadhwa, P. & Morrison, V. Infectious Complications of Chronic Lymphocytic Leukemia. *Seminars in Oncology* **33**, 240-249, doi:10.1053/j.seminoncol.2005.12.013 (2006).
459 Scarfò, L. *et al.* COVID-19 severity and mortality in patients with chronic lymphocytic leukemia: a joint study by ERIC, the European Research Initiative on CLL, and CLL Campus. *Leukemia* **34**, 2354-2363, doi:10.1038/s41375-020-0959-x (2020).
460 Roeker, L. E. *et al.* COVID-19 vaccine efficacy in patients with chronic lymphocytic leukemia. *Leukemia*, doi:10.1038/s41375-021-01270-w (2021).
461 Lyski, Z. L. *et al.* Cellular and humoral Immune response to mRNA COVID-19 vaccination in subjects with chronic lymphocytic leukemia. *medRxiv*, 2021.2011.2004.21265948, doi:10.1101/2021.11.04.21265948 (2021).
462 Kamar, N. *et al.* Three Doses of an mRNA Covid-19 Vaccine in Solid-Organ Transplant Recipients. *New England Journal of Medicine* **385**, 661-662, doi:10.1056/nejmc2108861 (2021).
463 Shroff, R. T. *et al.* Immune responses to two and three doses of the BNT162b2 mRNA vaccine in adults with solid tumors. *Nature Medicine*, doi:10.1038/s41591-021-01542-z (2021).
464 Mateus, J. *et al.* Selective and cross-reactive SARS-CoV-2 T cell epitopes in unexposed humans. *Science* **370**, 89-94, doi:10.1126/science.abd3871 (2020).
465 Bates, T. A. *et al.* Age-Dependent Neutralization of SARS-CoV-2 and P.1 Variant by Vaccine Immune Serum Samples. *JAMA*, doi:10.1001/jama.2021.11656 (2021).
466 Sun, C. *et al.* Partial reconstitution of humoral immunity and fewer infections in patients with chronic lymphocytic leukemia treated with ibrutinib. *Blood* **126**, 2213-2219, doi:10.1182/blood-2015-04-639203 (2015).

467 Roessner, P. M. & Seiffert, M. T-cells in chronic lymphocytic leukemia: Guardians or drivers of disease? *Leukemia* **34**, 2012-2024, doi:10.1038/s41375-020-0873-2 (2020).